UNIVERSIDAD COMPLUTENSE DE MADRID

FACULTAD DE CIENCIAS FÍSICAS

Departamento de Física de la Tierra, Astronomía y Astrofísica I (Geofísica y Meteorología) (Astronomía y Geodesia)

TESIS DOCTORAL

Estudio de compuestos secundarios inorgánicos del aerosol en atmósfera urbana: evolución temporal y caracterización de episodios

Study of secondary inorganic aerosol compounds in the urban atmosphere: temporal evolution and characterisation of episodes

MEMORIA PARA OPTAR AL GRADO DE DOCTOR

PRESENTADA POR

Mª Aránzazu Revuelta Menéndez

Directores

Begoña Artiñano Rodríguez de Torres
Francisco Javier Gómez Moreno

Madrid, 2013

UNIVERSIDAD COMPLUTENSE DE MADRID

DEPARTAMENTO DE FÍSICA DE LA TIERRA,
ASTRONOMÍA Y ASTROFÍSICA I
(GEOFÍSICA Y METEOROLOGÍA)

TESIS DOCTORAL

Estudio de compuestos secundarios inorgánicos del aerosol en atmósfera urbana: evolución temporal y caracterización de episodios

Study of secondary inorganic aerosol compounds in the urban atmosphere: temporal evolution and characterisation of episodes

Autora: Mª Aránzazu Revuelta Menéndez

Directores: Dra. Begoña Artíñano Rodríguez de Torres
Dr. Francisco Javier Gómez Moreno

Madrid, 2012

UNIVERSIDAD COMPLUTENSE DE MADRID

FACULTAD DE CIENCIAS FÍSICAS

Departamento de Física de la tierra, Astronomía y Astrofísica I

Estudio de compuestos secundarios inorgánicos del aerosol en atmósfera urbana: evolución temporal y caracterización de episodios

Study of secondary inorganic aerosol compounds in the urban atmosphere: temporal evolution and characterisation of episodes

Memoria que presenta para optar al grado de Doctor

Mª Aránzazu Revuelta Menéndez

Directores:

Dra. Begoña Artíñano Rodríguez de Torres

Dr. Francisco Javier Gómez Moreno

Centro de Investigaciones Energéticas, Medioambientales y Tecnológicas (CIEMAT)

Tutor en el Departamento:

Dr. Carlos Yagüe Anguis

AGRADECIMIENTOS

La elaboración de esta tesis ha supuesto, como suele ser habitual, una intensa etapa de transformación y maduración profesional y personal a la que han contribuido un sinfín de personas.

Empecemos por el principio agradeciendo a mi directora, Begoña Artíñano, el haberme brindado la posibilidad de realizar este trabajo. Aunque ya había tenido alguna experiencia previa, esta tesis ha supuesto mi formación como investigadora y la oportunidad de conocer en mayor profundidad el mundo de la ciencia. Asimismo, este trabajo ha mejorado enormemente gracias a su experiencia y conocimientos. A Paco Gómez Moreno, mi codirector, tengo que agradecerle el haberme enseñado casi todo lo que sé de química atmosférica. Pero sobre todo tengo que destacar su compromiso con la excelencia en el laboratorio. Además, agradezco especialmente a los dos su ayuda durante la fase final de la preparación de esta memoria, cuando el cansancio empezaba a hacer mella.

Al Profesor Roy Harrison, mi tutor en la Universidad de Birmingham, debo agradecerle su buena acogida así como todo su apoyo y ayuda, y un planteamiento del trabajo siempre constructivo. Esta colaboración no hubiera sido posible sin Juana Mari Delgado-Saborit, quien me ayudó a organizar mi estancia en la UoB y es una de las personas más eficientes y profesionales que he conocido. Gracias también a los compañeros con quien compartí la sala 425 y muchos buenos ratos, especialmente Forough y Eunh-Hwa. Y pensando en Birmingham, no puedo olvidar a mis muchos amigos de Wesley House, que hicieron de la casa un hogar y de mi estancia en el Reino Unido una experiencia inolvidable.

También quiero agradecer la organización de la campaña internacional DAURE, que me resultó enormemente formativa, a los Profesores Xavier Querol y José Luis Jiménez.

Son muchos los compañeros de la Unidad de Contaminación Atmosférica y de la Unidad de Emisiones Contaminantes del CIEMAT que me han prestado ayuda durante el desarrollo de este trabajo.

Es obligado comenzar por nombrar a Curro Molero. Sin Curro, el capítulo 7 de esta tesis no existiría. El trabajo sobre el evento volcánico del Eyjafjallajökull realizado con él me posibilitó asimismo el desarrollo de otros temas incluidos en esta tesis. Pero sobre todo tengo que agradecerle, desde un punto de vista personal, su obstinación en no permitirme desanimarme nunca.

También a Lourdes Núñez, mi compañera de despacho, por su apoyo constante y sus ganas de colaborar.

La primera parte del capítulo 4 (incluyendo análisis de tendencias, niveles y variaciones estacionales) se basa en un trabajo de Pedro Salvador, que compartió conmigo, y cuya metodología he seguido.

Con Javier Plaza† tuve la ocasión de trabajar durante mi primer año en el CIEMAT y colaborar en la primera fase del trabajo derivado de DAURE, en la que me enseñó el manejo, procesamiento de muestras y tratamiento de datos de MOUDI. La parte experimental de esta campaña la realicé en conjunto con Esther Coz. Ella y Elizabeth Alonso también han colaborado en la comparativa entre impactadores en cascada y equipos de continuo.

También debo recordar a José Luis Mosquera, siempre dispuesto a ayudar en lo que haga falta, ya sea elaborar mapas o arreglar equipos.

Asimismo, todos los compañeros del CIEMAT mencionados junto con Alfonso, Manuel, Alberto, Beatriz, Juan Carlos, Magdalena, Mariano, José Manuel y Begoña Aceña participaron en las campañas de muestreo de amoniaco que tuvieron lugar en 2011, y sin cuya ayuda hubiera sido imposible realizarlas.

También debo agradecer a Leonor Martín y Rosa García, de AEMET, su interpretación del paso de la nube volcánica del Eyjafjallajökull por la Península Ibérica.

Finalmente, quisiera mencionar a los profesores Encarna Serrano y Carlos Yagüe, de la facultad de Ciencias Físicas de la UCM, que me han ayudado en los diferentes trámites en el departamento, demostrando a la vez un apoyo que les agradezco enormemente.

Son numerosos los organismos que han colaborado en la realización de este trabajo proporcionando libremente datos de calidad de aire o herramientas de análisis.

La National Oceanic and Atmospheric Administration (NOAA) de los Estados Unidos proporciona el modelo de cálculo de trayectorias HYSPLIT, así como ficheros de datos meteorológicos.

El modelo de trayectorias FLEXTRA fue desarrollado por Andreas Stohl (NILU) en colaboración con Gerhard Wotawa y Petra Seibert (Institute of Meteorology and Geophysics, Wienna) y utiliza datos meteorológicos proporcionados por el European Centre for Medium Range Weather Forecast (ECMWF).

El Navy Research Laboratory de Estados Unidos proporciona el modelo de mapas de aerosol NAAPS.

El software OPENAIR es un proyecto del Natural Environment Research Council (NERC) del Reino Unido, y está dirigido por investigadores del Environmental Research Group del King's Collage de Londres y apoyado por la Universidad de Leeds.

Esta tesis se ha realizado con la ayuda predoctoral BES-2008-007079 del Ministerio de Ciencia e Innovación, incluyendo la estancia de 3 meses en el Reino Unido. El trabajo ha sido financiado mediante la participación en los siguientes proyectos:

- PROFASE CGL2007-64117, titulado “Procesos de formación y propiedades físico-químicas del aerosol secundario urbano”

- MICROSOL CGL2011-27020, titulado "Propiedades físico-químicas de la fracción submicrométrica del aerosol atmosférico"

- Acción Complementaria CGL2008-02817-E, titulada "Participación en la campaña de medidas internacional -DAURE 2009".

Y, ya en el aspecto personal, por supuesto, podría agradecer mil cosas a Daniel, con quien además de compartir la vida siempre tendré cerca el espíritu de la verdadera ciencia. Él y mi familia han sufrido los "efectos colaterales" de mi dedicación a esta investigación y me han apoyado siempre.

Este trabajo va dedicado a todas aquellas personas que he tenido la suerte de conocer que, a pesar de las dificultades inherentes al mundo de la investigación y especialmente en la situación actual, muestran una ilusión sin fisuras cuando se les habla del trabajo científico. Espero que esta memoria caiga en manos de algunas de ellas y sea de su interés.

ACKNOWLEDGEMENTS

The development of this thesis has been an intense period of personal and professional transformation and maturing which received the contributions of countless people.

First things first, I must start by thanking my supervisor, Begoña Artiñano, for giving me the opportunity of doing this work. Although I had had some previous experience, this thesis has made my training as a researcher and the opportunity to know in greater depth the world of science. Furthermore, this work has greatly improved thanks to her experience and knowledge. I have to thank Paco Gómez-Moreno, my co-supervisor, for teaching me almost everything I know about atmospheric chemistry. But mostly I have to emphasize his commitment to excellence in the laboratory. In addition, I must thank both of them for their help during the final stages of preparation of this memory, when fatigue began to take its toll.

I am grateful to thank Professor Roy Harrison, my supervisor at the University of Birmingham, for his welcome and for his support and help, always with a constructive approach to work. This collaboration would not have been possible without Juana Mari Delgado-Saborit, who helped me organize my stay in the UoB and is one of the most efficient and professional people I have ever met. Thanks also to the colleagues with whom I shared the room 425 and many good times, especially Forough and Eunh-Hwa. And thinking about Birmingham, I cannot forget my many friends at Wesley House, which made the house a home and my stay in the UK an unforgettable experience.

I also thank the organisers of the international campaign DAURE, which was extremely formative for me, Professors Xavier Querol and José Luis Jiménez.

Many colleagues from the CIEMAT Air Pollution Unit and Pollutant Emissions Unit have assisted me during the course of this work.

It must begin with Curro Molero. Without Curro, Chapter 7 of this thesis would not exist. The work on the Eyjafjallajökull volcanic event carried out with him also enabled me to develop other topics covered in this thesis. But mostly I have to thank him, from a personal point of view, his stubbornness in not allowing me to dishearten.

I must follow with Lourdes Núñez, my office mate, for her constant support and will to collaborate.

The first part of Chapter 4 (including levels, seasonal variations and trend analysis) is based on a work of Pedro Salvador, who shared it with me, and I followed the methodology used.

With Javier Plaza† I had the chance to work during my first year at CIEMAT and collaborate on the first phase of DAURE. He taught me the MOUDI handling, sample processing and data processing. The experimental part of this campaign was carried

out together with Esther Coz. She and Elizabeth Alonso have also collaborated on the comparison between cascade impactors and semi-continuous equipment.

I should also think of José Luis Mosquera, always willing to help in whatever is needed, whether mapping or fixing equipment.

Also, all mentioned CIEMAT mates together with Alfonso, Manuel, Alberto, Beatriz, Juan Carlos, Magdalena, Mariano, José Manuel and Begoña Aceña participated in the ammonia sampling campaigns that took place in 2011. Without them it would have been impossible to perform them.

I am grateful to Leonor Martin and Rosa Garcia, from AEMET, for their interpretation of the passage of the Eyjafjallajökull volcanic cloud over the Iberian Peninsula.

Finally, I would like to mention professors Carlos Yagüe and Encarna Serrano, from the Faculty of Physical Sciences at UCM, who helped me at different paperwork steps in the department, showing both a support I thank very much.

Many agencies have collaborated on this work by providing free air quality data and analysis tools.

The National Oceanic and Atmospheric Administration (NOAA) of the USA provide the trajectory model calculation HYSPLIT, together with meteorological data files.

The trajectory model FLEXTRA was developed by Andreas Stohl (NILU) in cooperation with Gerhard Wotawa and Petra Seibert (Institute of Meteorology and Geophysics, Wienna) and uses meteorological data provided by the European Centre for Medium Range Weather Forecast (ECMWF).

The Navy Research Laboratory of the USA provides the aerosol map model NAAPS.

The OPENAIR software is a project of the Natural Environment Research Council (NERC) of the UK. It is led by researchers of the Environmental Research Group del King's Collage of London and supported by Universidad of Leeds.

This thesis has been carried out under the grant BES-2008-007079 from Ministerio de Ciencia e Innovación, including the 3-month stay in the United Kingdom. This work has been funded by the participation in the following projects:

- PROFASE CGL2007-64117, entitled “Procesos de formación y propiedades físico-químicas del aerosol secundario urbano”
- MICROSOL CGL2011-27020, entitled “Propiedades físico-químicas de la fracción submicrométrica del aerosol atmosférico”
- Acción Complementaria CGL2008-02817-E, entitled “Participación en la campaña de medidas internacional -DAURE 2009”.

And, on the personal side, of course, I could mention a thousand things I should thank Daniel, who in addition to sharing life with me always keeps near me the spirit of true science. He and my family have suffered the "side effects" of my dedication to this research and have always supported me.

This work is dedicated to all those I have been lucky enough to meet that, despite the difficulties inherent to the research world and especially in the current situation, show a seamless illusion when speaking of scientific work. I hope this memory reaches some of them and will be of their interest.

INDEX

Page

RESUMEN

INTRODUCCIÓN

En las últimas décadas, el desarrollo tecnológico e industrial ha permitido a la humanidad alcanzar niveles de bienestar muy por encima de las generaciones anteriores. Sin, embargo, como consecuencia de este desarrollo el medio ambiente está sufriendo una degradación que no podemos ignorar. Este hecho está produciendo el desarrollo de muchas disciplinas científicas que buscan un mejor conocimiento de las complejas interacciones que gobiernan el sistema terrestre, incluyendo la atmósfera, hidrosfera, biosfera y litosfera. Las perturbaciones antropogénicas producidas en cualquiera de estas "esferas" pueden tener un impacto en las demás y dar como resultado alteraciones de la vida sobre la Tierra, incluyendo a los propios seres humanos. La ciencia de aerosoles es una de las disciplinas fundamentales que contribuyen a la comprensión de nuestro medio ambiente.

Aunque no existe una definición única, se puede considerar contaminación atmosférica a cualquier fenómeno producido en el aire por el que compuestos químicos naturales o artificiales alcanzan concentraciones suficientemente elevadas sobre los niveles ambientales para producir efectos mensurables sobre los seres vivos o el medio ambiente.

Los contaminantes atmosféricos se clasifican siguiendo diferentes criterios. De acuerdo con su estado físico, podemos distinguir: gases, partículas líquidas y partículas sólidas. También se dan partículas heterogéneas formadas por mezclas de fases sólidas y líquidas. La mezcla de partículas suspendidas en un gas se denomina "aerosol". No obstante, este término se extiende frecuentemente a las partículas en sí mismas, a las que también nos referimos como "material particulado" (*particulate material*, **PM**).

La generación de aerosoles puede ser tanto natural como antropogénica, es decir, debida a la actividad humana. Las fuentes naturales que emiten los mayores aportes de aerosol a la atmósfera incluyen volcanes, tormentas de polvo, incendios forestales y pulverización de agua marina. Las actividades humanas generan aerosol principalmente a través de industrias, estaciones de abastecimiento de energía y quema de combustibles en motores. El polvo generado en la construcción y la alteración de la

corteza terrestre (Ej. zonas arenosas donde se ha eliminado la vegetación o el agua) también son factores importantes.

Las partículas emitidas directamente a la atmósfera se denominan ***aerosol primario***, mientras que aquellas que se forman como producto de procesos físico-químicos ocurridos en el seno de la atmósfera se denominan ***aerosol secundario***. La composición del aerosol depende tanto de su origen como de la posterior transformación.

Con respecto al tamaño, Whitby (1978) observó que las distribuciones de tamaño de aerosoles naturales se podían caracterizar mediante un modelo trimodal consistente en tres distribuciones log-normales aditivas. La moda centrada entre 5 y 30 μm de diámetro formada por procesos mecánicos se denominó ***moda gruesa***; la moda centrada entre 0.15 y 0.5 μm formada por procesos de condensación y coagulación se denominó ***moda de acumulación***; y la moda centrada entre 0.015 y 0.04 μm debida tanto a condensación y coagulación como a nucleación de nuevas partículas se denominó ***moda de nucleación***. La suma de las modas de acumulación y nucleación constituye el ***aerosol fino***.

El diámetro de una partícula esférica puede determinarse mediante diferentes propiedades físicas: ópticas, eléctricas, o aerodinámicas. No obstante, las partículas atmosféricas no son esféricas. Así pues, sus diámetros deben describirse mediante "diámetros equivalentes" (diámetro de Stokes Dp, diámetro aerodinámico Da, etc).

La notación PM_x define aquellas partículas recogidas por un muestreador con una determinada curva de colección con un valor del 50% para partículas de un Da=x (μm). Los puntos de corte x con los que operan los dispositivos de muestreo se escogen teniendo en cuenta los efectos de los aerosoles en el organismo humano (capacidad de penetración) así como en una adecuada clasificación de las modas fina y gruesa. Los tamaños **PM_{10}-$PM_{2.5}$-PM_1** son los más utilizados en la actualidad en la clasificación de partículas y son los considerados en este trabajo.

Teniendo en cuenta tanto las fuentes como las propiedades físico-químicas, existen los siguientes grandes grupos de aerosoles: marinos, minerales, volcánicos, carbonáceos, biogénicos, y compuestos secundarios inorgánicos. De entre estos últimos, los

principales son los productos de azufre y nitrógeno. El estudio de estos compuestos en áreas urbanas constituye el tema central de esta tesis.

Los compuestos secundarios inorgánicos (**SIC**) conforman una fracción mayoritaria del material particulado urbano. En España, Querol et al (2008) encontraron que los SIC representaban el 20-33% y el 19-38% del aerosol fino en estaciones de fondo urbano y puntos calientes de tráfico o industriales, respectivamente. En aquel estudio SIC se definía como **SO_4^{2-}+NO_3^-+NH_4+.** Ésta es la definición que se recoge en esta tesis.

Una fracción mayoritaria del sulfato urbano proviene de la oxidación de dióxido de azufre, oxidación que a su vez puede producirse bien mediante reacciones homogéneas en fase gaseosa o bien mediante procesos heterogéneos en gotículas líquidas. Existe una fracción primaria de sulfato urbano generado en motores diesel, mientras que el precursor SO_2 es emitido en procesos de combustión de diferentes instalaciones. El sulfato particulado es químicamente muy estable, lo que permite su transporte a largas distancias.

A su vez, el nitrato particulado se genera esencialmente de las emisiones vehiculares de NOx (=NO+NO_2) mediante mecanismos tanto homogéneos como heterogéneos. Debido a su corto tiempo de vida en la atmósfera, sus efectos se han considerado generalmente locales o regionales.

Tanto el sulfato como el nitrato son neutralizados principalmente por el amonio, aunque el amoniaco gaseoso (NH_3) reacciona preferentemente con el sulfato y sólo el restante puede neutralizar el nitrato. En las áreas urbanas, el origen del amoniaco está en fuentes biológicas, procesos industriales y emisiones vehiculares. No obstante, la contribución de cada una de ellas a nivel local-regional no suele estar bien caracterizada.

La calidad del aire está regulada por organismos tanto nacionales como internacionales. Sin embargo, las concentraciones de compuestos secundarios del aerosol hasta el momento no están sujetas a ninguna regulación, ya que sus procesos de formación y transformación en la atmósfera son no-lineales y altamente complejos. Normativas europeas y nacionales regulan las emisiones y niveles ambiente de precursores y PM total. Por añadido, ordenanzas municipales en muchas ciudades,

como la ciudad de Madrid, han contribuido al control de emisiones contaminantes. El NH_3 es el único precursor que no está regulado hasta la fecha, existiendo únicamente una recomendación de vigilancia de sus niveles.

En este trabajo, el **área de estudio** principal será la cuenca aérea madrileña, situada en la parte central de la Península Ibérica. La región se encuentra en una extensa meseta y está bordeada por terreno montañoso al Nor-noeste, Noreste y Este. El clima presenta inviernos fríos y veranos cálidos y secos, con una predominancia de los días despejados. La situación sinóptica que da lugar a episodios de alta contaminación corresponde a anticiclones invernales, con la formación de inversiones radiativas nocturnas en superficie. En verano, en cambio, se caracteriza por el desarrollo de una fuerte actividad convectiva. La influencia de las montañas produce circulaciones características.

El área metropolitana de Madrid cuenta con aproximadamente 6.6 millones de habitantes, comprendiendo una flota de más de 4 millones de vehículos (aproximadamente el 50% diesel) con tráfico muy intenso los días de semana. Las emisiones procedentes de industrias ligeras y de calefacciones contribuyen en menor medida. La distancia entre Madrid y otras áreas urbanas o industriales es >200 Km., por lo que el penacho generado por el tráfico de la ciudad puede estudiarse de forma casi independiente de otras fuentes. No obstante, el transporte regional y a larga distancia debe ser tenido en cuenta en situaciones puntuales.

El **emplazamiento de referencia** utilizado en este estudio es una estación de fondo urbano situada en las dependencias del CIEMAT, en el sector nor-occidental de la ciudad. La mayor parte de los datos analizados en este trabajo se han medido en esta estación. No obstante, el análisis de la cuenca aérea ha incluido otras estaciones, y se han llevado a cabo estudios complementarios en otras regiones (sureste de Inglaterra y Barcelona) con el fin de contrastar las características específicas de la cuenca aérea madrileña y situarla en un contexto internacional.

OBJETIVOS

El **objetivo principal** de este trabajo es el de profundizar en el estudio del SIC en el área de interés, con especial énfasis en la fracción fina de nitrato y sulfato, cubriendo diversas lagunas localizadas en estudios anteriores. En primer lugar, la información de gases precursores es incompleta. Mientras que los NOx y SO_2 se han medido ampliamente y sus fuentes y niveles medios están bien caracterizados, la información relativa al NH_3 es muy limitada. Gómez-Moreno et al (2007) caracterizaron el comportamiento estacional del nitrato durante un año, así como la evolución horaria bajo condiciones de anticiclón invernal. Estos resultados debían confirmarse en periodos de tiempo mayores. Además, la evolución del nitrato en otras escalas temporales relevantes –semanal- no era bien conocida, y los episodios de transporte no se habían estudiado. Toda esta información quedaba pendiente en el caso del sulfato. Estudios anteriores en distintas fracciones de tamaño debían ampliarse para cubrir todo el rango desde la moda gruesa a tamaños nanométricos, centrándose en diferentes tipos de episodios (Ej. Acumulación y niebla) para así evaluar la relevancia de los distintos procesos de formación de SIC.

Para investigar las incógnitas detectadas se establecen los siguientes objetivos específicos:

- Caracterizar niveles, variaciones estacionales y tendencias temporales de precursors gaseosos del nitrato y sulfato particulados en la cuenca aérea de Madrid. Caracterizar los niveles medios y las principales fuentes de NH_3 gaseosos en el área metropolitana de Madrid.
- Caracterizar las variaciones en alta resolución temporal y la evolución estacional/interannual de nitrato fino obteniendo una base de datos en semi-continuo más larga.
- Caracterizar la evolución temporal en alta resolución y los patrones de variación temporal de sulfato fino a partir de una nueva base de datos en semi-continuo de al menos un año.
- Realizar un análisis conjunto de variaciones temporales de sulfato y nitrato particulados en alta resolución.
- Identificar y caracterizar episodios individuales que dan lugar a altas concentraciones de nitrato y sulfato en la región de Madrid.

- Caracterizar la distribución de tamaños de concentración de especies inorgánicas del aerosol en tamaños menores de 0.056 μm.
- Comparar y contrastar el comportamiento de estas especies en la cuenca aérea de Madrid con la fenomenología del aerosol en otras regiones.

METODOLOGÍA

En este trabajo, **medidas en alta frecuencia (10-20 min)** así como otras técnicas complementarias han permitido el estudio de los procesos de evolución de estos compuestos difíciles de identificar únicamente con las medidas tradicionales de muestras recogidas cada 12-24 h.

A continuación se enumeran los trabajos que se han llevado a cabo desde el punto de vista experimental:

1) Instrumentos en semi-contínuo:

- Instalación, puesta a punto y mantenimiento de de un analizador de sulfato particulado Thermo 5020i SPA.
- Mantenimiento de un analizador de nitrato particulado R&P 8400.
- Mantenimiento de instrumentación adicional (optical particle counters GRIMM1107 and GRIMM1108).

2) Muestreadores:

- Puesta a punto de un nano-MOUDI y ejecución de campañas de muestreo con impactadores en cascada MOUDI y nano-MOUDI.

3) Campaña de medida de amoniaco gaseoso.

Los instrumentos en semi-contínuo han operado en la estación del CIEMAT en Madrid. Las series temporales obtenidas se han analizado y comparado junto con datos análogos de la región de Londres. El impactador en cascada se empleó en el estudio de episodios específicos en Madrid, así como en una campaña de contraste en Barcelona. La campaña de amoniaco ha supuesto una primera aproximación a la caracterización

de fuentes y niveles ambiente de este contaminante, clave en la formación de nitrato y sulfato secundarios y cuya vigilancia recomienda el Real Decreto 102/2011.

Estos trabajos, con el análisis de series temporales de contaminantes proporcionadas por Redes de Calidad de Aire y el uso de modelos de trayectorias y de predicción de distribución de concentraciones de aerosol constituye el conjunto de herramientas empleadas.

ESTRUCTURA DE LA TESIS

En el **capítulo1** se describen las propiedades y procesos básicos que siguen los aerosoles en cuanto a origen, composición y tamaño, entre otras propiedades, con particular atención a los compuestos inorgánicos secundarios. También se describe el área principal de estudio y el marco regulatorio tanto en materia de emisiones como de concentraciones ambientales.

En el **capítulo 2** se presenta el estado del arte, describiendo los resultados más recientes en ciencia de aerosoles relacionados con el campo de estudio de la tesis, así como los resultados previos obtenidos en la región de Madrid. También se desarrollan los objetivos del presente trabajo.

En el **capítulo 3** se expone el conjunto de técnicas empleadas en el desarrollo de la tesis. En primer lugar, se describe la instrumentación disponible en la estación de medida del CIEMAT -incluyendo la utilizada directamente para el desarrollo de esta tesis y la que se ha empleado de manera complementaria-, así como los captadores pasivos empleados en la campaña de amoniaco. A continuación se presentan las redes de calidad de aire de las cuales se han utilizado datos. Después se exponen los modelos que se han manejado, o de los cuales se han empleado salidas. Para finalizar este capítulo, se explican las herramientas de tratamiento de datos empleadas en el análisis de las series temporales y para el tratamiento de distribuciones de tamaño de aerosol.

Como base para los resultados que se presentarán más adelante, en el **capítulo 4** se expone la evolución temporal y concentraciones de los contaminantes de interés en la cuenca aérea madrileña en la última década. Dada la escasa disponibilidad de datos sobre amoniaco gaseoso, esta información se completa con los resultados obtenidos en la campaña llevada a cabo en más de 60 emplazamientos del área urbana de Madrid.

En el **capítulo 5** se exponen los resultados del análisis de las series de datos de nitrato y sulfato obtenidas en el CIEMAT. Este análisis se centra en la búsqueda de patrones en tres escalas temporales distintas (anual, semanal y diaria), y se ha realizado en paralelo con el análisis de series análogas medidas en el sur de Inglaterra.

Tras exponer los patrones medios que siguen los contaminantes de interés en la ciudad de Madrid, en el **capítulo 6** se presenta una caracterización de los principales tipos de eventos que contribuyen a que se alcancen altas concentraciones. Estos eventos son de transporte regional, de transporte a larga distancia desde el continente Europeo y de acumulación local. Se discuten los métodos de identificación de cada uno, así como los niveles máximos a que dan lugar.

Durante el desarrollo del presente estudio se produjo un evento singular de particular interés que recibió un tratamiento más detallado. Este evento fue el impacto de la nube volcánica procedente del Eyjafjallajökull en la Península Ibérica. El análisis realizado se presenta en el **capítulo 7**.

Para complementar el análisis anterior, en el **capítulo 8** se presentan los resultados obtenidos en estudios previos de compuestos inorgánicos en distintas fracciones de tamaño en la ciudad de Madrid y se contrastan con los obtenidos en una campaña en Barcelona.

Para finalizar, el **capítulo 9** resume los principales resultados alcanzados en esta tesis, exponiendo las líneas que quedan abiertas y las posibilidades de continuación de estas investigaciones en el futuro.

CONCLUSIONES Y APORTACIONES FUNDAMENTALES DE LA TESIS DOCTORAL

En primer lugar se ha recopilado la información disponible sobre concentraciones de gases precursores (NO_2, NOx, SO_2 y NH_3), material particulado y SIC en tres emplazamientos representativos -urbano, fondo urbano y fondo rural- de la cuenca aérea de Madrid en la última década. En general, las concentraciones fueron máximas en el emplazamiento urbano y mínimas en el rural, presentando valores intermedios en el de fondo urbano. Se han encontrado patrones estaminales diferentes en función del contaminante y emplazamiento, que se discuten teniendo en cuenta sus fuentes y mecanismos de formación.

Los gases y PM han mostrado tendencias decrecientes en la última década excepto el NH_3 gaseoso, que mantuvo niveles anuales constantes en el emplazamiento rural. Los descensos en NOx y PM pueden ser debidos a varias medidas encaminadas a reducir las emisiones, como la incorporación de convertidores catalíticos en los vehículos. Se ha demostrado que estos catalizadores conducen a notables reducciones en las emisiones de NO, pero a la vez general amoniaco gaseoso. Los descensos en SO_2 y sulfato particulado se deben a las limitaciones en azufre en combustibles.

- Los resultados son compatibles con el predominio de la generación de nitrato local en el área urbana de Madrid con ciclos estaminales dominados por la descomposición térmica.
- Las fuentes locales han contribuido significativamente a los niveles de sulfato registrados en invierno en el emplazamiento urbano; sin embargo, el fondo rural en la cuenca aérea está dominado por la mayor oxidación fotoquímica del SO_2 en verano.

La Escasez de medidas de NH_3 gaseoso condujo a la campaña de caracterización de fuentes y niveles ambientales de amoniaco en el área urbana de Madrid en 2011. Se obtuvieron medidas integradas durante 10 días en invierno y verano utilizando captadores pasivos.

- Los emplazamientos cercanos a depuradoras de aguas residuales y a una incineradora registraron las mayores concentraciones de amoniaco, seguidas de los sitios de tráfico. Estos últimos mostraron valores significativamente más altos que los de fondo urbano en ambas estaciones.
- En Madrid, los niveles medios de amoniaco son similares a las medidas en otras ciudades y notablemente inferiores a las registradas en Barcelona en el mismo año.

Un análisis de patrones temporales medios de sulfato, nitrato y gases precursores en escalas anual, semanal y diaria se ha realizado para emplazamientos de fondo urbano y rurales en las regiones de Madrid y Londres en el periodo 2005-2010. Este estudio identificó similitudes y diferencias que contribuyen a determinar los principales procesos y los parámetros relevantes en cada caso.

- El patrón estacional de nitrato fino en Madrid está dominado por la evolución térmica. Por contraste, en Londres se aprecia la descomposición térmica en verano, pero también un notable máximo de Febrero a Abril que puede relacionarse con el transporte de contaminantes desde centro-Europa.

- En ambas ciudades se encontraron en verano reducciones de nitrato fino en torno al 20% con significancia estadística. En cambio, para el sulfato se encontraron reducciones en el rango 13-18% en invierno.

- El patrón diurno seguido por los NOx es similar en ambas ciudades, sin embargo, el comportamiento del nitrato en invierno es muy diferente. En Madrid, las bajas temperaturas permitieron el predominio de la fotoquímica en la formación de nitrato, dando como resultado un único máximo a mediodía. En Londres se registraron altas concentraciones durante la noche, como consecuencia de la formación acuosa de nitrato bajo altas humedades relativas. En verano, las mayores temperaturas y espesor de la capa de mezcla dan como resultado un pico matutino asociado a la hora punta de tráfico más un pico vespertino secundario. Este último se explica en términos de la contracción de la capa de mezcla.

- Los resultados de ambas ciudades indican que la evolución horaria de nitrato está determinada más por factores meteorológicos que por la evolución de los gases precursores.

- En Madrid en invierno el SO_2 y el SO_4^{2-} tienen sus máximos a mediodía. El mismo fenómeno se había observado en Londres para el SO_2.

El análisis de datos de Londres ha complementado el trabajo llevado a cabo en las campañas REPARTEE. Este trabajo también ha demostrado que los comportamientos identificados en Londres no son representativos de lo que ocurre en Madrid.

- Los procesos que controlan las concentraciones de nitrato y sulfato pueden variar sustancialmente a lo largo de Europa. No debe asumirse que las observaciones en una ciudad puedan extrapolarse a otros emplazamientos.

Se han caracterizado tres tipos de eventos que han dado lugar a altas concentraciones de nitrato y sulfato particulados en el área urbana de Madrid. Estos eventos son: un episodio de circulación regional (E1), transporte desde centro-Europa y Mediterráneo Occidental (E2a –sulfato- y E2b –nitrato y sulfato-) y acumulación local bajo condiciones anticiclónicas de invierno (E3). Aunque se confirma la importancia de las emisiones locales, los episodios de transporte regional y a larga distancia son también relevantes para las concentraciones ambientales de sulfato particulado en Madrid.

- Los valores más altos de nitrato en $PM_{2.5}$ (por encima de 20 $\mu g \cdot m^{-3}$) se asociaron con la situación de acumulación local E3, mientras que las concentraciones máximas alcanzadas bajo episodios de transporte E1 y E2b fueron inferiores a la mitad de ese valor.

- Los mayores niveles de sulfato en PM_1 registrados en el emplazamiento (7 $\mu g \cdot m^{-3}$) se asocian con el episodio de transporte a alrga distancia. Las concentraciones de sulfato alcanzaron 5 y tan sólo 3.5 $\mu g \cdot m^{-3}$ durante E1 y E3 respectivamente.

Un evento volcánico inusual que tuvo lugar durante el transcurso de las medidas llevadas a cabo en el CIEMAT se ha caracterizado en detalle. La erupción del volcán islandés Eyjafjallajökull trastornó el tráfico aéreo en Europa durante la primavera de 2010. El paso de la nube volcánica se identificó en las estaciones de la red EMEP. Las concentraciones de dióxido de azufre y sulfato particulado alcanzaron máximos relativos no correlacionados con otros contaminantes. El principal evento tuvo lugar entre los dáis 7 y 9 de mayo en el centro y sur de la Península. Se presenta una caracterización físico-química del aerosol que alcanzó el CIEMAT.

- Se calculó una estimación de los perfiles verticales de concentración a partir de los perfiles de coeficientes de extinción, obteniéndose un valor máximo de 77±9.6 $\mu g \cdot m^{-3}$, muy por debajo de el umbral establecido para el riesgo en la navegación aérea.

- Se detectó un gran aumento del aerosol en la moda fina en coincidencia con un aumento de la concentración de sulfato, mientras que la moda gruesa permanecía inalterada. Las distribuciones de volumen en superficie indicaron que las partículas se encontraron en al rango de tamaño 0.1-0.7 μm.

- Los resultados son consistentes con la distribución bimodal obtenida cerca de la fuente y sugieren el crecimiento de la moda fina a través de procesos de condensación y coagulación así como la eliminación de las partículas de ceniza.

Se han estudiado distribuciones de tamaño de iones en el rango desde 18 μm hasta <0.056 μm en invierno en un sitio de fondo urbano de Barcelona y se han comparado con un estudio previo en Madrid.

- En Barcelona, se encontraron modas de acumulación de 0.5 μm para el sulfato y amonio y 0.6-0.75 μm para el nitrato. En Madrid la moda de acumulación

estaba en torno a 0.35 μm para los tres iones. Esto es consistente con la presencia de una submoda droplet en Barcelona debida a valores superiores de la humedad relativa. En Madrid la moda de acumulación sólo mostró la submoda de condensación homogénea de gases.

- Se detecta la presencia de una moda gruesa de nitrato mineral en ambas ciudades, dominante en Madrid y en Barcelona durante la noche.

- Los balances iónicos muestran que la acidez está neutralizada, salvo para las partículas por debajo de <0.056 μm.

Para investigar estos fenómenos en mayor profundidad se realizó una nueva campaña en Madrid durante tres escenarios meteorológicos diferentes en invierno en el rango de 18 μm hasta to <0.010 μm: niebla densa (S1), estancamiento típico invernal (S2) y transición desde un periodo limpio a la niebla (S3).

- Las concentraciones más altas de sulfato y nitrato se registraron para S1 en el rango 1-1.8 μm (moda droplet). Este intervalo es notablemente mayor que el encontrado para S2 (sulfato 0.18-0.56 μm, nitrato 0.32-0.56 μm).

- Sólo para S2 se encontró una fracción significativa de nitrato y sulfato por debajo de 0.01 μm.

Estos resultados sugieren la generación acuosa en la moda droplet, aunque un desplazamiento de compuestos nanométricos a la moda de acumulación por procesos de agregación y coagulación en escenarios de alta humedad relativa también es posible.

Las medidas en semi-continuo confirmaron la eficiencia de la generación acuosa de SIC sobre los procesos de transporte y formación fotoquímica típicos de los escenarios de acumulación invernales.

LÍNEAS DE INVESTIGACIÓN FUTURAS

Esta tesis ha supuesto un estudio en profundidad del comportamiento del aerosol inorgánico secundario en la región de Madrid. Las técnicas en semi-continuo han permitido el estudio de características ocultas en trabajos previos. Sin embargo, todavía quedan problemas por resolver.

En el aérea urbana de Madrid la información sobre el amoniaco sigue siendo insuficiente. La campaña realizada supone un primer paso en esta dirección, pero se necesitan más estudios que cubran periodos temporales más largos. Las medidas en semi-continuo de este compuesto permitirían una mejor caracterización de la fuente de tráfico, puesto que se podrían realizar un análisis de correlaciones con contaminantes primarios emitidos por los vehículos.

La interpretación de la evolución diurna de los contaminantes secundarios ha demostrado ser compleja. En la literatura, los picos de la mañana y la tarde se relacionan con las horas punta de tráfico y con cambios vespertinos en la altura de la capa límite. Por el contrario, la ocurrencia de máximos a mediodía se ha explicado de diferentes maneras en varios emplazamientos de los Estados unidos. En algunos casos se han atribuido a producción fotoquímica local. En cambio, otros autores lo atribuyen a una combinación de fotoquímica local con transporte nocturno seguido por mezcla vertical durante el día. En el caso de Madrid, los patrones de evolución se pueden explicar en términos de la formación fotoquímica, pero teniendo en cuenta el transporte diurno dominante en la cuenca aérea.

Las medidas en semi-continuo han permitido diferenciar eventos de acumulación de contaminantes locales de eventos de transporte, ya que sólo en el primer caso se encuentran patrones de evolución diaria. La cuantificación de la proporción de nitrato y sulfato en la atmósfera de Madrid atribuible a cada tipo de evento permanece abierta.

Este trabajo ha proporcionado avances en el estudio de la fracción nanométrica de aerosol inorgánico presente en la atmósfera urbana de Madrid. Se han encontrado diferentes concentraciones de cada ión en cada fracción de tamaño en el rango nanométrico cuando se encuentran presentes aerosoles secos e hidratados. Para obtener resultados concluyentes se necesita determinar la respuesta de la técnica empleada a los distintos tipos de aerosol.

SUMMARY

INTRODUCTION

In the last decades, technical and industrial development has allowed humankind of a great part of the world to achieve a well-being high above previous generations. However, at the same time and as a consequence, the environment is suffering a degradation that we cannot ignore. This fact is leading to the development of many scientific disciplines with the objective of providing a better understanding of the complex interactions that govern the Earth's system, including the atmosphere, hydrosphere, biosphere and lithosphere. Anthropogenic perturbations in any of these "spheres" may impact the other ones and result in alterations of life on Earth, including the human beings ourselves. Aerosol science is one of the fundamental disciplines that contribute to understanding our environment.

Although there is not an unique definition, atmospheric pollution can be consider as any phenomenon produced in the air by which artificial or natural chemical compounds reach concentrations high enough over their natural ambient levels to produce measurable effects on living beings or the environment.

Atmospheric pollutants are classified following different criteria. According to their physical state we can distinguish gases, liquid particles and solid particles. Heterogeneous particles formed by a mixture of solid and liquid phases are also formed. The mixture of particles suspended in a gas is called "aerosol". Nevertheless, the term is frequently extended to the particles themselves, which are also referred as "Particulate Matter (**PM**)".

The generation of aerosols can be natural or anthropogenic, that is to say, due to the human activity. Natural sources that contribute with the highest loadings to the atmosphere include volcanoes, dust storms, forest and pasture fires and pulverization of seawater. Human activities generate aerosols mainly through fuel burning in vehicle motors, industry and power stations. The dust generated in construction works and alteration of the Earth's surface (i.e. sandy zones where water or vegetation has been removed) must be also considered.

Particles directly emitted to the atmosphere are denominated ***primary aerosols***, while those formed as the final product of physical and chemical processes occurred into the atmosphere are denominated ***secondary aerosols***.

The composition of an aerosol particle depends on its generation source as well as the physical and chemical transformation processes later undergone, being source/origin and chemical and physical properties closely linked.

Attending to size, Whitby (1978) observed that the aerosol size distributions could be usually well characterised by a trimodal model consisting on three additive log-normal distributions. The mode with a peak between 5 and 30 μm in diameter formed by mechanical processes is called the ***coarse mode***, the mode with a peak between 0.15 and 0.5 μm formed by condensation and coagulation processes is called the ***accumulation mode*** and the mode with a peak between 0.015 and 0.04 μm whose size was influenced by nucleation as well as by condensation and coagulation is called the ***nuclei or nucleation mode***. The ultrafine region defined by the nuclei mode is in turn split in the nucleation region (< 10 nm) and the Aitken region (10 – 100 nm). The sum of the accumulation and nuclei mode is called the ***fine aerosol***.

The diameter of a spherical particle may be determined attending to different physical properties: optical, light scattering and Mie theory, electrical mobility or aerodynamic behaviour. However, atmospheric particles are not spherical. Therefore, their diameters are described by "equivalent" diameters (Stokes Diameter Dp, aerodynamic diameter Da, etc).

The notation PM_x defines those particles collected by a sampler with a specified penetration curve yielding an upper 50% cut-point of x-μm aerodynamic diameter. The regulatory size cuts x for sampling devices are chosen according to aerosol effects on human health and accurate classification of the fine and coarse modes. **PM_{10}-$PM_{2.5}$-PM_1** are nowadays widely employed in the classification of particulate matter and will be the fundamental size fractions considered in this work.

Attending to both source and physico-chemical properties, aerosols can be classified as marine, mineral, volcanic, carbonaceous, biogenic, and secondary compounds. The

principal secondary inorganic compounds are sulphur and nitrogen by-products, and the study of these compounds in urban areas is the main topic of this thesis.

Secondary inorganic compounds **(SIC)** make a relevant fraction of urban fine particulate matter. In Spain, Querol et al (2008) found that SIC made 20-33% in urban background stations and 19-38% in traffic and industrial hotspots. In that study SIC was defined as $SO_4^{2-}+NO_3^-+NH_4+$. In this thesis we will also define SIC in the same way, although the availability of ammonium (NH_4+) measurements is smaller.

A major proportion of urban sulphate arises from the oxidation of sulphur dioxide. Reaction mechanisms in the atmosphere fall into two groups, either homogeneous reactions in the gas phase, or heterogeneous processes in aerosol droplets. Primary emissions of urban sulphate arise from diesel fuels, whereas the gaseous precursor SO_2 is emitted in combustion processes from different facilities. Particulate sulphate is chemically stable, allowing its atmospheric transport over long distances.

Particulate nitrate is generated in the urban areas essentially from vehicle gaseous NOx ($=NO+NO_2$) emissions, existing also homogeneous and heterogeneous formation mechanisms. Because of these relatively short atmospheric nitrate lifetimes, the major effects of emissions of nitrogen oxides are expected to be local or regional.

Both sulphate and nitrate are mainly neutralised by ammonium, but gaseous ammonia (NH_3) preferentially reacts with sulphate and only the remaining NH_3 can react with the nitric acid. In urban areas, ammonia sources include biological sources, industrial processes and vehicle emissions. However, the source apportionment usually is not well characterised.

Air quality is regulated by both national and international organisms. However, the concentrations of secondary compounds of the aerosol are not subject to any legal regulation at the moment, since their formation and transformation processes in the atmosphere are non-linear and highly complex. European and Spanish normatives regulate the emissions and ambient levels of precursor gases and total PM. In addition, in many cities such as Madrid, municipal ordinances have contributed to the control of pollutant emissions. NH_3 is the only main precursor which is not subject to regulation at the present time, existing only a recommendation of vigilance of levels.

The main **area of study** will be the Madrid air basin, located in the central part of the Iberian Peninsula. The area is characterized by an extended plateau bordered by mountainous terrain to the north-northwest, northeast and east. The weather in Madrid is typical of a mid-latitude continental area with hot dry summers and cold winters, most days being under clear-sky conditions. The general synoptic situation leading to the occurrence of episodic events corresponds in winter to stagnant anticyclone conditions, with the usual formation of radiative nocturnal surface inversions. In summer, the development of strong thermal convective activity and the influence of the mountains produce characteristic circulations.

The metropolitan area of Madrid has around 6.6 million inhabitants, comprising a car fleet over 4 million vehicles with very intense traffic on weekdays. Emissions from light industry and domestic heating in winter contribute in a lesser proportion. The distance between the Madrid metropolitan area and other significant urban or industrial areas in central Spain is >200 km. In this sense its urban plume could be studied as an isolated way. However long-range transport episodes significantly affect aerosol concentrations in the Madrid region.

The **reference sampling station** in this study is an urban background site located within the CIEMAT facilities, in the north-western area of the city of Madrid. A major part of the data analysed in this work has been measured in this location. Nevertheless, the analysis has been extended to other sites in south-eastern England and Barcelona, and complementary studies have been carried out to contrast the specific features of the Madrid air basin with other regions and situate it in an international context.

OBJECTIVES

The **main objective** of this work is to achieve a deeper insight on the secondary inorganic aerosol in an urban environment, with a special emphasis on the fine fraction of nitrate and sulphate. These species had been partially characterised in the Madrid air basin, and further research was needed to cover identified gaps found in previous studies. First, information on precursor gases is not complete. While NOx and SO_2

have been widely measured and their sources and mean levels well characterised in Madrid, information on gaseous NH_3 is very limited. A one-year study by Gómez-Moreno et al (2007) characterised nitrate seasonal behaviour and hourly evolution under winter episodic conditions. These results needed to be confirmed for a wider time period. At the same time, nitrate evolution in other timescales –weekly- was not well known, and nitrate events caused by other kind of episodes -such as air mass transport- had not been studied. The same information had to be acquired in the case of sulphate. Previous size-fractioned studies should be extended to cover a wider range from the coarse mode to nanometric sizes, focusing on distinct types of scenarios (e.g. stagnation and fog) to evaluate the relevance of the different SIC formation processes.

To fulfil these gaps the following specific objectives were established in this thesis:

- Characterise levels, seasonal variations and temporal trends of gaseous precursors of nitrate and sulphate in the Madrid air basin. Characterise mean levels and main gaseous NH_3 sources in the Madrid metropolitan area.
- Characterise the high-resolution variations and seasonal / interannual evolution of fine nitrate from a longer time series of semicontinuous measurements.
- Characterise the high-resolution temporal evolution and variation patterns of fine sulphate from a new database of at least one year of semicontinuous measurements.
- Perform a joint analysis of time variations of particulate sulphate and nitrate on a high-resolution temporal basis.
- Identify and characterise individual episodes leading to high nitrate and sulphate concentrations in the region of Madrid.
- Characterise the mass size distribution of inorganic aerosol species in size fractions smaller than 0.056 μm.
- Compare and contrast the behaviour of these species in the Madrid air basin with the phenomenology in other regions.

METHODOLOGY

In this work, **high frequency measurements (10-20 min)** together with ancillary techniques allowed the study of evolution processes of air pollutants difficult to identify solely with typical measurement of samples collected every 12-24 h.

From the experimental point of view, the works carried out are listed below:

1) Semi-continuous instruments:

- Installation, commissioning and maintenance of a Thermo 5020i Sulfate Particle Analyser.
- Maintenance of an R&P 8400 ambient particulate nitrate monitor.
- Maintenance of additional instrumentation (optical particle counters GRIMM1107 and GRIMM1108).

2) Samplers:

- Tuning of a nano-MOUDI and execution of sampling campaigns with nano-MOUDI and MOUDI cascade impactors.

3) Measurement campaign of gaseous ammonia.

The semi-continuous instruments have been operated at the CIEMAT site in Madrid. The time series obtained have been analysed and compared with analogous series of the London region. The cascade impactor was used to study specific episodic events in CIEMAT, and during a winter campaign in Barcelona. This works extended and complemented previous works in Madrid using a similar methodology. The ammonia campaign has been a first approach to the study of sources and levels of this pollutant, key in the formation of nitrate and sulfate particulates, and whose supervision is recommended by Royal Decree 102/2011.

This works, together with the joint analysis of pollutant time series provided by Air Quality Networks and the use of back-trajectory and aerosol distribution prediction models have allowed obtaining the results which will be summarised below.

THESIS STRUCTURE:

Chapter 1 describes the basic properties of the aerosols in terms of origin, composition and size, and the main processes the aerosol go through, with particular attention to secondary inorganic compounds. The main area of study is

also described as well as the regulatory framework regarding both emissions and ambient concentrations.

Chapter 2 presents the state of the art, describing the most recent results in aerosol science related to the field of study of this thesis as well as the previous results obtained in the region of Madrid. The objectives of the present work are also explained.

In **Chapter 3**, the techniques employed in the development of this work are exposed. In first place, the instrumentation available in the CIEMAT site is described – including main and ancillary instruments-, as well as the passive samplers employed in the ammonia campaign. Next, the models (or model outputs) which have been used are exposed. Finally, the data analysis tools employed in the treatment of temporal series and aerosol size distributions are explained.

As a basis for the results to be presented later, **Chapter 4** shows the time evolution and concentrations of the pollutants of interest in the Madrid air basin in the last decade. Given the limited availability of data on gaseous ammonia, this information is supplemented by the results of the campaign conducted in more than 60 sites in the urban area of Madrid.

Chapter 5 presents the results of the analysis of data sets obtained from nitrate and sulfate at CIEMAT. This analysis focuses on finding patterns in three different time scales (annual, weekly and daily), and has been performed in parallel with similar series analysis measured in southern England.

After exposing the mean patterns followed by the target pollutants in the city of Madrid, in **Chapter 6** a characterization of the main types of events that led to high concentrations is presented. These events were associated to situations of regional transport, long-distance transport from the European continent and local accumulation. We discuss the methods used for identifying each type of event as well as the maximum levels reached in every case.

During the course of this study there was a singular event of particular interest that received a more detailed treatment. This event was the impact of the volcanic ash cloud from the Eyjafjallajökull on the Iberian Peninsula. The analysis performed is presented in **Chapter 7**.

To complement the above analysis, **Chapter 8** presents the results of studies of inorganic ion mass size distributions in the city of Madrid contrasted with those obtained in a campaign in Barcelona.

Finally, **Chapter 9** summarizes the main results achieved in this thesis, exposing the open questions and the possibilities for continuing this research in the future.

CONCLUSIONS AND MAIN CONTRIBUTIONS OF THIS THESIS

First we have summarised the available information on concentrations of precursor gases (NO_2, NOx, SO_2 and NH_3), particulate matter and SIC at representative locations -urban, urban background and rural- of the Madrid air basin in the last decade. In general, concentrations were highest at the urban site and lowest at the rural, showing intermediate values at the urban background site. Different seasonal patterns have been found depending on the pollutant and sampling site.

PM and gases showed descending trends in the last decade except for gaseous NH_3, which kept constant annual values at the rural site. The falls in NOx and PM can be due to various measures to reduce emisions, such as the incorporation of catalytic converters in vehicles. These converters have been proved to lead to outstanding reductions in NOx emissions, but also to generate gaseous ammonia.Drops in SO_2 and particulate sulphate are due to the limitations of S in fuels. The urban site studied in Madrid (Escuelas Aguirre) showed a 40% reduction in SO_2 levels from winter 2008-2009 to winter 2009-2010. On 1 January 2009 the European Directive 2003/17/EC limited sulphur in all vehicle fuels to a maximum of 10 $mg \cdot kg^{-1}$.

- The results are compatible with prevailing nitrate local generation at the urban area of Madrid with seasonal cycles dominated by thermal decomposition.
- Local sources contributed significantly to sulphate levels in winter at the urban site studied; however, the rural background in the air basin is dominated by enhanced photochemical oxidation of SO_2 at summer.

The scarcity of measurements of gaseous NH_3 in comparison with other inorganic pollutants led to a characterisation of ammonia ambient levels and sources in the

Madrid atmosphere in 2011. 10-day integrated measurements were obtained in winter and summer using passive samplers.

- Sites close to sewage treatment plants and an incinerator registered the highest ammonia concentrations, followed by traffic sites. The latter showed significantly higher values than the urban background sites in both seasons.
- In Madrid, average ammonia levels were similar to measurements in other European cities and remarkably lower than the levels found in Barcelona on the same year.

An analysis of temporal mean patterns of sulphate, nitrate and precursor gases on annual, weekly and daily timescales has been performed for urban background and rural sites in the Madrid airshed and the London region in the period 2005-2010. This study identifyied similarities and discrepancies that contribute to determine the main processes and relevant parameters in each case.

- The seasonal fine nitrate pattern in Madrid was found to be dominated by temperature-driven evolution. In contrast, the annual nitrate pattern in London showed thermal decomposition in summer, but also a notable maximum from February to April which can be related to pollutant transport from mainland Europe.
- In both cities fine nitrate weekend reductions around 20% were found in summer with statistical significance. In contrast, weekend sulphate reductions in the range 13-18 % were found at both urban background sites in winter.

The daily pattern followed by NOx is similar in both cities; however, nitrate behaviour was very different in winter. In Madrid, low temperatures and the small vertical extent of the mixing layer allowed the dominance of photochemistry in nitrate formation, resulting in a single maximum at noon. High concentrations were registered in an urban background site in London at night-time, explained as a consequence of nitrate formation under high humidity conditions. In summer, higher temperatures and a greater mixing height resulted in a dominant morning peak associated to the traffic rush hour plus a secondary evening peak. The evening peak has been explained in terms of the contraction of the mixing layer by other researchers, which is consistent with our results.

- The results from both cities indicate that nitrate hourly evolution is predominantly determined by meteorological factors rather than by the evolution of precursor gases.

- In Madrid in winter SO_2 and SO_4^{2-} peaked at noon. The same phenomenon had been observed in London for SO_2.

The data analyses for London complement the process-based work carried out in the REPARTEE experiments. This work shows that behaviour seen in London is not representative of that in Madrid.

- The processes controlling nitrate and sulphate concentrations may vary substantially across Europe. Observations in one city should not be assumed to be applicable elsewhere.

Three types of events which led to high concentrations of particulate sulphate and nitrate at the urban area of Madrid have been characterised. These events are: a regional recirculation episode (E1), transport from Central Europe-Western Mediterranean (E2a –sulphate- and E2b –nitrate and sulphate-) and local accumulation in a winter stagnant anticyclonic situation (E3). These episodes were differentiated using HYSPLIT back-trajectory analysis, data from rural stations and FLEXTRA and NAAPS model results, and daily evolution of pollutants at the CIEMAT site. Since the importance of local emissions has been stated, regional and long range transport has also been found to be relevant for particulate sulphate ambient concentrations at a suburban site at Madrid.

- The highest $PM_{2.5}$ nitrate values (over 20 $\mu g \cdot m^{-3}$) were associated to the local accumulation situation E3, while the maximum concentrations reached under transport episodes E1 and E2b were less than half of that value.

- The highest short-term PM_1 sulphate values registered at the site (7 $\mu g \cdot m^{-3}$) were associated to the pollutant long-range transport E2a. Sulphate concentrations reached 5 and only 3.5 $\mu g \cdot m^{-3}$ during E1 and E3 respectively.

An unusual volcanic event which took place during the course of the measurements carried out at CIEMAT has been also characterised in detail. The eruption of the Icelandic volcano Eyjafjallajökull disrupted the air traffic in Europe during spring 2010.

The passage of the volcanic plume was identified in the EMEP network stations. The concentrations of sulphur dioxide and sulphate in PM_{10} and $PM_{2.5}$ reached relative maxima not correlated with other pollutants. The first effects appeared on 4 and 5 May, but they intensified between 7 and 9 May at the centre and south of the Peninsula. Physico-chemical characteristics of the aerosol that reached the CIEMAT site have been presented.

- An estimation of the vertical profiles of mass concentration was calculated from the extinction coefficient profiles, obtaining a maximum value (77±9.6 $\mu g \cdot m^{-3}$) well below the threshold established for safe aircraft operation.
- A large increase in the fine aerosol mode was detected in coincidence with an increase in sulphate concentration, while the coarse mode remained almost unaltered. Volume distributions at ground level indicate particles mainly in the 0.1-0.7 μm size range, in contrast with studies of the plume that affected Central Europe in April, where coarse particles were present.
- Results are consistent with the bimodal size distribution obtained near-source and suggest the growth of the fine mode through condensation and/or coagulation processes and also the removal of the larger ash particles.

Mass size segregated ions in the range 18 μm down to <0.056 μm have been studied in winter at a suburban site in Barcelona and compared with a previous study in Madrid. The ion concentrations measured in winter in Madrid were around half of the concentrations measured in Barcelona.

- In Barcelona, accumulation modes around 0.5 μm for sulphate and ammonia and 0.6-0.75 μm were found for nitrate. In Madrid the accumulation modal diameter was around 0.35 μm for all three ions. This is consistent with the presence of a droplet mode in Barcelona due to higher ambient relative humidity. In Madrid the accumulation range only showed the vapour condensation mode.
- Ion size distributions were dominated by the accumulation mode in the case of sulphate and ammonia, and by the coarse one (3.5-5.5 μm) in the case of nitrate in Madrid and also in Barcelona at night. This result shows the relevance of the reaction between nitric acid and mineral elements, especially $CaCO_3$, producing $Ca(NO_3)_2$.
- Balances show fully neutralised acidity except for the particles <0.056 μm.

In Madrid the sulphate concentration in the stage below 0.056 μm was the highest. In Barcelona non-neutralised sulphate and nitrate concentration were also found in the same stage, although concentrations were much smaller. To get a deeper insight into this problem size segregated secondary inorganic aerosol compounds were studied in Madrid during three different meteorological winter scenarios in the range 18 μm down to <0.010 μm: heavy fog (S1), typical winter stagnation (S2, which coincides with E3) and transition from a clean period to fog (S3).

- The highest sulphate and nitrate concentrations were found for S1 in the range 1-1.8 μm (droplet mode). This interval is significantly higher than the range found for S2 (sulphate 0.18-0.56 μm, nitrate 0.32-0.56 μm).
- A significant fraction of nitrate and sulphate below 0.01 μm was found only for S2.

The results suggest the aqueous phase generation in the droplet mode, but a shift of nanometric compounds to the accumulation mode through aggregation and coagulation processes in high ambient humidity scenarios is also possible. These processes can also explain the lower amount of sulphate and nitrate found below 0.056 μm in Barcelona.

Semi-continuous measurements confirmed the efficiency of aqueous-phase SIC generation over photochemical and transport processes which take place during the typical winter stagnation scenarios. Deviations were found in the mass ratios of nitrate and sulphate for S1, S2 and S3 measured with both techniques. This is probably related to variations in the detection efficiency of the various types of aerosol.

FUTURE RESEARCH AND OPEN QUESTIONS

This thesis has involved a deep study of the behaviour of secondary inorganic aerosol compounds in the region of Madrid. The semi-continuous techniques have allowed the study of features which were concealed in previous works. However, there are still unresolved problems.

In the Madrid air basin the measurements of some gaseous precursors (NOx and SO_2) are abundant, but existing information on ammonia is insufficient,

especially in the urban area of Madrid. The campaign carried out made a first step in this direction, but further studies covering larger time periods are needed. Semi-continuous measurements of this compound would allow a better characterization of the traffic source, since it would enable the analysis of correlations with primary pollutants emitted by vehicles.

The interpretation of the diurnal evolution of secondary compounds has proven to be complex. In literature, morning and evening peaks in urban areas are related to the traffic rush hours and changes in the height of the boundary layer. In contrast, the occurrence of maxima at noon-afternoon has been explained in different ways in several sites in the US. In the case of nitrate, Park et al (2005) and Rattigan et al (2006) interpreted that they were driven by local photochemical production and Wittig et al (2004) explained the same for sulphate. In contrast, Chow et al (2008) attributed them to a combination of local photochemical production in urban areas and nighttime transport followed by daytime vertical mixing. Recently, Doraiswamy et al (2010) found discrepancies between model forecasts and near real-time fine nitrate and sulphate. Underpredictions of sulphate concentrations at urban sites at noon were attributed to the underprediction of secondary formation due to sensitiveness to cloud properties, which influence water-phase production. In the case of Madrid, the evolution patterns found can be explained in terms of photochemical formation but taking into account the diurnal transport pattern prevailing in the air basin. The comparison of hourly evolution of precursors together with secondary compounds in two different cities highlighted the difficulties of this study.

Semi-continuous measurements allowed differentiating local events from transport events, since only in the former case a clear daily pattern is seen. Quantification of the amount of nitrate and sulphate which is attributable to each type of episode remains open, and especially to long-range transport of fine nitrate. The results shown indicate that the airborne nitrate contribution is less relevant than for sulphate, but noticeable.

This work has provided advances in the study of the nanometric fraction of inorganic aerosols present in the urban atmosphere of Madrid. Different mass contributions of every ion to each size fraction in the nanometric range has been found when dry and hydrated aerosols are present. To obtain conclusive results further research is needed, determining the response of the technique employed (cascade impactors) to different types of aerosol.

1-INTRODUCTION: ATMOSPHERIC AEROSOLS

1-INTRODUCTION: ATMOSPHERIC AEROSOLS

In the last decades, technical and industrial development has allowed humankind of a great part of the world to achieve a well-being high above previous generations. However, at the same time and as a consequence, the environment is suffering a degradation that we cannot ignore. This fact is leading to the development of many scientific disciplines with the objective of providing a better understanding of the complex interactions that govern the Earth's system, including the atmosphere, hydrosphere, biosphere and lithosphere. Anthropogenic perturbations in any of these "spheres" may impact the other ones and result in alterations of life on Earth, including the human beings ourselves. Aerosol science is one of the fundamental disciplines that contribute to understanding our environment.

Although there is not an unique definition, atmospheric pollution can be considered as any phenomenon produced in the air by which artificial or natural chemical elements or compounds reach concentrations high enough over their natural ambient levels to produce measurable effects on living beings or the environment.

Atmospheric pollutants are classified following different criteria. According to their physical state we can distinguish:

-Gases

-Liquid particles

-Solid particles

Heterogeneous particles formed by a mixture of solid and liquid phases are also formed.

The mixture of particles suspended in a gas is called "aerosol". Nevertheless, the term is frequently extended to the particles themselves, which are also referred as "Particulate Matter (PM)".

1.1-Fundamental properties and processes in aerosol science

1.1.1-Origin and sources

The generation of aerosols can be natural or anthropogenic, that is to say, due to the human activity. Natural sources that contribute with the highest loadings to the atmosphere include volcanoes, dust storms, sea-spray and forest and pasture fires. Although pulverization of seawater settle on the sea close to the emission area, it is also present in continental areas. Human activities also generate aerosols. The main anthropogenic aerosol sources are fuel burning in vehicle motors, industry and power stations. The dust generated in construction works and alteration of the Earth's surface (i.e. sandy zones where water or vegetation has been removed) must be also considered. The Intergovernmental Panel on Climate Change (IPCC), jointly established by the World Meteorological Organization (WMO) and the United Nations Environment Programme (UNEP) in 1988, estimated that, in global terms, artificial aerosols generated by human activities account roughly for 10% of the total aerosol mass load in the atmosphere (IPCC, 2001).

Particles directly emitted to the atmosphere are denominated primary aerosols, while those formed as the final product of physical and chemical processes occurred into the atmosphere are denominated secondary aerosols.

The chemical composition of an aerosol particle depends on its generation source as well as the physical and chemical transformation processes later undergone, being source/origin and chemical and physical properties closely linked.

Attending to source and physico-chemical properties, aerosols can be classified as follows:

-Marine aerosol-

Marine aerosol is the first type of particle in importance relative to the total emission load in a global scale, with more than 3000 million tonnes·year^{-1} (see Table 1.1). Marine PM is natural and mainly primary, although condensable vapours drive to secondary marine aerosol formation. Recent advances have identified specific chemical

compounds (iodine oxides and isoprene oxidation products, in addition to sulphuric acid), as contributing to formation and growth of secondary marine aerosol, although the exact roles remains to be determined (O'Dowd and de Leeuw, 2007).

Chemical composition of marine aerosol derives from that of seawater. The principal compound is sodium chloride NaCl, though other salts such as MgCl, $MgSO_4$ and Na_2SO_4 are also present.

	Northern Hemisphere	Southern Hemisphere	Global	Low	High
Carbonaceous aerosols					
Organic Matter (0–2 µm)					
Biomass burning	28	26	54	45	80
Fossil fuel	28	0.4	28	10	30
Biogenic (>1µm)	—	—	56	0	90
Black Carbon (0–2 µm)					
Biomass burning	2.9	2.7	5.7	5	9
Fossil fuel	6.5	0.1	6.6	6	8
Aircraft	0.005	0.0004	0.006		
Industrial Dust, etc. (> 1 µm)			100	40	130
Sea Salt					
d< 1 µm	23	31	54	18	100
d=1–16µm	1,420	1,870	3,290	1,000	6,000
Total	1,440	1,900	3,340	1,000	6,000
Mineral (Soil) Dust					
d< 1 µm	90	17	110	—	—
d=1–2µm	240	50	290	—	—
d=2–20µm	1,470	282	1,750	—	—
Total	1,800	349	2,150	1,000	3,000

Table 1.1. Primary particle emissions for the year 2000 ($Tg \cdot yr^{-1}$). From IPCC(2001)

-Mineral aerosol-

This group includes aerosol originated by suspension in the air of soil minerals by effect of the erosion of the Earth's crust. They are formed mainly by oxides (SiO_2, Al_2O_3, FeO, Fe_2O_3, CaO, etc) and carbonates ($CaCO_3$, $MgCO_3$).

Emissions of mineral dust in a global scale are estimated in more than 2000 million tons a year (Table 1.1), being a majority fraction attributed to deserts. In southern Europe, the principal contributor to mineral dust is the Sahara desert (see Figure 1.1) (Stuut et al, 2009).

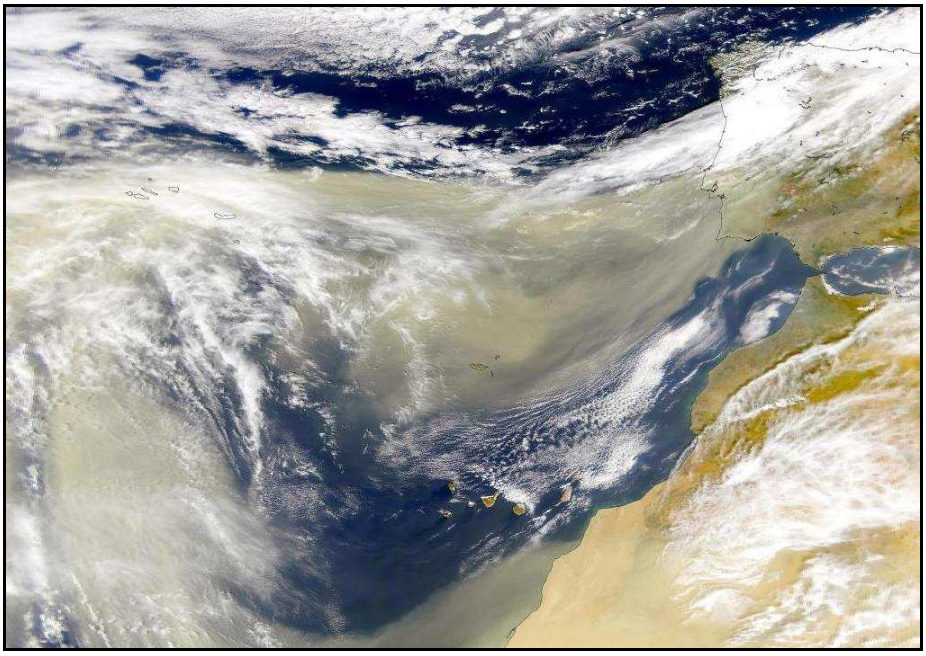

Figure 1.1. Saharan dust storm 28/02/2000 (SeaWiFS, NASA/Goddard Space Flight Center)

Although this type of aerosol is generally considered of natural origin, a fraction of the total mineral load in the atmosphere can be attributed to human activities. Indirectly, through desertification or inadequately land usage and directly, through activities such as construction, mining and ceramics and cement manufacture. Tegen et al. (2004) provided an estimate by comparing observations of visibility, as a proxy for dust events, from over 2000 surface stations with model results, and suggested that 5 to 7% of mineral dust comes from anthropogenic agricultural sources. Public construction/demolition works and road traffic can also constitute a significant source of mineral particles in urban areas through road surface erosion (Querol et al, 2001) as well as fugitive emissions from specific types of industrial activity (cement, ceramic) in industrial ones.

-Volcanic aerosol-

Volcanoes are very strong sources of sulphur, acids and other gases, as well as particles. There are several types of volcanic eruptions (explosive, phreatomagmatic, pyroclastic, etc) which lead to different kinds of fragmentation processes that generate airborne particles. Tephra is defined as any fragmental material produced by a volcanic

eruption regardless of composition and fragment size. Tephra can be generated in a size range from mm to the so-called fine ash, smaller than 63 μm. (Langmann et al, 2011). Estimated dust fluxes of primary volcanic ashes can vary from 4 to 10000 million tons per year (IPCC, 2001).

Both sulphur dioxide (SO_2) and sulphate (SO_4^{2-}) have been found in volcanic plumes. Volcanogenic sulphate can be either primarily emitted or result from the oxidation of gaseous SO_2. In the last case the aerosol falls in the submicrometric size range.

Residence time of volcanic aerosols in air has been estimated between 2-10 days depending on altitude and size. The extended lifetime of their emissions is due to their high altitude and latitude location (Mather et al, 2004).

-Carbonaceous aerosol-

Carbonaceous aerosol (excluding carbonates) can be divided in two fractions, elemental carbon EC and organic carbon OC.

EC is the elemental carbonaceous material that does not oxidise below a temperature threshold of 350°C (Cachier et al, 1989). EC is closely related to graphitic carbon and black carbon BC, although the three of them are defined according to different physico-chemical properties. While EC is defined in terms of chemical reactivity, graphitic carbon is defined in terms of molecular structure and BC refers to light absorption. EC is emitted to the atmosphere in incomplete combustion processes such as fuel burn or forest fires. OC includes a wide variety of species both anthropogenic and natural, including aerosol generated by living organisms (biogenic aerosol) (Park, R. et al, 2003). OC can be primary (mostly biogenic aerosol which will be commented following) or secondary organic carbon (SOC), which is formed through the condensation of volatile organic compounds (VOC), which also have both anthropogenic and natural sources (Kanakidou et al, 2005; Liao et al, 2007).

The main sources of anthropogenic carbonaceous primary PM are power generation, industry and traffic. Regarding the secondary, gasoline evaporation and vehicle emissions are the major source in the urban atmosphere. Likewise, the manufacture and handling of paints and solvents also contribute to the OC levels (Jacobson et al,

2000), as well as biogenic VOC's (BVOC's) emitted by several vegetation species. The source apportionment of organic components is a matter under discussion due to the large number of compounds that form atmospheric aerosol and the complexity of its experimental detection and data analysis (Ulbrich et al, 2009).

Global emissions of carbonaceous compounds are below 200 million tonnes·year^{-1}, very far from the marine and mineral loading. Nevertheless, it represents as much as 20-40% of the mass of particulate matter collected in urban stations in Europe (Putaud et al, 2010).

-Biogenic aerosol-

Biogenic aerosols are organic particles emitted from plants and animals by disintegration processes, and the dispersion of microorganisms. Living biogenic aerosols include bacteria, virus, pollen and spores, and non-living microorganisms and detritus. Primary and secondary biogenic aerosols comprise a wide range of aerosols with very different chemical and physical properties.

Estimations of global emission fluxes of emitted biogenic aerosols are in the order of 50 million tonnes·year^{-1} (Penner, 1995; Table 1.1), which are low in comparison with marine and mineral aerosols. Nevertheless, recent studies point to the possibility of these aerosols as an important primary source with emissions of at least 1000 million tonnes·year^{-1} (Jaecnike, 2005), which would mean that around 20% of the total primary emitted aerosols would be of biogenic origin.

-Secondary Inorganic Aerosol (SIA)-

The principal secondary inorganic compounds (SIC) in the atmosphere are sulphur and nitrogen by-products, followed by chloride by-products. It is considered that the secondary inorganic compound most often found in the atmospheric aerosol is sulphuric acid (H_2SO_4) alone or combined forming ammonium sulphate ($(NH_4)_2SO_4$) and ammonium bisulphate (NH_4HSO_4) or letovicite ($(NH_4)_3H(SO_4)_2$), and ammonium nitrate (NH_4NO_3) (Harrison and Pío 1967, 1983; Harrison and Jones, 1995).

Sulphates (SO_4^{2-}) present in the atmosphere are generally secondary particles formed as a result of oxidation of primary SO_2. The main source of sulphate aerosol is via SO_2 emissions from fossil fuel burning (about 72%), with a small contribution from biomass burning (about 2%), while natural sources are from dimethyl sulphide emissions by marine phytoplankton (about 19%) and by SO_2 emissions from volcanoes (about 7%) (IPCC, 2007). In 2001 the IPCC estimated total sulphate formed from precursors in 200 millions of tonnes·year^{-1} (Table 1.2)

Sulphates in the atmosphere are of special relevance due to their acid character related to the presence of H_2SO_4 and NH_4HSO_4, which triggers the well known "acid rain".

Nitrogen compounds (mainly nitrate NO_3^- and ammonium NH_4^+), are originated from the reactions of anthropogenic gaseous precursors. Feng and Penner (2007) estimated a large global, nitrate burden of 0.58 mg NO_3^- m^{-2}, which would imply an equivalent of 20% of the mean anthropogenic sulphate burden. In 2001 the IPCC estimated total nitrate formed from precursors in 18 millions of tonnes·year^{-1}.

	Northern Hemisphere	Southern Hemisphere	Global	Low	High
Sulphate (as NH_4HSO_4)	145	55	200	107	374
Anthropogenic	106	15	122	69	214
Biogenic	25	32	57	28	118
Volcanic	14	7	21	9	48
Nitrate (as NO_3^-)[b]					
Anthropogenic	12.4	1.8	14.2	9.6	19.2
Natural	2.2	1.7	3.9	1.9	7.6
Organic compounds					
Anthropogenic	0.15	0.45	0.6	0.3	1.8
VOC					
Biogenic VOC	8.2	7.4	16	8	40

Table 1.2. Estimates for secondary aerosol sources in millions of tonnes··year^{-1}. Calculated from precursor emissions using models (a) ECHAM/GRANTOUR and (b) UCI. From IPCC (2001)

Secondary sulphate and nitrate are the main topic of this thesis, and they will be further described in section 1.2.

1.1.2 - Size and chemical composition of atmospheric aerosols

The size of particles spans a range from a few nanometers to more than 200 μm in diameter, that is to say, from a few molecules to the maximum size that allows the particle to be suspended for at least a few hours before its deposition. In general, the smallest and lightest the particle, the longest its residence time in the atmosphere. Nevertheless, the very smallest are lost due to their higher diffusion which leads to impaction on larger particles (Tandon and Rosner, 1999).

-Size distributions-

Analysing over 1000 particle size distributions measured at various locations in the US, Whitby observed that the distribution typically had three peaks which he called "modes" (Whitby, 1978). The entire size distribution could be usually well characterised by a trimodal model consisting on three additive log-normal distributions (Figure 1.2). This model can be applied in most of aerosol studies.

Probability density function for the **lognormal distribution:**

$$f_X(x;\mu,\sigma) = \frac{1}{x\sigma\sqrt{2\pi}} e^{-\frac{(\ln x-\mu)^2}{2\sigma^2}} \quad , \ \mathbf{x > 0}$$

Where:
x=independent variable
μ=ln of the geometric mean of the distribution
σ=ln of the geometric standard deviation of the distribution

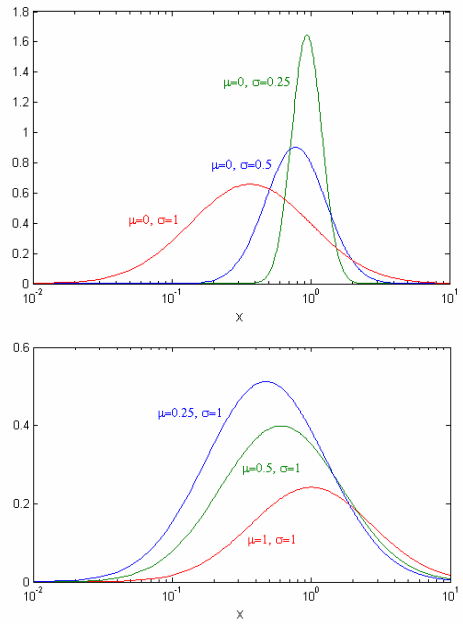

Figure 1.2. Lognormal distributions

The mode with a peak between 5 and 30 μm in diameter formed by mechanical processes is called the **coarse mode**, the mode with a peak between 0.15 and 0.5 μm formed by condensation and coagulation processes is called the **accumulation mode**

and the mode with a peak between 0.015 and 0.04 μm whose size was influenced by nucleation as well as by condensation and coagulation is called the **nuclei or nucleation mode**. The ultrafine region defined by the nuclei mode is in turn split in the nucleation region (< 10 nm) and the Aitken region (10 – 100 nm). The sum of the accumulation and nuclei mode is called the **fine aerosol**.

Size distributions are calculated in particle number, area, or volume, each one emphasizing the nuclei, accumulation or coarse mode respectively. Similarly to volume distributions, mass distributions emphasize the coarse mode. Figure 1.3 shows an idealised volume size distribution showing modes and the major formation and growth mechanisms of the four modes of atmospheric particles (EPA, 2004). Note that the nucleation mode can grow to the accumulation mode, but the accumulation mode does not grow to the coarse mode. The dynamics of fine particle growth ordinarily prevents the fine particles from growing larger than 1 to 3 μm. Thus, *the fine and coarse mode originates separately and evolves differently in the atmosphere*.

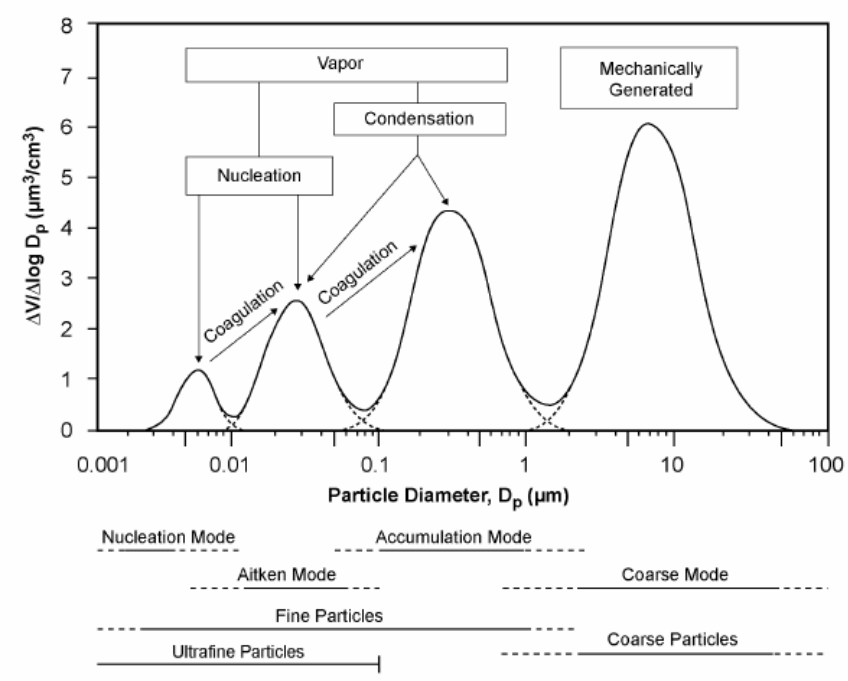

Figure 1.3. Idealised volume size-distribution. From US EPA (2004)

-Particle diameter-

The diameter of a spherical particle may be determined attending to different physical properties: optical, light scattering and Mie theory, electrical mobility or aerodynamic behaviour. However, atmospheric particles are not spherical. Therefore, their diameters are described by an "equivalent" diameter (i.e., the diameter of a sphere that would have the same physical behaviour).

The **Stokes diameter Dp** is defined as the diameter of a sphere having the same terminal settling velocity and density as the particle (Seinfeld and Pandis, 2006). Therefore, the Stokes diameter is defined for a uniform particle motion, where the external force applied on the particle and thus the drag force are independent of the particle density. For a smooth, spherically shaped particle Dp equals the physical diameter. For irregularly shaped particles, Dp is the diameter of an equivalent sphere that would have the same aerodynamic resistance.

Electrical mobility analysers classify particles according to their electrical mobility. The electrical mobility diameter can be considered the diameter of a spherical particle that would have the same electrical mobility as the irregular particle. The particle mobility can be related to the particle diffusion coefficient and Brownian diffusion velocity through the Stokes-Einstein equation. Thus, the Stokes diameter is the appropriate parameter for particle behaviour governed by diffusion. The optical particle diameter is based on the particle scattering when the particle is illuminated. Optical sampling devices are calibrated using spherical particles with known Dp and known refractive index. Therefore, Dp is used in size distributions based on light scattering and mobility analysis and is independent on density.

The **aerodynamic diameter Da** is defined as the diameter of a spherical particle of material density of 1 g cm^{-3} with an equal gravitational settling velocity. Da is used when the drag force depends on the particle density. For particles greater of 0.5 μm Da is the quantity of interest. For smaller particles, Dp can be more useful. Sampling devices based on Da include cascade impactors and high volume samplers (HVS).

-Regulatory size cuts-

The regulatory size cuts x for sampling devices are chosen according to a criterion related to aerosol effects on human health. This criterion is the penetration depth into the respiratory system and classifies particles in size fractions as follows:

- The **inhalable** fraction corresponds with those particles that can be inhaled by the nose and/or mouth and reach the respiratory tract. It accounts for a major fraction of the total aerosol.
- The **thoracic** fraction corresponds with those inhaled particles that reach the tracheo-bronchial region. As a function of total airborne particles, it is given by a cumulative lognormal curve with a median aerodynamic diameter of **10 μm** and a geometric standard deviation of 1.5
- **Respirable** particles penetrate to the gas-exchange regions of the lungs (alveolar region). This fraction is given by a cumulative lognormal curve with a median aerodynamic diameter of **4 μm** and a geometric standard deviation of 1.5
- **High risk respirable** particles are associated to high risk of infirmity or sickness. The median aerodynamic diameter is **2.5 μm** and the standard deviation 1.5.

The notation $\mathbf{PM_x}$ defines those particles collected by a sampler with a specified penetration curve yielding an upper 50% cut-point of x-μm aerodynamic diameter (EPA, 2004). Figure 1.4 shows the collection efficiency of a given sampler at different flow rates and its comparison with ideal convention curves.

Thus, respirable, thoracic, and inhalable sampling and PM_x sampling are based on particle aerodynamic diameter.

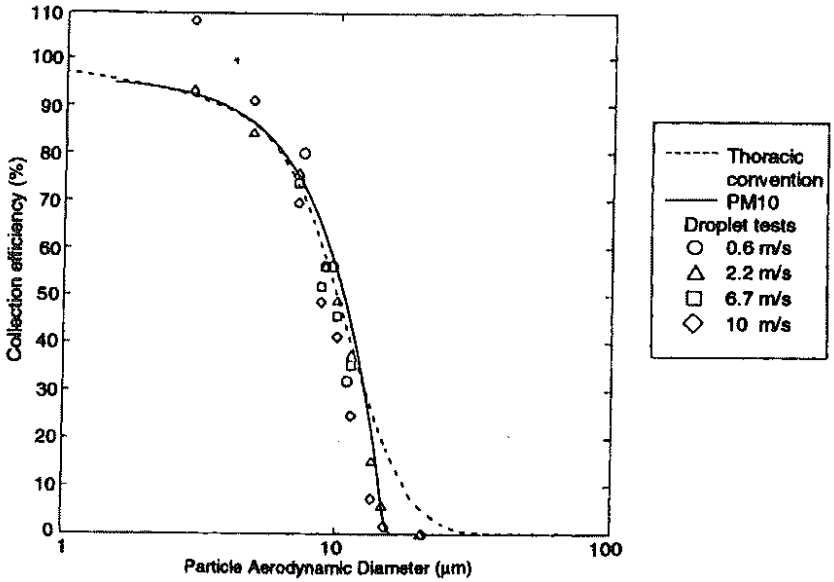

Figure 1.4. Collection efficiency at different flow rates for a Graseby-Andersen sampler. Comparison with ideal PM_{10} and Thoracic convention curves. From Harrison and Van Grieken (1998)

The size range between 1 and 3 μm may contain either accumulation mode or coarse mode material, or a mixture of both. A significant amount of either accumulation or coarse mode material can be found in the intermodal region 1-3 μm. The amount of material is larger under high relative humidity conditions due to heterogeneous aerosol production and water absorption. A $PM_{2.5}$ sample will contain the entire accumulation mode. However, $PM_{2.5}$ may also contain a small fraction of coarse PM. A cut point of 1 μm reduces the misclassification of coarse-mode material as fine. Due to this reason, PM_{10}-$PM_{2.5}$-PM_1 are nowadays widely employed in the classification of particulate matter and will be the fundamental size fractions considered in this work.

1.1.3-Effects of aerosols

Aerosols are constituents of the biosphere and interact with other elements present in the environment in many different ways. These interactions lead to effects that are studied by several disciplines as varied as occupational health, climate change and material sciences.

-Radiative effects and climate-

Aerosol radiative properties make them play a fundamental part in the Earth's climate since they interact with solar radiation as well as with infrared radiation emitted by the Earth's system. This interaction is called the **direct aerosol forcing of climate**. Changes in the composition of the aerosol layer would lead to changes in the Earth's climate.

The radiative properties of the aerosols depend on their size, morphology, chemical composition and mixing state. It is known that sulphates and mineral matter reflect solar radiation, producing a negative radiative forcing and contributing to the cooling of the system. On the other hand, elemental carbon absorbs infrared radiation, so it produces a positive forcing. Processes are complex and highly non-linear, and the result is that, locally, aerosols can both contribute to the cooling or warming of the Earth's surface. The global radiative effect of aerosols is not easy to be determined and still has not been reliably quantified. Information available indicates that the net effect of aerosols would lead to the cooling of the Earth's surface (IPCC, 2007).

Aerosol particles act as nuclei for cloud, ice and fog formation. Cloud (and fog) droplets scatter and absorb also solar radiation depending on the size and amount of incorporated absorbing material, respectively. These effects are called **indirect aerosol forcing of climate**. The number and size of cloud droplets strongly depends on the number size distribution of the aerosol greater than 100 nm and on the dynamics of the atmosphere (Dusek et al, 2006). In case the amount of condensable water is equal, a higher number of cloud condensation nuclei (CCN) may lead to more and smaller cloud droplets. This means that a change in size distribution and/or chemical composition of the aerosol may lead to a change in the cloud microphysics and optical properties. If these effects are caused by anthropogenic aerosols, then the indirect effects contribute to climate change.

-Hygroscopicity and cloud formation-

The presence of aerosols is necessary to allow water vapour condensation in the atmosphere to form cloud droplets. The efficiency of a certain particle to act as a CCN depends on its size and composition. There exist hydrophobic particles which do not

activate cloud formation (IPCC, 2007). Those who are or have a hygroscopic part (i.e., they form aqueous solutions at any relative humidity and maintain a solution vapour pressure over the entire range of relative humidity) activate cloud formation. Sulphates, marine aerosol and other water-soluble salts are common CCNs (Hudson & Da, 1996). Some organic compounds may also contribute to the hygroscopicity of the atmospheric aerosol. The equilibria involving organic compounds and water vapour, and, especially for mixtures of salts, organic compounds, and water, are not well understood. These equilibrium processes may cause an ambient particle to significantly increase its diameter at relative humidities above about 40%. A particle can grow to five times its dry diameter as the RH approaches 100%.

The interaction of particles with water vapour may be described briefly as follows. As relative humidity increases, particles of crystalline soluble salts, such as $(NH_4)_2SO_4$,

NH_4HSO_4, or NH_4NO_3, undergo a phase transition to become aqueous solution particles. For particles consisting of a single component, this phase transition is abrupt, taking place at a relative humidity that corresponds to the vapour pressure of water above the saturated solution (the deliquescence point). For particles consisting of more than one component, the solid to liquid transition will take place over a range of RHs. For particles of composition intermediate between NH_4HSO_4 and $(NH_4)_2SO_4$, this transition occurs in the range from 40% to below 10% relative humidity, indicating that for certain compositions the solution cannot be fully dried in the atmosphere. At low relative humidities, particles of this composition would likely be present in the atmosphere as supersaturated solution droplets (liquid particles) rather than as solid particles (Potukuchi and Wexler, 1995a and b; Cziczo et al 1997).

-Effects on visibility-

Visibility is defined as the degree to which the atmosphere is transparent to visible light and the clarity and colour fidelity of the atmosphere. Visual range is the farthest distance a black object can be distinguished against the horizontal sky. Visibility is measured by human observation, light scattering by particles, the light extinction-

coefficient, and parameters related to the light-extinction coefficient (visual range and deciview scale), and fine PM mass concentrations.

The air quality within a sight path will affect the illumination of the sight path by scattering or absorbing solar radiation before it reaches the Earth's surface. The rate of energy loss with distance from a beam of light is the light extinction coefficient. The light extinction coefficient is the sum of the coefficients for light absorption and scattering by gases and particles.

Visual range was developed for, and continues to be used as, an aid in military operations and to a lesser degree in transportation safety.

Visibility impairment is associated with airborne particle properties, including size distributions and aerosol chemical composition, and with relative humidity. With increasing relative humidity, the amount of moisture available for absorption by particles increases, causing the particles to increase in both size and volume. As the particles increase in size and volume, the light scattering potential of the particles generally also increases.

-Effects on vegetation and ecosystems-

The deposition of PM onto vegetation and soil, depending on its chemical composition (acid/base, trace metal, or nutrients, e.g., nitrates or sulphates), can produce direct or indirect responses within an ecosystem. The ecosystem response to pollutant deposition is a direct function of the level of sensitivity of the ecosystem and its ability to ameliorate resulting change. Changes in ecosystem structural patterns and the functioning of ecological processes must be scaled in both time and space and propagated to the more complex levels of community interaction to produce observable ecosystem changes.

The stressors of greatest environmental significance are particulate nitrates and sulphates whose indirect effects occur primarily via their deposition onto the soil (Gebauer et al, 1994; Bobbink et al, 1998). Upon entering the soil environment, they can

alter the ecological processes of energy flow and nutrient cycling, inhibit nutrient uptake, change ecosystem structure, and affect ecosystem biodiversity.

The effects on the growth of plants resulting from the deposition of nitrates and sulphates and the acidifying effect of the associated H+ ion in wet and dry deposition are the most important environmentally.

-Effects on materials-

Building materials (metals, stones, cements, and paints) undergo natural weathering processes from exposure to environmental elements (wind, moisture, temperature fluctuations, sunlight, etc.). Metals form a protective film of oxidised metal (rust) that slows environmentally induced corrosion. The natural process of metal corrosion from exposure to natural environmental elements is enhanced by exposure to anthropogenic pollutants, particularly gaseous SO_2 (Grabke et al, 1995).

A significant detrimental effect of particle pollution is the soiling of surfaces. Soiling changes the reflectance of opaque materials and reduces the transmission of light through transparent materials. Attempts have been made to quantify the pollutants exposure levels at which materials damage and soiling have been perceived (Pio et al, 1998). However, to date, insufficient data are available to advance our knowledge regarding perception thresholds with respect to pollutant concentration, aerosol particle size, and chemical composition.

-Health-

The effects of particulate matter on health have been widely studied on animals and also on human beings. From the 1980 and 1990 decades many epidemiological studies have investigated the relation between personal exposure to high concentrations of particulate matter and the increase in hospital admissions and deaths related to respiratory diseases (Pope and Schwarts, 1992; WHO, 2006; Miller et al, 2007).

Studies relate coarse particles to respiratory diseases while fine and ultrafine PM would also affect the cardiovascular system (Penttinen et al, 2001; Sioutas et al, 2005).

These effects include asthma, lung cancer, and premature death. As was exposed above, the size of the particle is key to determine the penetration in the body and thus the damage that the particle will cause (Venkataraman and Raymond, 1998), although aerosol chemical composition is also an important related variable that is being considered in present studies.

1.1.4-Aerosol removal processes

The lifetimes of particles vary with size. Nuclei-mode particles rapidly grow into the accumulation mode. However, the accumulation mode does not grow into the coarse mode. Accumulation-mode particles are kept suspended by normal air motions and have very low deposition rates to surfaces. They can be transported thousands of kilometres and remain in the atmosphere for a number of days. Coarse particles can settle rapidly from the atmosphere (within hours) and normally travel only short distances. However, when mixed high into the atmosphere, as in dust storms, the smaller-sized coarse-mode particles have longer lives and travel greater distances (Duce et al, 1980; Ansmann et al, 2003). Dry deposition rates are expressed in terms of a deposition velocity that varies with particle size. Accumulation-mode particles are removed from the atmosphere primarily by cloud processes. Fine particles, especially particles with a hygroscopic component, grow as the relative humidity increases, serve as cloud condensation nuclei, and grow into cloud droplets. If the cloud droplets grow large enough to form rain, the particles are removed in the rain. Falling rain drops impact coarse particles and remove them. Ultrafine or nuclei-mode particles are small enough to diffuse to the falling drop, be captured, and be removed by rain (Laakso et al, 2003).

Sulphate, nitrate, and some partially oxidised organic compounds are hygroscopic and act as nuclei for the formation of cloud droplets (Petters and Kreidenweis, 2007; Hameri et al, 2000). These droplets serve as chemical reactors in which (even slightly) soluble gases can dissolve and react (Donaldson, 1999; Kolb et al, 2010).

Sulphuric acid, ammonium nitrate, ammonium sulphates, and organic particles also are deposited on surfaces by dry deposition. The utilization of ammonium by plants leads to

the production of acidity. Therefore, dry deposition of particles can also contribute to the ecological impacts of acid deposition.

1.2- Secondary Inorganic Compounds

1.2.1- Concentrations and generation processes

The estimated global mass of sulphate and nitrate formed from precursors emitted per year is small compared to the annual loading of mineral and marine aerosol. Nevertheless, in urban air anthropogenic sources account for a relevant fraction of the aerosol and the chemical speciation differs greatly from the global average (see Figure 1.5).

Figure 1.5 shows a significant increase in fine nitrate in anthropogenic-influenced sites respect to those classified as representative of natural aerosol. On the other hand, both natural and anthropogenic sources contribute comparably to total sulphate atmospheric loading (Table 1.2). This results in similar or even higher percentage of sulphate in natural sites. Nevertheless, in urban sites we can expect a higher anthropogenic contribution to sulphate levels. Secondary inorganic compounds make a relevant fraction of urban particulate matter (Putaud et al, 2004). In Spain, studying 21 stations for the period 1999-2005, Querol et al (2008) found that the typical ranges of mean annual values for SIC made 28-36% of PM_{10} in rural backgroundg stations, 20-27% in urban backgroundg and 16-31% in traffic and industrial hotspots. These percentages rose to 33-34%, 20-33% and 19-38% respectively for $PM_{2.5}$. In that study SIC was defined as $SO_4^{2-}+NO_3^{-}+NH_4+$. In this thesis we will also define SIC in the same way, although the availability of NH_4+ measurements is smaller. Specifically, long term time series of sulphate and nitrate have been analysed, but ammonia time series are not available.

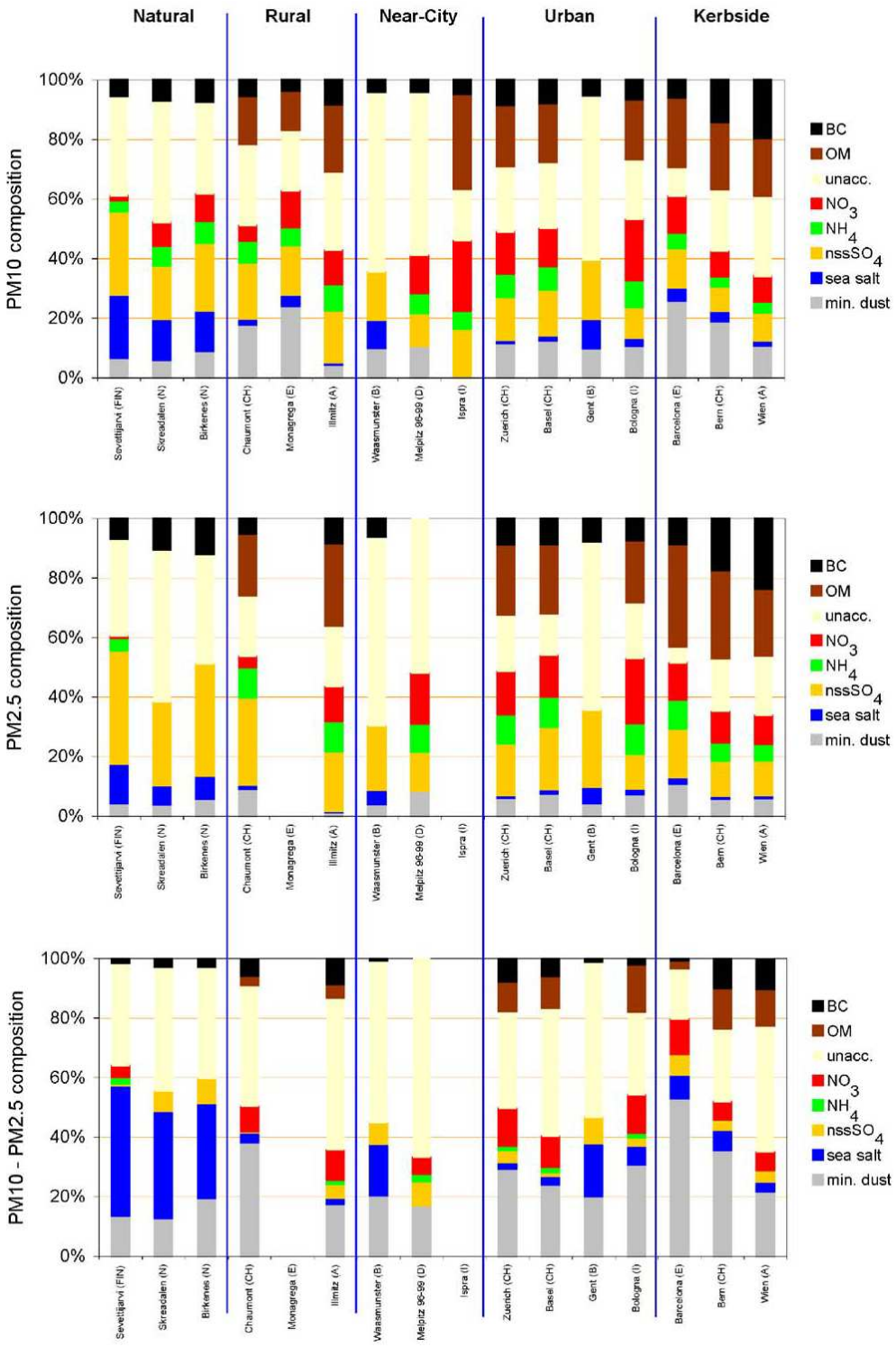

Figure 1.5. Annual average (%) of the main aerosol components in 16 European sites in (top) PM_{10}, (middle) $PM_{2.5}$ and (bottom) PM_{10}-$PM_{2.5}$. From Putaud et al (2004). Note: nssSO4 is non-sea-salt SO_4^{2-}

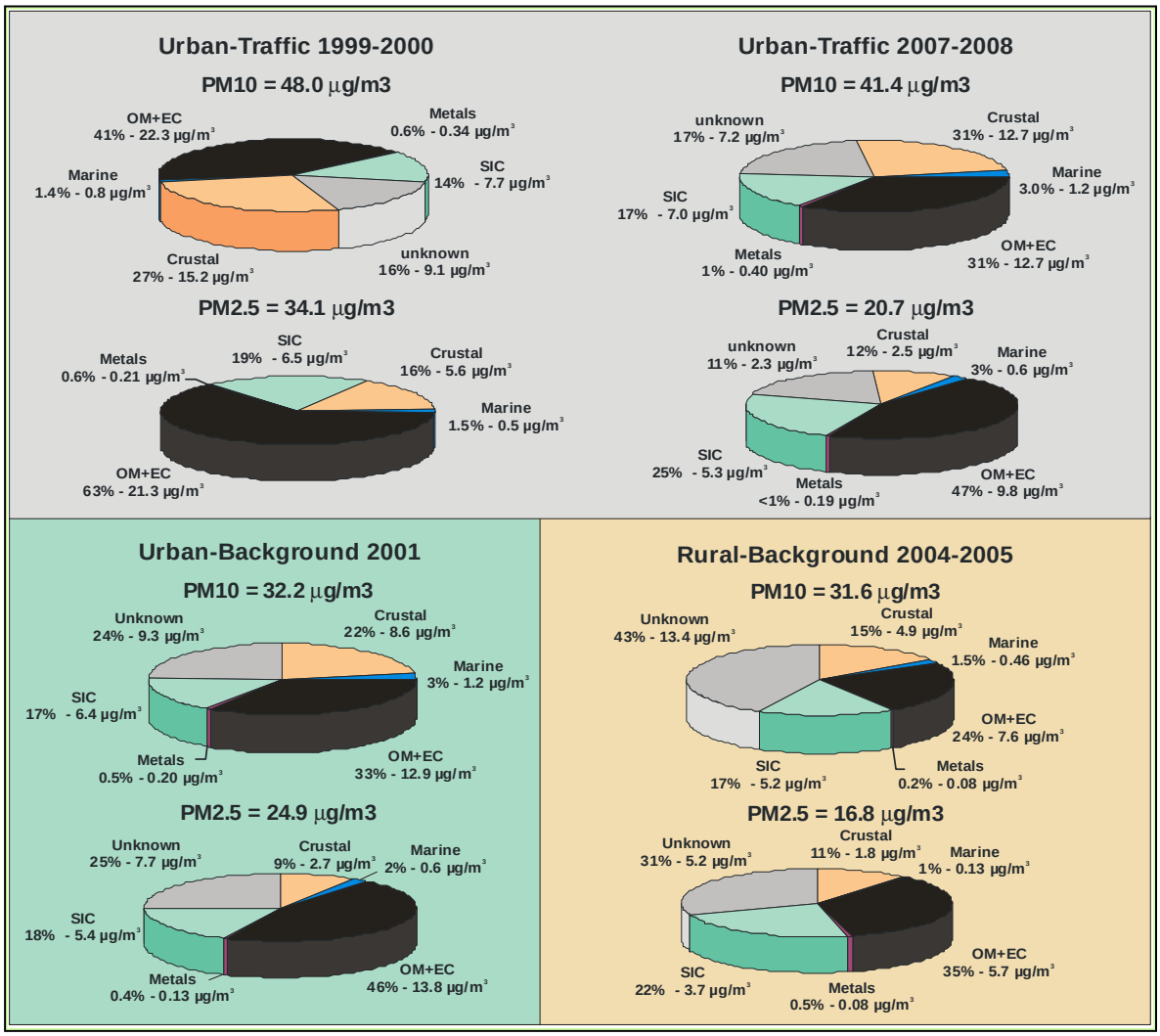

Figure 1.6. Mean contributions to PM_{10} and $PM_{2.5}$ of major constituents at rural, urban background and traffic at several sites of the Madrid air basin. From Querol et al (2009)

Figure 1.6 shows the mean contributions to PM_{10} and $PM_{2.5}$ of major constituents at rural, urban background and traffic sites of the Madrid air basin (Chapinería, Alcobendas and Escuelas Aguirre) obtained in different campaigns. SIC contribution to PM_{10} is in the range 14-25%, and 18-25% for $PM_{2.5}$.

-Sulphate-

A major proportion of urban sulphate arises from the oxidation of sulphur dioxide. Reaction mechanisms in the atmosphere fall into two groups, either homogeneous reactions in the gas phase, or heterogeneous processes in aerosol droplets involving

transfer of sulphur dioxide and oxidant species to the droplet phase with subsequent liquid phase oxidation.

The dominant homogeneous sulphate generation process is gaseous SO_2 oxidation by the hydroxyl radical (OH^-), formed by photochemistry. The hydroxyl radical is one of the main chemical species controlling the oxidizing capacity of the global Earth's atmosphere. This oxidizing reactive species has a major impact on the concentrations and distribution of pollutants in the troposphere.

The chemical reactions (cr) are the following:

$$\begin{aligned} &SO_2 + OH \rightarrow HSO_3 \\ &HSO_3 + O_2 \rightarrow SO_3 + HO_2 \qquad \text{(cr 1.1)} \\ &SO_3 + H_2O \rightarrow H_2SO_4 \end{aligned}$$

Sulphur dioxide is a highly water-soluble gas and hence in the presence of liquid water will tend to partition appreciably into the solution phase. In that case, the following heterogeneous chemical equilibria are established:

$$\begin{aligned} &SO_2(g) + H_2O(aq) \leftrightarrow SO_2 \cdot H_2O(aq) \\ &SO_2 \cdot H_2O(aq) \leftrightarrow HSO_3^-(aq) + H^+(aq) \qquad \text{(cr 1.2)} \\ &HSO_3^-(aq) \leftrightarrow SO_3^{2-}(aq) + H^+(aq) \end{aligned}$$

Neutralization of sulphuric acid in the urban atmosphere usually takes place through ammonia:

$$NH_3(g) + H_2SO_4(g) \rightarrow (NH_4)_2SO_4(s) \qquad \text{(cr 1.3)}$$

Primary emissions of urban sulphate arise from diesel fuels, whereas the gaseous precursor SO_2 is emitted in combustion processes from different facilities. Particulate sulphate is chemically stable, and this allows it to be transported over long distances. Its residence time in the atmosphere is estimated in more than 400 h by dry deposition and 80 hours by wet deposition (Rodhe, 1978). Sulphate is typically used as a tracer of regional background pollution levels.

-Nitrate-

Particulate nitrate is generated in the urban areas essentially from vehicle gaseous NO_2 emissions, being ozone O_3 and the OH radical involved through a photochemical cycle.

The main reactions considering nitric acid (HNO_3) generation are:

Daytime: $$NO_2(g) + OH(g) \rightarrow HNO_3(g) \qquad \text{(cr 1.4)}$$

Night-time:
$$\begin{aligned} & NO_2(g) + O_3(g) \rightarrow NO_3(g) + O_2(g) \\ & NO_3(g) + NO_2(g) \leftrightarrow N_2O_5(g) \\ & N_2O_5(g) + H_2O(aq) \rightarrow 2HNO_3(aq) \end{aligned} \qquad \text{(cr 1.5)}$$

During daytime, most of the nitric acid production is generated by 1.4 and is limited by the OH radical concentration. Reactions 1.5 occur only at night-time, because NO_3(g) is rapidly photolysed during the daytime (1.6). It reacts with NO fast enough so that NO and NO_3 cannot coexist at NO concentrations above a few parts per trillion (Wayne et al, 1991).

$$NO_3(g) + NO(g) \leftrightarrow 2NO_2(g) \qquad \text{(cr 1.6)}$$

As a consequence of 1.6, it is only possible to find the radical NO_3 during night-time and not at ground level in urban scenarios (Brown et al, 2003).

Night-time nitric acid generation occurs in hydrated aerosols rather than in the gas phase. The final product of the cycle cr 1.5 is gaseous nitric acid HNO_3, which can be transferred to the aerosol phase through two pathways:

(1) Neutralization by a base. This base is usually ammonia (NH_3):

$$HNO_3(g) + NH_3(g) \leftrightarrow NH_4NO_3(s) \qquad \text{(cr 1.7)}$$

Ammonia preferentially reacts with sulphate and only the remaining NH_3 can react with the nitric acid.

Both phases, solid and gaseous, are in thermodynamic equilibrium. This equilibrium displaces towards one or other phase depending on ambient temperature, favouring the

formation of the solid phase under high relative humidity conditions (Mozurkewich, 1993).

(2) Absorption of nitric acid by water droplets, producing acid aerosols. Nitric acid is one of the most water-soluble atmospheric gases and, after dissolution, it dissociates to nitrate increasing its solubility and the droplet acidity.

The mean tropospheric residence time for particulate nitrate has been estimated to be in the range of 3 to 9 days (72 to 214 hours) (Seinfeld and Pandis, 1998). Because of these relatively short atmospheric lifetimes, the major effects of emissions of nitrogen oxides are expected to be local or regional rather than global in nature.

-Ammonia-

Ammonia is, after N_2 and N_2O, the most abundant nitrogen-containing compound in the atmosphere (Seinfeld and Pandis, 2006) and also the principal alkaline gas responsible for the neutralisation of acid inorganic compounds in the atmosphere. Acidity produced by gaseous sulphuric and nitric acids is frequently neutralised by ammonia through the reactions 1.3 and 1.6, leading to the formation of inorganic salts. 1.3 prevails over 1.6, which means that only the free ammonia available after sulphuric acid neutralization would react to produce ammonium nitrate. Thus, both sulphuric acid and ammonia concentrations are related to the amount of ammonium nitrate that can be generated given a certain amount of nitric acid.

In 1997, Bouwman et al published a global high-resolution emission inventory for ammonia. The authors estimated the global emission for 1990 in about 54 Teragrams of Nitrogen per year (Tg N yr^{-1}). This value is four times the value estimated for NO for the same year (14.9 Tg N yr^{-1}) (Olivier et al, 1998). The total emission of NH_3 has more than doubled from 1860 to 1993 and there are estimations indicating that it may double again by 2050 (Krupa, 2003).

The major sources identified by Bouwman included excreta from domestic animals (21.6 Tg N yr^{-1}) and wild animals (0.1 Tg N yr^{-1}), use of synthetic N fertilisers (9.0 Tg N

yr^{-1}), oceans (8.2 Tg N yr^{-1}), biomass burning (5.9 Tg N yr^{-1}), crops (3.6 Tg N yr^{-1}), human population and pets (2.6 Tg N yr^{-1}), soils under natural vegetation (2.4 Tg N yr^{-1}), industrial processes (0.2 Tg N yr^{-1}), and fossil fuels (0.1 Tg N yr^{-1}). The regions with highest emission rates in Europe, the Indian subcontinent and China reflected the patterns of animal densities and type and intensity of synthetic fertiliser use. A more recent study obtained similar contributions to global atmospheric NH_3 primary emissions for livestock wastes (39%), natural sources (19%), volatilization of NH_3-based fertilisers (17%), biomass burning (13%), crops (7%) and humans, pets and waste water (5%) (Galloway et al, 2004). In 2009, Clarisse et al studied the global ammonia distribution using satellite observations. These authors pointed out the large uncertainties in the magnitude of ammonia emissions due to the scarcity of ground-based observations and atmospheric measurements.

1.2.2-Size distribution of sulphate and nitrate compounds in atmospheric aerosols

The greatest abundance of ammonium sulphate and nitrate is found in the accumulation mode, though these compounds are also present in the nucleation and the coarse modes.

Acid sulphate aerosol is found in the submicrometric range (Charlson et al, 1974). Marine and mineral primary sulphate can be found in the coarse range. Both sulphate and nitrate coatings have been observed on mineral dust particles (Li and Shao, 2009; Wurzler et al, 2000). Nitric acid vapour can react with particle surfaces, such as marine NaCl or mineral carbonate aerosols allowing the formation of thermally stable nitrates in the coarse range, i.e. sodium nitrate ($NaNO_3$), calcium nitrate ($Ca(NO_3)_2$) or magnesium nitrate ($Mg(NO_3)_2$).

Coarse ammonium sulphate and nitrate may be formed by the reaction of NH_3 gas on sulphate and nitrate enriched sea-salt and soil particles when excess NH_3 is available, in the presence of moisture. The NH_4NO_3 dissociation, which depends on temperature and relative humidity, may result in a nitrate size shift. The size shift lies in the fact that fine NH_4NO_3 releases HNO_3, which will be available for other chemical reactions in the

atmosphere, such as reactions with coarse soil and sea-salt particles. The reactions between nitrate and sea-salt and nitrate and calcium carbonate are described as:

$$NaCl(aq,s) + HNO_3(aq) \leftrightarrow NaNO_3(aq,s) + HCl(g) \qquad \text{(cr 1.8)}$$

$$CaCO_3(s) + 2HNO_3(g) \rightarrow Ca(NO_3)_2(s) + CO_2(g) + H_2O(g) \qquad \text{(cr 1.9)}$$

As a result of (cr 1.7) and (cr 1.8) or (cr 1.7) and (cr 1.9), nitrate is transformed from fine particles to coarse particles.

The reactions between sulphate and sea-salt and sulphate and calcium carbonate -also leading to the transformation of fine into coarse sulphate- are described as:

$$H_2SO_4(aq) + 2NaCl(aq,s) \rightarrow Na_2SO_4(aq,s) + 2HCl(g) \quad \text{(cr 1.10)}$$

$$H_2SO_4(aq,g) + CaCO_3(s) \rightarrow CaSO_4(s) + H_2O + CO_2(g) \quad \text{(cr 1.11)}$$

In 1.8 and 1.10, since gaseous HCl is formed, the process can be identified by the so-called ''chloride loss'', ''chloride depletion'', or ''chloride deficiency'', terms that are used to describe the excess of Na^+ relative to Cl^-. This effect has been studied by a wide number of researchers (Savoie and Prospero, 1982; Harrison and Pio, 1983; Wall et al., 1988; McInnes, 1994; Kerminen et al., 1997; Zhuang et al, 1999a).

Ion balances carried out in a traffic site at Madrid from June 1999 to July 2000 showed that, in average, 91% of fine sulphate and 30% of fine nitrate was neutralised by ammonium. For PM_{10} sulphate and nitrate, these percentages were 67% and 3% respectively. At an urban background site in 2001, 96% and 79% of fine sulphate and nitrate were associated to the ammonium ion (94% and 56% for the PM_{10} fraction). In the fine fraction, most of the sulphate and nitrate was found as ammonium salts, although in the coarse fraction other forms of sulphates and nitrates neutralised by the Na^+, Ca^{2+} and Mg^{2+} ions prevailed (Salvador, 2004a). Source apportionment studies performed using factor analysis allowed the identification of a secondary PM_{10} aerosol factor associated to the ions SO_4^{2-}, NO_3^- and NH_4^+ at a traffic site (Escuelas Aguirre) in Madrid (Salvador et al, 2004b). This factor explained 14% of the variance. All this information gives evidence of the dominance of ammonium salts in the secondary inorganic aerosol fraction in the main study area of this thesis.

1.3-Area of Study

The Madrid air basin is located in the central part of the Iberian Peninsula where extreme weather conditions associated with an inland climate are usually established. The area is characterised by an extended plateau. The Metropolitan Area is bordered to the north–northwest by a mountain range with heights over 2000 m (Sierra de Guadarrama), 40 km from the city, and to the northeast and east by lower mountainous terrain. The weather in Madrid is typical of a mid-latitude continental area, with hot dry summers and cold winters, most days being under clear-sky conditions. The general synoptic situation leading to the occurrence of episodic events corresponds in winter to stagnant anticyclone conditions, with the usual formation of radiative nocturnal surface inversions. In summer, the mixed layer evolution is quite different, because the development of strong thermal convective activity and the influence of the mountains produce characteristic circulations.

Table 1.3 shows relevant climate variables seasonally averaged 1971 to 2000. Winter is considered as December to February and summer is June to August.

	Temperature (°C)	Sunshine (hours)	Relative humidity (%)	Rainfall (mm)
Winter	6-8	425	65-75	130
Summer	20-25	1000	39-46	50

Table 1.3. Climatic parameters in Madrid. Seasonal average 1971-2000 (from AEMET, 2011)

The metropolitan area of Madrid has around 6.6 million inhabitants -data corresponding to 2011- (UN, 2012). It comprises a car fleet over 4 million vehicles (fifty percent of which are diesel powered, including more than six hundred thousand medium- and heavy-duty trucks) with very intense traffic on weekdays on the connecting radial roads and the several existing ring roads. Light industry and domestic heating in winter contribute in a lesser proportion to atmospheric pollutant emissions in the area. Gas boilers are the predominant domestic heating devices, while fuel-oil and coal boilers are also present but in a much lower percentage. Table 1.4

shows the sources (%) of PM and some of the most relevant gaseous pollutants as registered in the inventory of the Madrid city hall.

Source	Nitrogen oxides (%)	PM(%)	CO(%)	Sulphur oxides (%)	VOCs (%)
Road transport	77	72.8	91.4	17.3	33.2
Non-industrial combustion plants (residential boilers, etc)	6.5	13.2	5.4	68.5	
Industrial combustion plants	5.7			7.4	
Other modes of transport and mobile machinery	7.1	5.5	2.1		
Use of solvents and other products					53.5

Table 1.4. Inventory of pollutant sources (%) from the Madrid city hall (http://www.mambiente.munimadrid.es/opencms/opencms/calaire/ContaAtmosferica/portadilla.html May 2012)

The distance between the Madrid metropolitan area and other significant urban or industrial areas in central Spain is >200 km. In this sense its urban plume could be studied as an isolated way. However long-range transport episodes significantly affect aerosol concentrations in the Madrid region and are usually related to Saharan mineral dust outbreaks (Salvador et al, 2004b). The arrival of Atlantic or polar air masses generally has a cleansing effect on the atmosphere, significantly reducing particulate matter levels.

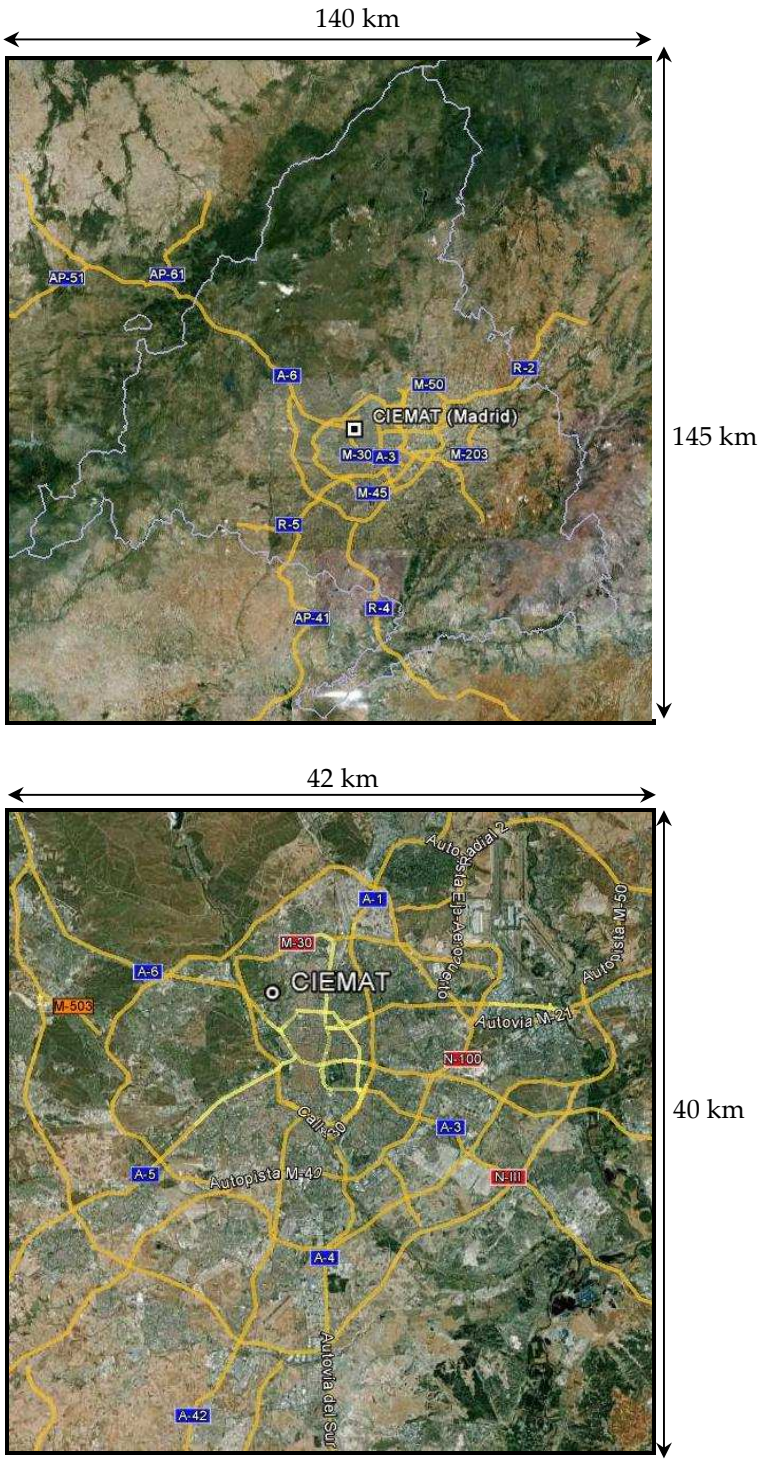

Figure 1.7. (Top) CIEMAT site and main roads in the Madrid Metropolitan Area. (Bottom) Urban area. Source: Google Earth

The features exposed above allow studying the Madrid plume as a typical urban plume, mainly fed by traffic and domestic urban emissions. The reference sampling site used in this study is located within the CIEMAT facilities (40° 27.5'N, 3° 43.5'W, 669 m. asl), in the north western area of the city of Madrid (Figure 1.7).

The European Environment Energy established a classification for air quality sampling stations (EEA, 1999). Table 1.5 shows the criteria for the urban background stations. According to this classification, the CIEMAT site is representative of urban background conditions. As can be seen in Figure 1.7, it is located in the north-west sector of the city, close to the outskirts of the city in an area largely covered by vegetation - a big urban park (Casa de Campo) and a Holm oak forest (Monte de El Pardo)- but with some heavily trafficked roads . Distance of any of these main roads to sampler exceeds 2 Km.

Type	Distance	Comments
Traffic	>50 m	Not more than 2500 vehicles per day within a radius of 50 m.
Industrial point sources	---	Expert judgement, depending on emission characteristics and prevailing wind direction, direct influence should be avoided
Small scale domestic heating with coal, fuel oil or wood, small boiler houses	>50 m	Should be avoided as much as possible

Table 1.5: Minimum distance to emission sources for urban background stations. (From the European Environment Agency, 1999).

A major part of the data analysed in this work has been measured in this location, for which atmospheric dynamics, air quality and meteorology features at local and regional scales are well known to the research group of CIEMAT involved in atmospheric pollution characterisation.

So that, to get an overview of the repesentativeness and reproducibility of the results obtained at this site, a comparison with those from other cities, with rather different characteristics from the point of view of emissions and meteorology, has been considered advisable. As it will be exposed in following chapters, several different and complementary studies have been carried out extending the analysis from the CIEMAT reference site to other locations.

1.4- Air Quality: Regulatory Framework

To preserve public health and ecosystems from air pollution undesirable effects, air quality is regulated by national and international organisms. The concentrations of secondary compounds of aerosol are not subject to any specific legal regulation at the moment, although the chemical characterization of the aerosol mass is advisable for some size fractions, as established in any normative document. Reductions in the concentrations of precursor gases involve reductions in the concentrations of particulate compounds derived from them. However, the formation and transformation processes are nonlinear and highly complex, making very difficult the estimation of the reduction in precursors that would lead to a certain reduction in secondary compounds. In fact, sometimes a reduction of precursors does not imply an abatement of secondary compounds (Harrison et al., 2008).

1.4.1- Atmospheric Emissions

-Sulphur-

The impurities of different fuels are the main source of anthropogenic sulphur in ambient air. These impurities can be removed, and therefore regulations have forced a progressive reduction of sulphur content in fuels. The most recent directive of the European Parliament on transportation fuels is 2003/17/EC, limiting the maximum sulphur content in petrol and diesel to 10 mg/kg from 1 January 2009. However, some types of petrol and diesel in different EU countries incorporated this limit in advance, and the reduction of sulphur in ambient air has been gradual. The Real Decreto 61/2006 is the document in force that introduced the requirements of directive 2003/17/EC in the Spanish legal framework.

As for fuel for heating facilities in the city of Madrid, the *Ordenanza General de Protección del Medio Ambiente Urbano* ANM 1985\3 prohibits the installation of new heating devices releasing more than 100 g of SO_2 to produce 100000 kcal. However, the removal of old generators is not mandatory, so they coexist with the less polluting facilities at present.

-Nitrogen Oxides-

The origin of anthropogenic nitrogen oxides is the reaction between ambient N_2 and O_2 due to the high temperatures reached in combustion engines. This reaction can be minimised through improved engines designs. In the last decade technologies have been also developed to reduce NOx to N_2 using selective catalytic reduction. Nevertheless, the latter solution has a disadvantage since catalysis leads to higher secondary emissions of NH_3 and HNCO originating from the reducing agent (Koebel et al, 2000).

Releases of nitrogen oxides (NOx), and also CO, hydrocarbons and particulate matter from vehicles are covered under the vehicle emission standards (so called Euro-standards). These are all measured separately for petrol and diesel cars as well as light and heavy goods vehicle classes, and contain maximum permitted emissions over a standard drive cycle. There are currently four stages for cars and Light Commercial Vehicles (LCVs) – conventionally labelled with Arabic numerals - that have progressively tighter emissions limits. Euro 4 has been in force for new types of vehicles since 1 January 2005 and since 1 January 2006 for all new vehicles. Euro 4 limits NOx emissions to 0.25 g/kWh. A further two new standards, Euro 5 and Euro 6, were introduced in Regulation No 715/2007 (2007). Euro 5 applies from 1 September 2009 and sets tighter emission limits of particles and NOx for new cars and vans sold in the EU, for example a 20% reduction in NOx emissions from diesel cars compared with Euro 4 limits. Euro 6, which will enter into force on 1 September 2014, sets significantly lower limits for NOx emissions from diesel cars (68% lower than the current Euro 4 limits).

1.4.2-Ambient concentrations

European Directive 96/62/CE, commonly referred to as “Framework Directive”, modified the regulation about air quality in the European countries existing at the time, adopting a general approach on the assessment of air quality, setting standards for the use and accuracy of assessment techniques and the definition of quality objectives to be achieved through proper planning. Directive 2008/50/EC updated the

Framework Directive, introducing regulations for new parameters, such as $PM_{2.5}$, and new requirements for the assessment and management of air quality.

In Spain, the legal framework regulating air quality is the *Ley* 34/2007. Its ultimate goal is to achieve optimal levels of air quality to avoid, prevent or reduce risks or negative effects on human health, the environment or property of any kind. The innovations introduced by the Directive 2008/50/EC were introduced by means of the *Real Decreto* 102/2011, which came into force on January 28, 2011. The purpose of this *Real Decreto* is to define and establish objectives for air quality with respect to concentrations of sulphur dioxide, nitrogen dioxide, nitrogen oxides and particles, among other pollutants. It also recommends the vigilance of levels of ammonia in ambient air due to the high reactivity of this gas, which favours the generation of secondary particles. However, defining quality objectives for this pollutant is not considered necessary at this time. It also determines the information to be given to the public and the European Commission on the concentrations of the substances to which it refers. The Real Decreto establishes the reference measurement methods for each pollutant and the type and number of measurement sites, with particular emphasis on urban and traffic sites. Limit values are set with certain tolerances and critical levels that should not be exceeded from fixed dates, so that the reduction in ambient concentration of pollutants is progressive. It includes the impact of transboundary pollution (i.e., transported from nearby countries) and due to natural causes (i.e., African dust events) that must be taken into account. Table 1.6 shows the current quality objectives for SO_2, NO_2, NOx, PM_{10} and $PM_{2.5}$

SO_2	Averaging time	Limit value	Date of meeting the limit value
1. Hourly limit value	1 hour	350 μg·m³, value not to be exceeded more than 24 times/year	From 01/01/2005
2. Daily limit value	24 hours	125 μg·m³, value not to be exceeded more than 3 times/year	From 01/01/2005
3. Critical level	Calendar year and winter (October 1 to March 31)	20 μg·m³	From 11/06/2008

NO_2	Averaging time	Limit value	Date of meeting the limit value
1. Hourly limit value	1 hour	200 μg·m³, value not to be exceeded more than 18 times/year	From 01/01/2010
2. Annual limit value	1 year	40 μg·m³	From 01/01/2010
3. Critical level	1 year	30 μg·m³ of NOx (Expressed as NO_2)	From 11/06/2008

PM_{10}	Averaging time	Limit value	Date of meeting the limit value
1. Daily limit value	24 hours	50 μg·m³, value not to be exceeded more than 35 times/year	From 01/01/2005
2. Annual limit value	1 year	40 μg·m³	From 01/01/2005

$PM_{2.5}$	Averaging time	Limit value	Date of meeting the limit value
1. Annual target value	1 year	25 μg·m³	From 01/01/2010
2. Annual limit value (stage I)	1 year	25 μg·m³	01/01/2015
3. Annual limit value (stage II)	1 year	20 μg·m³	01/01/2020

Table 1.6. Quality objectives for SO_2, NO_2, NOx, PM_{10} and $PM_{2.5}$ concentrations in ambient air in Spain (Real Decreto 102/2011)

2- STATE OF THE ART AND OBJECTIVES OF THIS WORK

2. STATE OF THE ART AND OBJECTIVES OF THIS WORK

The first studies on particulate nitrate and sulphate took place in the 50's last century. One of the longest time series was measured in the UK from 1954 to 1988 (QUARG, 1996). This series clearly showed a rising trend in sulphate until 1976 which since fallen, and a rising trend in nitrate which continued to the last of the measurements. The acid rain, which was associated with anthropogenic acid emissions, caused a serious environmental problem until the 70's (Likens et al, 1974). The introduction of strong acids into natural systems was then considered in order to develop proposals for new energy sources and in the development of air quality emission standards.

In the US, detailed chemical speciation of inorganic fine aerosol from traffic sources was performed (Dzubay and Stevens, 1979) and the production mechanisms of urban secondary inorganic compounds were investigated (Middleton et al, 1980) during the last quarter of the century. The size distribution of atmospheric aerosols (sulphate, ammonium and nitrate particulates) was also studied in Japan, and Kadowaki et al differentiated natural and anthropogenic fractions in 1976. In Europe, a great number of studies have been conducted from the 80's to obtain concentrations, chemical characterization and source apportionment of aerosol constituents (Harrison and Pío, 1983; Pío et al, 1991).

In Spain, Querol et al (1998a, 1998b) characterised ambient particulate sulphate evolution around big coal-fired power plant emissions, observing daily cycles associated to the SO_2 oxidation cycle, the power plant plume behaviour and the local atmospheric dynamics. Many other different types of environments and geographical areas have been characterised in Spain by this group and co-workers since then, compiling an extensive database on levels and composition of particulate matter.

The first mathematical models for pollutants transport and removal including conversion of sulphur dioxide, nitrogen oxides, and hydrocarbons to particulate sulphate, nitrate, and organics were developed in the 70's (Peterson and Seinfeld, 1977). Since then, enormous progress has been made in the knowledge of physical and chemical processes that govern production of secondary inorganic compounds in ambient air. However, important problems remain open.

2.1. State of the art

In previous sections the fundamental mechanisms that generate secondary sulphate and nitrate have been described. However, some aspects of these mechanisms are not fully understood yet. The rate of oxidation of SO_2 is a matter of discussion. Shindell et al. (2009) estimated the impact of reactive species emissions on both gaseous and aerosol forcing species and found that ozone precursors increased or decreased the rate of oxidation of SO_2 to sulphate aerosol. Studies with different formulations of sulphur cycle (Collins et al., 2010) have found lower sensitivity than Shindell et al. Recently, Stein and Saylor (2012) have analysed the influence of changes in oxidant levels and sulphur dioxide oxidation pathways to study the underlying pathways for sulphate formation. Comparison of modelled results and measurements demonstrates that the different pathways have significantly different responses in sulphate formation when the emissions of NO_x and/or VOC are altered, reflecting different photochemical regimes under which the formation of sulphate occurs. Heterogeneous reactions of gaseous nitrogen oxides on aqueous particles are also a subject of study. In 2009, Bertram and Thornton laboratory results showed that on aqueous particles the reactive uptake coefficient of N2O5 on particle liquid water was strongly dependent on the molar ratio of particle water to nitrate for low particle water concentrations. Measurements of N2O5 and nitrate were recently taken above London to study the night-time chemistry of these compounds (Benton et al, 2010).

Due to their low saturation vapour pressure and hygroscopic properties, sulphur compounds play a fundamental part in the formation of new particles. There exist experimental evidences indicating that reductions in sulphur emissions in urban environments lead to lower formation of ultrafine particles. A reduction of the measured ultrafine particle number concentrations has been observed in a kerbside site in Copenhagen from the period 2002-2004 to 2005-2007. Strong evidence indicates that a significant part of the reduction, especially in the size range <30 nm, is due to the transition to sulphur-free (<10 ppm) diesel fuel and petrol in Denmark at New Year 2005 (Wåhlin, 2009). A large reduction in airborne particle number concentrations at the time of the introduction of “sulphur-free" diesel has been detected in London (Jones et al, 2012).

Atmospheric new particle formation is generally thought to occur due to homogeneous or ion-induced nucleation of sulphuric acid. However, identification of precise compounds and exact mechanisms remains open. Recent studies on this matter have been performed in Northern Europe (Berndt et al, 2008; Laaksonen et al, 2008). Comparison of ambient nucleation rates with laboratory data from nucleation experiments involving either sulphuric acid or other forms of oxidised SO_2 indicate that intermediate radicals can play a key role in the production of nuclei of new aerosols. Zhang et al. proposed in 2009 a mechanistic explanation of the initial nucleation and formation of aerosols, which includes both biogenic VOCs and the anthropogenic pollutant SO_2. The resulting organosulphates were first discovered in both laboratory studies and ambient air samples by Surratt et al. (2007). A number of recent works study the formation of organosulphates and organonitrates observed in ambient secondary organic aerosol (SOA) (Darer et al, 2011).

The formation of secondary inorganic aerosols (SIA) including ammonium sulphate and ammonium nitrate has been modelled in Europe quite successfully. In 2004, Schaap et al presented a SIA model simulation validated for the year 1995 with special attention to nitrate. The chemistry-transport model LOTOS (Builtjes, 1992) was extended to account for secondary aerosol formation and deposition. Averaged over all stations the model reproduced the measured concentrations for NO_3^-, SO_4^{2-}, NH_4^+, total NO_3 (HNO_3+NO_3), total NH_4 (NH_3+NH_4) and SO_2 within 20%. The model underestimated wet deposition which was attributed to the insufficient representation of cloud processes. Inclusion of sea salt was found to be necessary to properly assess the nitrate and nitric acid levels in marine areas. The treatment of ammonia was found to be a major source for uncertainties in the model representation of secondary aerosols. The CALIOPE high-resolution air quality modelling system (Baldasano, 2008) has been recently used to investigate the formation of SIA (SO_4^{2-}, NO_3^- and NH_4^+), and their gaseous precursors (SO_2, HNO_3 and NH_3) over Europe during the year 2004. The CALIOPE system succesfully estimates SIA when compared to the measurements, although errors are larger for gaseous precursors. The temporal treatment of ammonia emission is a probable source of uncertainty in the model representation of SIA. Spatial distribution of key indicators is used to characterise chemical regimes and understand

the sensitivity of SIA components to their emission precursors. Results indicate that SO_4^{2-} is not usually fully neutralised to ammonium sulphate in ambient measurements, in spite of the presence of enough free NH_3. CALIOPE and the EMEP (European Monitoring and Evaluation Programme) network observations agree that the continental regions in Europe tend to be HNO_3 and not NH_3 limited for nitrate formation (Pay et al, 2012).

The source contribution to ammonia in urban areas is not yet fully characterised. These sources would include traffic, human and pets´ excretions, landfill, garbage, household products and sewage treatment plants. Observations suggest that the NH_3 emissions from the traffic exhaust could be a major source of the ambient NH_3 (Perrino et al, 2002), but more research in the topic is needed.

In Spain, aerosol ambient concentrations have been well characterised in numerous studies (Querol et al, 2008) at different types of environments and speciation and source-apportionment techniques have been applied to determine the contributions from the main aerosol fractions (Querol et al, 2004a). Special attention has been dedicated to the Saharan dust outbreaks, since they contribute significantly to PM levels, mainly in the spring and summer seasons (Rodriguez et al, 2001). These studies have been based on aerosol chemical speciation and size fraction although other optical and morphological aerosol properties have been characterised as well (Toledano et al, 2007; Coz et al, 2009). Saharan events contribute mainly to the coarse aerosol mode whereas the long-range transport of fine mode aerosol and SIC has been studied to a lesser extent. In 1998, Rúa et al studied the sources of SO_2, SO_4^{2-}, NOx, and NO_3^- in four Spanish rural stations using trajectory analysis and conditional probability functions. They identified the Mediterranean area as the main source of these pollutants, and smaller contributions from the north of Africa and Central Europe. In 2008, high fine SIC levels were associated to polluted air mass transport from Western Iberia through the Straits of Gibraltar in a rural site in south-western Spain (Pey et al, 2008).

Analysis of time series has been performed in several regions of the country. Viana et al (2003) analysed 5-year PM and gaseous pollutants time series for the period 1996-2000 in several locations of the Basque Country. The authors accounted for seasonal variations, finding a strong influence of precipitation. PM levels were highly influenced by African and European pollutant transport, apart from regional and local episodes. Weekend reductions and daily cycles were also discussed. In Santander, Moreno et al (2009) analysed a 12-month time series corresponding to 2007 to investigate annual, weekly and 24-h trends of gases and PM_{10}. In this work the daily evolution of pollutants is discussed in terms of the health effects attributed to exposure to high concentrations of pollutants during short time periods. PM_{10} and $PM_{2.5}$ samples were collected and analysed for 12 months in Elche (Nicolás et al, 2009). The authors studied water-soluble inorganic ions discussing ion balances, seasonal variations and the influence of African dust episodes.

Submicron size-distribution studies have also been performed in several locations in the Iberian Peninsula. In El Arenosillo, a rural and coastal environment in South-western Spain, the seasonal and annual variability of the total and modal particle concentration, and diurnal patterns features were investigated with complementary characterisation of emissions, secondary particle formation, meteorological analysis and long-term transport. The median size distribution for desert dust and continental aerosol was found to be dominated by the Aitken and accumulation modes, while nucleation events were strongly linked to the marine air mass origin (Sorribas et al, 2011). Other relevant studies have been performed in Barcelona (Pey et al, 2009) and Tenerife (Rodríguez et al, 2009).

Data from Spanish locations have been included in broader studies that consider the European aerosol phenomenology, to some extent (Putaud et al, 2004; Van Dingenen et al, 2004; Putaud et al, 2010). Few studies have compared aerosol processes and properties in Spanish cities with others from nearby countries. Querol et al (2004b) presented PM characteristics of seven European regions comparing levels and speciation studies of PM_{10} and $PM_{2.5}$. Regarding long-range transport, Borge et al found very different and characteristic transport patterns that affected PM_{10} concentrations in three European cities: Athens, Madrid and Birmingham (Borge et al, 2007). A

physicochemical characterization of the urban fine aerosol including aerosol number size distribution, chemical composition and mass concentrations in three European urban locations (Milan, Barcelona and London) was performed by Rodriguez et al (2007). The role of microphysical processes of the aerosol dynamic in the regular evolution of the urban aerosol (daily, weekly and seasonal basis) and in the day-to-day variations (from clean-air to pollution-events) was explored, as well as the link between aerosol chemistry and mass concentrations with the number size distributions.

One of the limiting factors in the study of aerosol compounds is the temporal resolution of the data acquired. Sampling techniques which allow obtaining chemical speciation on a daily basis are widely used, however, techniques based on aerosol collection on substrates or filters do not allow hourly resolution. Only a limited number of techniques allow obtaining aerosol speciation with hourly (or higher) resolution, and therefore, the short-time evolution of aerosol compounds is left out of most studies.

In his review on aerosol measurements McMurry (2000) noted that prior to the mid-1990s, the major "online" method for aerosol sulphate measurement involved Flame Photometric Detection in a hydrogen-rich flame (Tanner et al. 1980). Since that time a number of measurement methods for semi-continuous measurement of aerosol species, and different implementations of similar methods, have been proposed. These include, but are not limited to, the humidified impaction strip/flash volatilization/pulsed fluorescence of SO_2 method (Hering et al. 2003); the aerosol mass spectrometer (AMS) (Jayne et al. 2000); the particle-into-liquid sampler followed by ion chromatography (Weber et al. 2001; Orsini et al. 2003); the steam jet aerosol collector (Khlystov et al. 1995); and wetted filter collector (Al-Horr et al. 2003).

Particle mass spectrometers likely represent the greatest advancement in PM measurement technology during the last decade, although they are unlikely to be used in routine measurements in the foreseeable future because of their complex technical requirements and cost. The aerosol chemical speciation monitor (ACSM) is built upon

the same technology as the AMS, in which an aerodynamic particle focusing lens is combined with high vacuum thermal particle vaporization, electron impact ionization, and mass spectrometry (Ng et al, 2011). Modifications in the ACSM design, however, allow it to be smaller and simpler to operate than the AMS. The ACSM is also capable of routine stable operation for long periods of time (months). At present this is a highly promising instrument for the measurement of long time series of compounds aerosol. However, its development has been very recent and still did not allow obtaining time series of the order of years.

The technique used in this thesis for the semi-continuous measurement of particulate sulphate is the reduction oven plus pulsed fluorescence. It was patented by the Harvard School of Public Health and the commercial version was manufactured by Thermo Electron. The Sulphate Particle Analyzer (SPA) was first evaluated by Schwab et al in 2006 in the laboratory and a rural site in New York.

For the short-term nitrate detection, the technique used was based on reduction by humidified impaction with flash volatilization plus chemiluminescence. The Series 8400N ambient particulate nitrate monitor measures the mass concentration of ambient particulate nitrate contained in $PM_{2.5}$ in near real time using this technique and is based on prototypes described by Stolzenburg and Hering (2000). The Series 8400 was designed to meet the U.S. Environmental Protection Agency (EPA) $PM_{2.5}$ speciation monitor requirements.

Several studies using these instruments have been performed at the US Supersites. At Baltimore, a 9.5-month study allowed characterising seasonal and short-term variations in nitrate concentrations. Three kinds of transients were identified. The first was attributed to early morning traffic activity, the second type occurred during the afternoon due to photochemical activity, and the third occurred at night (Park et al, 2005). At Pittsburgh, semi-continuous $PM_{2.5}$ inorganic composition measurements were taken for one year to characterise seasonal and daily variations (Wittig et al, 2004).

However, studies using these techniques and exceeding one year are scarce in literature. Seasonal trends and diurnal nitrate patterns were observed for three years by Rattigan et al (2006) in New York State at one rural and one urban site. Chow et al

(2008) performed continuous and filter-based measurements of NO_3^- at the Fresno Supersite between 2000 and 2005. A seasonal pattern was observed for NO_3^-, with higher concentrations in winter than summer. In winter, NO_3^- increased around mid-day along with increasing temperature and decreasing BC concentration. The authors interpreted this result as NO_3^- formed aloft during transport and mixed to the surface with the breakdown of the nighttime inversion. Nitrate concentrations were measured at 10-min time resolution for a year or longer at four US urban sites by Millstein et al (2008). This study was focused on the fine particulate nitrate response to weekly cycles in emissions. Doraiswamy et al (2010) compared model-based forecasted $PM_{2.5}$ with the Thermo electron SPA and the R&P particulate nitrate monitor for 2 years, including hourly evolution of both pollutants at five sites in the Eastern US. The authors found some discrepancies with the model, in particular at urban sites around noon. In the case of sulphate, it was attributed to its sensitiveness to the accuracy of simulation of cloud properties, which influence heterogeneous cloud-phase reactions. However, there are aspects in the daily evolution of secondary inorganic compounds which have not been fully understood yet.

2.2. Previous results in the region of Madrid

PM mean levels in the Madrid air basin are within average ranges of PM_{10} and $PM_{2.5}$ concentrations obtained from a wide range of sites across Spain and also in many European sites. A summary of results for the Madrid air basin characterising mean PM_{10} and $PM_{2.5}$ concentration levels and their chemical composition was performed by Salvador et al (2012). The authors complied homogeneous time series of the main pollutants recorded by the air quality networks together with experimental data obtained in sampling campaigns at representative sites. The analysis ranged from 1999 to 2008, including data from 30 sites. Three campaigns took place in the following periods: June 1999-June 2000; 2001 and January 2007-April 2008. The results showed a mean annual PM_{10} ranging from 13 $\mu g \cdot m^{-3}$ in regional background sites to 40 $\mu g \cdot m^{-3}$ in traffic hotspots, and mean $PM_{2.5}$ concentrations ranging from 8 $\mu g \cdot m^{-3}$ in the regional background to 19 $\mu g \cdot m^{-3}$ in traffic hotspots. SIC was found to be the third major

component group of the aerosol mass in PM_{10} (16-60 %) and the second one at the urban and urban-background sites in the $PM_{2.5}$ fraction (19-26 %). Different behaviours were found for the single components of SIC. NO_3^- contributions reached 2.0-2.4 $\mu g \cdot m^{-3}$ in PM_{10} and 1.3-1.5 $\mu g \cdot m^{-3}$ in $PM_{2.5}$ at the different sites. In contrast, significant differences in SO_4^{2-} concentrations were found among sites in PM_{10} and $PM_{2.5}$, being the mean concentration significantly higher at the urban site in the 1999-2000 period. No statistically significant differences in NH_4^+ concentrations in $PM_{2.5}$ were found among sites. SIC mean content in PM_{10} did not show significant variations between the 1999-2000 and the 2007-2008 campaigns. Total SIC content decreased by 8% and 18% in PM_{10} and $PM_{2.5}$ respectively. However secondary compounds showed different evolutions. In the coarse fraction SO_4^{2-} concentrations diminished by 29% from 1999-2000 to 2007-2008. On the contrary NO_3^- and NH_4^+ concentrations increased by 17% and 31%, respectively, in the same period. In the fine fraction, the same behaviour was observed, i.e. a remarkable reduction in the concentration of SO_4^{2-} (38%) and an increase, lower than in the coarse fraction, in the concentration of NO_3^- (12%) and NH_4^+ (5%) from 1999-2000 to 2007-2008.

In the urban area of the region of Madrid, source apportionment studies have characterised PM_{10} sources identifying three main contributors: road traffic, crustal/mineral and secondary aerosol, and an almost negligible contribution of marine aerosol. Secondary inorganic aerosols were frequently discriminated as secondary sulphate and secondary nitrate. However both sources could be found grouped into a single one "Secondary Inorganic" depending at the site (Salvador et al, 2012). Positive Matrix Factorisation (PMF) analysis allowed the identification of industrial and biomass burning contributions in urban-background and rural background sites, as well as residential coal combustion in an urban site (Salvador et al, 2010).

Trend analysis in the city of Madrid showed a slight tendency of PM and SO_2 towards decreasing levels in the period 1979-1985 (Serrano et al, 1988). However, an extension of this analysis until 1989 revealed a reduction of the downward tendencies. This was attributed to the increase in number of heating systems installed in the city as well as the large number of diesel-engined vehicles. Daily patterns of PM_{10} and gases in

Madrid were depicted monthly from June 1999 to May 2000, showing a clear agreement between SO_2 evolution and the official heating season (November-March).

The most recent trend analysis performed in the region showed a significant downward trend in the concentrations of SO_2, CO, NOx and $PM_{2.5}$ in the city of Madrid in the period 1999-2008. These reductions can be attributed to a reduction in the emissions from residential coal burning and maybe in a lesser extent to traffic, since new vehicles incorporate transport emissions control technologies that might contribute to this decrease (Salvador et al, 2012). In that work, an increase in the ratio NO_2/NOx was also detected. This fact, together with the absence of a decreasing trend of NO_2 concentrations was attributed to the increase of the diesel fleet.

The influence of synoptic weather patterns and long-range transport episodes on the concentration of particulate matter (including PM_{10} and $PM_{2.5}$) and some major ions (SO_4^{2-}, NO_3^- and NH_4^+) has also been studied. The evaluation included PM_{10} and $PM_{2.5}$ concentrations and chemical composition data at three representative sites of the Madrid air basin and 6-years air mass back-trajectories arriving at a background rural station in central Spain by statistical methods, including a residence time analysis of trajectories, was also performed to detect remote sources and transport pathways. The analysis confirmed that elevated PM_{10} concentrations in central Spain are likely to be influenced significantly by long-range transport of desert dust from different desert regions in North Africa. Emissions from continental Europe with a high time of residence in the western and central areas of the Mediterranean basin seemed to significantly influence $PM_{2.5}$ and secondary inorganic aerosol concentrations in this region (Salvador et al, 2008).

In the last five years, some works have investigated characteristics of aerosol SIC in the Madrid metropolitan area in more detail. Particulate nitrate concentration in a suburban site has been semi-continuously measured and analysed together with gaseous pollutants and meteorological information during the course of one year, allowing the identification of the main formation mechanisms. Photochemical reactions dominate the nitrate generation, though nitrate maxima appeared under high humidity conditions occasionally. Strong thermal decomposition is observed in summer

(Gómez-Moreno et al, 2007). The mass size distribution of inorganic aerosol species show that the sulphate and ammonium mass is concentrated in the accumulation mode, so most of the sulphate is expected to be secondary. In contrast, the nitrate shows a bimodal distribution with a marked coarse mode. In most of the samples, the ammonium mass measured was enough or almost enough to neutralise inorganic acidity by formation of ammonium sulphate and nitrate. However, a significant sulphate mass not neutralised by ammonium was found in the aerodynamic diameter < 0.056 μm. The concentration of this sulphate and its contribution to the ultrafine fraction mass was higher under good dispersive conditions, when particle growth processes are not so favoured due to the higher atmospheric dilution factors. The origin of this ultrafine sulphate can be attributed to direct emissions from traffic, although further research is needed to characterise its formation processes (Plaza et al, 2011).

The particle number size distribution is related to the chemical composition of the aerosol and thus its study will be of interest for the investigation of SIC characteristics in a region. The time evolution of particle number concentration in Madrid was investigated by Gómez-Moreno et al (2011). It showed a clear seasonal influence, with maximum values in the period November-January, coinciding with atmospheric stagnant conditions and pollution episodes, and minimum values were measured in springtime, a period in which wind speed produces high atmospheric dilution. The Aitken and accumulation modes showed a similar seasonal behaviour, with two maxima related to vehicle emissions. The nucleation mode had a third maximum observed at noon during spring and summer. The size distributions were bimodal during most of the time: the first mode was centred on 20-50 nm and was associated with fresh particles related to vehicle exhaust emission; the second mode, between 50 and 160 nm, mainly corresponded to the evolution of the first mode. The evolution of the size distributions reveals a marked annual cycle, with an increase of median diameters during summer and a decrease during winter.

The work performed in this thesis, and also most of the results for the Madrid metropolitan area exposed above can be framed in two research projects:

- **PROFASE** was undertaken between October 2008 and December 2011. This project tackled the study of formation and transformation processes leading to secondary aerosol in an urban environment (Madrid). Under the frame of PROFASE a characterization of these processes following a methodology based on continuous measurements of ambient parameters and proper compounds was performed to provide key information to identify some mechanisms of secondary aerosol formation. Continuous measurements of number and size distribution of submicron particles were used to link physical and chemical processes.

- **MICROSOL** was programmed to be carried out between January 2012 and December 2014. The project aims to characterize major aerosol compounds (including inorganic, carbonaceous and organic) formation processes and evolution of the ambient urban aerosol mass in the sub-micrometric size range. The focus will be on some of the properties that play a relevant role in the understanding of processes related to the formation and evolution of particles once they have been emitted to the atmosphere and their source apportionment. Chemical composition is one fundamental aerosol property that determines not only its chemical behaviour and its effects on quality and health impact, but also influences physical properties such as the optical, having important consequences on the Earth's radiative balance.

2.3. Objectives of this work

The main goal of this work is to achieve a deeper insight on the secondary inorganic aerosol in an urban environment, with a special emphasis on the fine fraction of nitrate and sulphate. These species had been partially characterised in the Madrid air basin, and further research was needed to cover the identified gaps found in previous studies. First, information on precursor gases is not complete. While NOx and SO_2 have been widely measured and their sources and mean levels well characterised in Madrid, information on gaseous NH_3 is very limited. A one-year study by Gómez-Moreno et al (2007) characterised nitrate seasonal behaviour and hourly evolution under winter episodic conditions. However, these results needed to be confirmed for a wider time period. At the same time, nitrate evolution in other timescales –weekly- was not well known, and nitrate events caused by other kind of episodes -such as air mass transport- had not been studied. The same knowledge had to be acquired in the case of sulphate. Moreover, the nanometric sulphate fraction found had to be studied more closely.

To fulfil these gaps the following specific objectives were established in this thesis:

- Characterise levels, seasonal variations and temporal trends of gaseous precursors of nitrate and sulphate in the Madrid air basin. Characterise mean levels and main gaseous NH_3 sources in the Madrid metropolitan area.
- Characterise the high-resolution variations and seasonal / interannual evolution of fine nitrate from a longer time series of semicontinuous measurements.
- Characterise the high-resolution temporal evolution and variation patterns of fine sulphate from a new database of at least one year of semicontinuous measurements.
- Perform a joint analysis of time variations of particulate sulphate and nitrate on a high-resolution temporal basis.
- Identify and characterise individual episodes leading to high nitrate and sulphate concentrations in the region of Madrid.
- Characterise the mass size distribution of inorganic aerosol species in size fractions smaller than 0.056 μm.
- Compare and contrast the behaviour of these species in the Madrid air basin with the phenomenology in other regions.

The main novelty of this work is the focus on analysis of long time series of inorganic compounds in a semicontinuous basis. Seasonal and weekly variability can be studied with data from a greater variety of measuring techniques. However, the variability of PM compound concentrations on time scales shorter than a day, which are sometimes those at which several processes take place, can only be studied with a limited number of devices. This high resolution allows then obtaining more insight into some processes which can remain hidden in lower resolution data. On the other hand, few studies have characterised high-resolution time series of one year or longer, and in Madrid only two works of these characteristics had been carried out by Gómez-Moreno et al (2007) and Plaza et al (2011). This work provides novel information on some processes related with sulphate and nitrate evolution.

3-METHODOLOGY

3-METHODOLOGY

In the previous chapter the main objectives of this work were exposed, consisting mainly on achieving a deeper insight on the secondary inorganic aerosol in an urban environment, with a special emphasis on the fine fraction of nitrate and sulphate. This urban environment is the Madrid municipality. However, to characterise aerosol properties in this urban area the aerosol behaviour in other sites of the Madrid air basin must be considered. For these reasons, the principal sampling site chosen is the CIEMAT station -classified as an urban background site at Madrid- and further data from Air Quality Networks which operate in the Madrid air basin have been also used.

Chemical speciation of aerosols is usually based on filter-based sampling, which provides averaged PM concentrations, typically on a 24-hr basis. Filter samples collected over this or longer time periods lack sufficient temporal resolution to track short-term diurnal events (for instance, impact of traffic and photochemistry events) and in consequence processes that affect the chemical composition of the PM. Sampling techniques can also be subject to a number of sampling artefacts that can alter the result and hamper the actual chemical composition at the sampling time. In addition, filters require offline analysis techniques, which result in data availability delays. Therefore, the development of PM chemical composition analytical instrumentation with high temporal resolution provides information beyond the traditional filter-based analysis which allows further study of sulphate and nitrate formation and evolution processes at the same time scale at which they take place.

The methodological approach has been focused on the semi-continuous measurement of sulphate and nitrate, however, data or processed results from further instruments have been used to obtain a complete interpretation of the SIC behaviour. Filter-based measurements have been analysed when semi-continuous data were not available or in order to compare the information provided by both methods. Gaseous precursors have been analysed jointly with secondary products to obtain a full picture of the behaviour of the chemical compounds. Aerosol size distributions and vertical profiles have been used as additional information to characterise a volcanic event of special relevance occurred during the course of the measurement period. Ion mass distributions have

been measured to determine formation processes which cannot be identified studying a single aerosol size fraction.

Experimental data has been complemented with the use of trajectory models based on meteorological fields to study the origin of air masses and also with outputs from an aerosol distribution prediction model.

Data analysis has been focused on the analysis of pollutant time series. The availability of high frequency data has allowed studies in different time scales, from an annual basis to a 20-min time resolution. Size distributions obtained with different techniques have also been studied, implying data transformation which in general is not straightforward.

The results obtained for the Madrid air basin have been compared with results from other regions to get a broader perspective of the aerosol behaviour in the Madrid air basin and place in an international context. Specifically, time series have been analysed jointly with pollutant time series from South-Eastern England and size distribution have been contrasted with similar measurements in Barcelona.

All the instrumentation, including sites and networks information, models and data analysis tools used in this thesis are described in this chapter.

To achieve the specific objectives set out in Chapter 2, the following points have been covered.

- Analysis of the main pollutants (SIC) and related compounds (gaseous precursors and PM) from Air Quality Networks. The Madrid Township munipality network and the EMEP network have been used to characterise levels, seasonal variations and temporal trends these pollutants in the Madrid air basin in the last decade. Results from previous field campaigns have also been discussed. In the case of NH_3, no data were available in the Madrid municipality, so that a field campaign was carried out in two different seasons in Madrid.

- Acquisition of measurements of sulphate and nitrate on a semi-continuous basis. For this purpose a sulphate particulate analyser Thermo Electron 5020 was installed in the CIEMAT sampling station. Laboratory testing and intercomparison with filter-based measurements were performed. Maintenance of the R&P semi-continuous Ambient Particulate Nitrate Monitor already in use. Analysis of nitrate time series from 2004 to 2011 and sulphate time series from 2009 to 2011 in the CIEMAT site.
- Analysis of pollutant time series from Air Quality Networks in South-Eastern England and comparison with the Madrid air basin. Monthly, daily and hourly evolution of pollutants has been discussed.
- Identification and characterisation of individual episodes leading to high sulphate and nitrate concentrations in the region of Madrid. This was performed by trajectory clustering with the Hysplit model and comparison with data analysis from the CIEMAT station instrumentation, together with rural sites (EMEP network) data. The trajectory model FLEXTRA and the aerosol distribution prediction model NAAPS have been also used.
- Sampling of ion mass size distributions with a MOUDI cascade impactor. Measurements were performed in an urban background site at Barcelona. These measurements were carried out in the framework of the international sampling campaign DAURE. The data analysed were contrasted with previous results at an urban background site at Madrid.
- Sampling campaign under selected meteorological conditions and extension of the mass size distribution of inorganic aerosol species measured at Madrid to nanometric fractions. To this end, a nano-MOUDI was acquired and tested.
- Joint analysis of the results obtained in the previous phases.

The principal databases necessary to fulfill these points (based on semi-continuous sulphate and nitrate analysers and filter-based comparisons, MOUDI and nano-MOUDI) has been obtained by the author of this thesis since 2009, in addition to the basic information on PM and aerosol counts provided by optical particle counters. Ancillary data from other instruments operated by co-workers has been used to

complete the analysis and obtain a full picture of the aerosol phenomenology over extended time periods (information on gases) or specific events (aerosol size distributions and vertical profiles).

3.1- The CIEMAT station

The CIEMAT station is within the CIEMAT facilities in Madrid. These are located in the north western sector of the Municipality. The nearest road (Complutense Avenue) is separated from the site more than 300 m and no industrial or domestic heating sources are present in the vicinity, so according to the criteria established by the EEA (1999), the station can be classified as an urban background site.

Figure 3.1. (Top right) CIEMAT facilities. The red circle indicates the location of the air quality station. (Bottom left) Air quality station. Outdoor instrumentation and external part of the laboratory. (Bottom right) Detail of sampling pipes

Figure 3.1 shows the location of the station in the CIEMAT facilities (top) and the nearest road. A picture of the outdoor instrumentation and detail of the sampling pipes of the indoor instrumentation are also shown (bottom).

3.1.1- Instrumentation

This section describes the principal instrumentation available in the CIEMAT air quality station which has been used in this work.

3.1.1.1- Particulate Sulphate Analyser

As we mentioned in the previous chapter, a number of measurement methods for semi-continuous measurement of aerosol species and different implementations of similar methods have been proposed.

The reduction oven-pulsed fluorescence method was patented by the Harvard School of Public Health and the commercial version was manufactured by Thermo Electron. In 2009 a Thermo 5020 particulate sulphate analyser (SPA) was acquired to measure time series of particulate sulphate (Figure 3.2) in CIEMAT. The Model 5020 Sulphate Particulate Analyser (SPA) combines a continuous sulphate (SO_4^{2-}) to sulphur dioxide (SO_2) converter and a trace-level version of Thermo Electron's pulsed fluorescence SO_2 analyser to provide a system for near real-time measurement of sulphate aerosol.

As a result, a **semi-continuous time series of particulate sulphate concentrations on PM_1** has been obtained with this instrument on a 10 min time basis from **June 2009 to July 2011**. Interruptions due to instrumental failures have resulted in a total **77% of data coverage**.

Figure 3.2. Particulate Sulphate Analyser Thermo electron 5020 used by CIEMAT

-Principle of operation-

The sulphate measurement is based on reduction of particulate sulphate to gas phase SO_2 by thermal catalysis in a high-temperature converter module. The SO_2 formed in the converter module is conveyed to an analyser module where it is continuously measured using a pulsed fluorescence technique. The pulsed fluorescence measurement operates on the principle that SO_2 molecules become excited by absorbing ultraviolet (UV) light at one wavelength and then emit UV light at a different wavelength when decaying back to a lower energy state. The pulsed fluorescence instrument combined with a high efficiency SO_4^{2-} to SO_2 converter allows detection and measurement of particulate sulphate at low concentrations, typical of many ambient environments. When running with a 60 second averaging time, this analyser is capable of detecting SO_2 at concentrations of 0.05 ppb or less. This corresponds to a sulphate concentration of slightly below 0.20 micrograms per cubic meter $\mu g \cdot m^{-3}$ at standard conditions of temperature and pressure.

The Model 5020 quantifies sulphate by comparing the signal produced when aerosol-laden sample is drawn directly into the converter to a background signal that is produced when the sample stream is run through a high-efficiency particulate aerosol filter before conversion. The difference in signal between the filtered and unfiltered sample can be attributed to sulphur dioxide that is formed from sulphate particles in the unfiltered sample stream. The Model 5020 cancels out interference from ambient

SO_2 or other gases that might fluoresce, such as nitric oxide, and resets the instrument zero on every cycle.

The SPA measures particulate sulphate on a semi-continuous basis. The temporal basis is related to the measurement cycle and laboratory tests performed in CIEMAT that demonstrated that a measurement cycle of 20 min was necessary to obtain reliable data due to the equilibration times of the different parts of the cycle.

-Major Components-

The ambient particulate sulphate monitor is made up of the following major components (see Figure 3.3):

- **Inlet system**: composed of a rain cap followed by a concentric sample line. The sample flow is typically in the range 0.45-0.55 lpm.
- **Impactor:** for PM_1 selective inlet.
- **In-line denuder:** removes SO_2 and other acid gases from the sample stream to lower the background signal. The denuder is coated with a solution containing glycerol, and sodium carbonate.
- **"Background" sampling line:** runs parallel to the actual sampling line, but incorporates a HEPA filter to remove particulate sulphate. By routinely switching between the filtered and unfiltered sample streams, the instrument readings can be continuously adjusted or corrected for changes in background signal that might be produced by traces of SO_2 or other interfering gases. This frequent adjustment for changes in background signal improves the system stability, which in turn improves the limit of detection, though it introduces a limitation in temporal resolution. Excess volume flows back through the inlet.
- **Converter module:** contains the high-temperature reactor, a power supply and the sample handling hardware and electronics necessary to allow switching between the filtered and unfiltered air streams. In the reactor core, which is heated to 1000°C, the SO_4^{2-} particles vaporize and react with a reducing agent to produce SO_2. The converted sample is then filtered by a membrane filter.

This removes particles that are sometimes generated inside the converter core and that might otherwise contaminate the analyser optics.

- **Analyser module:** The analyser module includes the fluorescence based detector and a diaphragm pump that draws approximately 450 cc per minute of flow through the converter core and delivers it to the analyser bench. When the sample flows into the fluorescence chamber, pulsating UV light excites the SO_2 molecules. As the excited SO_2 molecules decay back to lower energy states, they emit UV light, with an intensity that is proportional to the SO_2 concentration. The fluorescence is detected by a photomultiplier tube. The SO_2 concentration is ultimately calculated by comparing the fluorescence signal to the signals generated by calibration gases containing known concentrations of SO_2, and the sulphate concentration is calculated by assuming a 1:1 molar conversion from SO_4^{2-} to SO_2. In order to improve analyser stability and improve self-diagnostic capabilities, the optical bench also incorporates a photodetector, which is located at the back of the fluorescence chamber. This detector continuously monitors the pulsating UV light source and is connected to a circuit that adjust the lamp voltage to compensate for fluctuations in the UV light that could occur due to aging of the lamp.

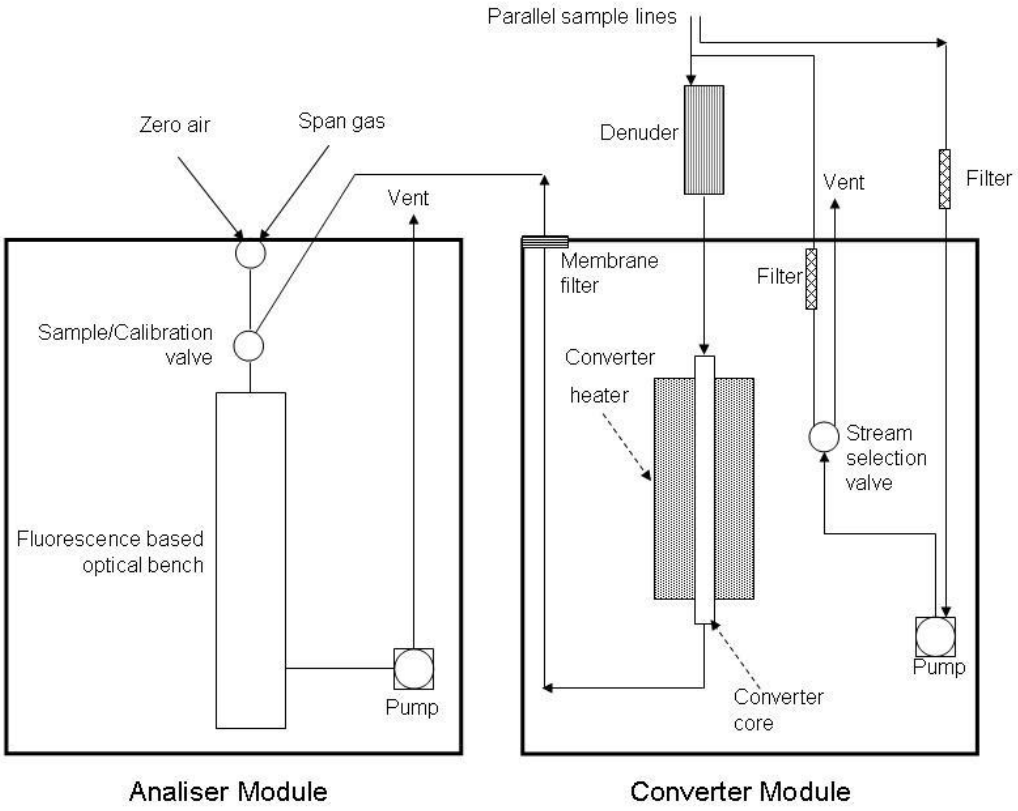

Figure 3.3. Basic scheme of the Sulphate Particulate Analyser (SPA)

-Maintenance and calibrations-

All the routine operations were carried out by following the recommendations of Thermo Electron including lamp voltage check, denuder cleaning and coating, flow check, quartz converter core replacement, pump rebuilding and filter replacement.

Calibration must be performed when any instrument is newly installed, moved, repaired or interrupted for long periods. In addition, in the case of the SPA, the manufacturer recommends an annual calibration of the analyser module. The analyser is calibrated by flowing gaseous purge purified air and span gas containing a known concentration of SO_2 from canisters into the pulse analyser. Theoretical and experimental SO_2 concentrations can be fitted to a straight line, where its coefficients give us the zero-offset and the span coefficient as follows:

$$SO_2\big|_t = (SO_2\big|_{\exp} - zero\_offset) \cdot (calibration\_factor) \cdot (span\_coefficient) \quad \text{(eq 3.1)}$$

The calibration factor is established experimentally at the factory and is an expression of detector sensitivity for a typical instrument of this design. A span coefficient that is

less than 1.00 would suggest that the instrument signal is slightly stronger than expected for a given SO_2 concentration and a span coefficient that is greater than 1.00 would suggest a signal slightly weaker than expected (e.g. due to dirt on the optical windows) for a given SO_2 concentration.

Commercial SO_2 canisters are high above SO_2 ambient concentrations. Nevertheless, according to the manufacturer, the relationship between the detector signal and SO_2 concentration has been demonstrated to be linear. Therefore, measurement of the zero signal and the detector signal at one span point should be sufficient to allow accurate SO_2 measurement over the entire operating range of this instrument.

In CIEMAT, after an initial stage when the span coefficient obtained was notably high (close to 2.00), after some necessary repairs it stabilised in the range 0.70-0.85.

-Comparison with other techniques-

The SPA was field and laboratory evaluated by Schwab et al in 2006. Laboratory tests concentrated on challenging the instruments with ammonium, sodium, potassium, and calcium sulphate aerosol. The instrument performed very well in field and laboratory settings, reporting values that were highly correlated with continuous mass measurements in the lab, and 24-hour filters in the field. Conversion/detection efficiencies for ammonium sulphate in the laboratory and for ambient sulphate aerosol in a rural site were both very close to 80%. Laboratory conversion efficiencies for calcium, sodium, and potassium sulphate salts ranged from 4% to 63%. These lower efficiencies for mineral-type sulphates would be an important consideration in areas with significant concentrations of sea salt or mineral dust sulphate, mainly if measuring coarse-mode aerosol. Laboratory tests performed recently by Chow et al (2012) confirmed that the conversion efficiencies for different salts were: 0.78 ± 0.12 for $(NH_4)_2SO_4$, 0.63 ± 0.05 for potassium sulphate (K_2SO_4), 0.20 ± 0.04 for sodium sulphate (Na_2SO_4), and 0.04 ±0.02 for calcium sulphate ($CaSO_4$).

In CIEMAT, the performance of the instrument was checked by comparison against daily filter-based measurements. Since a PM_1 cut size inlet was used, the mineral-type sulphate fraction is expected to be very low, and thus the efficiency should be good.

Filter samples were collected with a PARTISOL® sampler (section 3.1.1.3). Filters were analysed for soluble ions by ion chromatography (IC) (section 3.3). 46 samples were collected between August 2009 and February 2011 distributed along all the measurement period and covering different meteorological situations. Figure 3.4 shows the good agreement found between the filter-based analysis and the 24-h averaged semi-continuous concentrations.

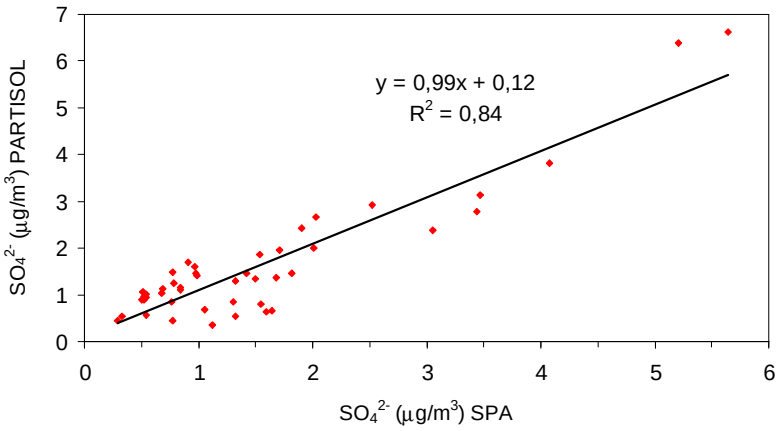

Figure 3.4. PM_1 filter-based (PARTISOL) vs. semicontinuos sulphate (SPA) measurements

We can calculate the error Δx derived from this linear regression by propagation of uncertainties:

for $X = f(A, B, ..., N)$

$$\Delta X^2 = \left|\frac{\delta f}{\delta A}\right|^2 \cdot \Delta A^2 + \left|\frac{\delta f}{\delta B}\right|^2 \cdot \Delta B^2 + ... + \left|\frac{\delta f}{\delta N}\right|^2 \cdot \Delta N^2 \qquad \text{(eq 3.2)}$$

obtaining the following approximation:

$$\Delta x \cong \Delta a \cdot y + \Delta y \qquad \text{(eq. 3.3)}$$

Δa=0.02

The standard error of the predicted y-value for each x in the regression is: Δy=0.28

Thus, this intercomparison gives an estimation of the error in the measure of particulate sulphate by the 5020 SPA around 0.4 $\mu g \cdot m^{-3}$ for the highest concentrations measured, and around 0.30 $\mu g \cdot m^{-3}$ for lower sulphate concentrations, typically found in this sampling point.

3.1.1.2-Ambient Particulate Nitrate Monitor

The Series 8400N ambient particulate nitrate monitor measures the mass concentration of ambient particulate nitrate contained in $PM_{2.5}$ in near real time. It measures all forms of inorganic nitrate, although the collection efficiency varies from one form to another.

The Series 8400 was designed to meet the U.S. Environmental Protection Agency (EPA) $PM_{2.5}$ speciation monitor requirements for the agency's national PM chemical speciation monitoring/sampling network. Studies conducted by this agency demonstrated its capability for the semi-continuous determination of particulate nitrate (and other water-soluble ionic species). Two instruments, an R&P Series 8400N Ambient Particulate Nitrate Monitor (8400N) and an ion chromatography (IC)-based prototype monitor developed at Texas Tech University were evaluated both in the laboratory using aqueous standards and simulated ambient aerosols and in the field during a 3-week period (July 1–21, 2003) by Long and McClenny (2006).

In the CIEMAT station, a time series of particulate nitrate concentrations on $PM_{2.5}$ has been semi-continuously measured by a Rupprecht and Patashnick Series 8400N Ambient Particulate Nitrate Monitor (Figure 3.5) on a 10 min time basis from 2004 to 2011. The UK Automatic Urban and Rural Network (AURN) installed in several stations this instrument in 2003 to obtain semi-continuous measurements of ambient nitrate.

Figure 3.5. Particulate nitrate analyser R&P8400N (Pulse generator and NOx analyser)

-Principle of operation-

The 8400N R&P Ambient Particulate Nitrate Monitor computes the concentration of ambient particulate nitrate by flashing the particulate material collected on a NiChrome (nickel-chromium alloy) strip. The strip is an exchangeable metal piece that serves as the PM impaction surface during sample collection, and undergoes resistive heating during the sample analysis. This strip is flashed in an N_2 atmosphere, producing the reduction of $\cdot NO_3$ to NOx. The resulting gas composition flows through a Pulse Analyser module for the gas concentration measurement. The system incorporates a NOx-chemiluminescence sensor optimised for pulse measurements for time-resolved analyses.

The base line stability and measurement resolution guaranteed by the manufacturer are 0.4 $\mu g \cdot m^{-3}$ and 0.2 $\mu g \cdot m^{-3}$ respectively. The default instrument cycle time is 10 minutes. Of this interval, eight minutes is for collection and the remaining time for the analysis phase.

The monitor's audit routine is automatic and occur due to the provision of a bottle of 5 ppm NOx in N_2 calibration gas. The calibration routines check for leaks and the proper operation of the NOx Pulse Analyser. The system software automatically performs audits; however, the Pulse Analyser and aqueous standards calibrations must be performed by the user.

The monitor has an initial sample flow rate of 5 $l \cdot min^{-1}$ that is surrounded by a high rate sheath flow. The 5 $l \cdot min^{-1}$ flow sample flow rate transports the aerosols into the system. The sheath flow maintains the sample stream at ambient temperature, as well as the analysis section of the Pulse Generator. A 1 $l \cdot min^{-1}$ portion of the sample flow passes through a $PM_{2.5}$ sharp-cut cyclone, followed by a activated carbon denuder, humidification system and a critical orifice that impacts the sample on the NiChrome flash strip, while the remaining 4 $l \cdot min^{-1}$ of the sample flow streams through a flow controlled bypass.

The monitor contains built-in sensors for the measurement of pressure, and the ambient temperature and percent relative humidity.

-Major Components-

The ambient particulate nitrate monitor is made up of the following major components:

- **Inlet system**: composed of a rain cap followed by a concentric sample line and flexible sheath flow line.
- **Pulse Generator:** for the collection, conditioning and flashing of the collected $PM_{2.5}$ material. The sample passes through a $PM_{2.5}$ sharp-cut cyclone, followed by an activated carbon denuder, humidification system, a critical orifice that impacts the sample and maintains a flow rate of 1 $l \cdot min^{-1}$, and impacts on the NiChrome flash strip. The carbon denuder absorbs ambient NOx to avoid interferences. The monitor humidifies the particle-laden sample stream using a Nafion humidification system to maximise the collection efficiency of the impactor .The highest collection efficiency is for particles bigger than 0.1 μm, which explains one of the objectives of the previous humidifier. The collection of humidified particles on the metal impaction plate (flash strip) achieves an efficiency of approximately 98%. The flash volatilization of the collected particulate matter takes place in a N_2 atmosphere at high temperatures through the resistive heating of the metal impactor plate. This creates a pulse of NOx that is quantified in the system's Pulse Analyser. The flash volatilization takes place under thermodynamically favourable conditions, ensuring no cross-interference from ammonium. Sample analysis does not involve any wet chemistry, and a constant sheath flow of ambient air keeps the analysis section of the Pulse Generator at ambient temperature (when the ambient temperature is greater than 5 °C) to avoid condensation/evaporation processes which would alter the final nitrate result.
- **NOx Pulse Analyser:** The Pulse Analyser is designed to measure the concentration of total oxides of nitrogen (NOx). Any possible NO_2 is reduced by a molybdenum converter and the instrument measures the light intensity of the chemiluminescent gas phase reaction of NO and ozone O_3. This process takes place in the reaction cell.

- **Pump:** provides the vacuum necessary to operate the system.
- **Gas canisters:** for the N_2/zero purge gas supply and the NOx in N_2 for calibration verification.
- **Meteorological built-in sensors:** measure ambient temperature, pressure and relative humidity.

-Maintenance and calibrations-

All the routine operations were carried out by following the recommendations of R&P (conversion efficiency, gas analyser calibrations, flow rate audits, etc.) and those included in Harrison (2004). In addition to the automatic routines, the manufacturer recommends performing two calibrations:

-Aqueous standards calibration

The performance of the Pulse Generator + Pulse Analyser modules can be checked through the aqueous standard calibration. 0.2 to 0.8 μl of solution of nitrate concentration (from 20 to 80 ng in 20 ng steps) are deposited on the flash strip and the resulting nitrate concentration given by the Pulse Analyser is measured. The comparison of deposited vs. measured mass is fitted to a least squares straight line, the slope being a measure of the efficiency of the instrument. This calibration was performed at least once a month and the efficiency was found to be in the range 60%-85%.

-Pulse Analyser Calibration

The pulse analyser was calibrated by flowing gaseous purge N_2 and span NO from the canisters into the pulse analyser. Cleaning and calibration of the Pulse Analyser was performed at least once a year. Theoretical and experimental NO concentrations were fitted to a straight line. The efficiency of the Pulse Analyser reached 85% after the annual cleaning and maintenance, and fell to 60% after one year of operation. Nevertheless, this drop is compensated through the aqueous standards calibration, so it does not affect the quality of the data.

-Reaction Cell Pressure Correction-

As the chemiluminescence product is collisionally relaxed, the analysis is sensitive to the absolute pressure of gas in the reaction cell (Rcell). In principle, the reaction cell pressure is maintained at 500 Hg by a regulator connected to the air sampling pump. However, the pump can not maintain this pressure for extended periods. For this reason an Rcell correction factor was developed by Harrison et al (2004) by observing the NO concentration reported for the span gas while artificially varying the total Rcell pressure between 16.6 and 24.4 kPa (absolute). The Rcell correction factor was calculated from the regression coefficients as follows:

$$R_{cellfactor} = \frac{1}{(-0.1177 \cdot R_{cellpressure} + 1.5809)} \qquad \text{(eq.3.4)}$$

This correction has been applied to the whole nitrate database.

-Comparison with other techniques-

Comparison of semi-continuous with off-line techniques is generally performed with the objective of identifying any artefact. Filter-based analysis are also subject to artefacts, however, they are already well-established and can be taken into account when comparing with other techniques. Chemical speciation on filter-based sampling provides averaged PM concentrations, typically on a 24-hr basis. Losses of semivolatile NH_4NO_3 from the particles can occur during sampling and equilibration (Long et al, 2003). The loss of nitric acid (HNO_3) from particles during sampling results in a negative artefact, or an underdetermination, of the ambient particulate nitrate concentration. In contrast, adsorption of gas-phase HNO_3 onto a collection surface result in a positive artefact, or an overdetermination, of ambient particulate nitrate levels (Long et al, 2005).

Measurements by Harrison et al., (2004) at the Baltimore Supersite showed that the R&P 8400N NO_3^- was significantly lower than 24-h filter NO_3^- with discrepancies ranging from 18% to 49% and averaging 33% for their 9.5 month study period. A study by Wittig et al., (2004) at the Pittsburgh Supersite also found that the R&P 8400N NO_3^- was lower (average 17%) than filter measured NO_3^-.

In flow chamber studies using laboratory generated aerosols of NH_4NO_3 and $NaNO_3$ showed that the R&P 8400N measured NO_3^- is in quantitative agreement with TEOM® total mass measurements (Hogrefe et al., 2004a). The manufacturer recommends using aqueous KNO_3 salt solutions to determine the NO_3^- to NO_x conversion efficiency. However, lower conversion efficiency when a mixed aqueous salt solution of $(NH_4)_2SO_4$ and KNO_3 is used has been observed (Rattigan et al, 2006). Furthermore, Long and McClenny (2006) observed NO_3^- on a Teflon filter placed downstream of the flash vaporization cell, implying incomplete conversion of the NO_3^- to NO_x. Therefore, it appears that the NO_3^- to NO_x conversion efficiency in the R&P 8400N instrument is somewhat dependent on the aerosol composition. The instrument response is therefore likely to vary with location. Variation in the 24-h filter comparisons between urban and rural location was observed by Rattigan et al (2006).

A comparison with PARTISOL daily filter-based measurements was performed in CIEMAT. The filters collected were analysed for soluble ions by ion chromatography. 24 samples were collected between November 2004 and June 2005.

The relation between the nitrate measured was found to be:

$$NO_3^-\big|_{PARTISOL} = 1.32 \cdot NO_3^-\big|_{R\&P} \qquad \text{(eq. 3.5)}$$

Like the cited studies above, the comparison performed in Madrid showed that the RP instrument underestimated the nitrate concentration value, observing also an increasing bias as the concentration increased. The incomplete collection of particles in the strip impactor (not all the particles are swollen to 0.14 μm by the humidity) and the temperature differences between the ambient and the impactor strip, especially for those samples taken during very cold days, could be some of the reasons for these differences. A partial evaporation due to the removal in the previous denuder of the gaseous HNO_3 in equilibrium with the solid phase, and an incomplete conversion of particulate nitrate to NO, which could be more difficult as the deposit thickness increases, could also contribute to the increasing disagreement at higher nitrate concentrations.

Taking into account the intercomparison results and also including offset and calibration errors, the overall accuracy in the measure of particulate nitrate by R&P

8400N analyser was estimated around 20% for concentrations below 10 μg·m^{-3} and 20–30% for higher concentrations (Gómez-Moreno et al, 2007).

The Ambient Particulate Nitrate Monitor R&P 8400N has been used in a semi-continuous basis in the CIEMAT sampling site from **2004 to 2011** except for the transfer of the monitor to Barcelona during the DAURE winter and summer campaigns in 2009. This fact, together with interruptions due to experimental failures has resulted in a total **75% of data coverage in Madrid**.

3.1.1.3-Sampling devices

-MOUDI and nano-MOUDI-

Particle size distribution was obtained by a rotating micro-orifice deposit impactor MOUDI M110R, manufactured by the MSP Corporation (Marple et al, 1991). This impactor collects ten size fractions according to aerodynamic size by inertial impaction in ten multi-nozzle stages. The equivalent cut-off diameters (at 50% efficiency) are: 10, 5.6, 3.2, 1.8, 1.0, 0.56, 0.32, 0.18, 0.1 and 0.056 μm, with a flowrate of 30 lpm (1.8 m^3·h^{-1}). The substrates used were 10 uncoated aluminium substrates and additionally a quartz fiber backup filter to collects particles < 0.056 μm. No coating material (typically grease) was used to avoid artefacts in the analysis procedure. After sampling the substrates and also the quartz filter were chemically analysed by ion chromatography (IC) for soluble ions, obtaining a size distribution for each of the ions (sulphate, nitrate, nitrite, ammonium, calcium, sodium, magnesium, potassium and chloride).

MOUDI sampling was performed in an urban background site in Barcelona and a rural site in the Montseny Natural Park during the winter DAURE campaign (February-March 2009). The results in Barcelona were compared with the previous study in Madrid carried out by Plaza et al (2011).

Nano-MOUDI (Marple and Olson, 1999) adds three stages to the M110R MOUDI. The cut sizes are 0.032, 0.018 and 0.010 μm, with a flowrate of 10 lpm (0.6 m^3·h^{-1}). When nano-MOUDI is used connected to MOUDI, the backup filter is deployed after the final stage of nano-MOUDI, collecting particles <0.010 μm.

An MSP Nano-MOUDI Model 115 was acquired in 2010. The performance of the instrument was tested and sampling during selected meteorological scenarios was performed.

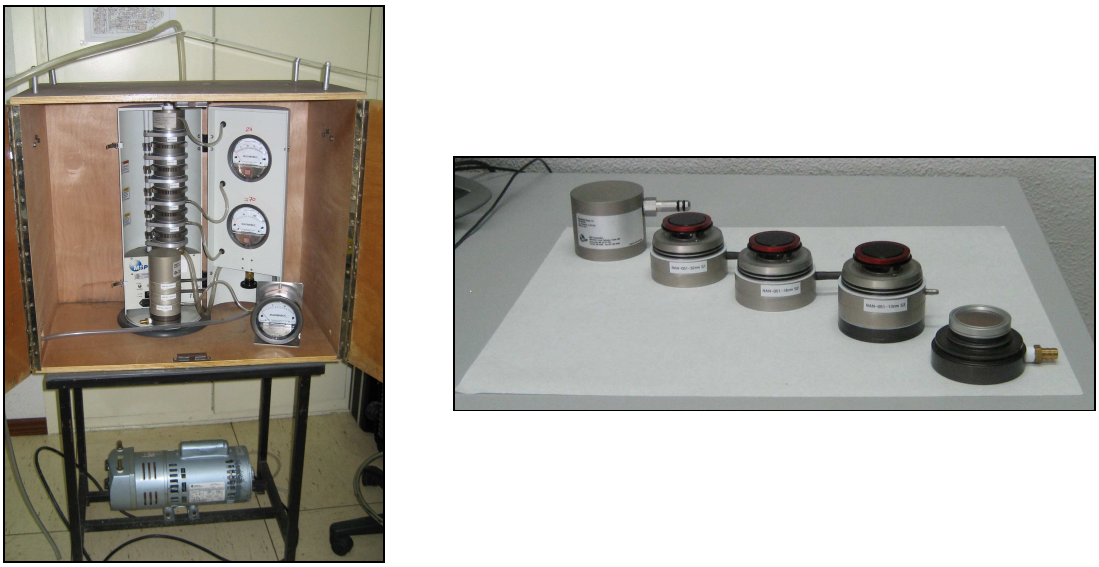

Figure 3.6. MOUDI and nano-MOUDI (left). Disassembled nano-MOUDI (right)

Potential artefacts in the MOUDI during the sampling have been studied by other researchers. The discrepancy found between MOUDI and high-volume samplers for gravimetrically determined PM_{10} mass is probably due to losses on the walls of the impactor or bounce-off from the collecting surface. A MOUDI using aluminium substrates can experience loss of particles due to bounce and re-entrainment at RH below 70% when particles are dry (Stein et al., 1994; Chang et al., 1999). Cabada et al. (2004) observed coarse particle losses affecting the PM_{10} fraction (15-20%) but not the $PM_{2.5}$ one. Comparing MOUDI and TEOM® measurements, an underestimation of 5% of the first instrument was found, which can not be considered a significant difference. The substrate material can account for a percentage of these differences. For instance, the use of aluminium non-greased substrates can reduce the collection efficiency because of bounce-off. High temperatures during summer or sun exposition of the MOUDI instrument can produce losses of the semivolatile compounds. A seasonal variation in losses was observed by Cabada et al (2004) for the inorganic material, with 70% losses for the aerosol nitrate during summer and good agreement during winter. In the case of sulphate, most of the studies have shown <20% differences between

MOUDI and filter samplers in winter and summer since it is not a semivolatile compound. Results from Nie et al (2010) indicate that the body of the MOUDI sampler was heated during daytime under direct sunshine, enhancing the losses of semivolatile compounds with respect to the nighttime. In order to minimise this kind of artefacts, in the studies discussed in this thesis the MOUDI impactor was introduced in an open wooden shelter to avoid the direct exposition to the sun radiance.

-PARTISOL-

The R&P Partisol 2300 Speciation Sampler is a 12-channel sampling platform for particulate matter and gaseous species analysis. The sampler meets the U.S. Environmental Protection Agency (USEPA) chemical speciation requirements for $PM_{2.5}$ sampling. The flow rate is 1 $m^3 \cdot h^{-1}$ (16.7 $l \cdot min^{-1}$)

Twelve Speciation Sampling Cartridges can be fitted to the 12 channels and the instrument can be programmed to perform sequential or simultaneous sampling, with the possibility of grouping the channels.

The Speciation Sampling Cartridges contain the following features:

- A sharp-cut $PM_{2.5}$ impactor.
- Up to two high-efficiency honeycomb denuders.
- A four-stage filter pack for 47 mm diameter filters.
- A straight flow path followed by the sample stream between the $PM_{2.5}$ impactor and the four-stage filter pack.
- A modified cartridge with a sharp-cut PM_1 impactor was also used.

Figure 3.7. R&P Partisol 2300 Speciation Sampler

PARTISOL sampling system was used to collect filter samples for intercomparisons with the nitrate and sulphate semi-continuous instruments. The particulate material was collected on a 47 mm quartz filter. Glass honeycomb denuders were used when particulate nitrate analyses were to be performed. These denuders were coated with a solution of Na_2CO_3 and glycerol to absorb nitric acid and other acidic gases (Koutrakis et al, 1993). This procedure prevents the adsorption of gas-phase HNO_3 on the quartz filter, which would react with gaseous ammonium to form ammonium nitrate and result in a positive artefact.

-High volume samplers-

Several MCV high volume samplers with DIGITEL® and MCV® PM_{10}, $PM_{2.5}$ and DIGITEL ® PM_1 size cut inlets were used. The flow rate was 30 $m^3 \cdot h^{-1}$ (500 lpm).

Figure 3.8. High-volume samplers (left) and PM_{10} size cut inlet (right)

High volume samplers were used for intercomparisons with GRIMM1107® optical monitor (described below). Particulate material mass collected on glass fibber filters was determined by gravimetry. Clean filters were conditioned for 24h in a controlled chamber at 20°C and 50% relative humidity before being weighted in a precision balance inside the chamber (see Figure 3.9).

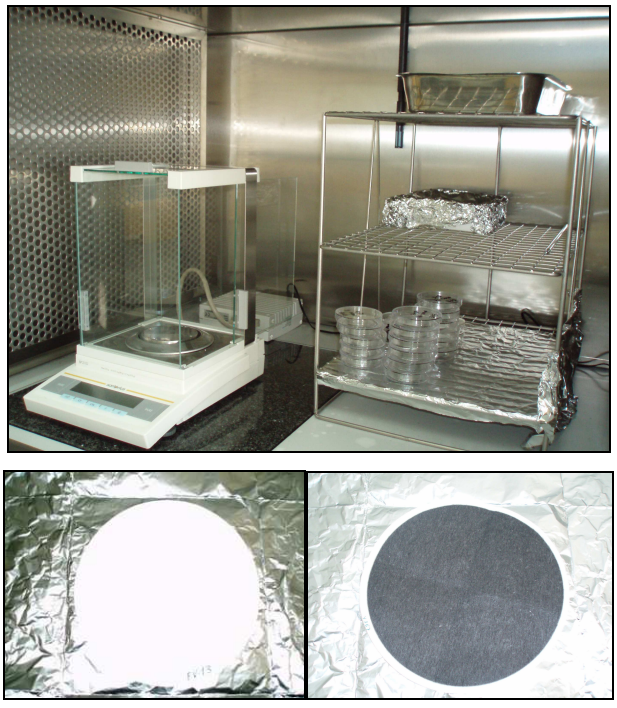

Figure 3.9. Controlled chamber (top). Quartz filter before and after 24-h sampling

After sampling, the filters were conditioned in the same conditions and then weighted again. The weight difference is related to the aerosol mass and, given the volume of air

sampled, can be converted to aerosol mass ambient concentration. The procedure was carried out following the European normatives EN12341 (1999) and EN14907 (2005) for PM_{10} and $PM_{2.5}$ sampling and gravimetric analysis.

3.1.2-Further instrumentation at the CIEMAT station

This section describes further instrumentation in the CIEMAT station used in this thesis as ancillary techniques. Data or processed results from these instruments have been used to complete the analysis of sulphate and nitrate and obtain a full picture of the behaviour of these pollutants.

-Differential Optical Absorption Spectrometer (DOAS)-

Figure 3.10. DOAS spectrometer OPSIS AR-500

Gaseous species were measured in the CIEMAT site by a DOAS (OPSIS AR-500) along a 228 m horizontal path with a mean height of 10 m above ground level and the optical receiver in the same location as the nitrate instrument. The measurement time is 1m 30s for NO and 30s for NO_2 and SO_2, and the full cycle for all species takes 7m 24s. Data were interpolated to a 10-min time basis before further analysis. Certified gas canisters and the calibration bench OPSIS CB100 with gas cells of 1.4 and 10 cm in length were used for the multipoint calibration of NO, NO_2 and SO_2. A careful offset assessment of their instrumental signals was carried out previously to obtain reliable concentration values for these species. This was necessary since relatively little is

known about the instrument analytical characteristics even with those species that are known to be reliable for DOAS measurements (e.g., SO_2, NO_2, and O_3). There are only a few studies that can actually provide an intensive interpretation of DOAS performance for particular trace gas (Virkkula, 1997).

Gaseous SO_2, NO and NO_2 concentrations measured by DOAS were jointly analysed with semi-continuous particulate sulphate and nitrate in the periods when there were reliable data.

-Optical Particle Counters-

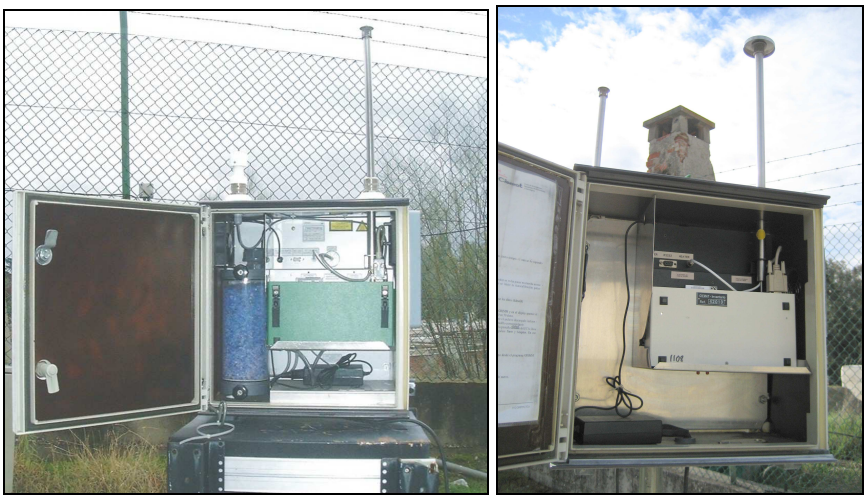

Figure 3.11. GRIMM 1107 (left) and GRIMM1108 (right) optical particle counters

Two optical particle counters (OPC), models GRIMM1108 and GRIMM1107 are operating in CIEMAT to measure aerosol counts and PM in a 10-min basis. GRIMM1108 OPC provides size distribution in the range from 0.3 to 20 μm. Each particle is sized by the amount of incident laser light scattered at an angle of 90°, obtaining a 15-channel particle number concentration by optical size (Peters et al, 2006). These data, in the form of particle counts, may be converted to a volume distribution -assuming spherical particles- or a mass distribution. In calculating the latter, particulate density information is required. Generally, this information is not available, so that a uniform density is assumed. According to the manufacturer, the reproducibility of the GRIMM1108 in particle counting is ±2%. GRIMM1107 OPC

employs 31 channels to obtain a similar distribution, which is converted into a mass distribution by the internal software in the same way as the GRIMM 1108 does, resulting in PM_{10}-$PM_{2.5}$-PM_1 ambient concentrations (Grimm and Eatough, 2009). Both instruments incorporate a heater at the sample inlet with the purpose of drying the aerosol. GRIMM1107 also incorporates a silica gel dryer to dilute the sample with dry air. This dryer is typically used only when relative humidity exceeds a certain value which was set to 70%.

Intercomparison campaigns between 24h-averaged GRIMM1107 PM_{10}-$PM_{2.5}$-PM_1 mass concentrations and aerosol mass obtained by gravimetry from filter-based collected high volume samplers have been carried out between October 2008 and April 2011. Linear relations were always found, however, they showed a high variability in different seasons and meteorological conditions. Thus, the GRIMM1107 data have only been used in selected periods, and mainly following a qualitative approach. The GRIMM1108 particle counts were converted to a volume distribution for some case studies.

- Scanning Mobility Particle Sizer-

Figure 3.12. SMPS 3936. Long DMA 3081+ CPC 3775

The particle size distribution in the particle size range 0.015-0.60 μm was measured using a Scanning Mobility Particle Sizer (TSI SMPS 3936 instrument), combining a long Differential Mobility Analyser (DMA) and a Condensation Particle Counter (CPC model 3775), and working in the scanning mode (Wang and Flagan, 1990). Before entering the DMA the sample was dried by a nafion drier, and particles were neutralised by a Kr-85 radioactive source. Once in the DMA, particles were classified according to their electrical mobility and then counted by the CPC.

The particle number size distribution obtained from the combined use of the GRIMM1108 and the SMPS were employed to characterise the size of the volcanogenic Eyjafjallajökull aerosol detected in Madrid in May 2010.

-Raman LIDAR-

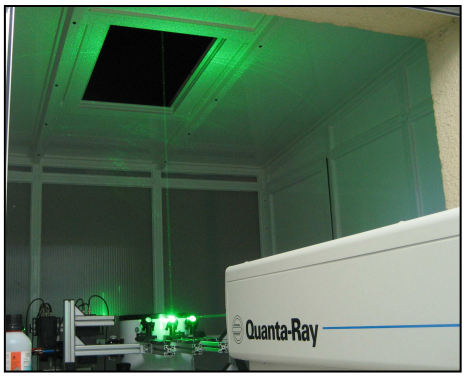

Figure 3.13. Raman Nd:YAG LIDAR NY82-20

At the CIEMAT site, a ground-based Raman LIDAR station belonging to the European Aerosol Research LIdar NETwork (EARLINET) (Bösenberg et al., 2001) is in regular operation. The LIDAR system is a laboratory equipment based on a Nd:YAG laser source (Spectra Physics LAB170-30) operating at the 2nd harmonic (532 nm), a 30 cm diameter Newtonian telescope and photon-counting acquisition system. The laser energy is 115 mJ/pulse, operated vertically due to safety reasons. Lidar signals are recorded with 1-min resolution (1800 laser pulses), but later 30- to 60-min files are averaged in order to derive resolved aerosol extinction coefficient profile with signal-to-noise ratio value larger than 3 up to the tropopause. The noise component is estimated from altitudes between 25 and 30 km, where the laser light contribution can

be considered negligible. The Klett-Fernald algorithm (Klett, 1981) is used in the inversion, with an aerosol extinction-to-backscatter ratio of 50 sr (continental aerosols). The Rayleigh extinction coefficient is calculated based on the revision of the theory (Bodhaine et al., 1999) using vertical profiles of meteorological data from the nearby AEMET radiosonde station at the Barajas airport.

-Meteostation-

Figure 3.14. CIEMAT meteorological station

Meteorological information in Madrid was obtained from a permanent tower installed at CIEMAT with the following parameters and heights: wind direction and speed at 52 m agl, precipitation and solar radiation at 31 m agl, temperature and humidity at 4m agl and pressure at ground level. Data were recorded every 10 min.

3.2-Passive high absorption ammonia samplers

During 2011 two field campaigns focused on NH_3 characterization in several Spanish cities were carried out. The first taken place in Madrid lasted from 17/03/2011-28/03/2011, 64 samplers being installed all over the Metropolitan Area of Madrid. The objective was to identify ammonia sources and also to obtain the highest possible spatial coverage in order to calculate mean levels. Out of these 64 samplers, 29 were placed in traffic sites, 28 in urban background, 6 close to sewage treatment plants and 1 close to an incinerator plant. Some of the samplers were placed close to sewers (with a duplicate separated some 10 m). The sampling points selected included the air quality

monitoring network of the Madrid city hall sites (Figure 3.15, left). The campaign was repeated in summer (01/07/2011-11/07/2011) to account for seasonal variations.

Figure 3.15: ALPHA samplers in the Madrid ammonia winter campaign

For NH_3 sampling, high sensitivity passive samplers (CEH ALPHA: Adapted Low-cost High Absorption) designed at the Centre for Ecology and Hydrology of Edinburgh (Tang et al., 2001) were used. Samplers are made up of circular polyethylene vial with one open end. An internal ridge supports a filter, which is coated with a solution of phosphorous acid in methanol, which serves to capture the ammonia. The open end is capped with a polytetrafluoroethylene (PTFE, also known as "Teflon") membrane (27mm diameter) allowing gaseous ammonia to diffuse through. After exposure, filters were stored at 4°C until analysis.

3.3-Analytical techniques

-Ion Chromatography-

The impactor substrates and quartz filters were analysed for soluble ions in the *Laboratorio de Cromatografía Iónica* of the *Departamento de Tecnología* of CIEMAT Solutions were prepared immersing the samples in 10-15 ml of distilled water prior to the analysis with a Dionex 300 and Dionex 500 ion chromatographs. The columns used were Dionex IonPac AG12A, AS12A (4x250 mm) for ammonium and Dionex IonPac AG9, AS9 (4x250 mm) for sulphate and nitrate with flow rates of 1.20 $ml \cdot min^{-1}$ (cations) and 1.0 $ml \cdot min^{-1}$ (anions). The eluents were 20 $mmol \cdot l^{-1}$ methanesulphonic acid (MSA) for cations and 2 mM Na_2CO_3 / 0.75 mM $NaHCO_3$ for anions. The injection volume was

50 μL and detectors were CSRS Suppressed conductivity for ammonium and AMMS Suppressed conductivity for sulphate and nitrate. For the external calibration standards of 0.1-2.5 $mg \cdot l^{-1}$ concentration were used. In addition to nitrate, sulphate and ammonium, chloride and nitrite anions and potassium, magnesium and calcium cations were also analysed.

Two replicates for each sample were analysed and their concentration values averaged. Blank values for each ion and substrate material were subtracted. The lower limit detectable in the ionic chromatographic analysis was 0.01 $\mu g \cdot m^{-3}$. The accuracy of the concentration determination for nitrate, sulphate and ammonium for the sampled period was estimated as 0.03, 0.01 and 0.02 $\mu g \cdot m^{-3}$, as obtained from the standard deviation of blank filter averages. Differences found in the blank concentrations were not significant for these ions.

-Analysis of ALPHA samplers-

The filters sampled in the 2011 inter-city ammonia campaign were leached in 3ml of distilled water to determine ammonium ion concentrations by ion selective electrode. The ambient air ammonia concentrations were calculated according to the principle of diffusion of gases from the atmosphere along a sampler of defined dimensions onto an absorbing medium, governed by Fick's law. The uptake rate of a sampler is a function of the length, L (m) and the cross sectional area, A (m^2) of the stationary air layer within the sampler, and can be calculated provided that the diffusion coefficient, D ($m^2 s^{-1}$) of the gas of interest is known.

Therefore, the effective volume of air sampled (V, m^{-3}) by the CEH ALPHA sampler is given by:

$$V = \frac{D \cdot A \cdot t}{L} \quad \text{(eq. 3.6)}$$

where: t=time of exposure (h)

D=2.09 x 10-5 $m^2 s^{-1}$ at 10°C
A= 3.4636 x 10^{-4} m^2
L=0.006 m

The air concentration of a pollutant (X, $\mu g \cdot m^{-3}$) can then be calculated as:

$$X = \frac{(m_e - m_b)}{V} \qquad \text{(eq. 3.7)}$$

Where: m_e= amount of NH_3 collected on sample

m_b= amount of NH_3 in blank sample

3.4-Air Quality Networks

Data from the following air quality networks have been used:

Red de Vigilancia de la Calidad del Aire del Ayuntamiento de Madrid. This is the local air quality network belonging to the Madrid Township. This network was created in the 1970s to monitor air pollution in the city, being mainly oriented to traffic, the main source of atmospheric pollutants in this city. As a consequence, the majority of the stations, which could be classified as hot spots, were located within the urban area, whereas only one station measured urban background ambient levels. In 2009 the network was adapted to the EU directive 2008/50 on ambient air quality and cleaner air for Europe and at present it comprises 26 stations including 9 traffic, 12 urban background and 3 suburban sites. A number of gaseous pollutants, PM_{10} and $PM_{2.5}$ are monitored, although not all of the pollutants are monitored in every station. PM_{10}, $PM_{2.5}$, SO_2, NO_2 and NOx evolution in Madrid has been studied in two stations from 1999 to 2011: 1 traffic (Escuelas Aguirre) and 1 urban background (Casa de Campo) sites, on a time resolution of 1 h (see Table 3.1, figure 3.16).

Station	***Coordinates***	***NO_2-NOx***	***SO_2***	***PM_{10}-$PM_{2.5}$***
Escuelas Aguirre	40° 25' 17.76" N 3°40' 56.34" W 672 m asl	**Chemiluminescence**	UV-fluorescence	**Microbalance**
Casa de Campo	40° 25' 9.68" N 3° 44' 50.4" W 645 m asl	**Chemiluminescence**	UV-fluorescence	**Microbalance**

Table 3.1. Air Quality Monitoring Network sites of the Madrid city hall and sampling techniques of the parameters used in this study

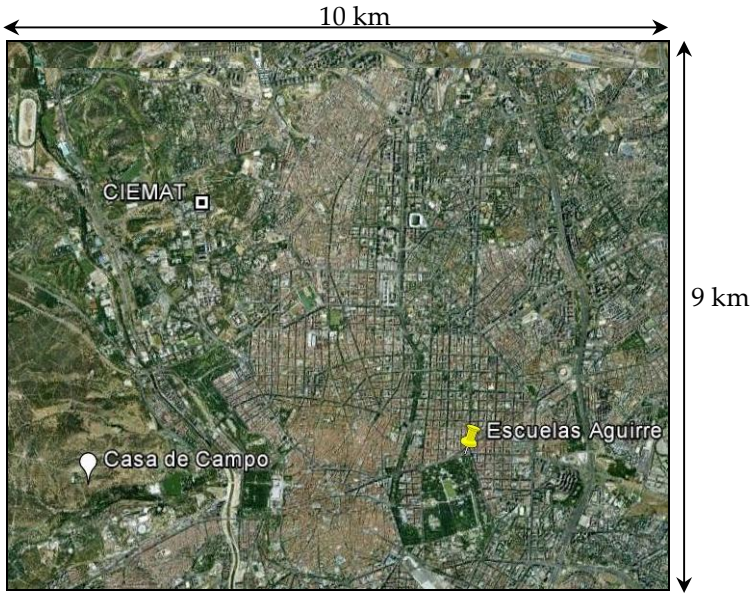

Figure 3.16. Location of Escuelas Aguirre, Casa de Campo and CIEMAT

EMEP (European Monitoring and Evaluation Programme) is a scientifically based and policy driven programme created to study transboundary air pollution problems. A monitoring network formed by more than 250 rural stations is operated across 37 European countries. 17 of these stations are located in Spain (13 operative in 2012) and managed by the Spanish Meteorological Agency (AEMET). Gaseous pollutants are semi-continuously monitored at the Spanish stations. The EMEP network in Spain takes samples of PM_{10} and $PM_{2.5}$ filters in 24-h periods and perform chemical speciation (major ions) of particulate matter. Variations of PM, particulate SO_4^{2-}, NO_3^- and NH_4^+ in PM_{10} and precursor gases were studied in the central Iberian Peninsula (ES09) from 1999 to 2011. The EMEP pollutant data were also relevant in the identification of transport events.

Figure 3.17 shows the location of the 17 Spanish EMEP stations together with the CIEMAT site.

Figure 3.17. Geographical situation the Spanish EMEP stations -represented by circles- and the CIEMAT site -square-

The names, coordinates and measurement techniques of the parameters used in this work can be consulted in Appendix I.

UK Automatic Urban and Rural Network (AURN)

The AURN is the UK's largest automatic monitoring network, currently formed by 109 sites. It includes automatic air quality monitoring stations measuring $PM_{2.5}$ nitrate, oxides of nitrogen (NOx), sulphur dioxide (SO_2) and particles (PM_{10}, $PM_{2.5}$) among others. These sites provide high resolution hourly information and daily ion concentrations based on filter sampling followed by ion chromatography.

NOx, SO_2, and particulate NO_3^- and SO_4^{2-} time evolution has been studied in three sites:

1 traffic (Marylebone Road), 1 urban background (North Kensington) and 1 rural (Harwell).

Station	*Coordinates*	*$PM_{2.5}$ nitrate*	*NOx*	*SO_2*	*Ions in PM_{10}*
Marylebone Road	51° 32.6′ N 0° 9.92′ W 27 m asl	R& P 8400N Nitrate Analyser	Chemiluminescence	UV-fluorescence	PARTISOL sampler + IC
North Kensington	51° 31.27′ N 0° 12.8′ W 27 m asl	R& P 8400N Nitrate Analyser	Chemiluminescence	UV-fluorescence	PARTISOL sampler + IC
Harwell	51° 34.72' N 1° 20.26' W 137 m asl	R& P 8400N Nitrate Analyser	Chemiluminescence	UV-fluorescence	PARTISOL sampler + IC

Table 3.2. Air Quality Monitoring sites of the AURN and sampling techniques of the parameters used in this study.

3.5- Air quality models

Air Quality modelling is the mathematical prediction of ambient concentrations of air pollution, based on measured inputs. Air quality modelling is the necessary substitute for ubiquitous air quality monitoring, which is impossible.

Modelling for air quality management purposes typically falls into two broad categories: dispersion modelling and receptor-based modelling. Dispersion models are used to predict ambient concentrations and receptor (or source apportionment) models use ambient data to determine the sources. When they are differentiated taking into account the treatment of the transport equations they can be classified in Lagrangian and Eulerian models. Both Lagrangian and Eulerian dispersion models have been used in this work and will be described below.

Lagrangian models based on trajectories computed from meteorological fields became available in the mid 1970s (Heffter and Taylor, 1975). They are a widely used tool for the description of transport processes and to identify the source regions of pollutants. Until early 1980s, trajectory calculations were done on constant pressure surfaces,

commonly referred to an isobaric trajectory model. Other types of trajectory models were then scarcely available because of limited vertical levels of meteorological data and limited computer resources. It was experimentally approved that trajectories resulted from the isobaric model, which neglects the vertical transport, were not as accurate as those obtained from the isentropic model (transport on the surface of constant potential temperature) and 3D-wind model (estimating transport from 3D-wind field). These two models are commonly included in recent trajectory programs. HYSPLIT and FLEXTRA are two of the free trajectory models. Both models use the method of Petterssen (1940) for the time integration, but FLEXTRA uses a flexible time steps in integration that achieves both good integration accuracy and fast computing speed.

Eulerian box models are based on the mass conservation of a species inside a fixed box of volume $\Delta x \Delta y \Delta z$. They simulate the atmosphere in varying degree of detail by mathematically representing emissions; initial and boundary concentrations of chemical species; the chemical reactions of the emitted species and of their products; and the local meteorology such as sunlight, wind, and temperature. In this way, an understanding of the atmosphere's chemistry and meteorology is combined with estimates of source emissions.

Backtrajectories obtained from FLEXTRA and Hysplit models and results from the Eulerian aerosol distribution prediction model NAAPS have been used in this thesis.

-FLEXTRA-

The Lagragian trajectory model was developed at the Norwegian Institute for Air Research in the Department of Atmospheric and Climate Research (Stohl et al., 1995) The FLEXTRA model uses bicubic horizontal, quadratic vertical and linear time interpolation to determine the three wind components at a trajectory position and employs the numerical method of Petterssen for the trajectory calculation. The model has been validated with constant level balloon flights, manned gas balloon flights and meteorological tracers.

FLEXTRA backtrajectrories can be obtained from the Nilu webpage (http://www.nilu.no/projects/ccc/trajectories/) for EARLINET sites (including Madrid)

for fixed daytimes (0, 6, 12 and 18 UTC) and heights (1500, 3000 and 5000 m. agl). These backtrajectories have been used in this work for the identification of aerosol transport episodes.

-HYSPLIT-

The HYSPLIT (HYbrid Single-Particle Lagrangian Integrated Trajectory) model is a complete system for computing sample air parcel trajectories to complex dispersion and deposition simulations. The initial development was a result of a joint effort between the US NOAA (National Oceanic and Atmospheric Administration) and Australia's Bureau of Meteorology (Draxler and Hess, 1998). Without the additional dispersion modules, Hysplit computes the advection of a single pollutant particle. The model's default configuration assumes a 3-dimensional fluid particle distribution (horizontal and vertical). The trajectories module computes single or multiple (space or time) simultaneous trajectories forward or backward in time. Default vertical motion uses omega field, although other motion options are isentropic, isosigma, isobaric and isopycnic. Hysplit can use a variety of meteorological data files, providing links to ARL and NWS meteorological data servers. Access to forecasts and archives includes NCAR/NCEP reanalysis and additional software converts MM5, RAMS, COAMPS, WRF, and other data.

The model allows performing integrated trajectory clustering. Cluster analysis is an exploratory data analysis tool which sorts different objects into groups in a way that the degree of association between two objects is maximal if they belong to the same group and minimal otherwise. Trajectory cluster analysis is used to discover structures in large groups of trajectories.

Hysplit groups trajectories in order to minimise the cluster spatial variance (SPVAR). Initially, total spatial variance is zero. Each trajectory is defined to be a cluster, in other words, there are N trajectories and N clusters. For the first iteration, for every combination of trajectory pairs, the cluster spatial variance (SPVAR) is calculated. SPVAR is the sum of the squared distances D between the endpoints of the cluster's component trajectories and the mean of the trajectories in that cluster. Then the total

spatial variance (TSV), the sum of all the cluster spatial variances, is calculated. The pair of clusters combined are the ones with the lowest increase in total spatial variance. After the first iteration, the number of clusters is N-1.

$$SPVAR = \sum_{traj\_in\_cluster} \left(\sum_{traj\_endpoints} D^2 \right) \qquad \text{(eq 3.8)}$$

$$TSV = \sum SPVAR \qquad \text{(eq 3.9)}$$

The iterative process follows in the same way, pairing either clusters formed by individual trajectories or groups of trajectories. The iterations continue until the last two clusters are combined, resulting in N trajectories in one cluster.

The iterative steps just before large increases of TSV indicate the possible final number of clusters. The program will usually produce at least one possible outcome set of clusters. Typically more than one outcome is given, and the user must then subjectively choose one for the final result.

Hysplit backtrajectory clustering has been used in this work to classify air masses according to their origin and relate them to pollutant levels measured in Madrid on ground level on autumn 2009 and winter 2010-2011. This has allowed identifying the presence of aerosol SIC transported from the European continent.

-NAAPS (Navy Aerosol Analysis and Prediction System)-

NAAPS is a global aerosol model developed by the Naval Research Laboratory (NRL) in Monterey (California, USA). It is a near-operational system for predicting the distribution of tropospheric aerosols. The model is a modified form of that developed by Christensen (1997). The NRL version uses global meteorological fields from the Navy Operational Global Atmospheric Prediction System (NOGAPS) (Hogan and Rosmond, 1991; Hogan and Brody 1993) analyses and forecasts on a 1 X 1 degree grid, at 6-hour intervals and 24 vertical levels reaching 100 mb. The model performs 120-hour forecasts in near-real-time and simulates sulphate, dust and smoke ambient

concentrations. Sulphate formation is modelled using GEIA (Global Emissions Inventory Activity) sulphur emissions databases.

NAAPS results can be downloaded in plotted format in http://www.nrlmry.navy.mil/aerosol/. Regional plots of NAAPS results are presented in a 4-panel format, containing:

- Optical depth at a wavelength of 0.55 microns for three components: sulphate, dust, and smoke.
- Sulphate mass mixing ratio ($\mu g \cdot m^{-3}$) at the surface.
- Dust mass mixing ratio ($\mu g \cdot m^{-3}$) at the surface.
- Smoke mass mixing ratio ($\mu g \cdot m^{-3}$) at the surface.

NAAPS maps have been used to determine the sulphate aerosol distribution across Europe during the identified events and compare the predicted with the measured concentrations in Madrid in the case of the European transport episodes.

3.6-Data analysis tools

A consistent set of tools for air quality data analysis does not exist. Data treatment has been performed using several standard data analysis software: Excel, OriginPro and Matlab. The Openair software has also been used (Carslaw et al, 2011). The Openair project is a UK Natural Environment Research Council (NERC) knowledge exchange project that provides a collection of open-source tools for the analysis of air pollution data. The project is led by the Environmental Research Group at King's College London, and supported by the University of Leeds. The Openair project makes available a range of existing techniques and develops new ones for the analysis of air pollution data. Openair uses the statistical/data analysis software environment R as a platform.

3.6.1-Time series analysis

Time series of the pollutants studied have been analysed. The temporal evolution of nitrate, sulphate and their precursor gases in the central Iberian Peninsula have been

studied to account for significant increments or reductions. Data from air quality networks has been used for this analysis. Further analysis was performed in four selected sites, with the focus on temporal patterns in three timescales: yearly, weekly and daily. Data were averaged monthly, daily and hourly (when available) for a time period from December 2004 to July 2011 always when data coverage was over 50%. Errors were estimated using the 95% Confidence Intervals of the arithmetic means, thus obtaining:

$$95\%CI = 1.96\frac{\sigma}{\sqrt{n}} \qquad \Longrightarrow \qquad x \in \left[\bar{x} \pm 1.96\frac{\sigma}{\sqrt{n}}\right] \qquad \text{(eq. 3.10)}$$

σ=standard deviation

n=number of samples

Pearson's correlation coefficient r (eq. 3.11) was used to correlate two samples of simultaneous data (Xi, Yi), being Xi a time series of a pollutant concentration and Yi a time series of a meteorological parameter.

$$r = \frac{1}{n-1}\sum_{i=1}^{n}\left(\frac{x_i - \bar{x}}{\sigma_x}\right)\left(\frac{y_i - \bar{y}}{\sigma_y}\right) \qquad \text{(eq. 3.11)}$$

3.6.2-Aerosol size number and volume distributions

The SMPS software provides aerosol number and volume distributions assuming spherical particles. To study the number distribution of aerosols obtained jointly with SMPS and GRIMM1108 optical particle counter the counts data given by the latter must be transformed into a number distribution.

The output of the OPC are 15 channels i of counts l-1 of particles with diameter > xi μm

We must obtain the following discrete distribution in integral form (figure 3.18), where the aerosol number N is normalised by $\log_{10}(D)$ to take into account the size of the channel:

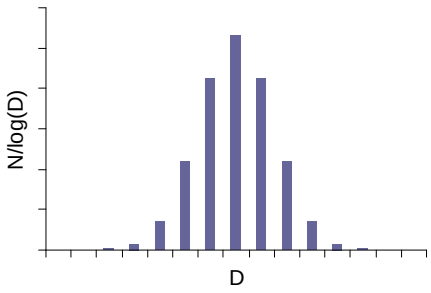

Figure 3.18. Discrete aerosol number distribution

For every channel i we need $\left.\frac{N}{\Delta \log(D)}\right|_i = \frac{\mathrm{N_i}}{\log(\mathrm{D_{i\,upper}}) - \log(\mathrm{D_{i\,lower}})}$ (eq 3.12)

If we want to obtain the volume distribution V/log(D) we need:

$$\left.\frac{\Delta V}{\Delta \log(D)}\right|_i \approx \frac{N_i \frac{4}{3}\pi (R_{mean})^3}{\log(D_{iupper}) - \log(D_{ilower})} \qquad \text{(eq 3.13)}$$

Rmean= (1/2) particle diameter in the middle of the channel

This volume distribution assumes spherical particles.

Similarly, we would obtain the mass distribution by multiplying by the aerosol density ϱ. However, the aerosol density is not usually available, and it would be necessary to assume a certain ϱ based on bibliography.

The SMPS data and the GRIMM1108 data points obtained by these transformations can be fitted to a probability distribution, as well as the ions mass concentrations obtained by MOUDI and nano-MOUDI. Empirically, it is found that the lognormal distribution is the one which fits best to the experimental aerosol size distributions (Hinds, 1982).

Lognormal unimodal and bimodal distributions were fitted using the OriginPro 7.5 software. The equation for the unimodal distribution given by OriginPro 7.5 is:

$$y = y_0 + \frac{A}{\sqrt{2\pi}wx}\exp\left\{\frac{-\left[\ln\left(x/x_c\right)\right]^2}{2w^2}\right\} \quad \text{(eq 3.14)}$$

Where: y0= offset, typically set to 0

xc=center of the mode (geometric mean d_g)

w=width of the mode. w=lnσg where σg is the geometric standard deviation of the distribution

A=amplitude

Given these parameters, the modal diameter m, which is the diameter D at which the distribution reaches its global maximum, is obtained using the Hatch-Choate equations (Hinds, 1982, pp 91)

$$m = d_g e^{-\ln^2 \sigma_g} \qquad \text{(eq 3.15)}$$

OriginPro provides statistical error values for the fitted parameters xc and w. The errors of m and σg calculated from them can be obtained by propagation of uncertainties (eq. 3.2)

Bimodal lognormal distributions were also fitted with OriginPro adding a new term to equation 3.14.

$$y = y_0 + \frac{A}{\sqrt{2\pi}wx}\exp\left(\frac{-\left[\ln\left(x/x_c\right)^2\right]}{2w^2}\right) + \frac{B}{\sqrt{2\pi}w'x}\exp\left(\frac{-\left[\ln\left(x/x'_c\right)^2\right]}{2w'^2}\right) \quad \text{(eq 3.16)}$$

4- TIME EVOLUTION AND CONCENTRATIONS OF SECONDARY INORGANIC COMPOUNDS AND PRECURSORS IN SELECTED SITES OF THE MADRID AIR BASIN

4- TIME EVOLUTION AND CONCENTRATIONS OF SECONDARY INORGANIC COMPOUNDS AND PRECURSORS IN SELECTED SITES OF THE MADRID AIR BASIN

4.1- Introduction

This thesis focuses on the analysis of the behaviour of particulate nitrate and sulphate in the fine fraction in the city of Madrid. But, before going into more detail on these issues, it is interesting to know, as a preliminary framework, the time evolution on an historical basis, of these compounds and related pollutants in the Madrid air basin. This chapter identifies the basic features of the time series and other previous results of the pollutants of interest in the last decade.

For this purpose, the concentrations of particulate matter and precursor gases (NO_2, NOx and SO_2) at three representative locations (traffic, urban background and rural) of the Madrid air basin has been described. Gaseous ammonia and particulate sulphate, nitrate and ammonium have been also depicted for the rural site, belonging to the EMEP network, together with the sulphate and nitrate time series registered at the CIEMAT site. Annual patterns of sulphate, nitrate and ammonium obtained in previous sampling campaigns at the traffic site are also discussed.

The most recent publications on time series comprehend time periods up to the year 2008 (Salvador et al, 2012) and 2010 (IDAEA-CSIC, 2012). These PM and gases time series have been extended in this work until the end of 2011 to include the full time range covered in this thesis. This information is discussed taking into account the evolution of primary emissions of these compounds in the European Union and Spain. It has been observed that reductions in emissions of primary pollutants do not translate directly into reductions in ambient levels concentrations of them and their chemically derived compounds (Harrison et al., 2008). The generation processes of secondary PM -highly nonlinear- and the contribution of the natural fraction causes important differences between variations in emissions and ambient concentrations. Further insight can be obtained by exploring the relationships between secondary compounds and their precursors. Available data allowed comparing particulate sulphate and nitrate concentrations with gaseous precursors in the EMEP rural stations.

Ammonia is the SIC gaseous precursor which has been studied to a lesser extent up to date in the region. Real Decreto 102/2011 recommends the vigilance of levels of ammonia in ambient air, establishing the requirement of measuring ambient ammonia at five rural background stations and one traffic site in every city with more than 500000 inhabitants. Quality objectives are not defined yet in Spain, but the main role of this gas in the formation of secondary particles raises the interest in its study. In general terms, it is recognised that the main source of ambient ammonia is livestock waste, followed by vegetation and agriculture. However, the source contribution to ammonia in urban areas is not yet fully characterised. These sources would include traffic, human and pets´ excretions, landfill, garbage, household products and sewage treatment plants. In 2002, Perrino et al studied the relationship between gaseous ammonia and traffic in the urban area of Rome. The authors found at traffic sampling sites a high correspondence between the hourly time evolution of a primary gas emitted by traffic, carbon monoxide, and NH_3. This study also corroborated the result of Kean et al (2000) who found that in the USA the petrol-engine vehicles equipped with three-way catalytic converters generated gaseous ammonia. NH_3 would be generated through the reaction taking place in the converter between NO and H, which is produced particularly when the air:fuel ratio of the combustion is lower than the stoichiometric value (fuel-rich engine). In contrast, three-way catalytic converters are associated to outstanding reductions in NOx emissions, which raises controversy on the use of these devices. Most recent observations also suggest that the NH_3 emissions from the traffic exhaust could be a major source of the ambient NH_3 in other urban areas such as New York (Li et al, 2006) Manchester (Whitehead et al, 2007) or Beijing (Meng et al, 2011).

A study conducted in the city of Madrid with the aim of characterizing levels of ammonia took place in 2011. It focused in two different periods - winter and summer, and allowed to make a first estimation of the main contributing sources. Madrid campaigns formed part of a larger study conducted in 6 Spanish cities: Barcelona, A Coruña, Valencia, Huelva and Santa Cruz de Tenerife. The results obtained in Barcelona were presented by Reche et al (2012). High ammonia levels were found compared with other European cities. In winter, traffic sites registered the highest

concentrations, but in summer biological sources –humans, sewage systems and garbage containers- dominated ammonia emissions. These results were extended in Barcelona with a summer campaign in which real-time measurements of ammonia were performed (Pandolfi et al, 2012). The contributions of both road traffic and biological sources to ambient levels were confirmed. The high ammonia concentrations found were pointed out as the cause of high secondary nitrate and sulphate levels and the importance of the gas-to-particle phase partitioning (volatilization or ammonium salts formation) was also stated. The results obtained in the campaigns in Madrid are presented in this thesis.

4.2-Methods

-Sites-

In addition to the CIEMAT site, the following representative stations have been chosen:

- Escuelas Aguirre (40° 25' 17.63" N, 3° 40' 51.90" W, 672 m asl) – urban traffic station belonging to the Madrid Township network (*Red de Calidad de Aire del Ayuntamiento de Madrid)*. PM_{10}, NO_2, NOx and SO_2 data available.
- Casa de Campo (40° 25' 6.07" N, 3° 44' 14.19" W, 645 m asl) - urban background station belonging to the Madrid Township network (*Red de Calidad de Aire del Ayuntamiento de Madrid)*. PM_{10}, $PM_{2.5}$, NO_2, NOx and SO_2 data available.
- Campisábalos (41° 15' 53.44" N, 3° 7' 36.31" W, 1 360 m asl) - rural station included in the EMEP network. NO_3^-, SO_4^{2-}, NH_4^+, PM_{10}, $PM_{2.5}$, NO_2, NOx, SO_2 and NH_3 data available.

Escuelas Aguirre is located in the Madrid city centre, in a residential and business area. The distance to the very busy streets Alcalá and O'Donnell (yearly average 47812 and 49756 vehicles day^{-1}) is <50 m. The Retiro park is at a distance <100 m.

Casa de Campo is located in a big green area on the western part of the city. Some minor roads with low traffic density (< 5000 vehicles day^{-1}) are within a distance <100 m.

Campisábalos is located in the centre of the Iberian Peninsula, on the far north-eastern limit of the Madrid air basin and 100 km away from the city. It is surrounded mainly by coniferous forest and in a small proportion by farmland and pasture. Ancillary data

from other EMEP stations in the central Peninsula (San Pablo de los Montes, Risco Llano and Peñausende) have been depicted.

At Escuelas Aguirre and Casa de Campo, pollutants were registered continuously with automatic devices. PM_{10} was registered with a Tapered Element Oscillating Microbalance (TEOM). A comparison with particulate matter collected on quartz fibre filters was performed during 2011 at Escuelas Aguirre. Samples were collected twice a week with an MCZ-16 sampler with a flow rate of 68 $m^3 \cdot h^{-1}$. The size cut inlet was a DIGITEL PM_{10}. The correlation coefficient was over 0.95. A 1.02 correction factor was determined and applied to the whole sampling time period.

In the EMEP stations, samples of particulate matter are taken in 24-h periods, from 07:00 to 07:00 UTC. PM_{10} and $PM_{2.5}$ are collected with high volume samplers on quartz fibre filters. Ion concentrations in PM_{10} are determined by ion chromatography, atomic absorption spectrometry or visible spectrometry, depending on the compound. Sulphur dioxide is continuously monitored with UV pulsed fluorescence analysers. NOx and NO_2 are also continuously monitored using the chemiluminescence technique. Gaseous ammonia is determined on a weekly basis using visible spectrophotometry.

At the CIEMAT station, particulate nitrate and sulphate were semicontinuously measured following the methodology described in Chapter 3.

Trend analysis has been performed using the Openair software. The trends depicted together with the monthly mean concentrations have been calculated using the smoothTrend function. Figures 4.2 to 4.4, 4.6 to 4.9, 4.11 and 4.14 show pollutant monthly concentrations together with the smooth lines fitted to the data. The shaded areas indicate the 95 % confidence intervals (CI) of the fit. Monthly means have been calculated when the data capture was over 50%. The line is determined using Generalised Additive Modelling (GAM). The model is a relationship between time and pollutant concentration, i.e. a trend. The amount of smoothness in the trend is optimised in the sense that it is neither too smooth -therefore missing important features- nor too variable -fitting noise rather than real effects (Carslaw et al., 2007). The model accounts for autocorrelation. Autocorrelation happens when consecutive

points in time are related to one another, which is the case for data with a strong seasonal effect.

Information regarding time trends in $\mu g \cdot m^{-3}$ $year^{-1}$ has also been calculated with Openair using the Theil-Sen method. Given a set of n (x, y) pairs, the method calculates the slopes between all pairs of points. The Theil-Sen estimate of the slope is the median of all these slopes. The Theil-Sen estimator is very robust and tends to provide accurate confidence even when outliers are present. The case when the seasonal variation is removed before calculation has been considered.

All information regarding emissions, including data used to calculate the reductions, and the information on pollutant trends in the EU has been extracted from the European Union emission inventory report 2011 (EEA, 2011) and the Air Quality in Europe 2012 Report (EEA, 2012). Following the methodology used in EEA 2011, reductions in emissions have been calculated as $\frac{C_f - C_0}{C_0}$ (%), where C_f and C_0 are the final and initial yearly concentrations.

-NH_3 campaign-

The samplers (dosimeters) were prepared and analysed using the techniques described in sections 3.2 and 3.3. Laboratory and field blanks were prepared. Laboratory blanks were stored at 4°C after preparation. Field blanks were carried to the campaign in the same box as the dosimeters deployed and subsequently stored at 4 °C until analysis.

City	Winter campaign	Summer campaign
Madrid	17/03/2011 - 28/03/2011	01/07/2011 - 11/07/2011
A Coruña	7/10/2010 - 18/10/2010	15/07/2011 - 25/07/2011
Huelva	04/11/2010 - 18/11/2010	31/05/2011 - 10/06/2011
Sta. Cruz de Tenerife	02/12/2010 - 15/12/2010	06/09/2011 - 19/09/2011
Barcelona	17/01/2011 - 28/01/2011	07/07/2010 - 21/07/2010
Valencia	14/02/2011 - 02/03/2011	17/06/2011 - 27/06/2011

Table 4.1. Cities and dates corresponding to the NH_3 campaigns

The ammonia concentrations detected were slightly higher for field with respect to laboratory blanks. NH_4^+ values were less than 0.2 times the smallest concentrations found in the exposed dosimeters. The method was validated in Barcelona by Reche et al (2012). Analysis of samples was performed as part of the whole study in carried out in 6 Spanish cities. The full study was carried out between October 2010 and September 2011. A 10-14 days sampling was performed in each of the participating cities twice: one in a period representative of winter conditions and the other in a period representative of summer conditions. Table 4.1 shows the dates when the passive samplers were deployed and collected for every city.

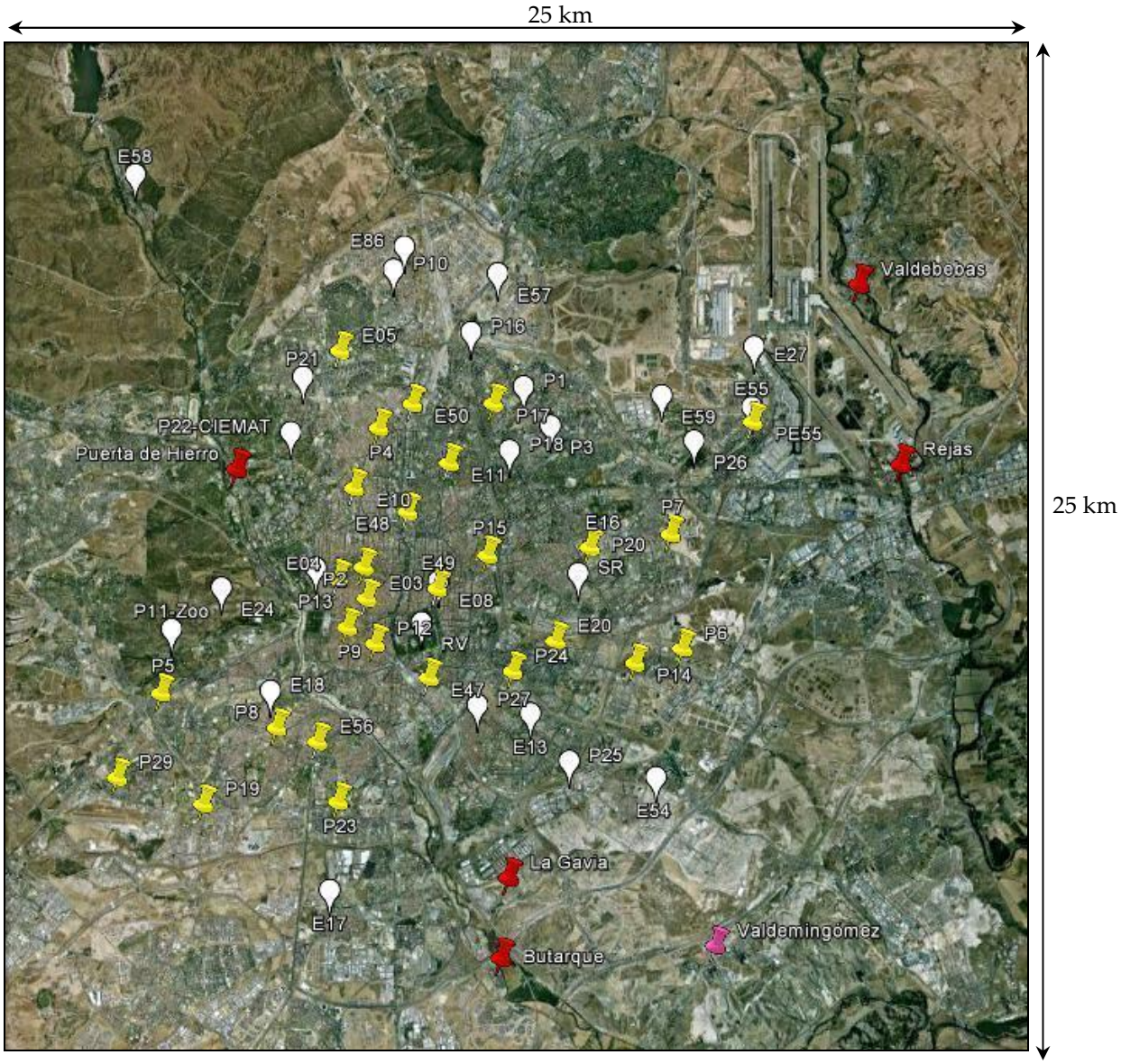

Figure 4.1. Sampling sites during the winter NH_3 campaign in Madrid.

Figure 4.1 shows the sampling sites selected for the winter NH_3 campaign in Madrid.

For the NH_3 characterization within Madrid from 17/03/2011-28/03/2011, 64 samplers were deployed all over the Metropolitan Area of Madrid with the objective of identifying ammonia sources and also obtaining the highest possible spatial coverage in order to calculate mean levels. Out of these 64 samplers, 29 were placed in traffic sites (yellow drawing pins), 28 in urban background sites (white balloons), 6 close to sewage treatment plants (red drawing pins) and 1 close to an incinerator plant (purple drawing pin). Some of the samplers were placed close to sewers (in this case with a duplicate separated at least 10 m). The sampling points selected included some of the air quality monitoring network of the Madrid city hall sites (points labelled as EX-EXX, RV and SR). The campaign was repeated in summer (01/07/2011-11/07/2011) to account for seasonal variations. In the summer campaign the number of available passive samplers was smaller. As a consequence some sites had to be removed from the campaign and 51 samplers were deployed in total. Table AII.1, in Appendix II, shows the names and coordinates of all sites in the winter and summer ammonia campaigns in Madrid.

4.3-Time Series and Concentrations

4.3.1-Particulate matter

Figure 4.2 shows the PM_{10} monthly evolution at Escuelas Aguirre, Casa de Campo and Campisábalos for the period 2001-2011.

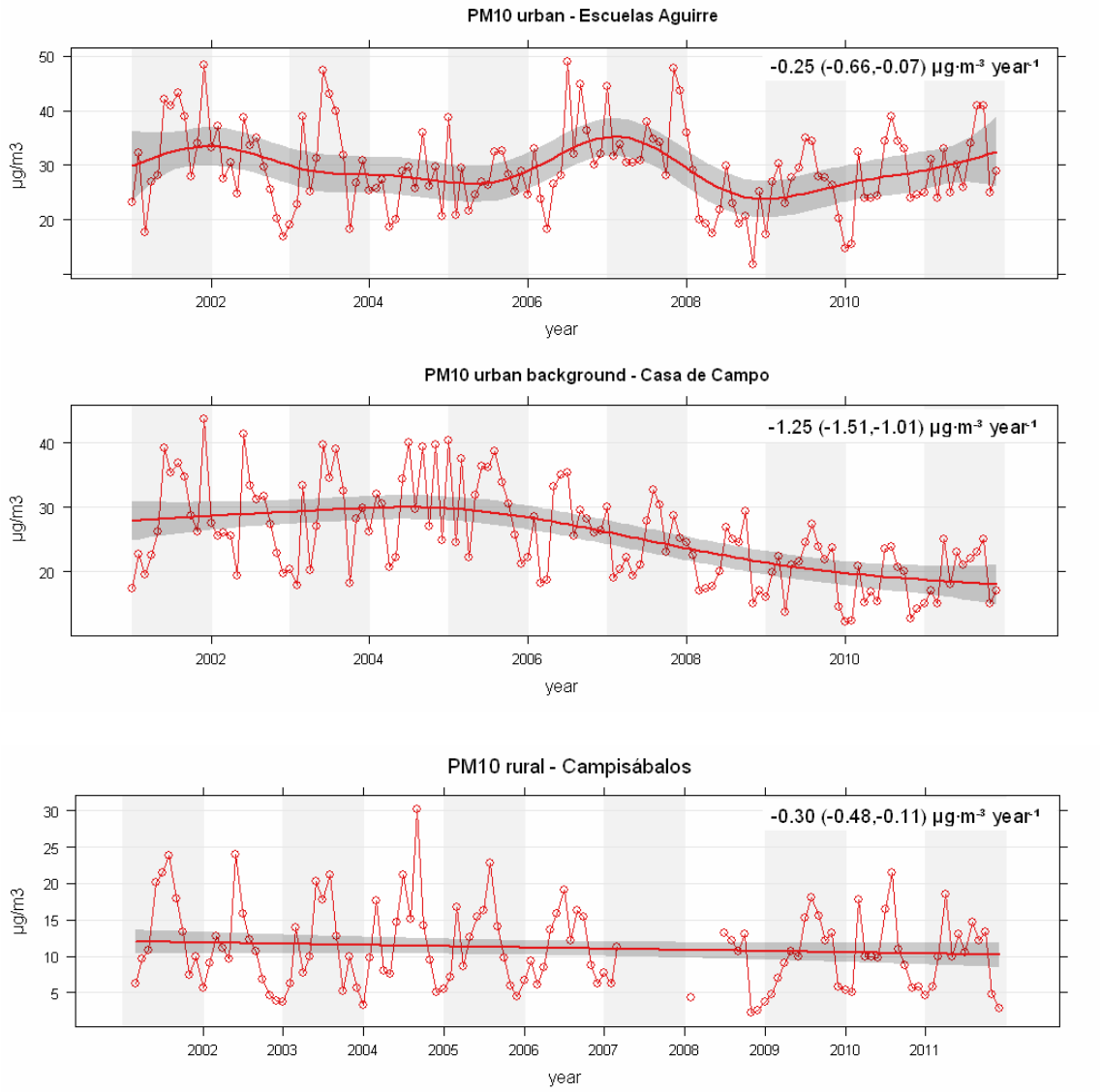

Figure 4.2. PM_{10} monthly evolution

PM_{10} mean yearly levels are in the range 25-40 µg·m^{-3} and 15-35 µg·m^{-3} in the urban and urban background sites, and <15 µg·m^{-3} at Campisábalos. PM_{10} showed a seasonal cycle in the rural and urban background sites, with maximum values at summer. The trend analysis showed a slight decreasing trend at the rural site when the seasonal variability is removed (-0.30 µg·m^{-3} year^{-1}). The decrease is enhanced at the urban background site (-1.25 µg·m^{-3} year^{-1}), but not at Escuelas Aguirre

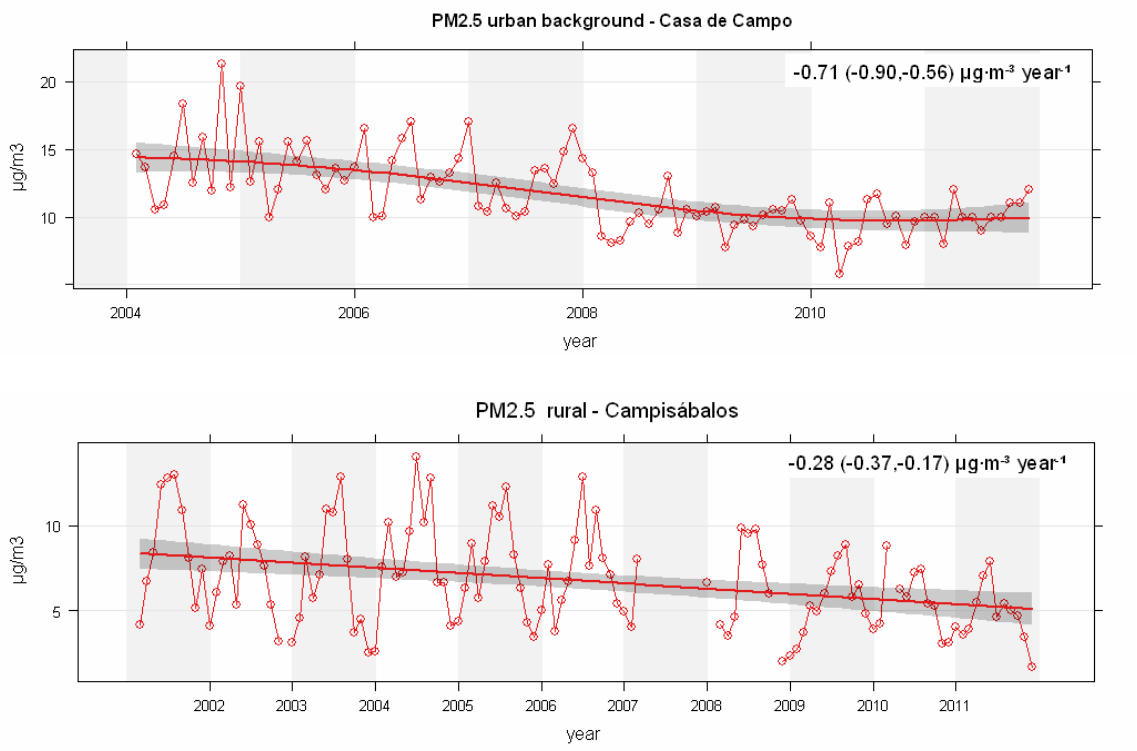

Figure 4.3. $PM_{2.5}$ monthly evolution

Figure 4.3 depicts the monthly evolution of the fine particulate matter concentration at Casa de Campo and Campisábalos. Concentrations are about half PM_{10} concentrations at Casa de Campo, but only slightly smaller at Campisábalos. $PM_{2.5}$ showed a seasonal cycle at Campisábalos, peaking at summer, the same as PM_{10}. Decreasing trends were seen at the two stations, with slightly smaller variations in concentration units per year than PM_{10} (~0.28 $\mu g \cdot m^{-3}$ $year^{-1}$ at Campisábalos and ~ 0.71 $\mu g \cdot m^{-3}$ $year^{-1}$ at Casa de Campo). There was a clear drop in $PM_{2.5}$ levels in 2008 at the urban background site. The lack of data for 2007 at the rural site does not allow confirming the decrease of fine particulate matter concentrations in the whole Madrid air basin in 2008, although figures suggest this.

In the European Union, PM_{10} and $PM_{2.5}$ emissions decreased by 14% and 20% between 2000 and 2009. Outstanding particulate matter emission reductions took place in Spain in this period (24% and 23%), in agreement with the decreasing trends found. In average, in Europe the highest relative reductions were achieved in public electricity, heat production and heavy duty vehicle emissions; but emissions from passenger cars also decreased in the last decade. Increased PM concentrations due to the eruption of

the Eyjafjallajökull volcano in Iceland have been noted in 2010 in a number of European sites.

4.3.2-Nitrate, NO_2 and NOx

-Nitrate-

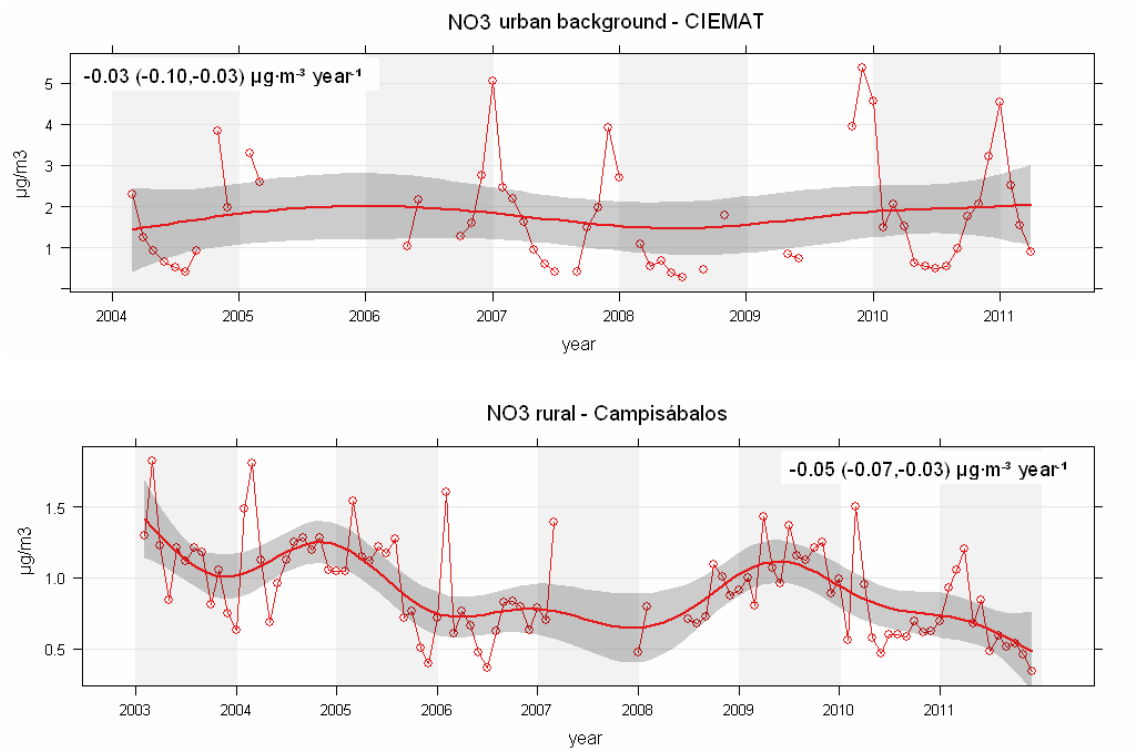

Figure 4.4. Nitrate in $PM_{2.5}$ at CIEMAT and nitrate in PM_{10} at Campisábalos monthly evolution

Time series of secondary inorganic compound concentrations are only available in the EMEP sites and the CIEMAT station. Nonetheless, filter-based sampling campaigns took place at Escuelas Aguirre in 1999-2000, 2007 and 2011. Figure 4.4 (top) shows the monthly evolution of fine nitrate at CIEMAT from 2004 to 2011. A clear seasonal pattern is observed, with maximum concentrations in winter reaching 4 $\mu g \cdot m^{-3}$ or higher, while in summer values are below 1 $\mu g \cdot m^{-3}$. A secondary maximum appears in March 2010. A small decrease can be seen. Figure 4.4 (bottom) shows the monthly evolution of nitrate in PM_{10} at Campisábalos, with levels always under 2 $\mu g \cdot m^{-3}$, significantly lower than fine nitrate at CIEMAT. Although seasonal maxima usually

took place in winter time, the pattern is quite irregular, with a maximum in summer 2009. The trend was slightly downwards in the studied time period. In general, at Escuelas Aguirre (Figure 4.5) the highest particulate nitrate values are registered in the cold season, but similarly as at Campisábalos, no clear annual patterns are observed. Fine nitrate monthly concentrations were smaller at Escuelas Aguirre than at CIEMAT, which is probably related to sampling losses due to the semivolatile nature of NH_4NO_3.

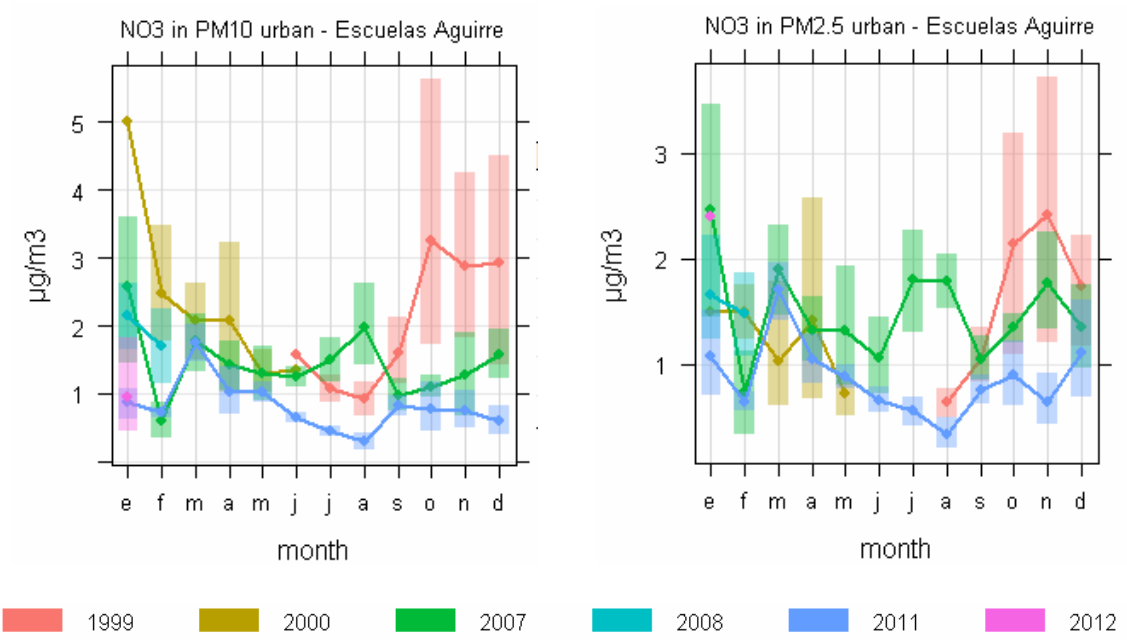

Figure 4.5. Nitrate in PM_{10} and PM2.5 monthly evolution at Escuelas Aguirre. The shading shows the 95% CI of the mean.

To get more insight into the nitrate monthly evolution this parameter has been plotted at two additional EMEP sites.

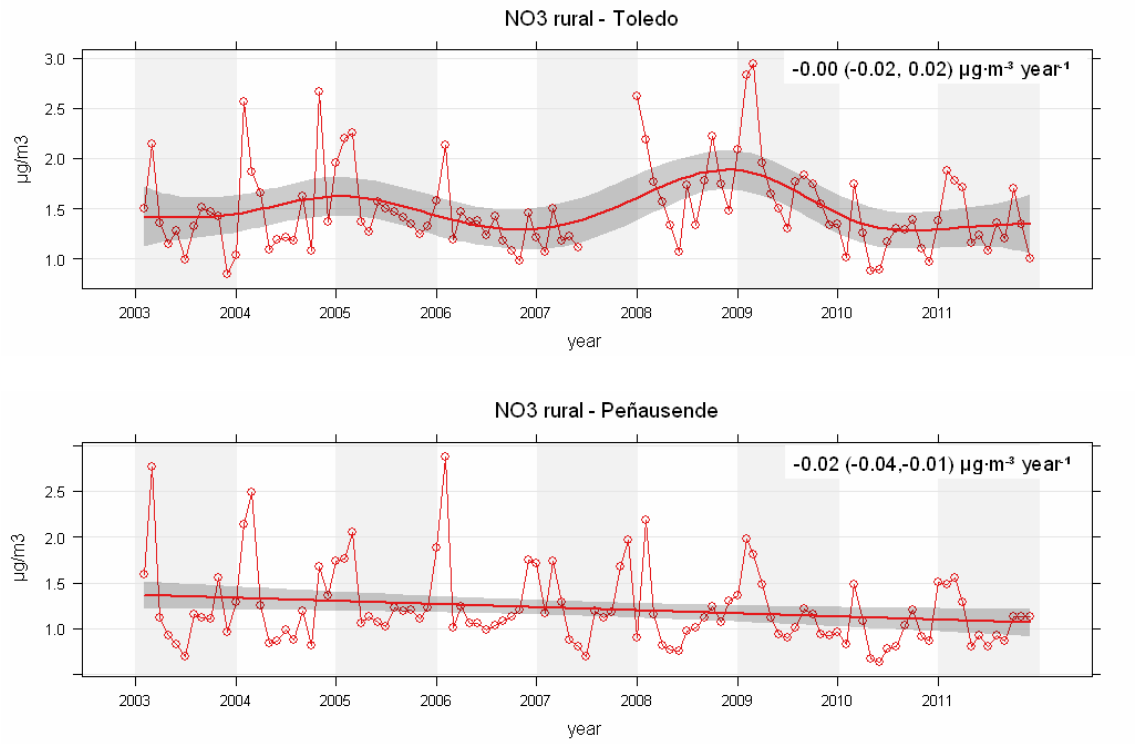

Figure 4.6. Nitrate in PM_{10} monthly evolution at EMEP sites in Toledo and Peñausende

Figure 4.6 (top) shows the evolution in ES01 (San Pablo de los Montes) and ES15 (Risco Llano), two equivalent stations in the province of Toledo which have been in use in the last decade (ES15 2003-2007; ES01 2008-2011). The bottom panel corresponds to ES13 (Peñausende). In Toledo, the time evolution of nitrate shows similarities with Campisábalos, although the 2008-2009 maximum is reached earlier. This maximum cannot be confirmed at the CIEMAT station with the data available. No trend is found at this station. In Peñausende, also in the Central Iberian Peninsula but out of the Madrid air basin, nitrate shows a seasonal pattern peaking in winter. The yearly maximum in 2010 appears in March at all the rural stations studied. In this month nitrate transport from the European continent took place, as will be exposed in Chapter 6.

We can conclude that nitrate evolution in the stations of the central Iberian Peninsula tends to show maximum concentrations during the cold season, according to the thermal phase equilibrium of particulate and nitric acid. However, there might be regional superimposed effects in the Madrid air basin which do not affect other stations.

-NO_2 and NOx-

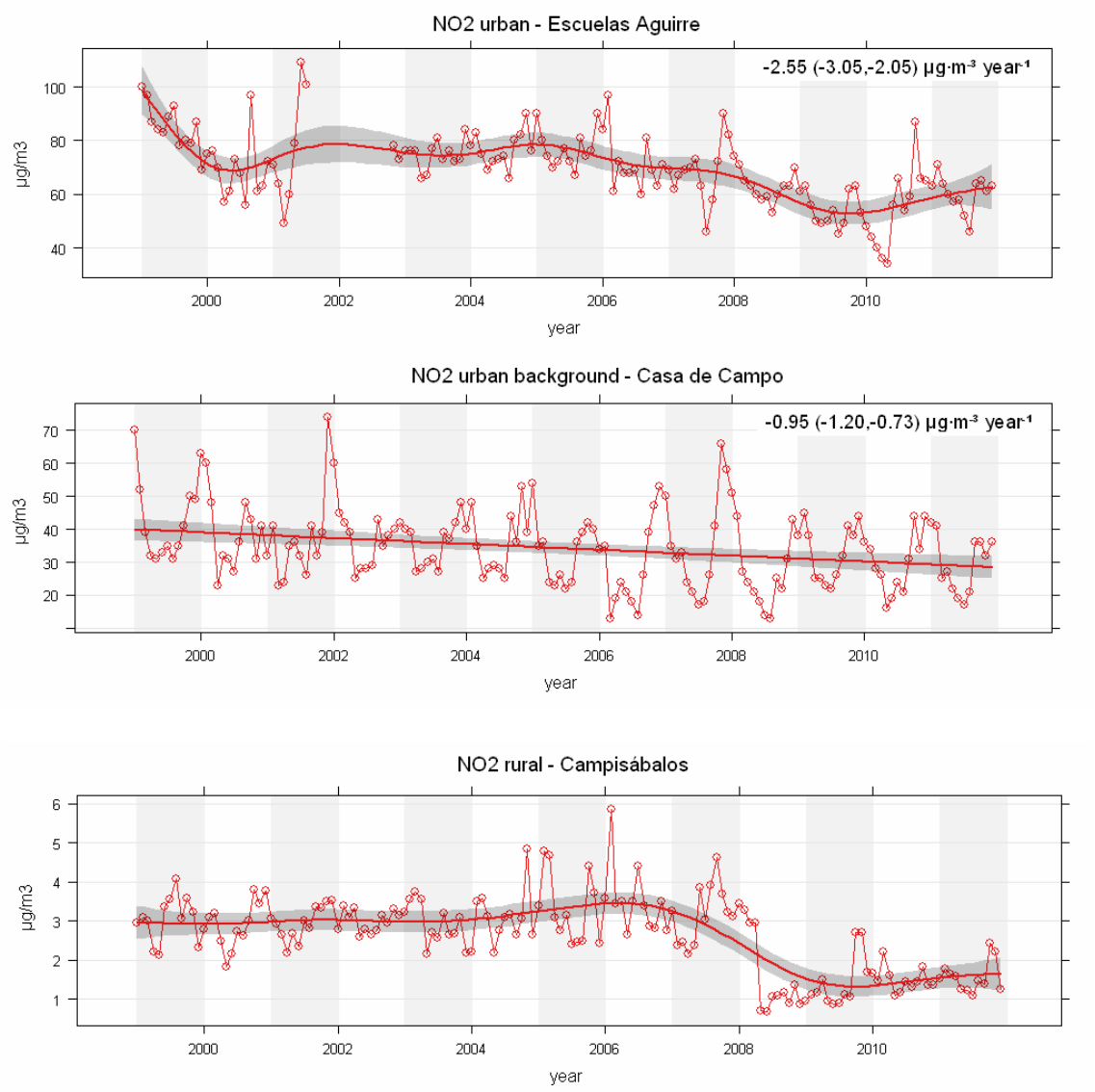

Figure 4.7. NO_2 monthly evolution

NO_2 yearly average concentrations are in the range 50-90 µg·m^{-3} at the urban site (Figure 4.7, top), and about half these values at the urban background site (Figure 4.7, middle). Levels at Campisábalos (Figure 4.7, bottom) are more than one order of magnitude lower. NO_2 showed a clear seasonal cycle only at Casa de Campo, peaking in winter. The analysis indicated a decreasing NO_2 trend in the period 1999-2010 for the two first sites (-2.55, -0.95 µg·m^{-3} year^{-1}). In contrast with nitrate, its gaseous precursor NO_2 showed a marked drop at the beginning of 2008 at Campisábalos. This was due to changes in the instrument calibration procedure currently under revision. The smooth curve modelled is nearly constant both after and before the drop.

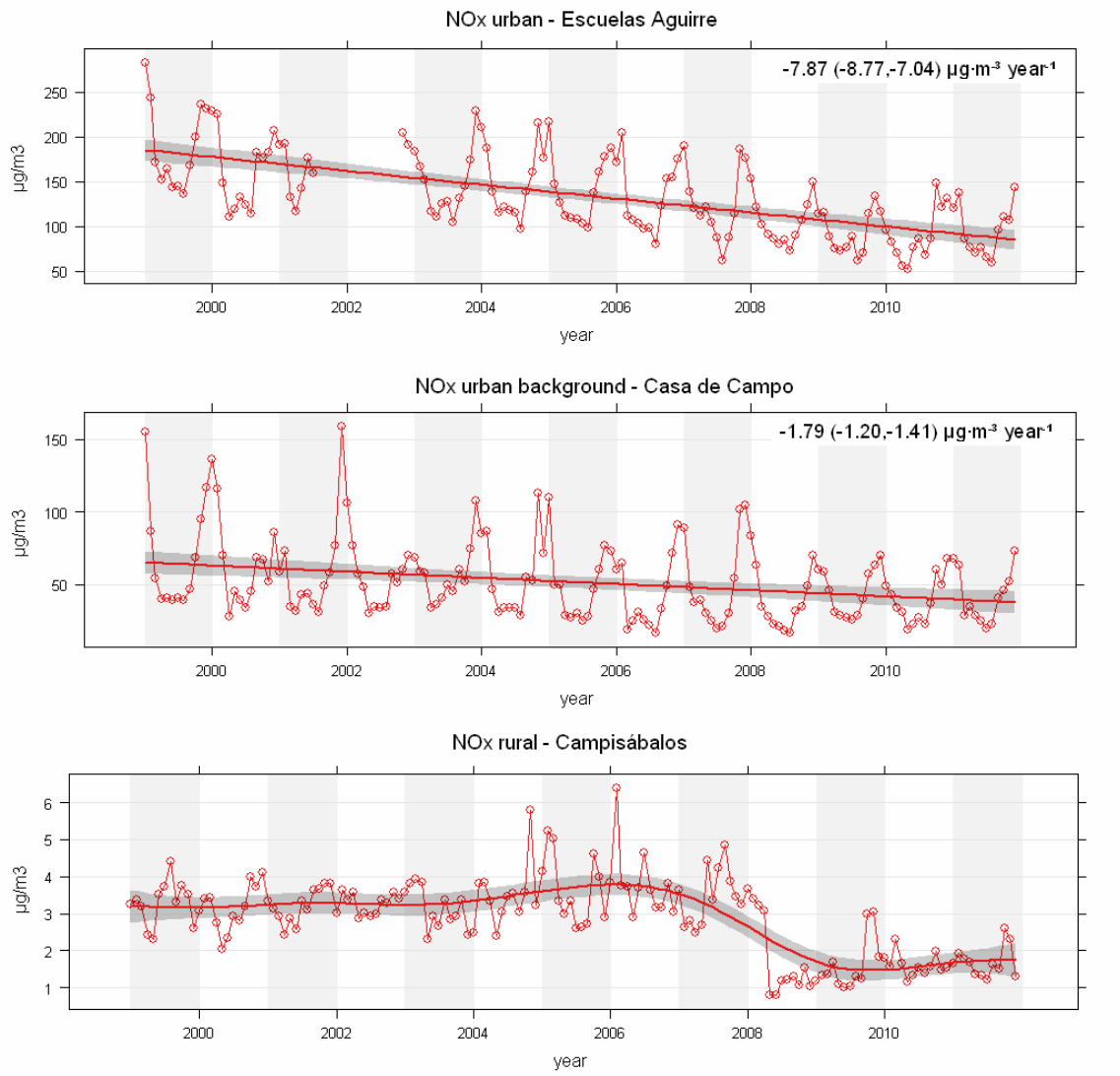

Figure 4.8. NOx monthly evolution

NOx yearly averages are in the range 90-190 µg·m^{-3} at Escuelas Aguirre, and three times lower at Casa de Campo (Figure 4.8). Seasonal cycles of NOx were found at Escuelas Aguirre and Casa de Campo, peaking in winter, due to the higher traffic emissions and the accumulation effect in a narrower mixing layer in this season. NOx was very similar to NO_2 evolution at Campisábalos, with slightly higher values. The annual ratio NO_2/NOx increases with the distance to the traffic sources, being 0.40-0.60 for Escuelas Aguirre, 0.60-0.75 for Casa de Campo, and ~0.90 for Campisábalos. All this information indicates the oxidation of NO before arriving to the urban background and rural sites. A downward tendency is observed at the urban and urban background sites, highly enhanced at Escuelas Aguirre (-7.87, -1.79 µg·m^{-3} year^{-1}). The decreasing trend was more pronounced than for NO_2. Studies have identified increments in the

NO_2/NOx ratio in European urban sites. In Madrid, this was observed for two kerbside and one urban background site for the period 1999-2006 (Plaza et al, 2007). The increment in the proportion of NO_2 has been associated to the increase in diesel vehicles in the urban fleets (Carslaw et al, 2011; Keuken et al, 2012). A remarkable drop in NOx maximum concentrations was observed at Campisábalos in 2008.

Between 2000 and 2009, NOx emissions decreased in the EU by 26%, mainly because the reductions reported in the UK, Spain and Germany. In Spain, this reduction reached 23%. In the period from 2009 to 2010 NOx emissions fell by 1.4 % in the EU. The transport sector is clearly the largest contributor to the NOx emissions and in accordance the highest relative reductions were achieved in passenger cars' emissions, which accounts for the enhanced decreases at Escuelas Aguirre. Reduced emissions from the road transport sector have mainly resulted from the introduction of three way catalytic converters on cars and stricter regulation of emissions from heavy duty vehicles.

4.3.3-Sulphate and SO_2

-Sulphate-

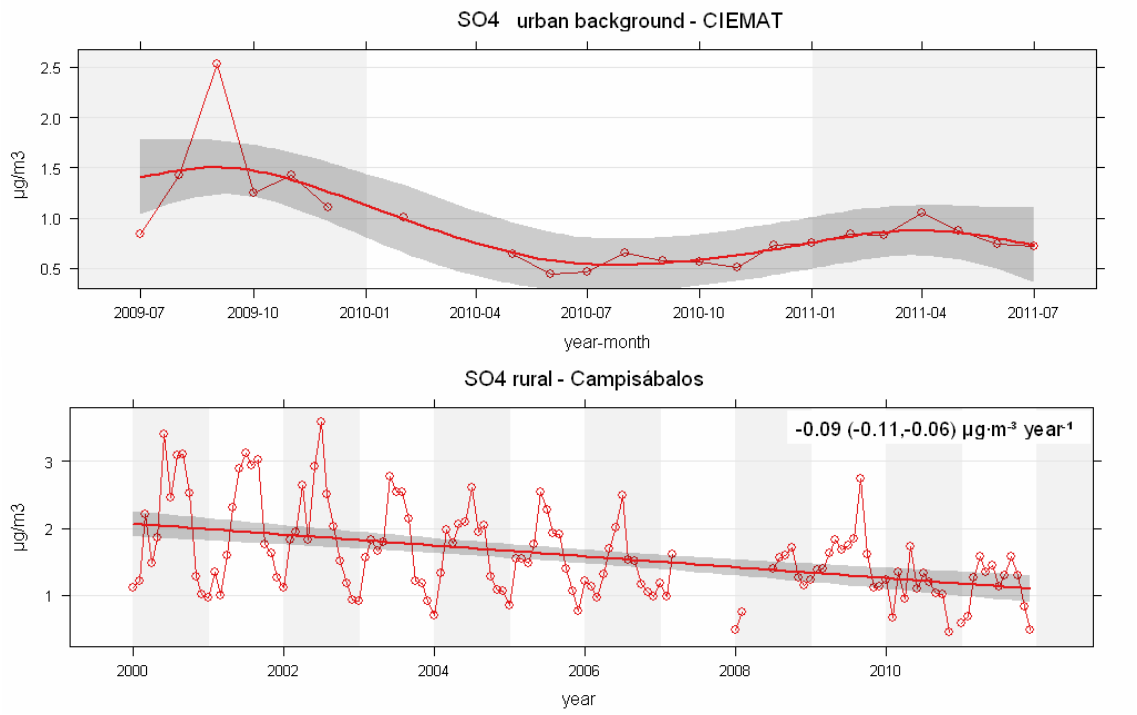

Figure 4.9. Sulphate monthly evolution. PM_1 sulphate at CIEMAT (top) and PM_{10} sulphate at Campisábalos (bottom)

Figure 4.9 shows the monthly evolution of sulphate at CIEMAT and Campisábalos. Measurements at CIEMAT (top) ranged from June 2009 to July 2011. In this time period no clear seasonal pattern can be observed. An overall downward tendency is seen, with an outstanding maximum in September 2009, when remarkable sulphate transport from the European continent took place, as will be exposed in Chapter 6. The time series has not been considered long enough to perform a representative trend analysis.

Figure 4.9 (bottom) depicts the evolution of sulphate in PM_{10} at Campisábalos. This pollutant showed a yearly cycle peaking in summer. Sulphate are higher than nitrate concentrations. Yearly averages are up to 2 $\mu g \cdot m^{-3}$ and monthly averages close to 3.5 $\mu g \cdot m^{-3}$. The seasonal pattern is more marked before 2008. Afterwards maximum concentrations were smaller, with the exception of September 2009. An overall downward tendency is observed (-0.09 $\mu g \cdot m^{-3}$ $year^{-1}$).

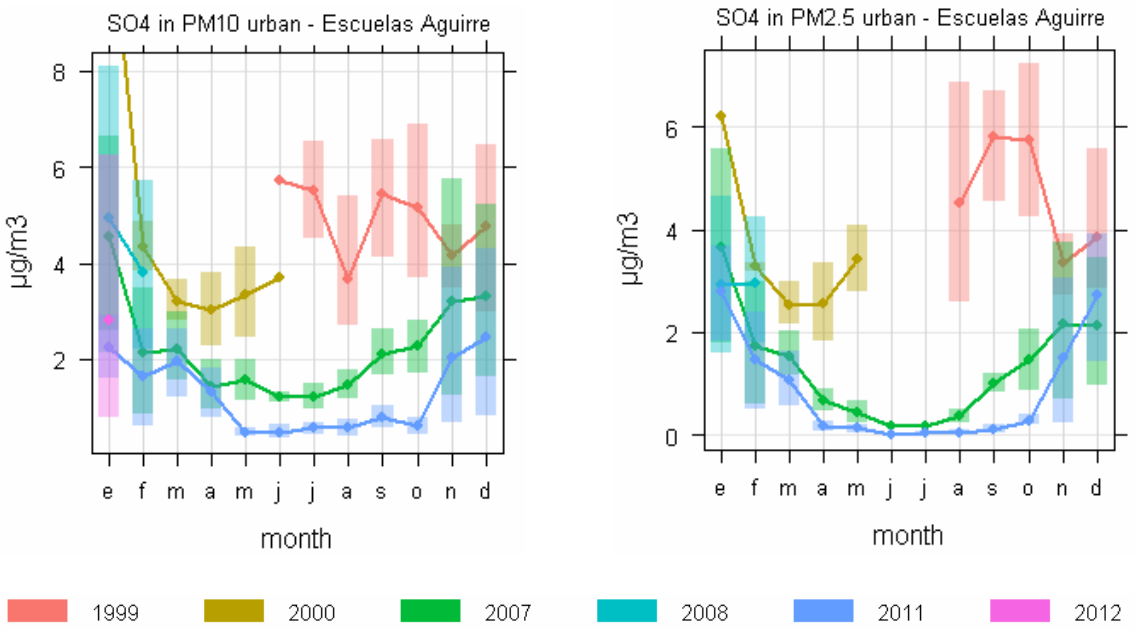

Figure 4.10. Monthly evolution of sulphate in PM_{10} and $PM_{2.5}$ at Escuelas Aguirre. The shading shows the 95% CI of the mean.

The monthly concentrations of particulate sulphate obtained in sampling campaigns at Escuelas Aguirre can be seen in Figure 4.10. A clear seasonal pattern was observed in 2007 and 2011 with higher concentrations in winter, coinciding with the months when the heating devices are operative in Madrid. This contrast with the results obtained for

PM_1 sulphate at CIEMAT, where no seasonal pattern was seen. In 2011, the levels registered in this traffic site for $PM_{2.5}$ sulphate are also notably higher than the concentrations registered at CIEMAT. Sulphate concentrations descended at the urban site from the first campaign (1999-2000) to the last (2011) in the two size fractions measured.

-SO_2-

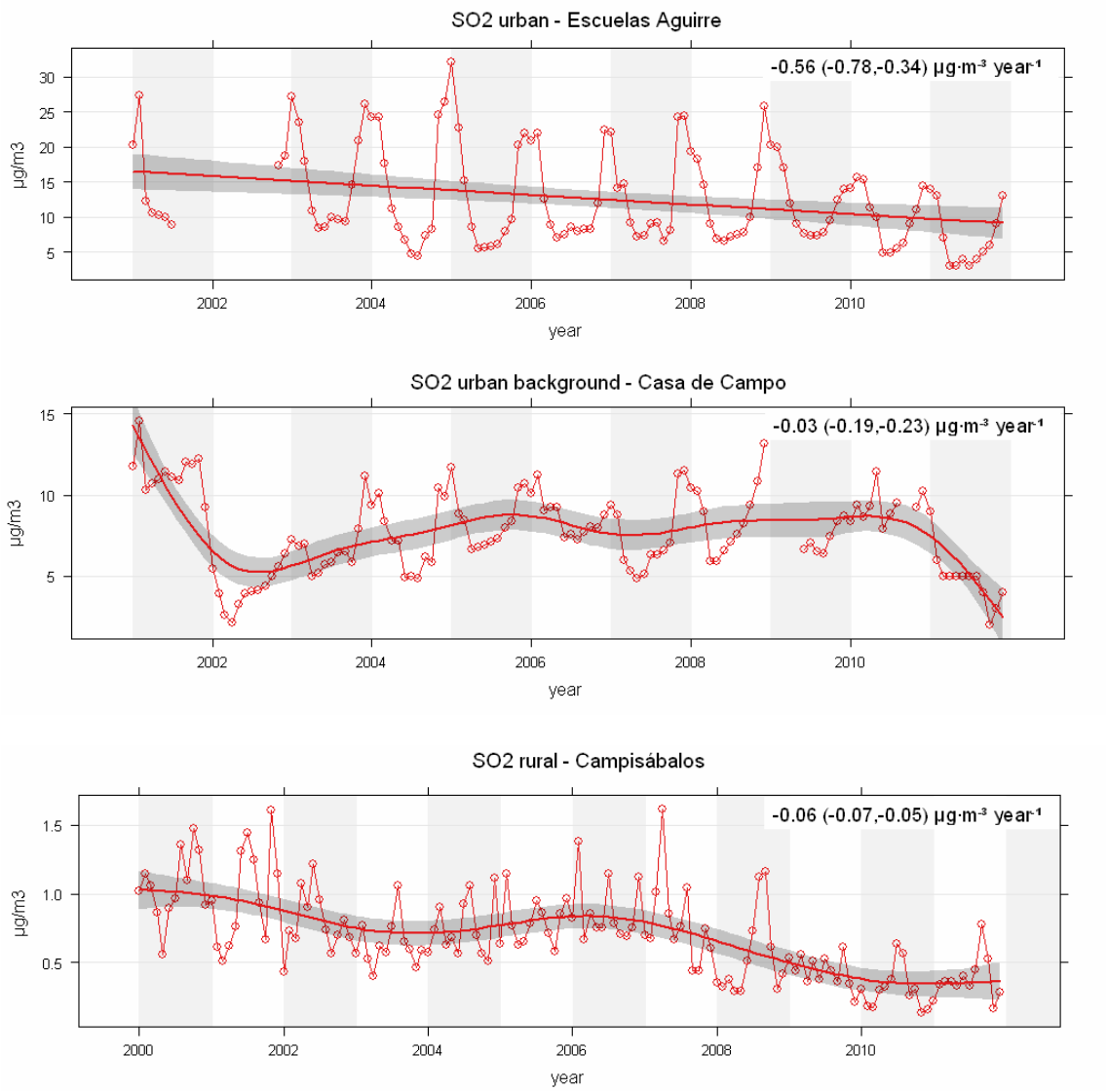

Figure 4.11. SO_2 monthly evolution

SO_2 (Figure 4.11) shows remarkably lower concentrations than NOx. At Campisábalos, SO_2 levels are lower than sulphate levels, as a result of the absence of near sources at the rural site. The stations in the Madrid Metropolitan Area showed a seasonal SO_2

cycle peaking in winter, coinciding with the emissions from heating systems. In contrast, SO_2 annual maximum were often found in summer at Campisábalos. Mean yearly reductions were -0.56 $\mu g \cdot m^{-3}$ at Escuelas Aguirre and only -0.03 and -0.06 $\mu g \cdot m^{-3}$ at Casa de Campo and Campisábalos. The decrease at Escuelas Aguirre is dominated by a 40% reduction in SO_2 levels from winter 2008-2009 to winter 2009-2010. This is likely to be related to the reductions in permitted sulphur in fuels required by the European Directive 2003/17/EC which came into force on 1 January 2009. An SO_2 reduction can be also seen at Campisábalos after winter 2008-2009, however, at Casa de Campo a remarkable reduction was not found until 2011.

The European Environmental Agency reports the evolution in emissions of sulphur oxides (SOx) in Europe. The major sulphur oxides are sulphur dioxide (SO_2) and sulphur trioxide (SO_3). When SO_2 combines with ambient oxygen some SO_3 is slowly formed. Between 2000 and 2009, SOx emissions decreased in the EU by 70% in average, reaching as much as 76% in Spain in that period. The reduction was 54% for the EU in the period 2001-2010. This was a result of a combination of measures, including switching fuel away from high sulphur solid and liquid fuels to low fuel sulphur fuels in energy-related sectors and also road transport. In the Madrid Metropolitan Area the gradual replacement of coal heaters with cleaner devices might also have played a role.

In view of this information, the small annual reductions reported for Casa the Campo before 2011 are surprising.

4.3.4-Ammonium and NH_3

-Ammonium-

Particulate ammonium has been measured at Campisábalos since 2006. However, data available are scarce (255 daily samples in the period 2006-2011) and do not allow obtaining reliable monthly means. Figure 4.12 shows the daily NH_4^+ in PM_{10} measurements performed at this site. The concentrations seem to descend from 2009 onwards in comparison with the three previous years, keeping values under 2 $\mu g \cdot m^{-3}$, except for two data points.

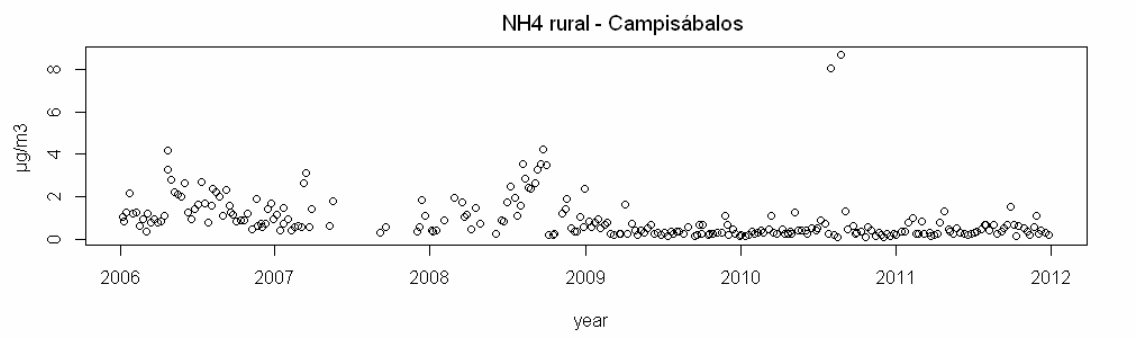

Figure 4.12. Daily NH_4^+ in PM_{10} at Campisábalos

The results for particulate ammonium obtained in sampling campaigns at Escuelas Aguirre can be seen in Figure 4.13. Some seasonal variation would be expected, since particulate NH_4^+ is formed through the neutralization of sulphate and nitrate ions, the latter presenting higher concentrations in winter. However, no seasonal variations are observed. Monthly concentrations are similar or higher than the values registered at the rural site. In 2007 concentrations seemed to be higher than in the other periods measured, however, the scarcity of data for that same year at Campisábalos does not allow obtaining any conclusion.

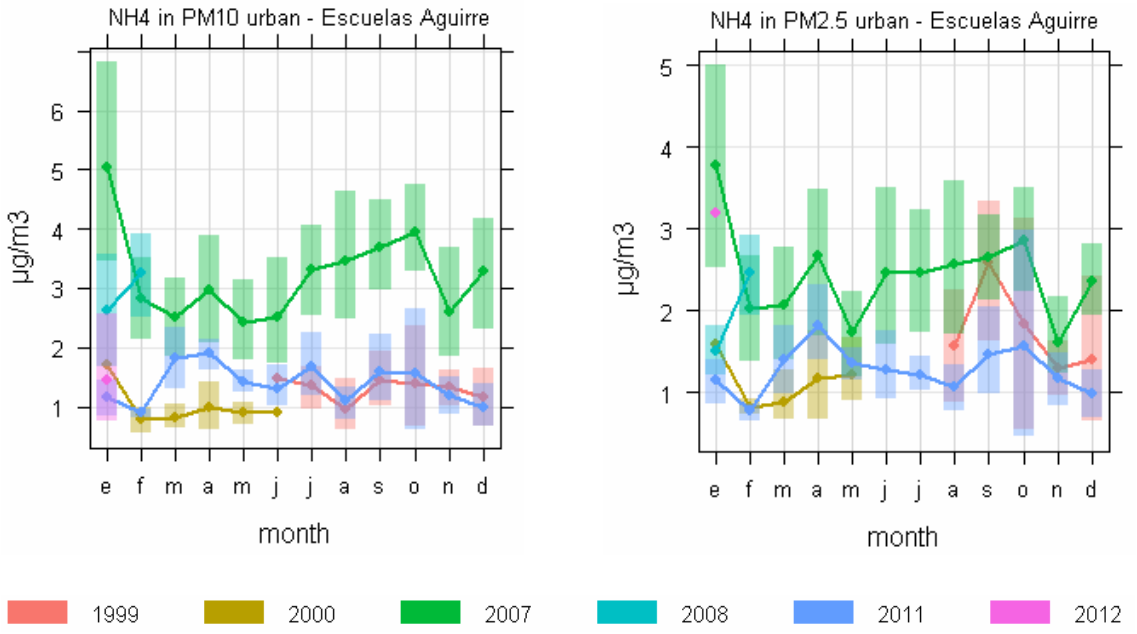

Figure 4.13. Ammonium in PM_{10} and $PM_{2.5}$ monthly evolution at Escuelas Aguirre. The shading shows the 95% CI of the mean.

-NH_3-

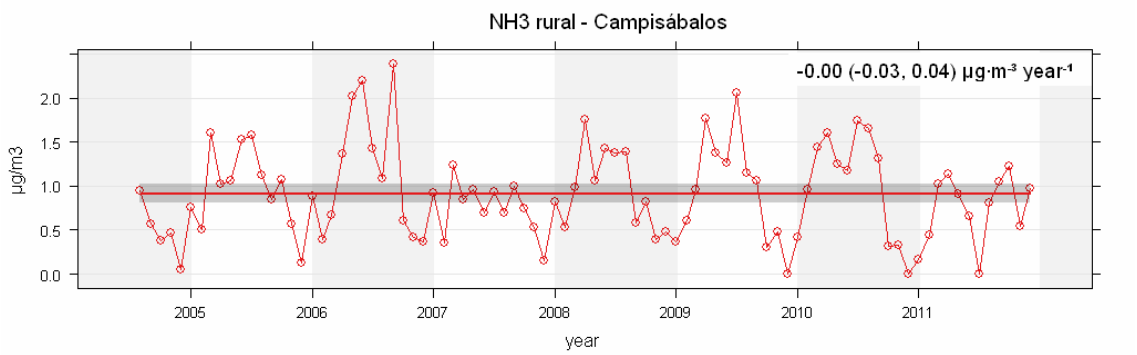

Figure 4.14 Ammonia monthly evolution at Campisábalos

Weekly integrated ammonia measurements have been obtained at Campisábalos since August 2004. Monthly mean concentrations are in the range 0-2.5 µg·m^{-3} and a seasonal pattern with summer maxima is observed most of the years. Nevertheless, a drop in the middle of the summer is clearly observed in 4 out of the 7 years sampled, very pronounced in 2011. Theil-Sen analysis does not show any tendency, i.e., annual mean concentrations remained constant at this site in 2005-2011. Regarding the Madrid municipality, no gaseous ammonia is routinely measured at the *Red de Calidad de Aire del Ayuntamiento de Madrid*. The results from the sampling campaign carried out in 2011 are presented below.

The European Union emission inventory for 1990–2009 reported decreasing ammonia emissions in most Member States. However, in Spain there was a 12% increase in that study period. In the period 2001-2010 NH_3 emissions fell about 10% in the EU.

4.4- Relationships between SIC and precursor gases at rural sites

Finding mathematical relationships between ambient concentrations of SIC and their precursors is extremely difficult due to the variety and complexity of the formation and transformation processes of secondary aerosol compounds.

The availability of long-term measurements of SIC concentrations together with precursor gases in the EMEP stations allows exploring these relations. Jones et al (2011) found for the annual means a potential relationship of the form

$$[SO_4^{2-}] = a[SO_2]^b \qquad \text{(eq. 4.1)}$$

for EMEP sites in several countries. In Denmark the coefficient of determination R^2 of the fitted curve was close to 0.95. The authors proposed a potential relationship of the form of eq. 4.2 to estimate the reductions in SO_2 necessary to achieve a certain reduction in SO_4^{2-}.

$$[SO_4^{2-}] = a[SO_2]^b + c \qquad \text{(eq. 4.2)}$$

Figure 4.15 shows SO_4^{2-} vs. SO_2 annual averages in the Spanish EMEP network for the period 1987 (start of the measurements) to 2011. Table 4.2 shows the EMEP stations and time intervals which have been used in Figure 4.15. The blue diamonds correspond to SO_4^{2-} in total suspended matter (TSP), while the orange squares correspond to SO_4^{2-} measured in PM_{10}. The two datasets are consistent. For the sulphate in PM_{10}, the concentration of gaseous SO_2 entailed a minimum value for the sulphate concentrations. However, no empirical relation which could be fitted to a curve was observed for all the stations.

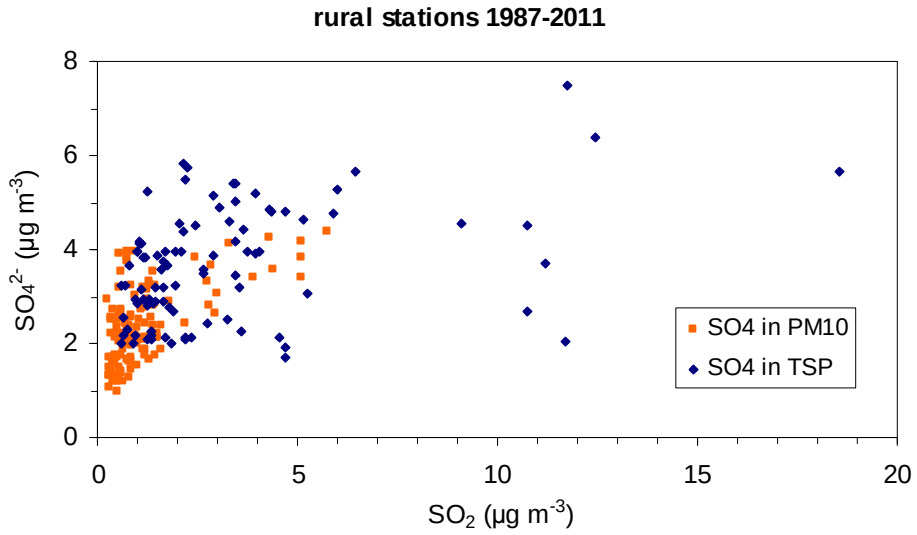

Figure 4.15. Annual averages of sulphate against SO_2 in the EMEP network

SO_4^{2-} in TSP		SO_4^{2-} in PM_{10}	
Code	Time span	Code	Time span
ES01	1987-2000	ES01	2008-2001
ES02	1987-1995	ES05	2008-2001
ES03	1987-2000	ES06	2008-2001
ES04	1988-2001	ES07	2000-2011
ES05	1992-2000	ES08	2000-2011
ES06	1992-1998	ES09	2000-2011
ES07	1995-2002	ES10	2000-2011
ES08	1999-2002	ES11	2000-2011
ES09	1998-2002	ES12	2000-2011
ES10	1999-2002	ES13	2001-2011
ES11	1999-2002	ES14	2000-2011
ES12	1999-2002	ES15	2003-2006
ES13	2000-2002	ES16	2001-2011
ES14	2000-2002	ES17	2008-2011
ES15	2000-2002		
ES16	2001-2002		

Table 4.2. Stations codes and time intervals in Figures 4.15 and 4.16

In figure 4.16 the SO_4^{2-} in PM_{10} vs. SO_2 is plotted separately for the 14 stations. When $[SO_2] > 2$ µg·m^{-3}, higher concentrations of particulate sulphate are often found. Equation 4.1 has been fitted for ES08 (Niembro-Llanes, Asturias), the only one with SO_2 annual concentrations over 3.5 µg·m^{-3}. The coefficient of determination R^2 is over 0.80.

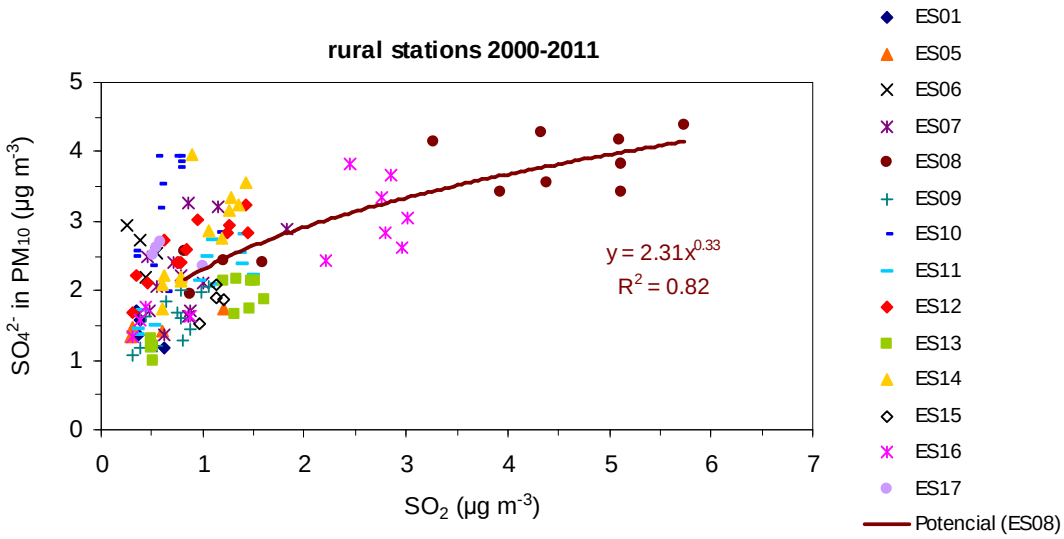

Figure 4.16. Annual averages of sulphate in PM_{10} and SO_2 at 14 EMEP stations. Potential function fit for ES08

Figure 4.17 shows the annual averages of nitrate in PM_{10} vs. NO_2. No relationships can be found for all or individual stations. Table 4.3 shows the EMEP stations and time intervals which have been used.

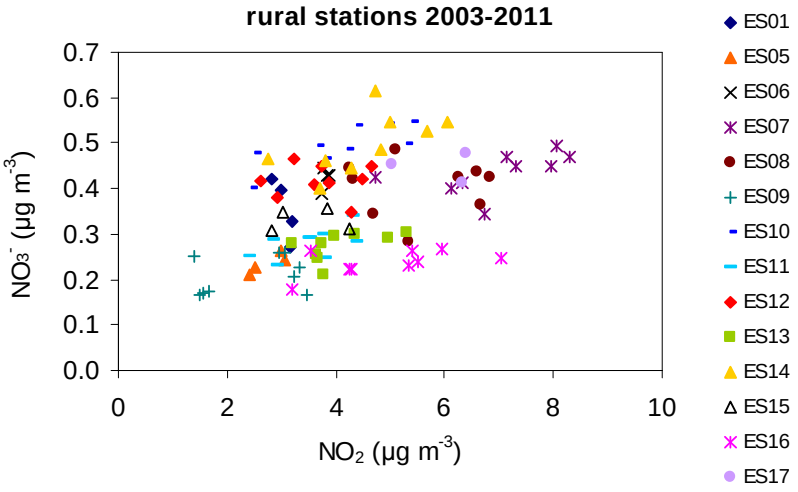

Figure 4.17. Annual averages of nitrate in PM_{10} against NO_2 in the EMEP network

NO_3^- in PM_{10} and NO_2

Code	Time span
ES01	2008-2011
ES05	2008-2011
ES06	2008-2011
ES07	2003-2011
ES08	2003-2011
ES09	2003-2011
ES10	2003-2011
ES11	2003-2011
ES12	2003-2011
ES13	2003-2011
ES14	2003-2011
ES15	2003-2006
ES16	2003-2011
ES17	2008-2010

Table 4.3. Station codes and time intervals in Figure 4.17

4.5- Ammonia levels and sources in Madrid

Two sampling campaigns covering more than 50 sites in the Metropolitan Area of Madrid were performed with the objective of estimating the levels of this pollutant seasonally, and at the same time identifying the sources which contribute most to increasing ammonia concentrations in the city. To perform this source identification the results obtained in the campaigns are presented according to the type of site below.

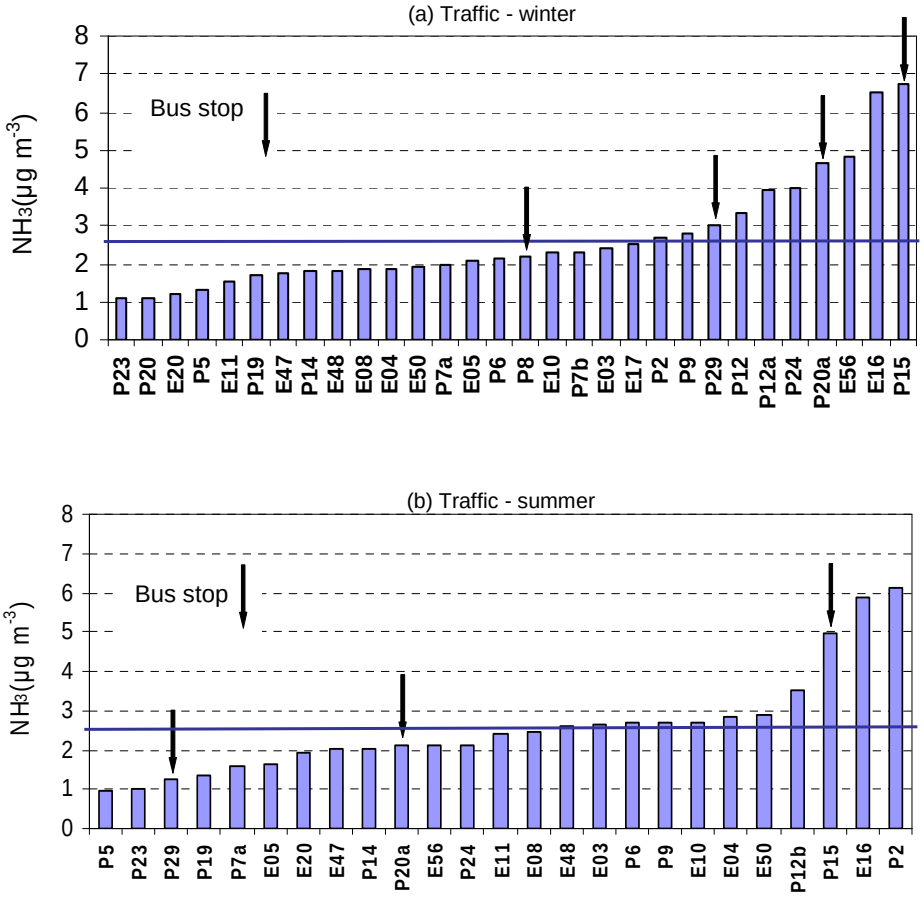

Figure 4.18. Mean NH_3 concentrations in the traffic sites in (a) winter and (b) summer

Figure 4.18 shows the mean NH_3 concentrations calculated for the traffic sites in the winter and summer campaigns. The mean values were very similar in both seasons (2.7± 0.5 $\mu g \cdot m^{-3}$ in winter and 2.6±0.4 $\mu g \cdot m^{-3}$ in summer) (see Table 4.5). In winter, three of the four samplers placed very close to bus stops registered concentrations above the mean. In P15 and E16 very high concentrations were measured in both

seasons. These sites were nearby the very busy streets Alcalá and Arturo Soria (yearly average 47812 and 29087 vehicles day^{-1})

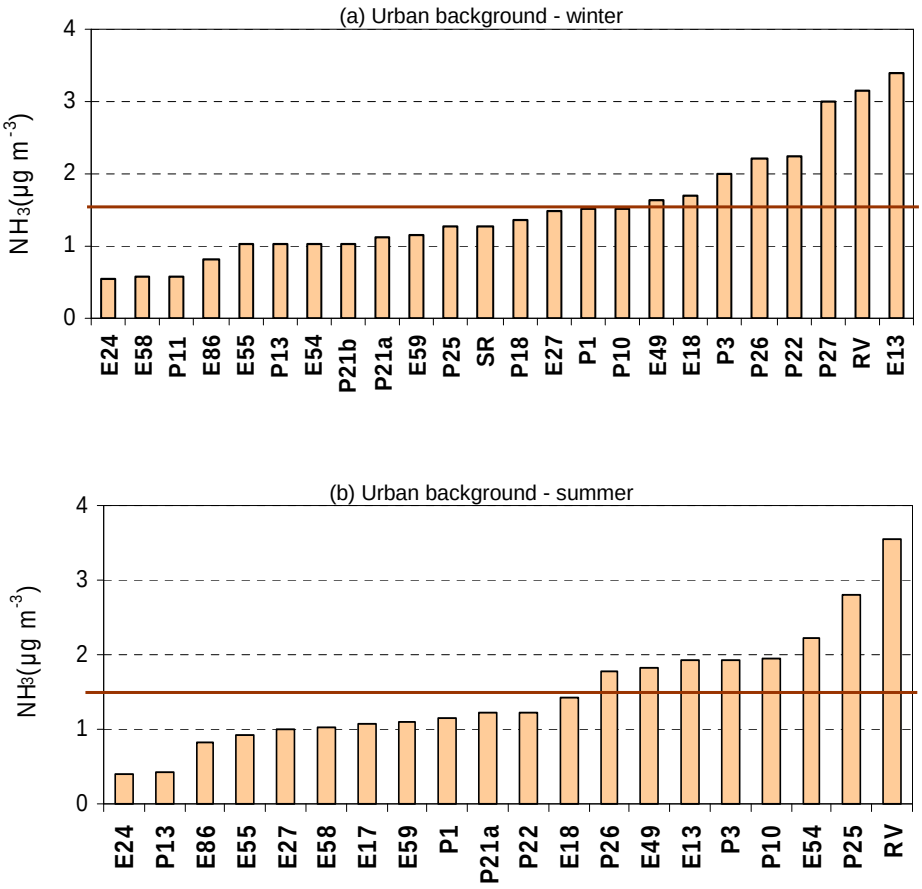

Figure 4.19. Mean NH_3 concentrations in the urban background sites in (a) winter and (b) summer

Figure 4.19 shows the mean NH_3 concentrations calculated for the urban background sites in the winter and summer campaigns. Urban background sites also registered very similar mean NH_3 concentrations in both seasons (1.6±0.3 µg·m^{-3} and 1.5±0.3 µg·m^{-3}). RV (Retiro Viveros) showed very high concentrations both in winter and summer. The sampler was placed in a big urban park, close to the park's nursery. The lowest values were registered at Casa de Campo (E24), a big forested area located on the western part of the city.

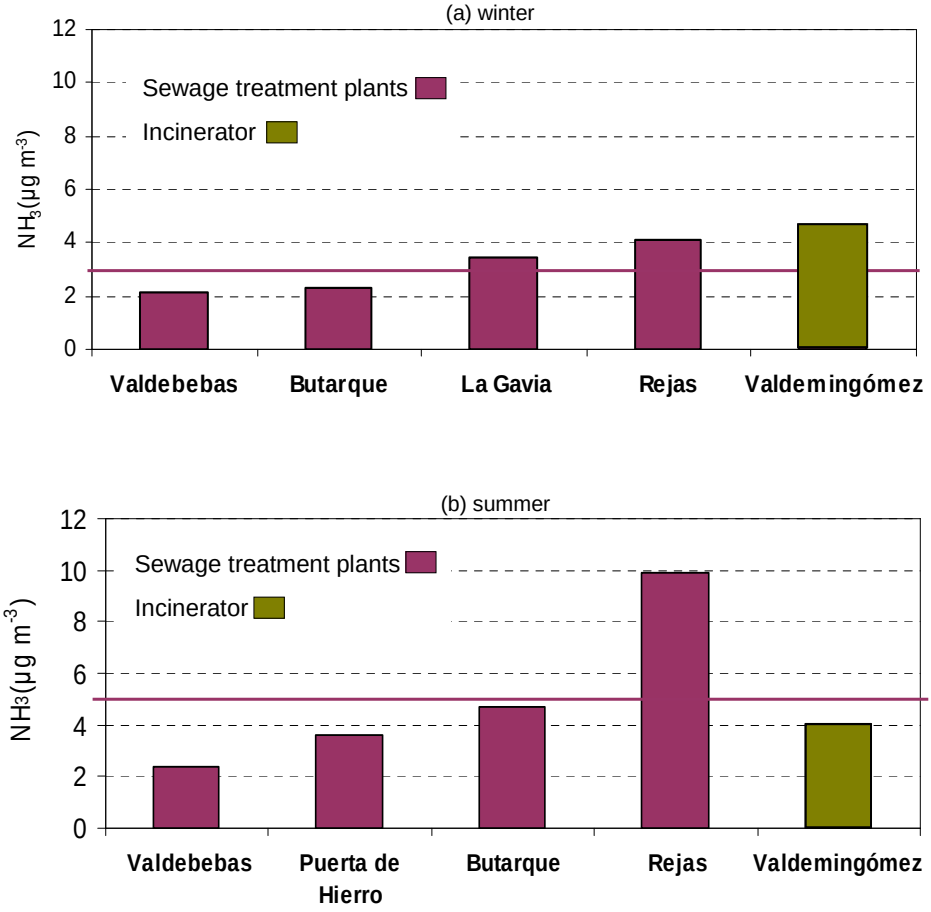

Figure 4.20. Mean NH_3 concentrations in the sewage treatment plants and the incinerator in (a) winter and (b) summer

Figure 4.20 shows the mean NH_3 concentrations calculated for the sewage treatment plants and the incinerator sites in winter and summer. The Rejas sewage treatment plant registered concentrations more than two times higher in summer, being the highest value obtained (~4 $\mu g \cdot m^{-3}$ winter; ~10 $\mu g \cdot m^{-3}$ summer). The rest of the plants and the incinerator showed values in the range 2-5 $\mu g \cdot m^{-3}$ in both seasons.

Site	Sewer adjacent	NH_3 ($\mu g\ m^{-3}$)	Sewer >10m	NH_3 ($\mu g\ m^{-3}$)
Traffic	P7b	2.3	P7a	2.0
	P20b	1.1	P20a*	4.7
	P12a	4.0	P12b	3.4
Urban bg	P21a	1.1	P21b	1.0

*Table 4.4. Mean NH_3 concentrations ($\mu g \cdot m^{-3}$) in sites adjacent to sewers and duplicates. * bus stop*

Table 4.4 shows the results obtained in the sites adjacent to sewers and the duplicates, separated >10 m. The sampler closer to the sewer showed slightly higher ammonia concentrations at P7 and P12 (traffic sites) and P21 (urban background). However, P20a, located on a bus stop, showed a much higher ammonia concentration than P20b. Thus, the proximity to sewers might influence ambient ammonia levels locally, but the results obtained are not conclusive.

At the CIEMAT site (P22) NH_3 concentration in winter was 2.2 $\mu g \cdot m^{-3}$, higher than the average of the urban background sites (1.6 $\mu g \cdot m^{-3}$). The averaged registered values for $PM_{2.5}$ nitrate and PM_1 sulphate in the same time period were 1.46 $\mu g \cdot m^{-3}$ and 0.71 $\mu g \cdot m^{-3}$ respectively. In summer, NH_3 concentration was 1.2 $\mu g \cdot m^{-3}$, slightly under the average of urban background sites (1.5 $\mu g \cdot m^{-3}$). Information on particulate nitrate and sulphate is not available for comparison.

Table 4.5 summarises the results obtained in both seasons at the different types of sampling sites.

Sites (average)	Winter ± 95% CI	Summer ± 95% CI
Traffic	2.7±0.5	2.6±0.4
Urban background	1.6±0.3	1.5±0.3
Sewage treatment plants	3.0±0.8	5.1±2.8
Incinerator	4.7	4.0
Total	**2.2±0.3**	**2.4±0.4**

Table 4.5. Mean NH_3 concentrations ($\mu g \cdot m^{-3}$) registered in Madrid during the winter and summer 2011 campaigns.

Comparing the mean values calculated in traffic and urban background sites we can see there is a statistically significant difference in both seasons, with higher mean concentrations in the traffic sites. In contrast, the sewage treatment plants and incinerator showed the highest NH_3 levels, but the difference with the mean ammonia levels registered in the traffic sites was not significant. This result is in agreement with the studies in other cities which had pointed to traffic emissions as a major source of ammonia in urban areas. No significant differences between winter and summer were registered for any kind of sampling site. In winter the mean concentrations registered at the urban background sites were slightly higher than the monthly mean in March

2011 at Campisábalos (~1 μg·m^{-3}). However, in July 2011 mean NH_3 at Campisábalos were surprisingly low.

The results obtained allow plotting NH_3 concentration maps for the metropolitan area of Madrid in winter and summer (see Figure 4.21).

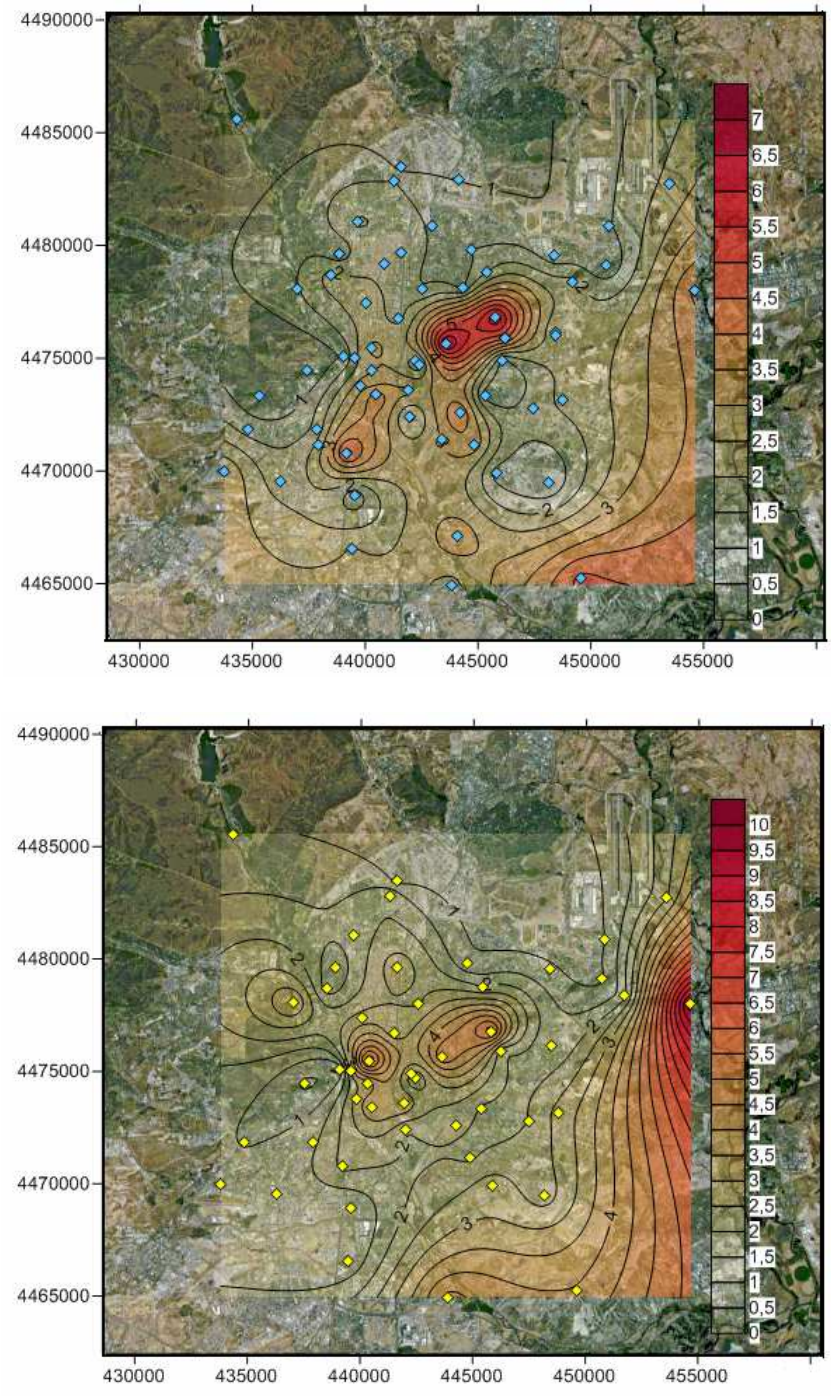

Figure 4.21. Maps of NH_3 concentration in Madrid obtained in the 2011 winter (top) and summer (bottom) campaign. Legend represents μg·m^{-3}. Scale: UTM coordinates, zone 30.

Both maps show high ammonia concentrations in the east and south of the city associated to sewage treatment plants and the incinerator. The lower density of sampling sites in the outskirts of the city magnifies the impact of these emission sources, especially in summer. In winter, the highest concentrations are observed in the central zone of the map (which does not coincide with the historical city centre) associated to the traffic hotspots Alcalá and Arturo Soria. High concentrations are also remarkable at E56 (the very busy Plaza Fernández Ladreda). In summer, Alcalá and Arturo Soria showed high ammonia levels again, although the highest value in the urban area was registered in P2 (Calle de Ruiz, close to Glorieta de Bilbao).

Average NH_3 levels measured in this campaign are notably lower in Madrid than in Barcelona, where 4.4 and 9.5 $\mu g \cdot m^{-3}$ were registered in winter and summer respectively. In winter, traffic sites registered higher levels than urban background sites, but the opposite happened in summer. The ammonia behaviour in summer was explained by the fact that the higher temperatures and solar radiation in summer will increase emission from biological sources in the city, such as humans, sewage and garbage collection systems, dominating over traffic emissions, together with the volatilization of NH_3 from the aerosol phase (Reche et al, 2012).

4.6-Conclusions

In this chapter we have presented the time evolution in the last decade of concentrations of precursor gases (NO_2, NOx and SO_2) and particulate matter at three representative locations -urban, urban background and rural- of the Madrid air basin. Particulate sulphate and nitrate were depicted for the rural station and the CIEMAT urban background site and specific sampling campaigns at the urban site. Some information on gaseous ammonia and particulate ammonium is also available at the rural and urban sites. This information provides a necessary basis before addressing more specific issues in the following chapters.

Relationships between SIC and precursors have also been explored at rural sites.

In general, concentrations were highest at the urban site and lowest at the rural, showing intermediate values at the urban background site. These differences were highly enhanced for gaseous traffic-emitted pollutants.

Different seasonal patterns have been found depending on the pollutant and sampling site. Particulate matter presented maximum levels in summer at the rural site. In contrast, the traffic-derived NO_2, NOx and NO_3^-, and also SO_2 -originated mainly in domestic heating devices in the Madrid Metropolitan Area- in general showed more marked seasonal cycles in the urban stations, with maximum values in winter. For nitrate, there might be regional superimposed effects in the Madrid air basin which do not affect other stations. NH_3 also showed higher concentrations in summer at the rural site.

Particulate sulphate presented maximum levels in summer at the rural site, and the opposite at the urban site. This can be explained by the enhanced photochemical oxidation of SO_2 at summer which dominates the annual pattern at the rural site while the urban site is dominated by the nearby higher emissions in winter. Mean values registered at Campisábalos, CIEMAT and Escuelas Aguirre did not show large variations among sites. Particulate nitrate concentrations are significantly higher at the CIEMAT station than at Campisábalos. Filter-based measurements at the urban site resulted in lower monthly concentrations and noisier seasonal patterns than the ones registered at CIEMAT, which can be a consequence of sampling losses of this semivolatile compound.

PM and gases showed descending trends in the period 1999-2010 except for gaseous NH_3, which kept constant annual values at the rural site. The most significant reductions in this period were found for NOx at the urban site. Escuelas Aguirre showed a 40% reduction in SO_2 levels from winter 2008-2009 to winter 2009-2010. This is likely to be related to the reductions in permitted sulphur in fuels. An SO_2 reduction can be seen also at Campisábalos after winter 2008-2009. However, at Casa de Campo a remarkable reduction was not found until 2011, in spite of the outstanding reported reductions in emissions in Spain. Some pollutants also present a marked drop in 2008 (fine PM at Casa de Campo and NOx-NO_2 at Campisábalos). Descending trends in

NOx and PM are due to various measures to reduce pollutants emitted by energy production plants and traffic, such as the incorporation of catalytic converters in vehicles. These tendencies are not reflected in the nitrate monthly evolution registered at CIEMAT. Reductions in SO_2 and particulate sulphate are due to the limitations of S in fuels.

In the rural stations of the EMEP network in Spain the annual averages in concentration of gaseous SO_2 entailed a minimum value for the sulphate in PM_{10}. In ES08 (Niembro-Llanes, Asturias) a potential relationship has been found between both pollutants, as proposed by Jones et al (2008). No relationships were found between annual averages of nitrate in PM_{10} and the nitrate gaseous precursor NO_2.

A characterisation of gaseous NH_3 ambient levels and sources in the Madrid atmosphere was carried out in 2011. A winter campaign was performed from 17/03/2011 to 28/03/2011 and a summer campaign was performed from 01/07/2011 to 11/07/2011. Passive samplers were used, obtaining a measurement integrated over the exposure time period.

Sites close to sewage treatment plants and an incinerator registered the highest concentrations. The traffic sites showed significant higher values than the urban background sites in both seasons. Traffic emissions could be related to catalytic converters, which have been proved to lead to outstanding reductions in NOx emissions, but also to generate gaseous ammonia, raising controversy on the use of these devices. At this stage of the research a statistically significant difference between sewage treatment plants and the incinerator with traffic sites cannot be established. No significant differences between winter and summer were registered for any kind of sampling site in the Madrid Township, in contrast with the summer maxima observed at the rural EMEP site most of the years. In winter the mean concentrations registered at the urban background sites were consistent with the monthly mean in March 2011 at Campisábalos, but in summer 2011 the mean NH_3 registered at the rural site was extremely low.

At the CIEMAT site NH_3 concentration in winter was higher than the average of the urban background sites. In contrast, NH_3 concentration in summer was slightly under the average of urban background sites.

In Madrid, average ammonia levels were similar to measurements in other European cities such as Aveiro (Pio et al, 1991), Münster (Vogt et al, 2005) and Thessaloniki (Anatolaki and Tsitouridou, 2007). Remarkably higher levels were found in Barcelona on the same campaign (Reche et al., 2012)

5- TEMPORAL PATTERNS OF SULPHATE AND NITRATE AT URBAN AND RURAL SITES

5- TEMPORAL PATTERNS OF SULPHATE AND NITRATE AT URBAN AND RURAL SITES

5.1-Introduction

In this chapter the analysis of the most extensive SIC time series measured in CIEMAT that has been done in the course of this thesis is presented. In Gomez et al, 2007, a series of one year of particulate nitrate at the CIEMAT sampling station was analysed. The authors described episodes of nitrate photochemical formation and heterogeneous formation in the gas-aqueous phase, as well as nitrate local or regional transport. In this thesis, specific episodes in which high concentrations of particulate sulphate and nitrate have been reached will be also described (Chapters 6 and 7). Nevertheless, to obtain a full picture of the behaviour of pollutants in the region studied analysis of temporal properties over extended time periods is also necessary and complementary to event analysis. The method chosen for this characterization is the study of average patterns in three scales: annual, weekly and daily. For the case of the weekly and daily patterns, winter and summer conditions have been analysed separately.

Secondary inorganic aerosol is the result of transformation processes of primary pollutants in the atmosphere which depend on emissions as well as on meteorology. Such pollutants can be transported from the source region to thousands of km away, which means that an interpretation of aerosol behaviour in a zone not only requires information on sources and pathways in that region but also on pollutants transported from other source areas.

Both meteorology and emissions show large differences in different regions of Europe, and conclusions from a certain region cannot be extrapolated to other parts of the continent. A compendium of European aerosol phenomenology including chemical characteristics of particulate matter at kerbside, urban, rural and background sites is presented in Putaud et al (2004) and Putaud et al (2010). Querol et al (2004b) analysed PM characteristics of seven European regions comparing levels and speciation studies of PM_{10} and $PM_{2.5}$. They found in Central Europe (including UK) annual mean values of SIC slightly higher than those found in Southern Europe, where the difference between rural and urban sites was larger. It was noticeable that SIC levels were very

similar in all urban areas, with an extra input in intensively industrialised regions or heavily polluted urban areas. Regarding long-range transport, Borge et al (2007) found very different and characteristic transport patterns that affected PM_{10} concentrations in three European cities: Athens, Madrid and Birmingham.

The joint analysis of pollutant and meteorological data on different timescales provides information on the dominant processes that govern aerosol formation and transport. Competing effects lead to different patterns in different locations. Nitrate in the fine fraction, mainly ammonium nitrate, is partitioned into a gaseous and a particulate phase, this partition depending on temperature. As sulphate and coarse nitrate are more thermally and chemically stable, they are more affected by transport processes, whereas fine nitrate evolution is expected to be more affected by local meteorology and formation/dissociation processes.

Time evolution of pollutants on a yearly timescale reveals a seasonal pattern related to emissions and climate. Weekday/weekend analysis provides information on the formation and accumulation time of secondary pollutants in the atmosphere, but moreover, since there is no natural process which follows a seven day cycle, it can provide information on the anthropogenic influence on a certain site. The daily pattern not only gives us information about the origin of pollutants, since a marked anthropogenic emission pattern indicates anthropogenic local/regional provenance, but also on the formation processes involved. In the last decade, several researchers have analysed aerosol behaviour on different timescales. Rattigan et al (2006) reported fine nitrate and sulphate seasonal patterns in a rural and an urban site in the state of New York, finding maximum sulphate concentrations in the warmer months, and highest nitrate in the colder periods. They concluded that photochemistry was the dominant formation mechanism for sulphate aerosol, while nitrate concentration was driven by thermal dissociation of ammonium nitrate. Millstein et al (2008) investigated the fine particle nitrate response to weekly changes in emissions at four US urban sites. They found a reduction in measured concentrations of PM nitrate on weekends associated with lower NOx emissions, indicating the potential to reduce $PM_{2.5}$ nitrate via NOx control. Recently, Bampardimos et al (2011) investigated the weekly cycle of coarse and fine mode PM in different types of rural and urban stations in Switzerland to calculate

the contribution of traffic to the coarse mode urban ambient concentrations. Some authors have point out the possibility that a cloud cover weekly cycle can be found conducted by the change of aerosol concentrations through the semi-direct aerosol effect, which leads to weekly cycles of meteorological variables such as RH and solar radiation (Wang et al, 2012).

Wittig et al (2004) studied diurnal patterns of nitrate and sulphate on a seasonal base at the Pittsburgh Supersite, relating features of the patterns to temperature, RH, and ultraviolet radiation that affected the formation processes of secondary aerosol.

In this study an analysis of temporal features of nitrate and sulphate in the Madrid air basin has been performed. Given the differences in the emission profiles and meteorology, different processes and relevant parameters can produce characteristic behaviours that cannot be observed at other European sites. For this reason this analysis has been performed in parallel with other sites at south-eastern UK. The comparison with the UK is interesting given the large climatic difference between the two regions, which necessarily affect the formation and temporal evolution of secondary compounds. It is also particularly favourable given the high availability of data provided by the air quality networks in the UK. Besides gas measurements at high resolution, which are common in many sampling stations worldwide, $PM_{2.5}$ nitrate is taken at high resolution with the same instrument used in the CIEMAT site, R&P 8400N and in a similar temporal range.

The study was conducted in five representative sites, including urban background sites in the two capitals, Madrid and London, and nearby rural sites (Revuelta et al, 2012a,b).

5.2-Sampling sites and techniques

5.2.1-Meteorology and topography

The Madrid air basin, described in section 1.3, is characterised basically by an extended plateau (Meseta Central) bordered by mountainous terrain, with heights over 2000 m to the north-northwest. In contrast, the geography of south-eastern England consists of lowland terrain, with heights not exceeding 400 m. The main meteorological

influence is the proximity to the Atlantic Ocean, which results in a humid and windy maritime climate, subject to frequent changes.

Climatic information can be obtained from the meteorological services of both countries (http://www.aemet.es/es/serviciosclimaticos and http://www.metoffice.gov.uk/climate/uk/). Seasonal comparison of relevant meteorological parameters averaged from 1971 to 2000 shows important differences that are likely to influence aerosol formation and transformation. Mean temperatures are higher in Madrid than London, but the difference is larger in summer (mean values are 6-8 °C in Madrid and 4-5 °C in London in winter; 20-25 °C Madrid and around 17°C London in summer). However, sunshine and precipitation make the largest differences. Sunshine in winter is around 425 hours in Madrid and 170 in London, while in summer it reaches 1000 hours in Madrid and 600 in London. On the other hand, average rainfall is 130 mm in winter and only 30 mm in summer in Madrid, while precipitation in southern England is over 200 mm in both seasons.

Since the Spanish rural site is significantly elevated above the level of the city, meteorological features are different. The wind regime is affected by the mountainous topography. Temperatures are lower and mean precipitation is higher. In contrast, climatic differences between the UK sites are small.

5.2.2-Spain sites and measurements

Gaseous pollutants, particulate SIC concentrations and meteorological parameters were continuously recorded in the CIEMAT air quality station (40° 27.5'N, 3° 43.5'W, 669 m asl).

The rural station selected for this study is Campisábalos (41° 17' N, 3° 09' W, 1 360 m asl), one of the sites selected for the preliminary analysis presented in the previous chapter, as representative of the Madrid air basin regional background. In this station PM_{10} filters are collected daily and analysed for ions.

Temperature and insolation data were collected from the Spanish Meteorological Service (AEMET) station in Puerto de Navacerrada (40° 46.83' N, 4° 0.62', 1 894 m asl). Puerto de Navacerrada is located in the mountain chain to the North-West of the air basin with similar characteristics as Campisábalos (figure 5.1, left).

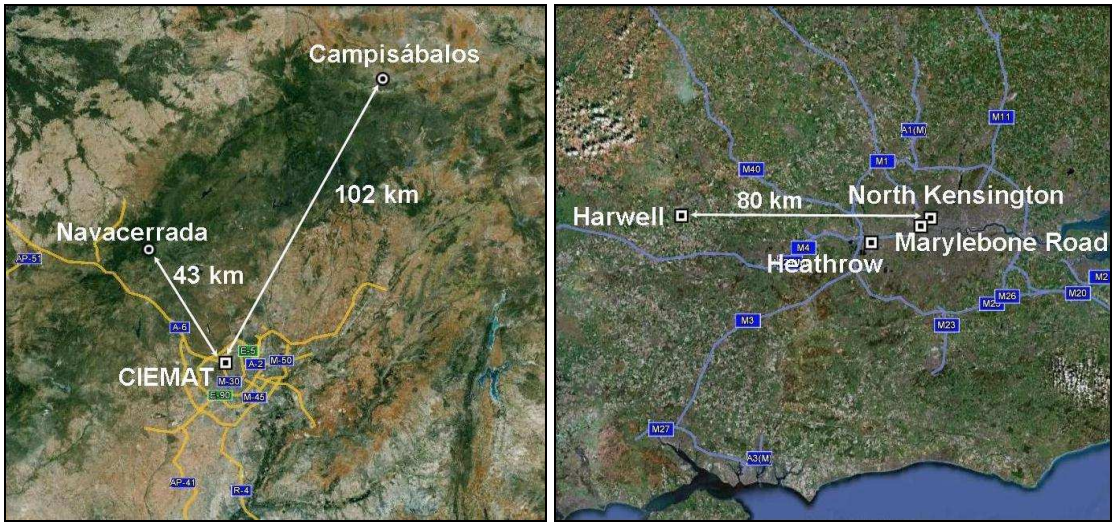

Figure 5.1. Maps of the two regions. (Left) Spanish sites, (right) UK sites.

5.2.3-UK sites and measurements

UK data have been obtained for sites that form part of the UK Automatic Urban and Rural Network (AURN) and the London Network (figure 5.1, right).

With a population over 7 million inhabitants, London is by far the largest city in the UK.

The Marylebone Road monitoring station (51° 32.6′ N, 0° 9.92′ W, 27 m asl) is one of the sites selected for this study. It is located on the kerbside of a major arterial route within the City of Westminster in London. Traffic flows of over 80 000 vehicles per day pass the site on 6 lanes with frequent congestion.

North Kensington (51° 31.27′ N, 0° 12.8′ W) is an urban background site located in a residential area to the west of central London, approximately 4 km from the Marylebone Road site. The nearest road is approximately 30 metres from the station with an average daily traffic flow of 8 000 vehicles per day. There are a number of retail and light industrial units located within the vicinity to the east and west of the monitoring station.

The Harwell rural site (51° 34.72' N, 1° 20.26' W, 137 m asl) is also an EMEP site and is located within the grounds of the Harwell Science Centre, in the middle of an unfarmed field and surrounded by predominantly agricultural land. It is around 80 km from London. There is limited activity in the area. Distant sources include the busy A34 dual carriageway about 2 km to the east and the Didcot power station about 5 km to

the north-east. A careful analysis of the influence of the power station has shown that it accounts for only 3.3% of the annual mean sulphur dioxide measured at Harwell (Jones and Harrison 2011).

These sites are equipped with continuous monitors recording fine nitrate concentration and gases. PM_{10} filters are collected daily and analysed for ions.

5.2.4 – Techniques

Spain: At the CIEMAT site, fine nitrate concentration was measured using the Rupprecht and Patashnick 8400N Nitrate Analyser with a $PM_{2.5}$ sampling inlet on a 10-min time basis. Semicontinuous PM_1 sulphate concentration was registered with the Thermo 5020 sulphate particulate analyser (SPA) on a time basis of 20 minutes. Gaseous species (SO_2, NO and NO_2) were measured by the DOAS spectrometer (OPSIS AR-500) along a 228 m horizontal path with a mean height of 10 m above ground. The measurement frequency was similar to the particulate nitrate instrument. Meteorological information was obtained from a permanent tower installed at CIEMAT with temperature at 4 m. Data were recorded every 10 min. At Campisábalos, PM_{10} filters are collected with an Andersen GUV15H sampler, and particulate sulphate and nitrate concentrations are subsequently determined by Ion Chromatography (IC).

U.K.: Fine nitrate concentration was measured using also a Rupprecht and Patashnick 8400N Nitrate Analyser with a $PM_{2.5}$ sampling inlet. Gaseous nitrogen oxides in the UK sites are measured hourly using the chemiluminescence technique. Gaseous SO_2 is measured by UV fluorescence. Filters at UK sites are collected using a Partisol sampler with a PM_{10} inlet and analysed for ions by IC. Meteorological data in the UK have been obtained from London Heathrow (51° 28.74′ N, 0° 26.94′ W, 25 m asl) which lies between the London sites and Harwell.

All plots use UTC time and averages have been computed if 50% of the data was captured over the averaging interval. Error bars are based on 95% confidence intervals (CI) of the mean.

5.3-Results

5.3.1-Annual patterns

Monthly averages have been computed to obtain a seasonal pattern for nitrate and sulphate in four sampling sites. Six years of data (2005 to 2010) have been computed except for the sulphate in Madrid, where available data started in June 2009. Due to this fact and the significant differences found in the years 2009 to 2011, measurement periods were plotted separately. In London, the site selected to calculate the seasonal evolution is Marylebone Road due to the higher data availability. A comparison with the urban background site did not show significant differences in the nitrate and sulphate monthly means (see Figure 5.2).

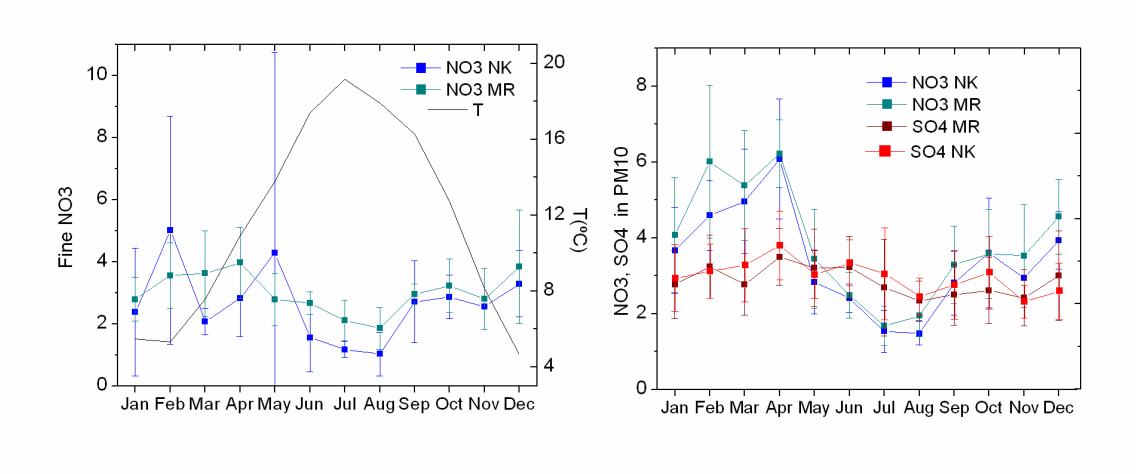

Figure 5.2. Monthly averages in North Kensington and Marylebone Road. (Left) Fine nitrate and temperature. (Right) Nitrate and sulphate in PM_{10}

Similar monthly averages and seasonal fine nitrate patterns were found in Marylebone Road and North Kensington, with matching data within the error bars. In North Kensington there are only two years of data available which showed large differences on some months. Similar monthly averages and seasonal PM_{10} nitrate and sulphate evolution were found in both sampling sites. Fine nitrate in North Kensington ranges 2008-2009, while all the other parameters range 2005-2010.

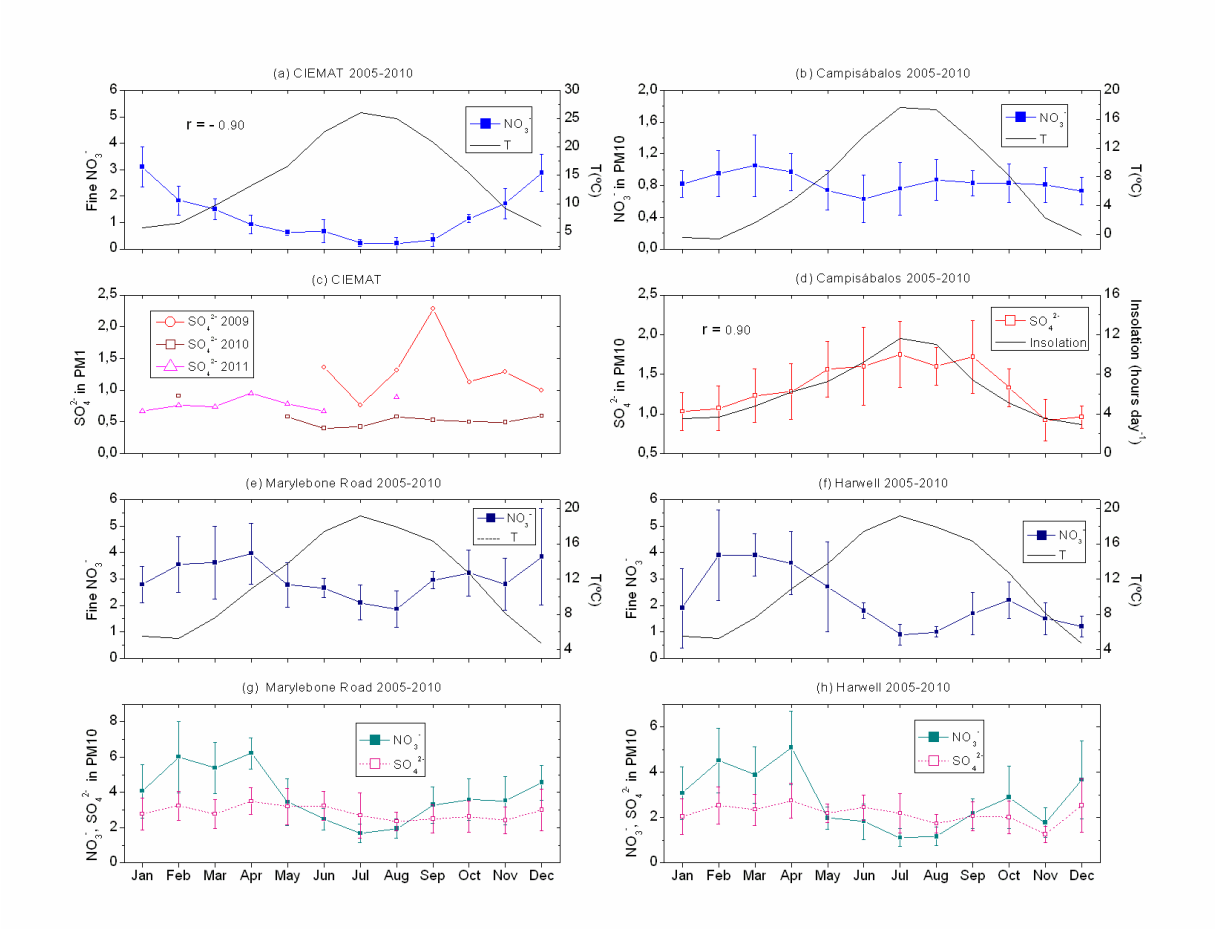

Figure 5.3. Monthly average concentrations (in μg· m^{-3}) of nitrate and sulphate in the size fractions and time intervals indicated

In central Spain, the highest nitrate monthly means are around 3 μg·m^{-3} at the urban background site and three times lower at the rural site. The sulphate concentrations show smaller differences, being below 2.5 μg·m^{-3}. In London and also at the rural Harwell site the fine nitrate monthly means are above the Madrid concentrations, reaching 4 μg·m^{-3}. PM_{10} nitrate and sulphate concentrations in Harwell are smaller than in London, but well above Campisábalos.

The behaviour of pollutants at both Spanish sites is very different, unlike the UK sites. This is thought to be a result of the different orography of the two regions and its interaction with meteorology. While southern England is flat, thus allowing a synoptic flow to be dominant at the regional scale, the Madrid Metropolitan Area lies within an air basin with a characteristic mesoscale wind circulation. Although the two rural sites are at similar distances from the main cities, Madrid and London, the rural site in the

UK is only 100 m higher than the city, though in Spain it is 700 m above. All this results in a small urban influence at the Spanish rural site, whereas Harwell is strongly influenced by the regional sources that influence London. The fine nitrate in Madrid (Figure 5.3a) showed a marked pattern, with small error bars, clearly dependant on temperature (linear correlation coefficient r = -0.90). This suggests that most of the nitrate is in a thermally unstable state, most probably ammonium nitrate and thus displaced towards the gas phase at high temperatures. At the rural Campisábalos site concentrations of PM_{10} nitrate are much lower (Figure 5.3b) than urban fine nitrate. Seasonal differences are not statistically significant. This suggests the presence of sodium or calcium, rather than ammonium, nitrates.

In the London site the lowest concentrations were also recorded in summer (Figure 5.3e) and the highest values mainly in springtime from February to April. As dependence on temperature was not as clear as in Madrid, other processes or source behaviour should be present. Analysing a 2002-2003 data set, Abdalmogith and Harrison (2005) found that the UK received the highest amounts of particulate nitrate and sulphate due to long range transport from central Europe during spring. This finding was recently confirmed by Baker (2010). Pollutant transport is reflected in the fine nitrate annual pattern. This type of external factor was also found by Salvador et al (2008) who, analysing PM_{10} and $PM_{2.5}$ filter-based SIC data from traffic, urban background and regional background monitoring sites from the Madrid airshed, showed that the Madrid air basin was also influenced by long range transport of SIC, in this case from Europe and the Western Mediterranean, in the warm season months. However, impact of long-range transport was not seen in the fine nitrate annual pattern at the Spanish sites for the study period analysed in this work.

At Harwell, fine nitrate levels (Figure 5.3f) are very similar to those at Marylebone Road. Both patterns showed similarities, but Harwell displayed a more marked minimum in summer and a less pronounced secondary maximum in autumn-winter. As Harwell is less influenced by local emissions, it is more representative of long-range transport and meteorological conditions.

PM_{10} nitrate (Figure 5.3g, 5.3h) showed slightly higher concentrations and a similar pattern to fine nitrate at Harwell. At Marylebone Road, the Feb-Apr maximum is

enhanced in PM_{10} nitrate. This reinforces the hypothesis of dominant locally generated ammonium nitrate in autumn and early winter and a significant contribution of transported nitrate in Feb-Apr.

PM_1 sulphate in Madrid (Figure 5.3c) showed a very flat pattern from 2010 on. In September 2009 concentrations were remarkably higher due to regional and long-range transport episodes from central Europe and the Western Mediterranean. These episodes will be analysed in detail in Chapter 7. PM_{10} sulphate at the rural site (Figure 5.3d), on the contrary, shows an insolation-dependent pattern (correlation coefficient r =0.90). Other researchers found higher fine sulphate concentrations in summer at urban sites in New York (Bari et al, 2003; Rattigan et al, 2006). They attributed it to the photochemical formation of sulphate from SO_2 through the OH radical, more effective in this season. This effect is not clearly seen in the Madrid sulphate.

Both of the UK sites present flat annual PM_{10} sulphate patterns (Figure 5.3g, 5.3h); nevertheless, levels are higher than in the Spanish sites. The remarkable maximum seen in nitrate in springtime is not reflected in the sulphate averages. The explanation may be related to aqueous phase oxidation processes making a greater contribution to sulphate in winter in the UK context (Jones and Harrison, 2011), and the lack of a temperature-dependent dissociation of ammonium sulphate.

5.3.2-Weekly patterns

24-hour averages by day of the week have been computed on a seasonal basis. Figure 5.4 depicts the weekly evolution of SIC and in some cases also the precursor gases NOx and SO_2 for the urban background sites. Winter (December to February) and summer (June to August) months have been chosen following a temperature criterion. The time periods selected for each pollutant and season have been determined by the minimum capture of 50% of data.

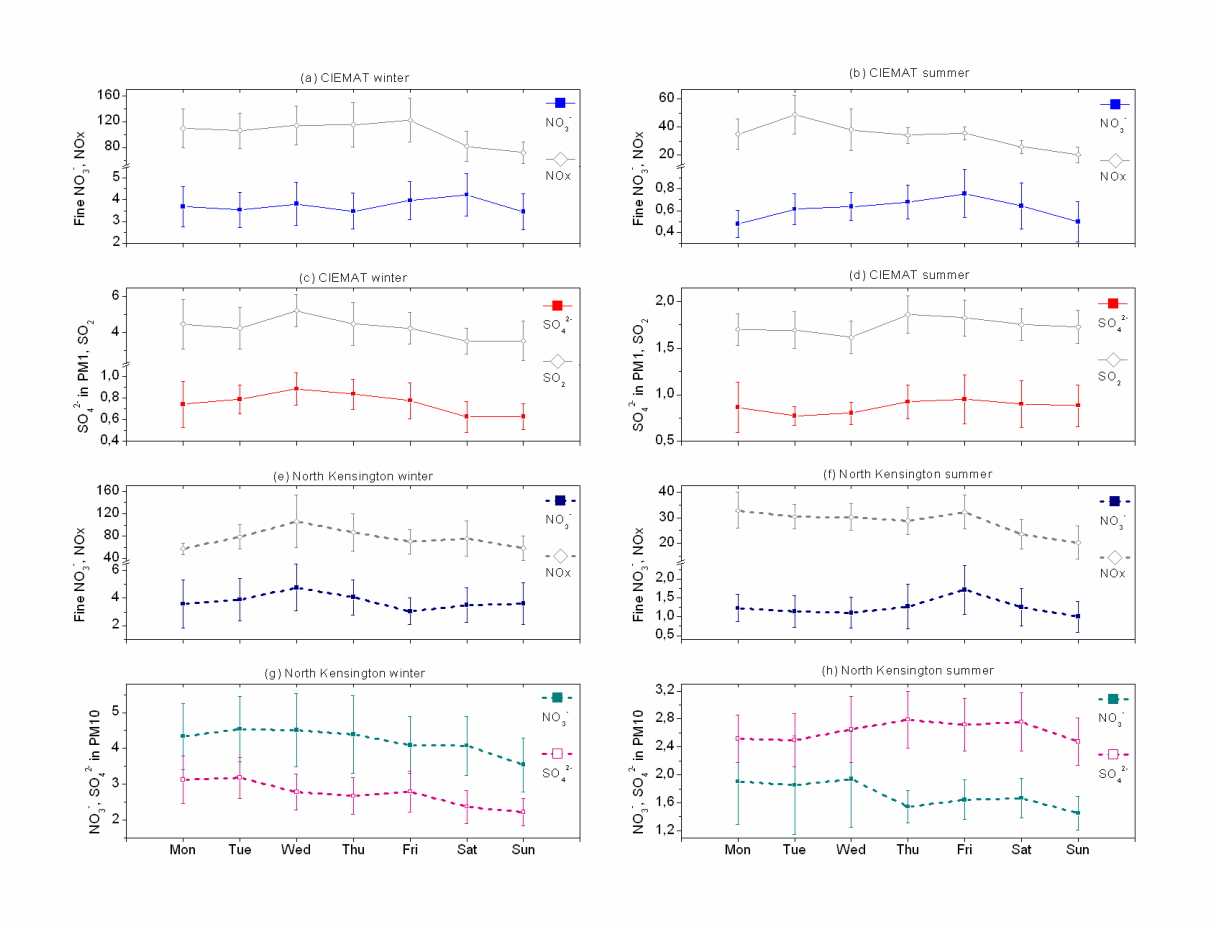

Figure 5.4. Daily averages. (a): CIEMAT winter. Nitrate 2004/2005-2010/2011 and NOx 2009/2010-2010/2011. (b): CIEMAT summer. Nitrate 2005-2011 and NOx 2011. (c) CIEMAT winter. Sulphate and SO_2 2010/2011. (d) CIEMAT summer. Sulphate and SO_2 2011. (e) North Kensington winter. Nitrate and NOx 2007/2008-2008/2009. (f) North Kensington summer. Nitrate and NOx 2008-2009. (g) North Kensington winter. Nitrate and Sulphate 2004/2005-2009/2010. (h) North Kensington summer. Nitrate and Sulphate 2005-2010. Concentrations in $\mu g \cdot m^{-3}$

Fine nitrate daily averages are much lower in summer in CIEMAT than in North Kensington and similar in winter, while NOx concentrations are similar or even higher (Fig. 5.4a, 5.4b, 5.4e and 5.4f). This is probably a result of summer thermal decomposition of nitrate in Madrid. A pattern related to emissions is seen for NOx both in Madrid and London. Ambient concentrations are lower during the weekend, most notably in Madrid in winter. In general, nitrate evolution is related to NOx evolution, though it does not follow it closely.

The weekend reduction R of a given pollutant for one week is calculated as:

$$R = \frac{[P_{day}] - [\overline{P}_{week}]}{[\overline{P}_{week}]}$$

Where:

P=pollutant

Table 5.1 shows the mean reduction for all the weeks considered $\overline{R}$ (± 95% CI) at CIEMAT and North Kensington. Non-statistically significant reductions are not shown. In Madrid, a significant nitrate weekend reduction can be seen in summer, although the minimum concentrations reached are displaced from Saturday-Sunday to Sunday-Monday, with mean reductions around 20%. In North Kensington, fine nitrate summer reductions of 21±16 % are found on Sundays. In a similar study, Millstein et al. (2008) calculated fine nitrate variations by day of week at four US urban sites for one year. In three of these sites the authors found nitrate weekly minima on Sundays or Mondays with mean annual reductions of 21-29% related to the weekly mean. Reductions found in Madrid and London are consistent with these values. In winter, at both urban sites fine nitrate weekend reductions were not significant.

	CIEMAT nitrate in $PM_{2.5}$	CIEMAT sulphate in PM_{10}	North K. nitrate in $PM_{2.5}$	North K. sulphate in PM_{10}
Winter				
Sat	---	18 ± 12 %	---	---
Sun	---	16± 15 %	---	13 ± 11 %
Mon	---	---	---	---
Summer				
Sat	---	---	---	---
Sun	18±11 %	---	21±16 %	---
Mon	20±13 %	---	---	---

Table 5.1. Mean weekend reductions in SIC ± 95% CI

Results for SO_2 and sulphate at CIEMAT are depicted for winter 2010-2011 (Figure 5.4c). In winter 2009-2010 meteorological conditions favoured the ventilation of the city and, with sulphate concentrations very low, no pattern was seen. In winter 2010-2011 several intense atmospheric stagnation episodes took place, favouring pollutant

accumulation. Under these conditions, a regular sulphate weekly evolution appeared, with reductions above 15% for Saturdays and Sundays. This behaviour corresponds with the SO_2 weekend reduction. This points to urban SO_2 as a source for sulphate although it does not rule out a diesel primary sulphate source. Artíñano and other researchers stated that the seasonal evolution of SO_2 in Madrid reflected the influence of heating devices in autumn and winter, causing levels considerably higher from November to March (Artíñano et al, 2003). In summer (Figure 5.4d), although SO_2 concentrations are significantly lower than in winter, the similar sulphate concentrations reflect the great oxidising capacity and reaction rates in this season.

On 1 January 2009 the European Directive 2003/17/EC limited sulphur in all vehicle fuels to a maximum of 10 $mg \cdot kg^{-1}$. These reductions were adopted earlier for some kinds of fuels in several EU countries, including Spain and the UK. Fuels for heating devices have also been refined. The installation of new facilities emitting more than 0.86 g of SO_2 to produce 1kW is forbidden in Madrid since 1985 (Ayuntamiento de Madrid, 2009). However, older devices still exist. In spite of these reductions weekly SO_2 and sulphate patterns demonstrate the anthropogenic influence on sulphur-derived pollutant ambient concentrations when meteorological conditions favour accumulation.

PM_{10} SIC in winter and PM_{10} nitrate in summer at North Kensington show a slight weekly downward tendency (Figure 5.4g, 5.4h). Significant reductions are found for sulphate on winter Sundays. Analysing data from filter-based measurements averaged between 2000 and 2002, Jones et al (2008) did not find any SIC weekend reduction at the North Kensington or Harwell sites; nevertheless, statistical differences were found at both stations for particulate matter. In this study, a small SIC weekend reduction can be derived for the PM_{10} fraction, although the summer reduction for the fine nitrate is clearer.

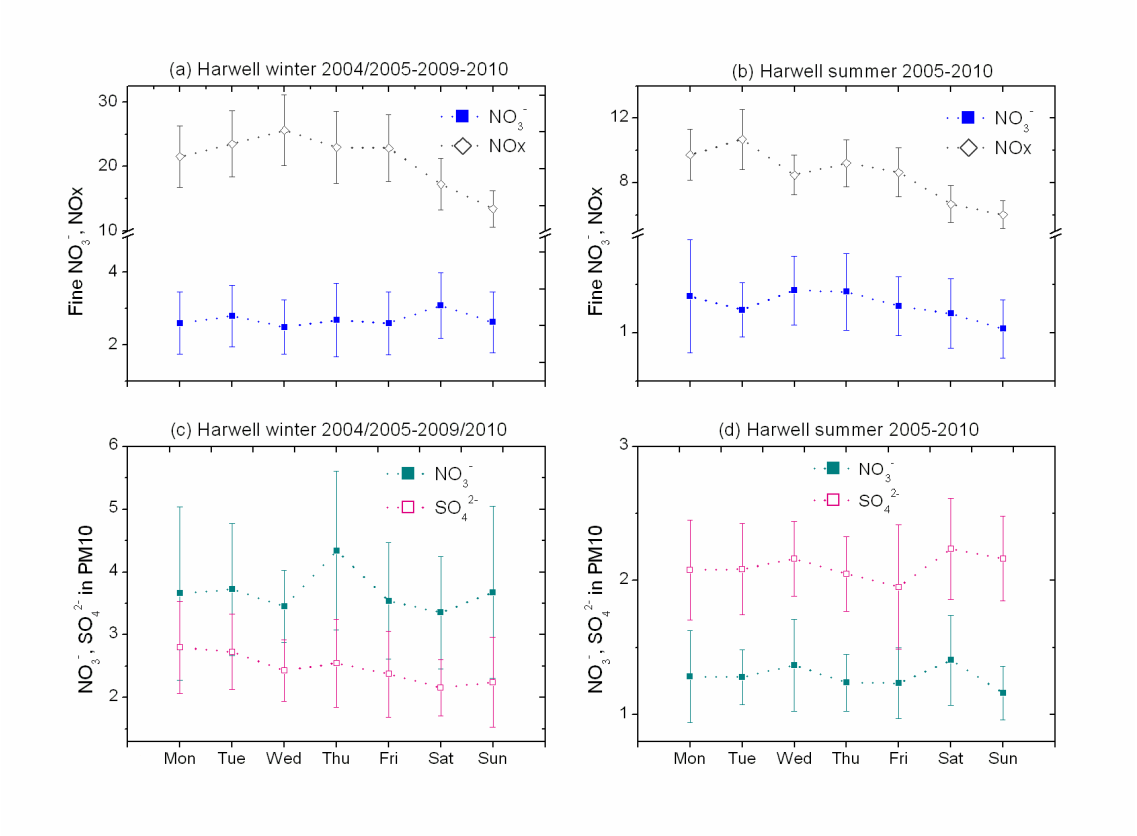

Figure 5.5. Daily averages in Harwell (a) Fine nitrate and NOx in winter. (b) Fine nitrate and NOx in summer. (c) Nitrate and sulphate in PM_{10} in winter. (d) Nitrate and sulphate in PM_{10} in summer

The weekly evolution of pollutants was also investigated at Harwell, since this site might have some local anthropogenic influence (see Figure 5.5). NOx levels were considerably lower than in North Kensington, however, nitrate levels were not so much smaller. No statistically significant SIC weekend reductions were found. No weekend PM_{10} SIC reduction is seen at the Spanish rural site (see Figure 5.6).

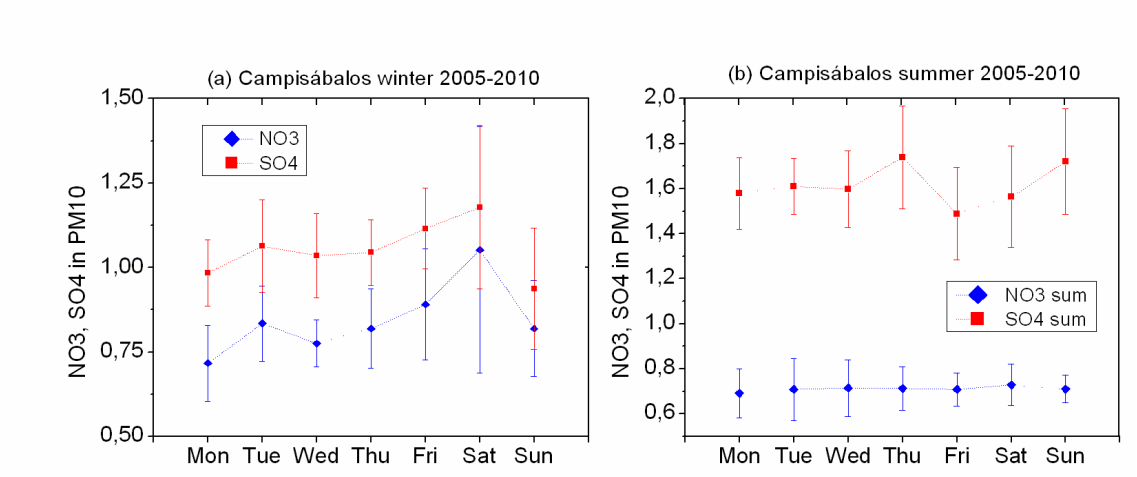

Figure 5.6. Daily averages in Campisábalos (a) Nitrate and sulphate in PM_{10} in winter. (d) Nitrate and sulphate in PM_{10} in summer

In short, significant nitrate weekend reductions have been observed in both cities in summer, while sulphate weekend reductions were significant in winter also in the two cities studied. Assuming that in winter precursor emissions are higher and meteorological conditions favour the accumulation of pollutants, this facts would lead to the presence of secondary compounds formed in week days during the weekend. In summer, emission and meteorological conditions do not favour pollutant accumulation and this, together with the fast reaction velocity of nitrate would allow identifying weekend reductions for this pollutant. The behaviour of sulphate might be associated to the presence of a primary diesel source.

5.3.3-Daily patterns

Average daily SIC and precursor gas profiles have been computed seasonally from 1h averages, separating weekdays and Sundays. Weekdays are Tuesday to Friday when a significant Monday reduction was observed.

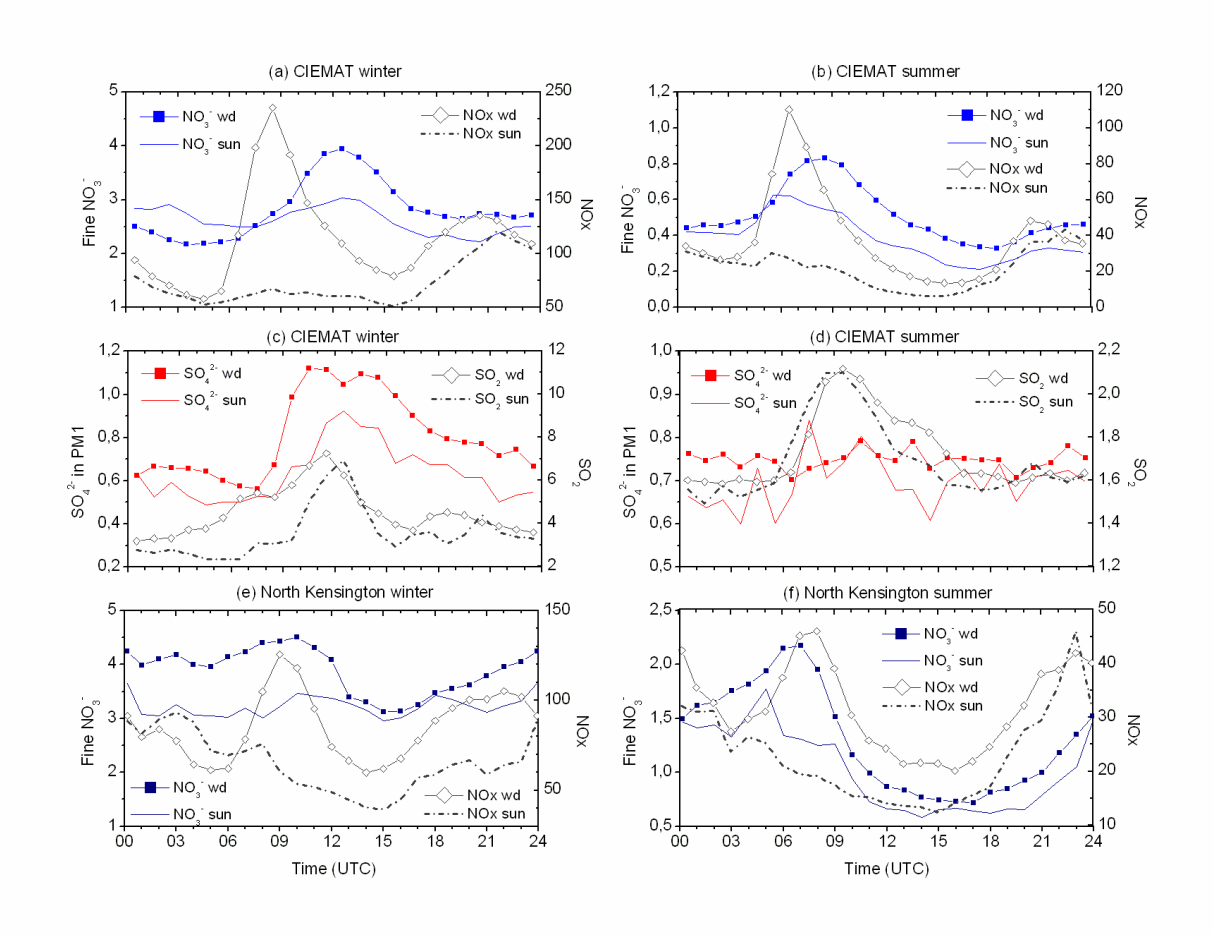

Figure 5.7. Hourly averages in concentration. Time periods correspond to Figure 5.4. Concentrations in μg·m⁻³

NOx rises corresponding to the morning traffic rush hour and the secondary rush hour during the evening. In winter in Madrid, nitrate (Figure 5.7a) follows closely the diurnal change in solar radiation (not shown for clarity) on weekdays. This suggests the dominance of photochemical processes in nitrate formation in Madrid, as Gomez-Moreno et al (2007) have already stated. In summer, the morning nitrate rise started before dawn (6 UTC in average) (Figure 5.7b). After 9 UTC the combined effect of the rise of the mixing height and the diurnal increase of temperature dominated over the photochemical formation of nitrate. NOx concentration is significantly lower than in winter, which can be partly explained by lower traffic emissions, but is also probably related to the greater mixing depth. The secondary evening traffic peak also appeared in nitrate in summer, but not in winter. This peak has been explained by other authors in terms of the contraction of the mixing layer (ML), which is consistent with our

results, since it is hardly exhibited on Sundays, unlike the morning peak. In general, the evolution of the convective ML in the Madrid area begins 1h after dawn, reaching the maximum value at 12-15 UTC and decreasing usually around 16 UTC (Crespí et al, 1995). Crespí et al (1995) studied the evolution of the ML in Madrid under different synoptic conditions, obtaining a classification according to different meteorological scenarios. Under synoptic situations typically found in autumn and winter the ML is very shallow, not exceeding 700 m agl. In spring and summer the mixing height can be well above 2000 m agl.

In winter 2010-11 a daily PM_1 sulphate pattern was found in Madrid (Figure 5.7c). Both SO_2 and sulphate peaks are centred at noon, and concentration increased earlier in the morning on weekdays. An evening increment appeared in SO_2 in winter weekdays. For Sundays, the lesser data available resulted in a noisy pattern that made this increment unclear. In summer, a daily pattern with no remarkable differences between weekdays and Sundays was also seen for SO_2, peaking earlier than in winter, but not for sulphate (Figure 5.7d). This suggests that the increase is driven by meteorological processes rather than low-level emissions. Sulphate daily evolution differs from the results found by Wittig et al (2004) in Pittsburgh. They found diurnal variation only in summer, consistent with local photochemical production.

To infer the source of precursor gases polar diagrams have been plotted using the OPENAIR software (Carslaw et al, 2011). Figure 5.8 shows NOx and SO_2 concentrations at the CIEMAT site in winter as a function of wind direction and time-of-day. NOx maximum concentrations arrive in the morning from the East, while SO_2 arrives later in the morning and noon from the south-eastern sector. Wind directions indicate that the air masses come from the city and are a consequence of mean wind circulation in the Madrid air basin. The delay of SO_2 indicates that road traffic is not the main source. In North Kensington, Bigi and Harrison found a similar behaviour of SO_2 in both seasons. The authors suggested that the timing of the maximum was driven by the entrainment of high level emissions into the mixing layer, since polluted air from aloft is mixed downwards as the boundary layer increases in depth in the morning (Bigi and Harrison, 2010).

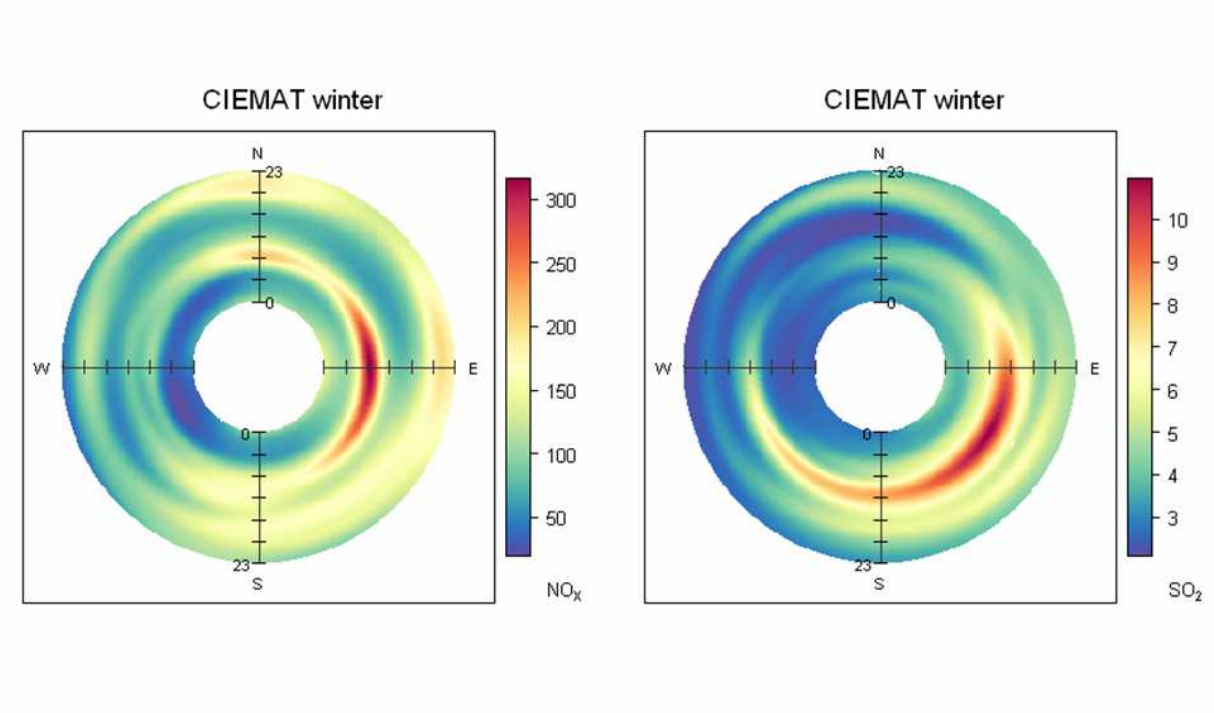

Figure 5.8. Polar plots of (left) NOx and (right) SO_2 ($\mu g \cdot m^{-3}$) at the CIEMAT site in winter as a function of wind direction and time-of-day. Inside of circle is 00:00-01:00 h UTC running through the day to 23:00-24:00.

NOx hourly evolution is similar in both cities, though the evening increment is more marked in London. However, in North Kensington, nitrate behaviour was very different to that in CIEMAT in winter. On winter weekdays, nitrate kept steady values (Figure 5.7e) with a drop in concentrations in the afternoon. In summer, the morning evolution is similar to that in Madrid, but the evening and night concentration rise is notably higher. The presence of the afternoon drop was detected in 2009 hourly averages in North Kensington and Harwell (Harrison et al, 2012a). North Kensington fine nitrate profiles are more similar to the ones found by Wittig et al (2004) at the Pittsburgh Supersite, located in an urban park. Nocturnal high values are explained by low temperature and high relativity humidity. In Madrid, nocturnal high nitrate levels related to very high relative humidity have been observed only occasionally (Gomez-Moreno et al, 2007).

During the REPARTEE-II campaign, which took place in London in autumn 2007, Barlow et al (2011) studied the daily evolution of the boundary layer during three weeks using a Doppler lidar. On average, they found an 800 m maximum mixing

height at 13-15 h, and a delayed 600 m maximum aerosol layer height at 15-17 h. In the present work, averaged winter NOx concentrations showed a deep minimum at 14h on weekdays, while fine particulate nitrate showed a delayed minimum at 15-16h on winter weekdays. The response of reactive gaseous and particulate pollutants to changes in the mixing layer is not known with certainty. A different response of NOx and particulate nitrate is not surprising, since NOx is only affected by the dilution, whereas the reduction in gaseous HNO_3 and NH_3 concentration shifts the phase equilibrium causing particulate nitrate disintegration. Thus, particulate nitrate concentration is reduced due to a double effect. This result supports the hypothesis that the expansion of the mixing layer in the warmest hours of the day plays a major role in the formation of the afternoon aerosol concentration minimum.

Finally, comparing seasonally the levels reached by NOx and nitrate, it is found that hourly NOx concentrations are noticeably higher in Madrid. However, nitrate maximum hourly concentrations are higher in North Kensington, most notably in summer. The smaller seasonal difference in London can be attributed to smaller summer increments in temperature and mixing height in London (Rigby et al, 2006). This suggests, as inferred above from the weekly patterns, that nitrate formation is more efficient in London. This is likely to be related to the lower temperatures. However, in urban environments, nitrate in the fine fraction is mainly formed through the neutralization of gaseous nitric acid by a base, usually ammonia. A second pathway involves heterogeneous formation from $\cdot NO_3$ or N_2O_5 on water droplets, producing acid aerosols. Thus, the higher efficiency of nitrate formation in London could be related to ammonia availability or higher relative humidity; however, there is insufficient information on ammonia in Madrid or London to go into this topic in greater depth. Pollutant apportionment between long-range transport and local formation should be also quantified.

5.3.4-Ratios NO_3^-/NOx, SO_4^{2-}/SO_2 and SO_4^{2-}/NO_3^- in Madrid

Seasonally averaged ratios of nitrate and sulphate to precursor gases and SO_4^{2-}/NO_3^- ratios have been calculated on a daily basis when more than 50% of data were

available simultaneously (Table 5.2). This corresponded to one or two seasons except for the summer 2011, when only data from 1 June to 7 July were available.

	NO_3^-	NOx	NO_3^-/NOx	r
Winter 2010/2011	2.60	119.24	0.03	0.74
Summer 2011	0.33	38.42	0.01	0.20

	SO_2	SO_4^{2-}	SO_4^{2-}/SO_2	r
Winter 2009/2010-2010/2011	4.32	0.88	0.29	0.31
Summer 2009	2.76	1.15	0.42	-0.13

	NO_3^-	SO_4^{2-}	SO_4^{2-}/NO_3^-	r
Winter 2009/2010-2010/2011	3.59	0.87	0.71	0.40
Summer 2009-2010	0.58	0.78	1.81	0.38

Table 5.2. Ratios NO_3^-/NOx, SO_4^{2-}/SO_2 and SO_4^{2-}/NO_3^-, and correlation coefficients r in Madrid

Ratios of the secondary inorganic pollutants to precursor gases NO_3^-/NOx and SO_4^{2-}/SO_2 give some more clues about formation processes and/or aerosol sources. The gas-phase reactions responsible for the formation of particulate SIC involve the slow oxidation of SO_2 to sulphate and NO_2 to nitrate mainly by the OH radical, generated photochemically by the action of solar radiation on oxidants, and by heterogeneous processes. In principle, if photochemistry is dominant, higher oxidation ratios at summer would be expected. However, aqueous-phase reactions also generate secondary nitrate and sulphate and are more likely to take place in winter. Other processes, such as thermal decomposition of nitrate and pollutant transport can also influence the ratios.

In CIEMAT, **NO_3^-/NOx** was higher in winter. In this case, it is probably a consequence of thermal decomposition, but the role of heterogeneous formation is very hard to quantify. The correlation coefficient r in summer was low. The small number of simultaneous NOx and nitrate data make difficult to draw representative conclusions.

The $\mathbf{SO_4^{2-}/SO_2}$ ratio was higher in summer. Sulphate levels did not show a big seasonal variation, and the ratio difference can be attributed to lower summer SO_2 concentrations. A small negative **r** appears in summer. This is consistent with the hypothesis of a relevant fraction of sulphate in Madrid in summer not originated from oxidation of local SO_2, but being the result of a regional background with contributions from long range transport. Finally, $\mathbf{SO_4^{2-}/NO_3^-}$ was higher in summer, as a consequence of nitrate variations. Correlations were low, supporting again the hypothesis of different controlling processes for sulphate and nitrate.

5.4-Conclusions

An analysis of temporal patterns on annual, weekly and daily timescales has been performed for urban and rural sites in the Madrid airshed. This analysis has been performed in parallel with a study performed in south-eastern UK, to identify similarities and discrepancies that contribute to identify main processes and relevant parameters in each case. Patterns in precursor gases have also been considered. Results indicate the dominant processes affecting the formation and evolution of nitrate and sulphate in both regions.

NOx concentrations are higher in Madrid; nevertheless, nitrate concentrations are higher in London, most notably in summer. This might indicate that nitrate formation is more efficient in London, although thermal dissociation processes also influence nitrate concentrations. The seasonal fine nitrate pattern in Madrid was dominated by temperature-driven evolution. Concentrations at the rural site Campisábalos were comparatively very low. These factors suggest that fine nitrate in Madrid has mainly a local production origin. In contrast, the annual nitrate pattern in London shows thermal decomposition in summer, but also a notable maximum from February to April. This maximum is more clearly seen in PM_{10} than in $PM_{2.5}$ nitrate and also at the rural UK site, Harwell, relative to the London sites which allows it to be identified with well known pollutant transport from mainland Europe.

Higher PM_{10} sulphate concentrations were registered in the UK. No seasonal evolution was seen though. The absence of a spring maximum attributable to European transport is surprising, but may relate to the involatility of ammonium sulphate. In Spain,

photochemical formation in summer was seen at the rural site, but not in urban PM_1 sulphate.

SIC weekend reductions were investigated. In both cities fine nitrate reductions around 20% are found in summer with statistical significance. These results are consistent with the findings of Millstein et al (2008) in the US in 2008. Weekend sulphate reductions in the range 13-18 % were found at the urban background sites in winter. The hypothesis to explain this result are related to the different behaviour of the atmosphere in winter and summer in the case of nitrate. While in winter meteorological conditions favour accumulation of pollutants, in summer the pollutant removal is favoured instead. In the case of sulphate, the presence of a primary diesel source might explain the result found.

In Madrid, the daily evolution of urban nitrate was a consequence of meteorological effects. In winter, low temperatures and the small vertical extent of the mixing layer allowed the dominance of photochemistry in nitrate formation. In summer, higher temperatures and a greater mixing height resulted in a more complex pattern. A secondary evening peak appeared in nitrate in summer. This peak has been explained in terms of the contraction of the mixing layer, which is consistent with our results, since it is not inhibited on Sundays. The pattern followed by NOx is similar in both cities; however, nitrate behaviour was very different in winter. High concentrations were registered in North Kensington at night-time, explained as a consequence of nitrate formation under high humidity conditions. Winter NOx concentration showed a deep minimum in the afternoon followed by a delayed maximum in particulate nitrate on winter weekdays in North Kensington. This behaviour is consistent with afternoon changes in the mixing layer. The results from both cities indicate that nitrate hourly evolution is predominantly determined by meteorological factors rather than by the evolution of precursor gases. For a complete interpretation of daily pollutant evolution a complementary mixing layer study and measurement of vertical gradients is needed.

In Madrid in winter SO_2 and SO_4^{2-} peaked at noon. The same phenomenon is observed in London for SO_2, where it is explained by the entrainment of pollutants emitted at high level into the mixing layer.

SO_4^{2-}/SO_2 ratio in Madrid was very low, especially in summer. This is consistent with the premise that a relevant fraction of sulphate is not locally generated, but is the result of a regional background with a long range transport component.

These data analyses complement the process-based work carried out in London in the REPARTEE experiments (Harrison et al., 2012b). Campaign-based measurements using both ground-based and an elevated sampling platform showed the influence of regional transport of sulphate upon sulphate concentrations in London, with concentrations aloft exceeding those at ground-level during an episode. On the other hand, nitrate fluxes were less clearly uni-directional and were much influenced by the potential of ammonium nitrate for dissociation/association. The diurnal processes involved in transfer of nitrate between the condensed and vapour phases were clearly observed using single particle mass spectrometry (Dall'Osto et al. 2009) and the potential for nitrate formation via NO_3 and N_2O_5 was demonstrated by observations aloft on the BT Tower (ca 160 metres) (Benton et al., 2010). The data analyses in this work show strong seasonal influences, upon nitrate especially, and that behaviour seen in London is not representative of that in Madrid. The overall conclusion is therefore that the processes controlling nitrate and sulphate concentrations may vary substantially across Europe and hence observations in one city should not be assumed to be applicable elsewhere.

6-CHARACTERISATION OF EVENTS OF FINE PARTICULATE MATTER IN MADRID I

6-CHARACTERISATION OF EVENTS OF FINE PARTICULATE MATTER IN MADRID I

6.1-Introduction

In chapter 4 we saw that decreasing SIC and precursor gases trends have been recorded at the Madrid air basin in the last decade. In chapter 5, the average evolution in different timescales of sulphate and nitrate was characterised. The high correlation between sulphate and radiation at Campisábalos showed the enhanced photochemical sulphate formation in summer. At the urban area of Madrid, Sunday reductions in winter and SO_4^{2-}/SO_2 ratios indicated the relevance of local sources in winter, whereas in summer the results were consistent with the dominance of a regional sulphate background. The chemical stability of particulate sulphate allows it to be considered as a tracer of the regional recirculation but this pollutant can also travel thousands of kilometres in the atmosphere. The impact of sulphate transport can have a significant impact on the fine aerosol concentrations (Wagstrom et al, 2011). Thermal decomposition of particulate nitrate make more difficult the identification of its transport, however, nitrate can also be transported over long distances.

At six regions of Spain –including the Madrid air basin- in the period 1996–2000, in addition to the local pollution events, high PM_{10} episodes were recorded during African dust outbreaks, regional atmospheric recirculation events (mainly in spring to autumn), and to a lesser extent, under the influence of European and Mediterranean long range transported air masses (Querol et al, 2004c). Identification of intensive air pollution events from the European continent in PM_{10} is complex. However, the authors suggested that most of these episodes may increase sulphate levels at the Iberian Peninsula in the range of $< 5\ \mu g \cdot m^{-3}$, in accordance with the observations made by the Marine Meteorology Division of the Naval Research Laboratory of the US (http://www.nrlmry.navy.mil/aerosol/#aerosolobservations).

Using electronic microscopy techniques, Coz et al (2010) characterised particulate material at Madrid under four different types of events (regional, local, African and Atlantic). This work showed that the percentage of sulphate in particle mass in three size fractions was a maximum in regional episodes, followed by local pollution events.

References to regional pollutant transport at the Madrid air basin are frequent in literature (e.g. Salvador et al, 2004b; Plaza et al, 2011; Fernández-Gálvez et al, 2012). However, the studies of long-range transport of SIC into the Madrid air basin are rare in literature, and are probably limited to Salvador et al (2008). Using back-trajectory clustering during the 1999–2005 period, the authors identified the highest SIC concentrations in PM_{10} and $PM_{2.5}$ for clusters representing:

1- low speed air circulation or regional transport. Cluster containing short trajectories of air mass recirculating within the Iberian Peninsula. This situation occurred predominantly in the summer and early autumn months.

2- transport of air masses from the European Continent towards the Iberian Peninsula, through the Mediterranean Sea. On average March, June and December were the months with a higher occurrence of this transport pattern.

The existence of other source areas which might contribute to sulphate and nitrate levels in the Madrid air basin must not be discarded either. North-African anthropogenic emissions are increasingly being considered in air pollution studies. Studying transport patterns and trends in precipitation chemistry of a rural site in North-Eastern Spain in the period 1984-2009, Izquierdo et al (2012) discovered that industrialisation in Eastern Europe and North Africa seemed to be acquiring a greater role in the recent period. For sulphate, source areas extended over a vast stretch of central Europe in the early period, but were drastically reduced in the last years due to the effectiveness of pollution abatement measures for S. Meanwhile, NO_3^- sources areas from central Europe strikingly increased.

Episodes giving rise to significant fine nitrate increases at Madrid were described by Gomez-Moreno et al (2007). Two different types of events, which corresponded with daytime and night-time under low dispersive conditions, were found. Morning increases were associated to photo-oxidation processes in a narrow mixing layer, while nocturnal increases took place under high humidity conditions. Two events of each kind were described in detail. Peaks attributed to transport were also identified.

In this chapter, a characterisation of episodes giving rise to high fine sulphate and nitrate concentrations at Madrid is presented. Three examples of basic kinds of

episodes are described. The first kind corresponds to regional recirculation of pollutants. The type of meteorological scenario which gives rise to air mass recirculation processes is characterised by strong thermal convection that favours particle resuspension. It is typical of the warmest days of the summer season (Millán et al, 1997). The second kind corresponds to long-range transport from Central Europe and the Western Mediterranean. Despite the predominance of the general Western circulation, polluted air masses from the European continent may reach the Peninsula through the Mediterranean basin or the Gulf of Biscay. The third kind corresponds to a typical winter anticyclonic situation. The stagnation of air during winter thermal inversion favours concentration in a local scale during the coldest months of the year. PM accumulates under stable atmospheric conditions favoured by the presence of high pressures at surface level.

6.2-Methods

The objective of this chapter is the identification of different kinds of events giving rise to high sulphate and nitrate concentrations at an urban background environment at Madrid. Long range transport events are more easily identified and characterised at remote stations where influence from local sources can be neglected. Back-trajectory clustering has been performed for separate periods with the objective of a more reliable identification of transport episodes.

Back-trajectory clustering was performed with the HYSPLIT model for two periods:

> 1 - Aug-Nov 2009, characterised by recirculation of air at the Mediterranean basin. The atmospheric stability led to high pollutant concentration at the Western Mediterranean and Central Europe.
>
> 2 – Dec 2010-Mar2011, characterised by several intense atmospheric stagnation episodes and local pollution accumulation at the Madrid air basin.

The SIC concentrations registered at Madrid were depicted for each cluster.

The episodes selected were described using the following techniques:

-The time evolution of air pollutants and meteorological parameters was depicted in high temporal resolution (20 min). Semicontinuous PM_1 sulphate concentration, semicontinuous $PM_{2.5}$ nitrate concentration, gaseous species (SO_2, NO and NO_2), particulate mass concentration (PM_{10}, $PM_{2.5}$ and PM_1), wind direction and wind speed were monitored at the CIEMAT sampling station using the instrumentation described in chapter 3.

-SIC evolution at Madrid was compared with the PM_{10} SIC evolution at three EMEP rural stations at the central Iberian Peninsula: ES01 (San Pablo de los Montes; Toledo), ES09 (Campisábalos; Guadalajara) and ES13 (Peñausende, Zamora). Information from rural stations helped to identify transport events.

- In addition to the HYSPLIT clustering analysis, 7 days back-trajectories were obtained at fixed times for the specific events described using the FLEXTRA model.

-The distribution of surface concentration of sulphate across the European continent was estimated with the NAAPS model at the same times selected for FLEXTRA back-trajectories calculation.

6.3-Results

6.3.1-Cluster analysis

Two 4-day back-trajectories per day (0h and 12h UTC) arriving at Madrid were computed. A fixed height of 2000 m agl was chosen as the arrival level. This height is in general above the boundary layer, which allows avoiding surface artefacts, but not too high. The meteorological variables used for the first period were obtained from the NCEP/NCAR Reanalysis datasets files (Kalnay et al., 1996), provided by the NOAA/OAR/ESRL PSD, USA. For the second period, reanalysis data were not available, so GDAS meteorological files, also provided by NCEP, were used. The vertical velocity field used was the one included in the meteorological data files.

• **Aug-Nov 2009**

244 trajectories were computed for this period.

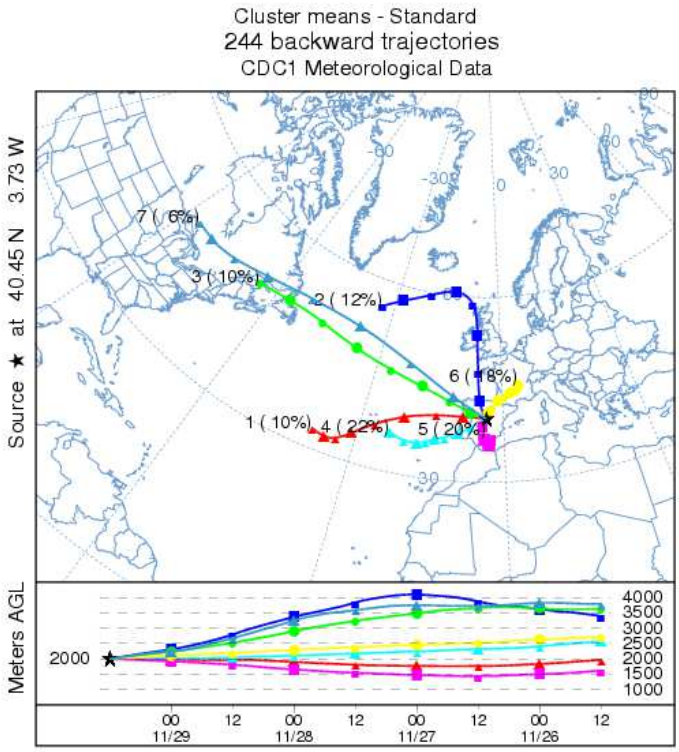

Figure 6.1. Cluster means for the period Aug-Nov 2009

The HYSPLIT software found solutions for 3, 4 or 7 clusters. In all cases there was a very stable cluster characterised by low wind speeds and recirculation over the Western Mediterranean basin. The 7-cluster model differentiated two clusters, one formed by trajectories arriving from Central Europe (no. 6, yellow) and another formed by trajectories recirculating within the central and southern Peninsula, sometimes starting at the North of Africa (no. 5, pink). The 3 and 4-clusters models merged these two cases together. The 7-cluster analysis was selected. Back-trajectories grouped in each cluster can be consulted in Appendix III.

PM_1 sulphate measured at CIEMAT was rescaled into a 12-hour basis. Figure 6.2 depicts the sulphate concentrations measured for every trajectory at the CIEMAT sampling station. Error bars in cluster means represent the 95% confidence intervals.

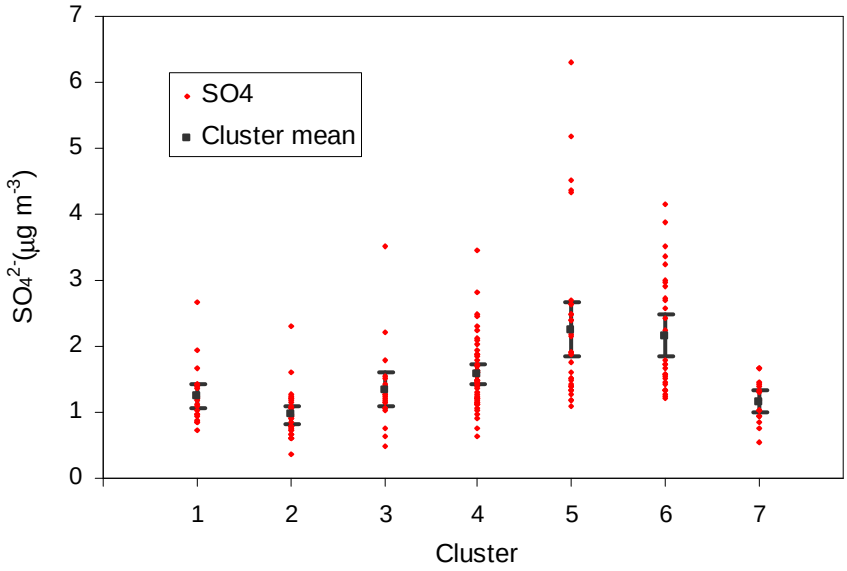

Figure 6.2. Sulphate concentration per cluster for the period Aug-Nov 2009

The sulphate means are significantly higher for clusters 5 and 6. The 4 data points attributed to cluster 5 exhibiting the highest sulphate concentrations correspond to the dates 29 Sept to 1 Oct. This period is included in the E2a event -which will be described below-. E2a is characterised by 25 back-trajectories in total, 21 of them belonging to cluster 6 and 4 belonging to cluster 5.

Nitrate data capture (30%) in this period was insufficient to perform the same analysis.

- **Dec10-Mar11**

230 trajectories were computed for this period.

In this case a 6-clusters model has been selected. Again, the model differentiated two clusters, one formed by trajectories arriving from Central Europe (no. 1, red) and another formed by trajectories recirculating within the Peninsula and north of Africa (no. 3, green). Back-trajectories grouped in each cluster can be consulted in Appendix III.

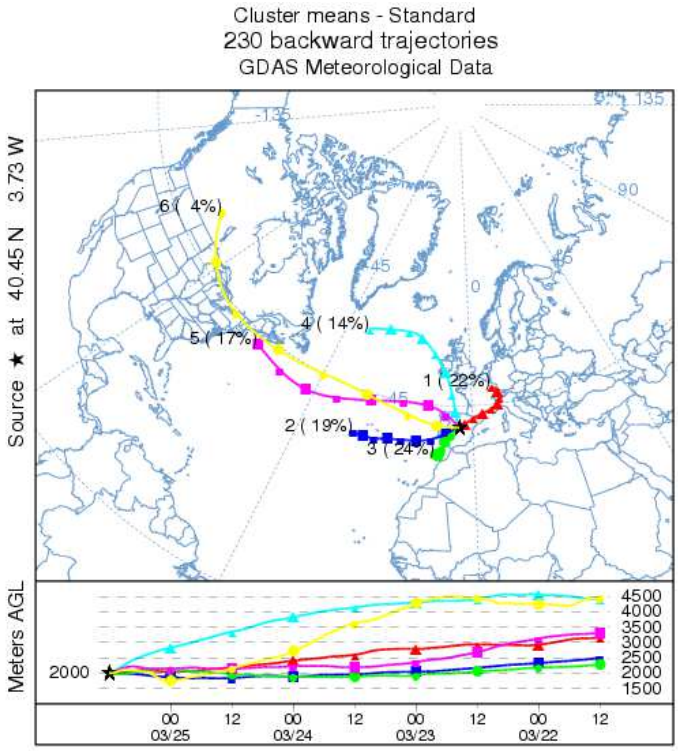

Figure 6.3. Cluster means for the period Dec 2010-Mar 2011

Figure 6.4 depicts the sulphate and nitrate concentrations measured per cluster for Dec 2010-Mar 2011. The highest concentrations of both pollutants are found for cluster 2 (slow trajectories starting in the Atlantic Ocean) and 3 (regional recirculation). Looking at the back-trajectories included in cluster 2 (Appendix III) we can see that all of them are originated in the Atlantic Ocean, but some of them show recirculation over the Iberian Peninsula and North of Africa before arriving in Madrid. The trajectories associated to the highest concentrations of sulphate and nitrate belong to recirculation or local events in which sometimes some trajectories are included in cluster 2. The corresponding dates are the following: 28/12/2010, 13-14/1/2011, 17-19/01/2011 and 10/2/2011.

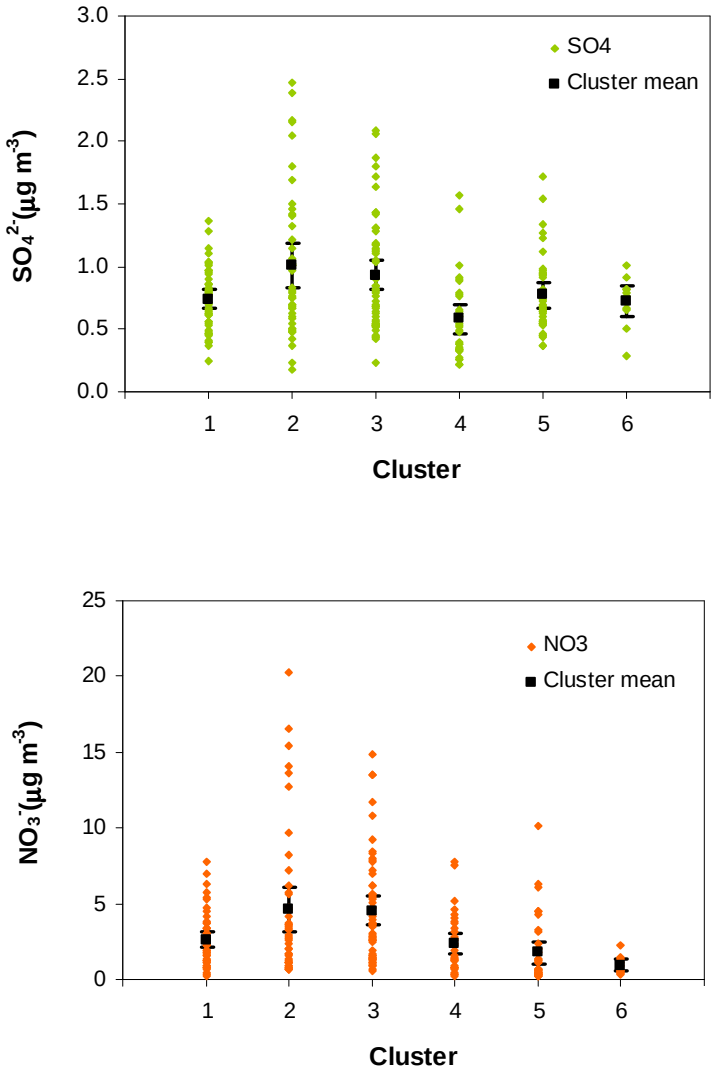

Figure 6.4. Sulphate (top) and nitrate (bottom) concentration per cluster for the period Dec 2010-Mar 2011

In contrast with the period Aug-Nov 2009, the cluster formed by back-trajectories arriving from Central Europe does not correspond to high concentrations of PM_1 sulphate.

6.3.2-Regional recirculation and European long-range transport events

Events E1, E2a and E2b have been selected as examples of different situations which led to high SIC concentrations in the period Aug-Sept 2009.

-E1: regional transport-

E1 took place between 1 and 2 September 2009 (see Figure 6.5).

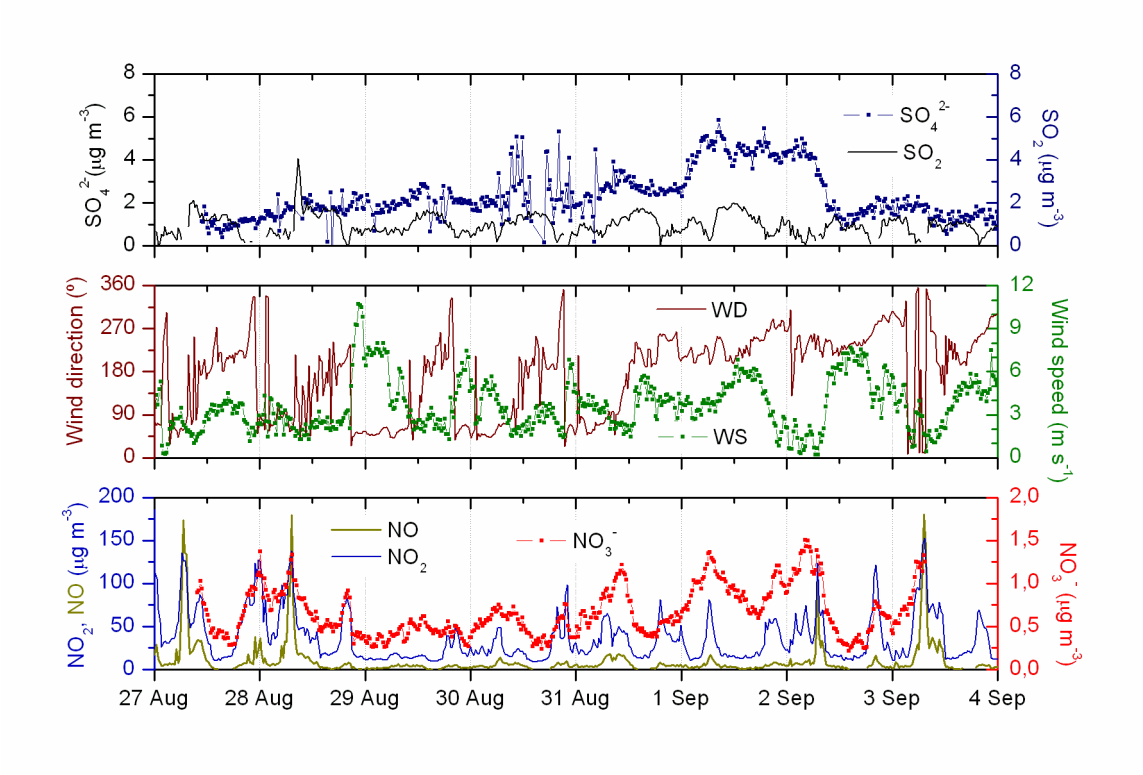

Figure 6.5. E1. SO_4^{2-}, SO_2 (top); Wind direction, wind speed (middle) and NO, NO_2, NO_3^- (bottom)

During this event SO_4^{2-} registered steady short term values over 5 $\mu g \cdot m^{-3}$ from 1 Sept night to 2 Sept night. The typical diurnal wind pattern was inhibited, appearing S-SW dominant wind directions which suggest E1 as a transport event. In this period NO_3^- showed a simultaneous rise and fall, although the levels reached were low (under 2 $\mu g \cdot m^{-3}$) due to the strong thermal decomposition of nitrate in this season. In addition, nitrate exhibited variations probably due to the effect of temperature. There was no correspondence between the pattern followed by SIC and the gases measured.

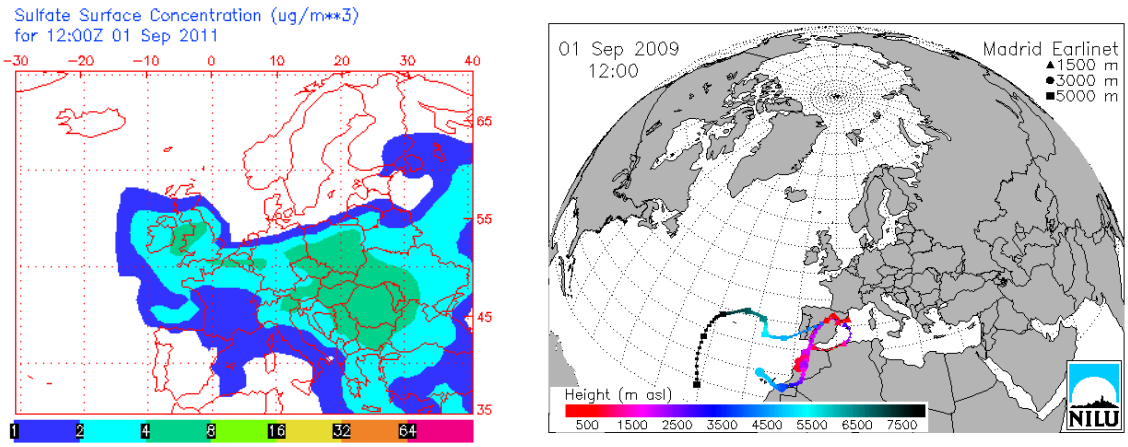

Figure 6.6. E1. (Left) Sulphate surface concentration estimated by NAAPS. (Right) Trajectories arriving at Madrid on 01 Sept 2009 at 12:00 UTC

Back-trajectory analysis performed with the FLEXTRA model showed low trajectories recirculating across the South-Eastern Peninsula and going around the African coast on 1 Sept. The NAAPS model shows the usual sulphate cloud over Europe, which does not affect the Peninsula (see Figure 6.6). The model does not account for the regional event originated by air recirculation at the central Iberian Peninsula. A possible influence of emission sources in the North of Africa cannot be ruled out.

-E2a: European sulphate transport-

E2a took place between 22 and 30 September 2009. In this period the sulphate concentration (short-term value) rose from 2 $\mu g \cdot m^{-3}$ to over 7 $\mu g \cdot m^{-3}$, reaching the maximum registered on the sampling site (see figure 6.7). Nitrate data were not available. Wind speeds between 4-9 $m \cdot s^{-1}$ and dominant NE wind directions suggest E2a as a transport event. During 28 September the clearest arrival of sulphate was registered. SO_4^{2-}, wind direction, wind speed and SO_2 keep steady values until 29 Sept morning. On the contrary, no correlation was found with NO and NO_2. On 22-28 Sept these anthropogenic gases followed a daily emission pattern, peaking at rush traffic hours. On 28-30 September NO and NO_2 concentrations descended due to the dilution caused by the arrival of a new air mass, sulphate enriched.

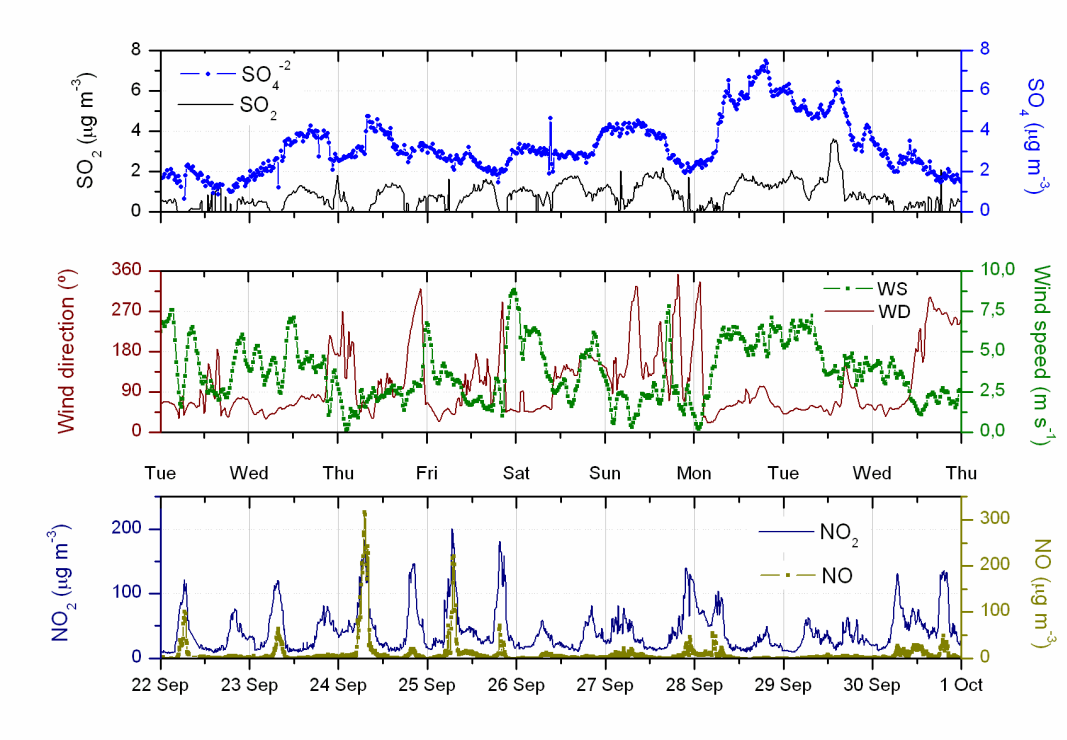

Figure 6.7. E2a. SO_4^{2-}, SO_2 (top); Wind direction, wind speed (middle) and NO, NO_2 (bottom)

FLEXTRA back-trajectories showed European and Western Mediterranean provenance of wind flows at low heights from 22 to 30 Sept. These have previously been identified as potential source areas of fine aerosol and particulate sulphate by Salvador et al (2008). The authors explained this result by the transport of polluted air masses originated in European source areas and moving southward the Mediterranean Sea. There are experimental evidences that, during the warm season, there is a persistent southward flow of European pollution into the western and central Mediterranean basin at the lower troposphere. European emissions together with local emissions are trapped into atmospheric recirculation flows (Gangoiti et al, 2001). Figure 6.8 depicts 7 days FLEXTRA back-trajectories ending on 28 Sept at 12:00 UTC, after the highest sulphate increase had been observed. The NAAPS model shows high sulphate concentrations in Central Europe. The sulphate cloud extends over the northern Mediterranean Sea and the Iberian Peninsula.

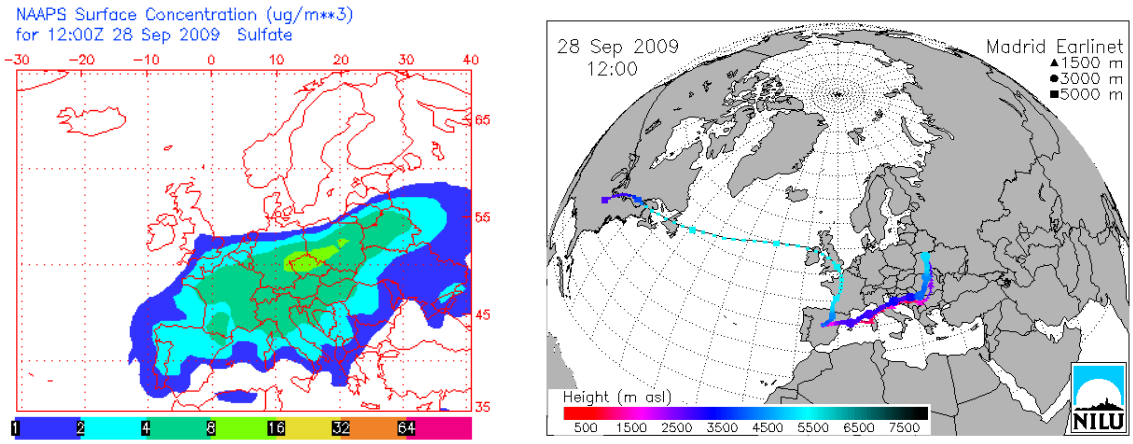

Figure 6.8. E2. (Left) Sulphate surface concentration estimated by NAAPS. (Right) Trajectories arriving at Madrid on 28 Sept 2009 at 12:00 UTC

All this information suggests identifying E2a as a long-range transport process. However, it is interesting to see the evolution of sulphate concentration on rural stations on the same time period. A similar pollutant evolution is a strong evidence of phenomena affecting a whole area, and thus local processes can be dismissed.

Figure 6.9 shows the evolution of particulate sulphate and nitrate at CIEMAT and three EMEP stations at the central Iberian Peninsula. Event E1 is seen at CIEMAT, ES01 and ES09. ES13, located to the North-West of the Madrid air basin, showed a nitrate increase three days before the other sites and only a small sulphate increment. This is consistent with the back-trajectories found recirculating across the south-eastern Iberian Peninsula. E2 was seen for sulphate at all the stations, but not for nitrate at EMEP stations (nitrate data at CIEMAT are not available). This information reinforces the previous hypothesis and allows classification of **E1** as a **regional transport event (RT)** and **E2a** as a **European sulphate transport event (ET)**.

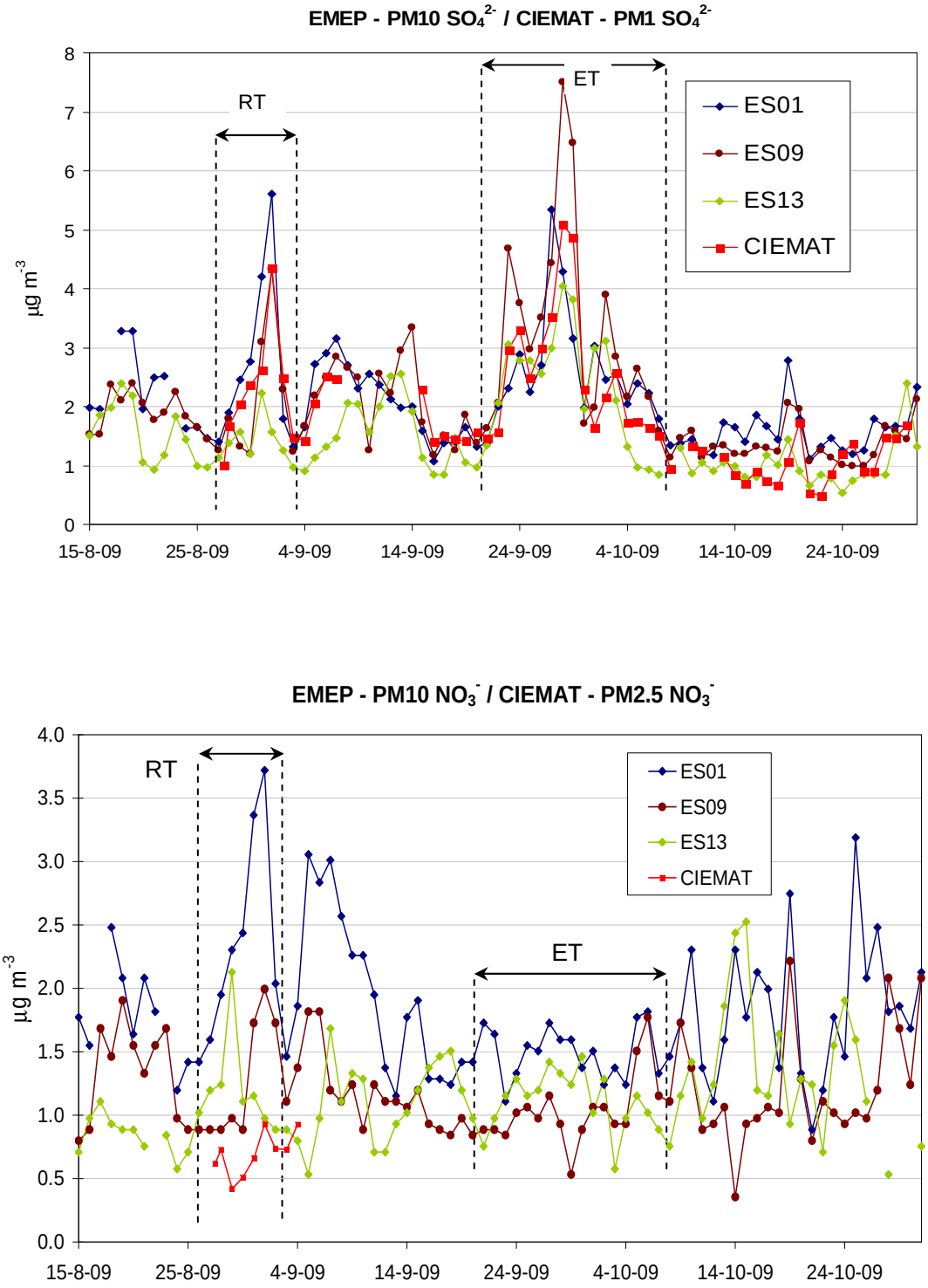

Figure 6.9. Evolution of daily averaged particulate sulphate (top) and nitrate (bottom) at CIEMAT and three EMEP sites (see Appendix I) during E1 (RT) and E2a (ET)

The evolution of sulphate concentration given by NAAPS in the region studied is in reasonable good agreement with the evolution measured on the second half of September and beginning of October, although the concentration values are underestimated (Appendix III). Event E1 is not described by the model.

- E2b: European nitrate transport-

Data captured by the semicontinuous instruments did not allow identifying a simultaneous event of European transport affecting both sulphate and nitrate.

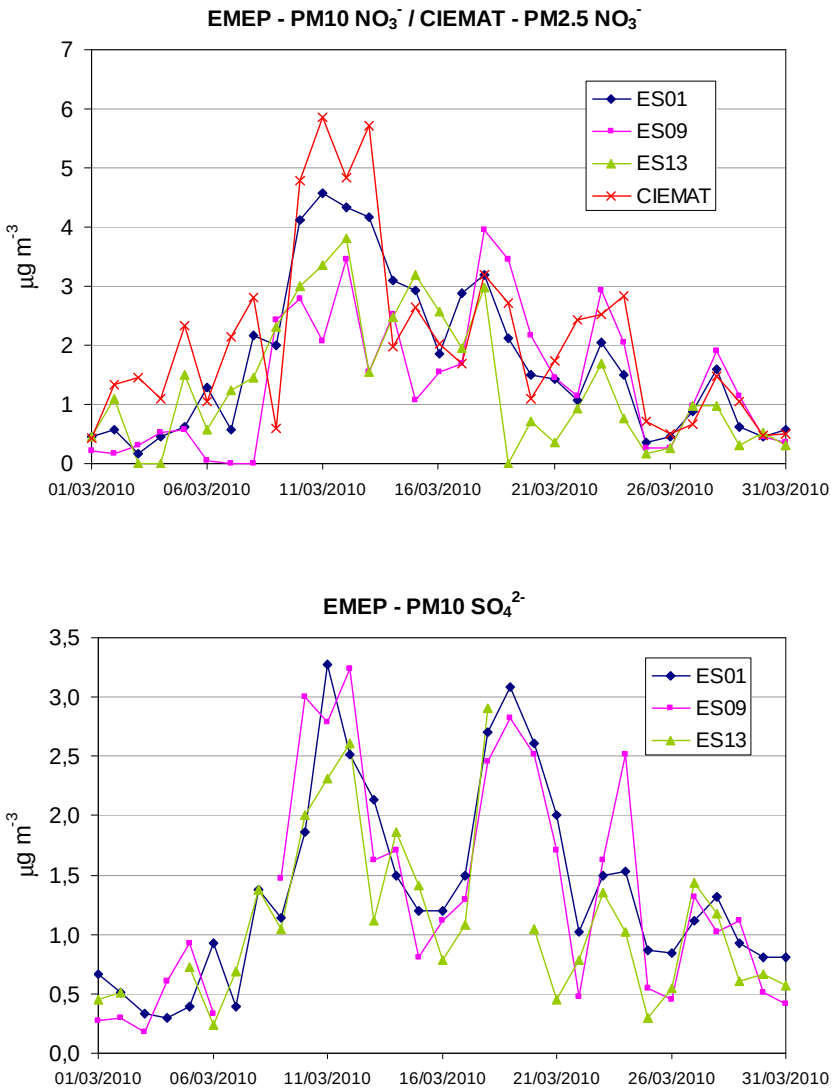

Figure 6.10. (Top) Evolution of daily averaged particulate nitrate at CIEMAT and three EMEP sites.(Bottom) Evolution of daily averaged particulate sulphate at three EMEP stations

Nevertheless, results from Salvador et al (2008) demonstrated that a nitrate flux originated in Central Europe and/or the Eastern Mediterranean is established on certain meteorological situations, and therefore it must be possible to detect its effects at Madrid.

In March 2010, FLEXTRA show persistent back-trajectories from Europe from day 5 to 20. The NAAPS model shows a sulphate cloud spreading over the Iberian Peninsula on this period (Figure 6.11, left). Although model information on nitrate is not available, NAAPS sulphate and trajectories give evidence of the circulation of pollutants on these dates.

Figure 6.10 (top) shows the nitrate daily concentration on EMEP stations and CIEMAT. Evolution is similar, with a remarkable maximum on 10-13 March on ES01, ES13 and CIEMAT. The same maximum is observed for PM_{10} sulphate in the EMEP sites. Particulate sulphate is not available at CIEMAT in that time period.

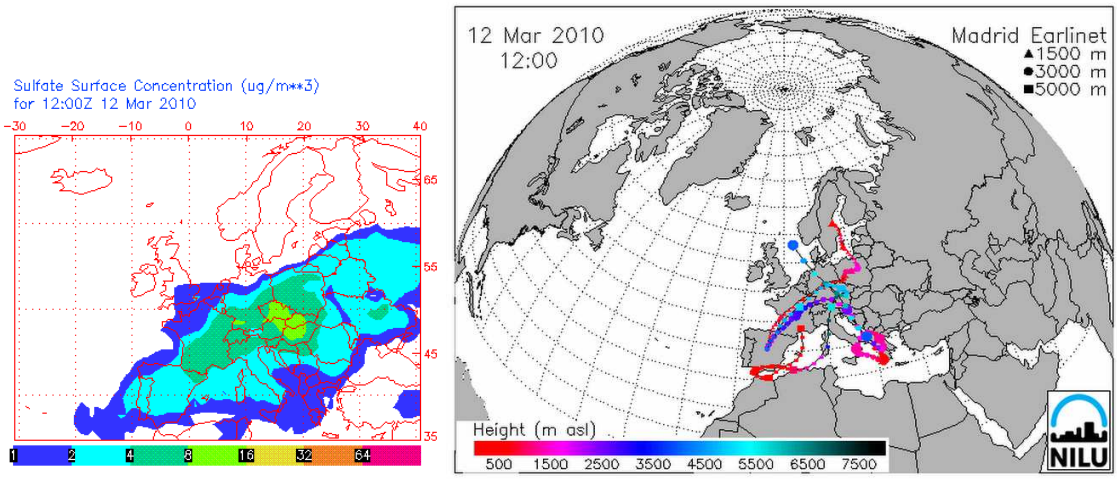

Figure 6.11. (Left) Sulphate concentration by NAAPS. (Right) FLEXTRA back-trajectories on 12 Mar 2010 at 12 UTC

FLEXTRA back-trajectories (Figure 6.11, right) show a clear European air mass origin on 12 March, and for the same day NAAPS model predicted a large sulphate cloud spreading over all Europe giving rise to sulphate concentrations in the range 3-4 $\mu g \cdot m^{-3}$ in the central Peninsula, in coincidence with the levels registered by the EMEP network.

All this information suggests the classification of **E2b** as a **European nitrate and sulphate transport episode** which could be identified in the fine nitrate evolution in an urban background site in Madrid.

6.3.3-Winter stagnation event

The **E3** event took place between 6 and 12 February 2011, coinciding with **anticyclonic meteorological conditions**. The atmospheric stagnation led to an intense pollutant accumulation episode that raised progressively the levels of both particulate matter and gases, including the nocturnal values. Under this kind of episodes, back-trajectory analysis sometimes shows short trajectories moving around the central part of the Iberian Peninsula, indicating air stagnation. However, anticyclonic conditions are difficult to identify with trajectory analysis alone.

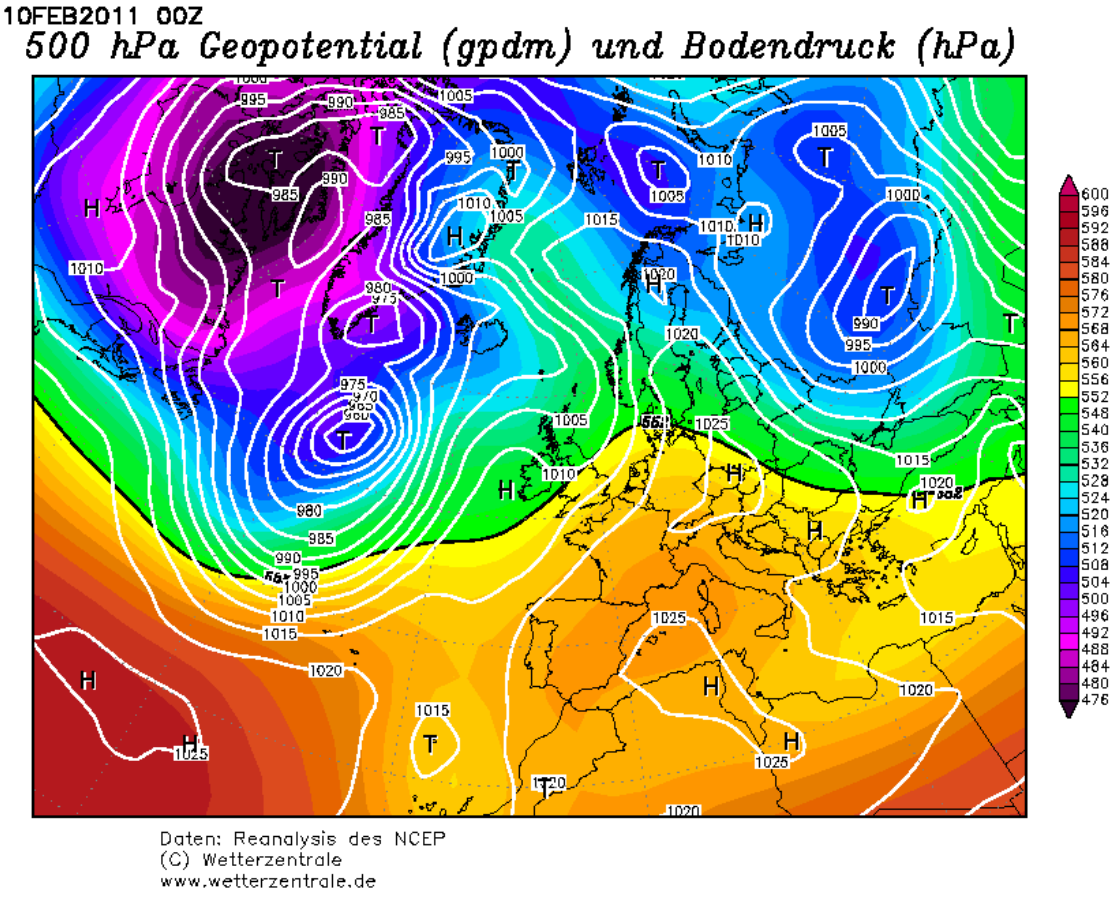

Figure 6.12. 500 hPa geopotential surface over Europe on Feb 10 at 0h UTC

For this reason, in this case the synoptic map showing the 500 hPa geopotential surface is presented for February 10 at 0h UTC (see Figure 6.12). The map is provided by the Wetterzentrale and uses NCEP Reanalysis data (http://www.wetterzentrale.de/topkarten/fsreaeur.html).

Figure 6.12 clearly shows that the Iberian Peninsula was under the influence of an anticyclone system when E3 event took place in Madrid.

Figure 6.13 depicts the evolution of PM_{10}, PM_1; NO, NO_2, NO_3^-, wind direction, wind speed and SO_4^{2-}, SO_2 at the CIEMAT site. During E3 wind speed was low and wind direction showed the typical local-regional circulation pattern. All the parameters registered followed a clear daily pattern, which during E1 and E3 faded away. The highest PM, nitrate, sulphate and SO_2 concentrations were recorded at noon. Maximum concentrations reached 3.5 $\mu g \cdot m^{-3}$ for sulphate -very far from E1-E2a values- while for nitrate exceeded 20 $\mu g \cdot m^{-3}$ -high above E1 and E2b values-.

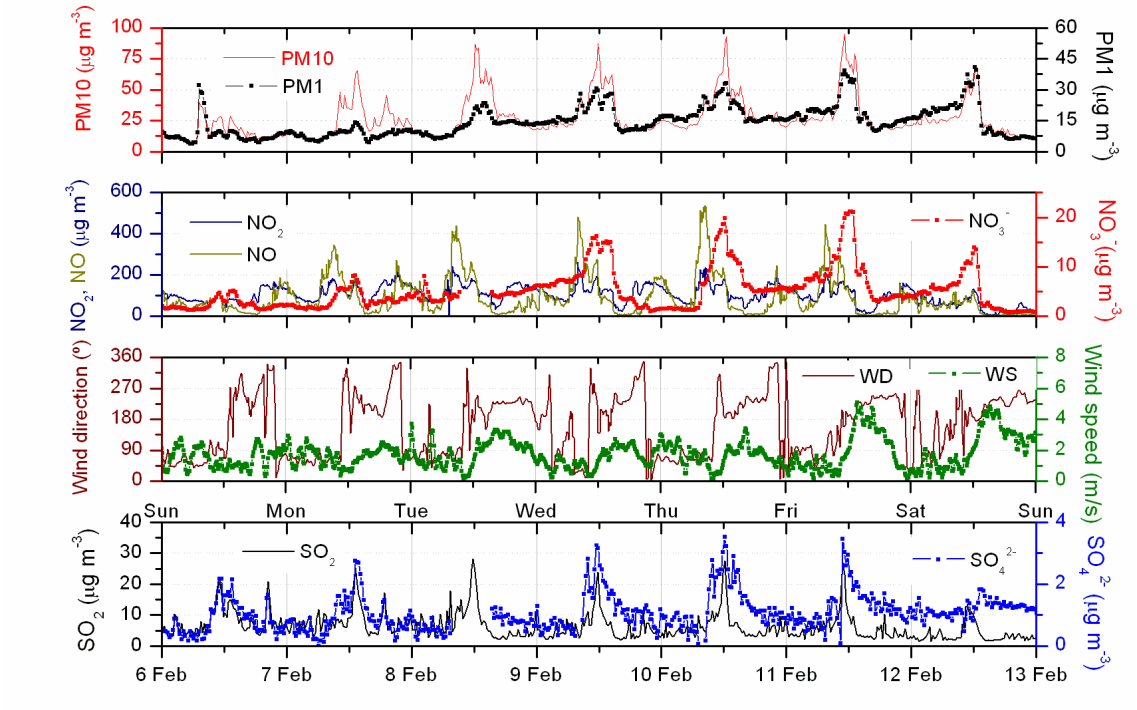

Figure 6.13. PM_{10}, PM_1; NO, NO_2, NO_3^-, wind direction, wind speed and SO_4^{2-}, SO_2 during E3 at CIEMAT

Figure 6.14 depicts the averaged daily evolution of SO_2, $SO_4^{2-}$and NO_2, NO_3^- during E3 weekdays. SO_2 pattern was similar to sulphate, though differences have been identified

from the peak shapes. Both SO_2 and SO_4^{2-} morning rises are similar. SO_2 fell earlier than SO_4^{2-} in the afternoon. NO_2 rose in the early morning (traffic rush hour) and evening, but also showed a secondary maximum at noon, coinciding with the nitrate maximum.

The daily evolution of sulphate, SO_2 and nitrate on weekdays is very similar to the winter averaged patterns described in chapter 5 (see Figure 5.7), although the maximum concentrations reached are significantly higher for E3. This indicates that the averaged patterns are dominated by the behaviour of pollutants under anticyclonic conditions. The effects of episodes such as regional or long-range transport are compensated since they do not exhibit any characteristic daily evolution.

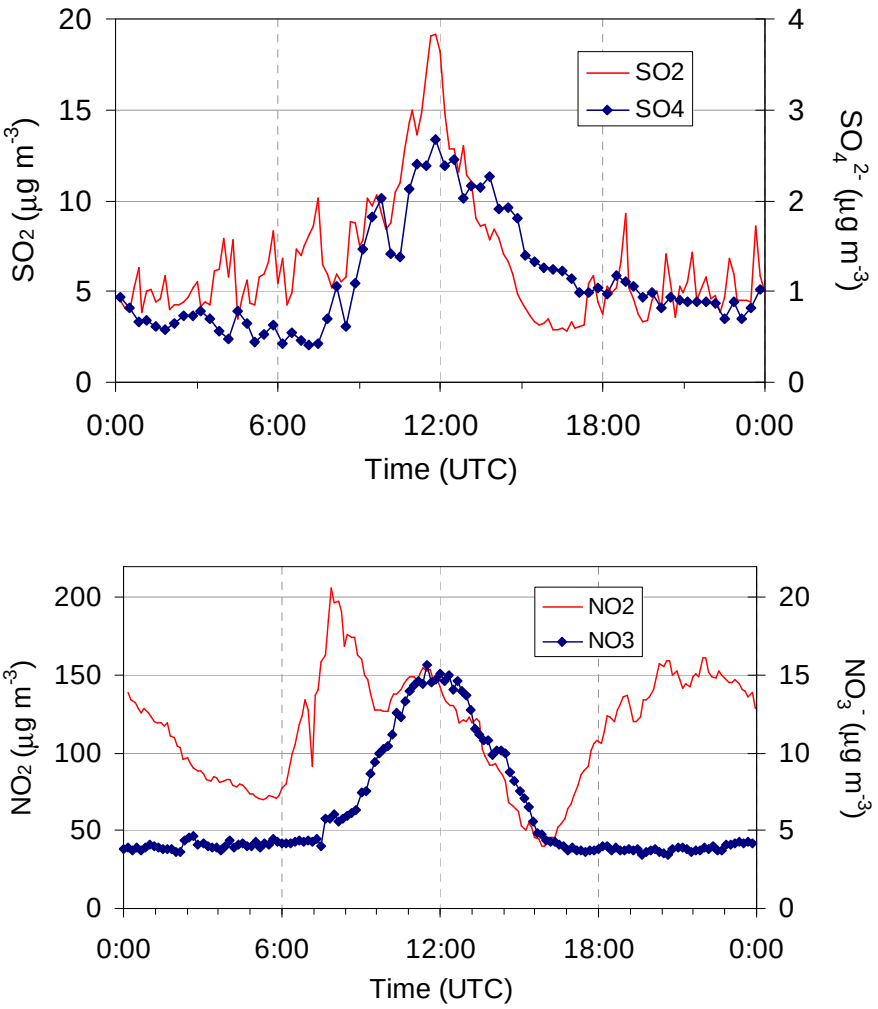

Figure 6.14. Weekday (7 to 11 Feb) pattern of SO_2, SO_4^{2-} (top) and NO_2, NO_3^- (bottom) during E3.

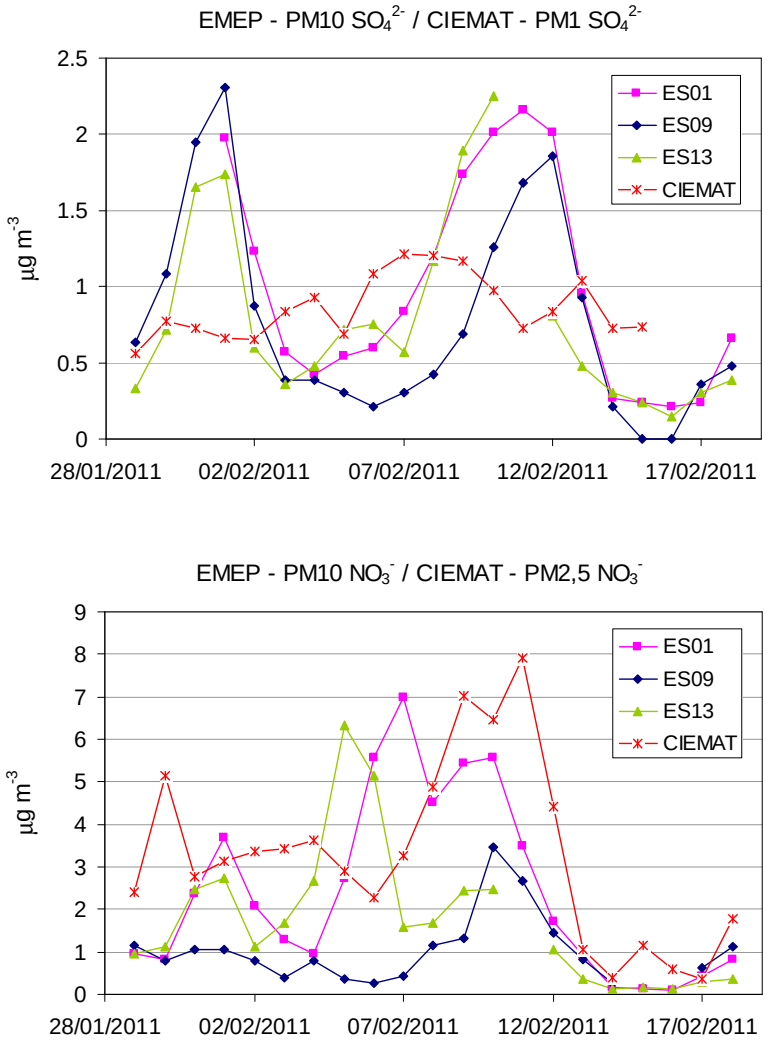

Figure 6.15. Evolution of daily averaged particulate sulphate (top) and nitrate (bottom) at CIEMAT and three EMEP sites during E3.

The evolution of particulate sulphate and nitrate at EMEP stations exhibited significant differences with CIEMAT (see Figure 6.15), reflecting the effect of the local accumulation episode in the Madrid township atmosphere. It is noticeable that the concentrations registered in the EMEP PM_{10} sulphate are significantly above those reached by PM_1 sulphate in Madrid under the strong local accumulation event described.

6.4-Conclusions

In this chapter three types of events which led to high concentrations of particulate sulphate and nitrate at the urban area of Madrid have been characterised. These events are: a regional recirculation episode (E1), transport from Central Europe-Western Mediterranean (E2a –sulphate- and E2b –nitrate and sulphate-) and local accumulation in a winter stagnant anticyclonic situation (E3).

A cluster analysis of back trajectories with the HYSPLIT model has allowed identification of two distinct clusters describing regional recirculation and European transport, and the comparison of the sulphate concentrations reached in these situations. In the period Aug-Nov 2009 -coinciding with the time of the year when typically pollutants are accumulated in the Mediterranean air basin- both clusters were associated to sulphate concentrations significantly higher than the other clusters. In the period Dec 2010-Mar 2011, the regional circulation cluster led to high concentrations of sulphate and nitrate, but not the European cluster.

The EMEP stations at the Central Iberian Peninsula and the CIEMAT site showed similar daily SIC evolution for the regional and European transport events. Both kinds of episodes were differentiated using the information provided by the FLEXTRA back-trajectories model and the NAAPS model. NAAPS usually depicts a sulphate cloud over the European continent, reaching the Peninsula when the episodes E2a and E2b were detected, although the concentrations were underestimated for E2a. Nonetheless, the model does not account for the regional circulation episode E1. A nitrate episode which can be attributed to transport from Central Europe (E2b) was identified on March 2010. Further research is needed to characterise the impact of nitrate transport at urban sites at Madrid.

At Madrid, the synoptic situation leading to the occurrence of episodic accumulation events tipically takes place in winter under stagnant anticyclone conditions. In one episode of this kind (E3) pollutant concentrations rose slowly for a period of days. All recorded parameters showed marked diurnal cycles inhibited during the transport episodes. PM, sulphate, nitrate and gaseous SO_2 and NO_2 exhibited maxima at noon.

The daily evolution of sulphate, SO_2 and nitrate during E3 on weekdays is very similar to the winter hourly patterns described in chapter 5. This indicates that the averaged patterns are dominated by the behaviour of pollutants under anticyclonic conditions, while the effects of episodes such as regional or long-range transport are compensated since they do not exhibit any characteristic daily evolution.

The highest PM_1 sulphate values were associated to the pollutant long-range transport situation. The highest short-term PM_1 sulphate concentrations registered at the site (7 $\mu g \cdot m^{-3}$) were reached during E2a. Sulphate concentrations reached 5 and 3.5 $\mu g \cdot m^{-3}$ during E1 and E3 respectively. Thus, the highest sulphate concentrations during the European transport event were approximately twice the values reached during the local event.

The highest $PM_{2.5}$ nitrate values were associated to the local accumulation situation. The highest short-term $PM_{2.5}$ nitrate concentrations were over 20 $\mu g \cdot m^{-3}$, while the maximum concentrations reached under transport episodes were less than half of that value.

Thus, since the importance of local emissions has been stated, regional and long range transport is also relevant for particulate sulphate ambient concentrations at a suburban site at Madrid. Quantification of the amount of sulphate and nitrate which can be attributed to distant and local/regional sources is an interesting issue to address in future works.

7-CHARACTERISATION OF EVENTS OF FINE PARTICULATE MATTER IN MADRID II

7-CHARACTERISATION OF EVENTS OF FINE PARTICULATE MATTER IN MADRID II

7.1-Introduction

During the course of the measurement of the semi-continuous sulphate time series analysed, two sulphate events coinciding with eruptions of European volcanoes were identified in Madrid. The first episode took place in May 2010 and was caused by the eruption of the Icelandic volcano Eyjafjallajökull, located about 2800 km north-northwest of the Iberian Peninsula. The evolution in space and time of the volcanic plume was forecasted by several models and monitored by a variety of ground level, airborne and satellite sensors (Schumann et al., 2011). The impact of this plume at the CIEMAT station was characterised in particular detail with all the instrumentation available at the time (Revuelta et al, 2012c).

The European airspace was closed from 15 to 20 April 2010 due to the volcanic eruption in Iceland. The Eyjafjallajökull volcano (63.63°N, 19.62°W, 1660 m asl) had remained dormant for several decades, but on 20 March 2010 an eruption started, forcing the evacuation of the local population and interfering with air traffic in the region. The eruption entered a strong phase of ejection of ash to the atmosphere on 14 April 2010, with large aerosol plumes rising up to the high troposphere during the following days (14-17 April). These were rapidly advected down the North Sea and then dispersed over a very large area of central and northern Europe (Colette et al., 2010; Flentje et al., 2010). The eruption shifted to a lava producing phase throughout late April (18-30 April), but after more than a week of relatively subdued activity, the volcano began a new round of explosive ash eruptions in the first week of May (Langmann et al., 2012). The meteorological conditions favoured the arrival of the volcanic cloud in Spain. The plume crossed over the Iberian Peninsula from West to East between 7 and 9 May, and then over the Mediterranean and the Balkans.

The most effective ground-level measurement system for detecting the presence of volcanic plumes aloft is lidar (Light Detection And Ranging). During the days of the event, lidar systems were the only remote sensing measurements from which vertically-resolved mass concentrations could be estimated, although large

uncertainties remain in the conversion from extinction coefficient to mass concentration profiles. The impact on air traffic generated a demand for timely mass loading estimates in order to determine the damaging potential of the plume. A special effort was made by EARLINET (European Aerosol Research LIdar NETwork) (Bösenberg et al., 2001) to monitor the ash plume dispersion in order to provide vertically-resolved ash optical properties. The temporal development of the plume was documented in near real-time, and further analysis of the optical profiles provided optical and even microphysical properties of the ash (Wiegner et al., 2011).

Madrid is located about 1700 km west of the Etna volcano. Despite being an active volcano with frequent eruptions, the prevailing wind circulation in these latitudes prevents the material ejected from being transported to the west. However, the meteorological conditions present during the eruptive phase that began on 28 Sept 2011 made that aerosol from the Sicilian volcano could get to Madrid.

Volcanoes are very strong sources of sulphur, acids and other gases, as well as particles. Sulphur dioxide (SO_2) is a major component of volcanic clouds and subsequently sulphuric acid (H_2SO_4) may be formed by oxidation processes, thus giving rise to secondary sulphate (SO_4^{2-}) formation. Sulphate can be either primarily emitted or result from the oxidation of gaseous SO_2 (Allen et al., 2002). A recent study has shown increasing SO_2 depletion and gas phase sulphuric acid enrichment in the volcanic plume of an Antarctic volcano with the distance to the emission source, suggesting a fast SO_2 to SO_4^{2-} oxidation (Oppenheimer et al., 2010). The chemical stability of sulphate makes it a feasible candidate for detecting long-range transported volcanogenic aerosols. Accordingly, volcanic ash plumes are generally formed by gaseous pollutants, mainly SO_2, primary ash particles (micrometer size range) and also secondary smaller particles (submicrometer size range). Ground-based measurements of volcanic emissions have traditionally focused on sulphur dioxide concentrations, but a few studies have also reported continuous measurements of aerosol chemical compounds of volcanogenic origin such as sulphate. In one recent work of this type (Ovadnevaite et al., 2009) the authors also demonstrated that a large amount of sulphur released from Icelandic volcanoes could travel over distances greater than 1000 km. On the other hand, research on volcanic aerosol has been mainly oriented to

coarse particles, while the fine fraction has received less attention. Thus, it is interesting to jointly investigate gases, fine and coarse aerosols to know the spatial distribution of the different kind of pollutants produced at the eruption.

In this chapter we report measurements of the Eyjafjallajökull volcanic plume at ground level, identified by an increase in gaseous SO_2 and particulate sulphate concentrations in several background air pollution Spanish monitoring stations of the Iberian Peninsula, and observations of the volcanic layer over Madrid provided by the CIEMAT ground-based lidar during the aforementioned event in May. The contribution of the Etna eruption to the increase in sulphate concentration occurred in autumn 2011 in Madrid is also discussed.

7.2-Experimental setup

The CIEMAT-Madrid lidar station provided timely measurements from the beginning of the Eyjafjallajökull event. In the CIEMAT lidar station, due to low quality signals in the Raman channel during most of the Eyjafjallajökull episode, only the elastic channel was employed to derive vertical profiles. The Klett-Fernald algorithm (Klett, 1981) was used in the inversion, with an aerosol extinction-to-backscatter ratio of 50 sr. This value is typically used for continental aerosol but it seems to be appropriate for volcanic aerosols, as recent studies obtained ratios ranged from 49 to 60 sr for the volcanic plume over Germany (Wiegner et al, 2011, Ansmann et al 2010).

The PM_{10}, $PM_{2.5}$ and PM_1 temporal evolution and volume distributions in the range 0.015-20 μm, along with particulate sulphate temporal evolution, were obtained in this station. The temporal evolution of particle number, sulphate, nitrate, PM_{10}, $PM_{2.5}$, PM_1 and meteorological parameters were also obtained at surface level in the CIEMAT site. All data were recorded every 10 min except for the sulphate, which were recorded every 20 min. Time series of particulate sulphate on PM_1 were obtained by means of the Thermo 5020 sulphate particulate analiser. Particulate nitrate concentrations on $PM_{2.5}$ were semi-continuously measured by the Rupprecht and Patashnick Series 8400N Ambient Particulate Nitrate Monitor. GRIMM1107 OPC obtained the PM_{10}-$PM_{2.5}$-PM_1 temporal evolution. GRIMM1108 OPC provided size distribution in the range from 0.3

to 20 μm. The particle size distribution in the size range 0.015-0.60 μm was measured using the Scanning Mobility Particle Sizer (TSI SMPS 3936 instrument). The GRIMM1108 and the SMPS overlap in the size range from 0.3 μm to 0.661 μm. Therefore, it is possible to obtain a single plot for number distributions from 0.015 to 20 μm by joining the data of both instruments. The diameter of a particle can be determined by measuring different physical properties such as light scattering (OPC) or electrical mobility (SMPS). For spherical particles, the electrical mobility diameter would equal the Stokes diameter Dp, and also the diameter given by optical particle counters would equal Dp if light absorption is negligible and the refractive index is constant. Under these assumptions, particle counts were converted to a volume distribution (dV/dlog(Dp)). The overlap region shows some discrepancies due to the different techniques employed. However, the results are consistent.

Data from the 13 EMEP stations located throughout the Iberian Peninsula and the Balearic Islands was analysed. The EMEP network took daily samples of particulate matter filters, from 07:00 to 07:00 UTC. Particulate sulphate and nitrate concentrations were determined by Ion Chromatography. Sulphur dioxide was continuously monitored with UV pulsed fluorescence analisers.

Isentropic backward trajectories of the air mass arriving to each of the Spanish EMEP and CIEMAT sites were computed with the FLEXTRA model (Stohl et al, 1995). The meteorological fields used come from the upper air analysis of the HIRLAM/AEMET Numerical Weather Prediction operational suite at 00, 06, 12 and 18 h UTC, with 16 km horizontal resolution and 40 hybrid vertical levels, driven by the meteorological forecast fields from the European Centre for Medium-Range Weather Forecasts as boundary conditions. Back-trajectories started at altitudes of 500, 1500 and 2500m above model ground with a length of 96h backward in time.

During the Etna eruption, sulphate in PM_1 was continuously monitored in CIEMAT. Data from EMEP stations have also been analysed. NAAPS predictions and FLEXTRA back-trajectories were used to identify the origin of the event.

7.3-Results

The eruption of the Eyjafjallajökull volcano went through several explosive phases before the final degassing phase. The eruption that started on 14 April affected mainly the British Isles and Central Europe, while a new round of explosive ash eruptions occurred in the first week of May, affecting the Iberian Peninsula.

The HIRLAM/AEMET meteorological fields analysis at 500 hPa depicted a strong ridge over the West of Iceland located between two depressions, one of them over Newfoundland whereas the other one over the Balearic Islands. This situation favoured the arrival of the volcanic plume at the Iberian Peninsula, being detected at ground level in most EMEP stations and also at the CIEMAT site.

Measurements in the time period from 4 to 14 May were analised, as the first effects were recorded on 4 May on several stations, the main event was observed from 7 to 9 May 2010 and a smaller event was detected on 13 May. During this period, there was rainfall irregularly distributed through Spain, which in some cases could contribute to the wet deposition of pollutants by precipitation scavenging and then reduce observed gaseous pollutants and particulate matter in ambient air.

7.3.1-First effects of the Eyjafjallajökull plume and main event

Figure 7.1 shows the temporal evolution of SO_2 at San Pablo de los Montes (ES01), Peñausende (ES13) and O Saviñao (ES16) between 4 and 14 May 2010 (top left panel), and the precipitation at the same sites (bottom left); the top right and bottom right panels show the same information at the eastern stations of Víznar (ES07), Zarra (ES12) and Els Torms (ES14). The volcanic impact on surface raised the SO_2 concentrations, without correlation with other anthropogenic pollutants such as nitrogen oxides and ozone. These are the stations in which this effect can be seen more clearly.

A sulphur dioxide peak appeared on 4 May at O Saviñao, 13:30 UTC, Peñausende at 15:00 UTC, San Pablo at 15:30 UTC and Víznar, on 5 May at 00:00 UTC, showing a northwest to southeast trend. The main SO_2 event happened on 7-9 May, appearing

from the West to the East of Spain so that the highest values were recorded at EMEP stations as follows: San Pablo on 7 May, at 17:00 UTC; Víznar on 8 May at 11:00 UTC; Zarra, on 8 May at 16:00 UTC; and Els Torms on 9 May at 8:00 UTC. The observed values of SO_2 were higher at the eastern stations, where the precipitation came days later than in the west of Spain and was less abundant.

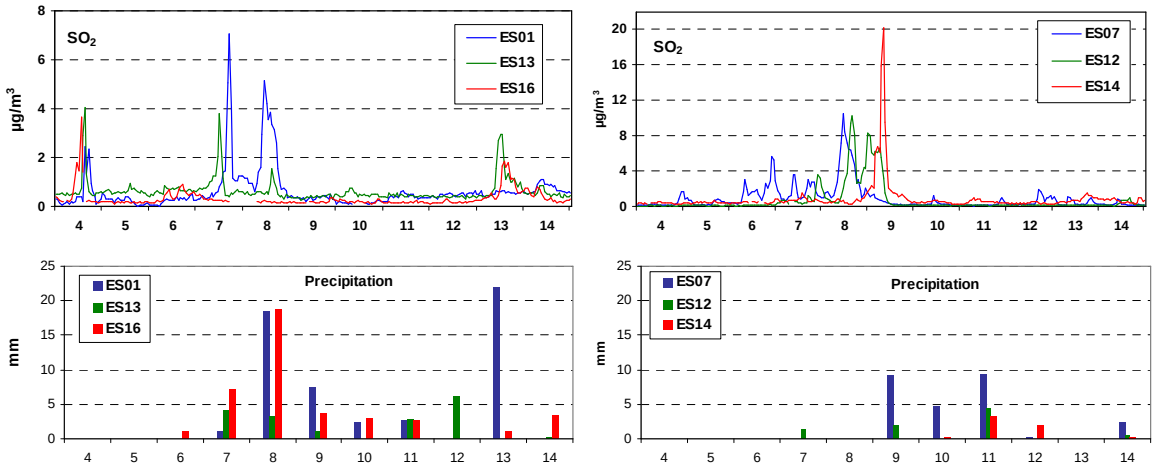

Figure 7.1. Top left panel: SO_2 concentration at San Pablo (ES01), Peñausende (ES13) and O Saviñao (ES16). Bottom left panel: precipitation at the same stations. Top right panel: SO_2 concentration at Víznar (ES07), Zarra (ES12) and Els Torms (ES14). Bottom right panel: precipitation. 4-14 May 2010.

At other stations the origin of SO_2 peaks is disguised by the presence of high values of NOx and no influence is observed at the Cabo de Creus and Mahón stations. FLEXTRA air mass back-trajectories calculated in AEMET show that the Cabo de Creus and Mahón stations were out of the influence of the air mass coming from South Iceland. In addition, the model proves that this air mass reached Els Torms later than the rest of the sites.

Figure 7.2 shows the arrival of the volcanic aerosol over Madrid, observed by means of the lidar system in a double layer located between 4.5 and 5.4 km asl (top panel). The provenance of these layers is confirmed by the back-trajectories provided by FLEXTRA model ending over Madrid at 1500 m (triangles), 3000 m (circles) and 5000 m (squares) on 6 May 00:00 UTC (bottom panel).

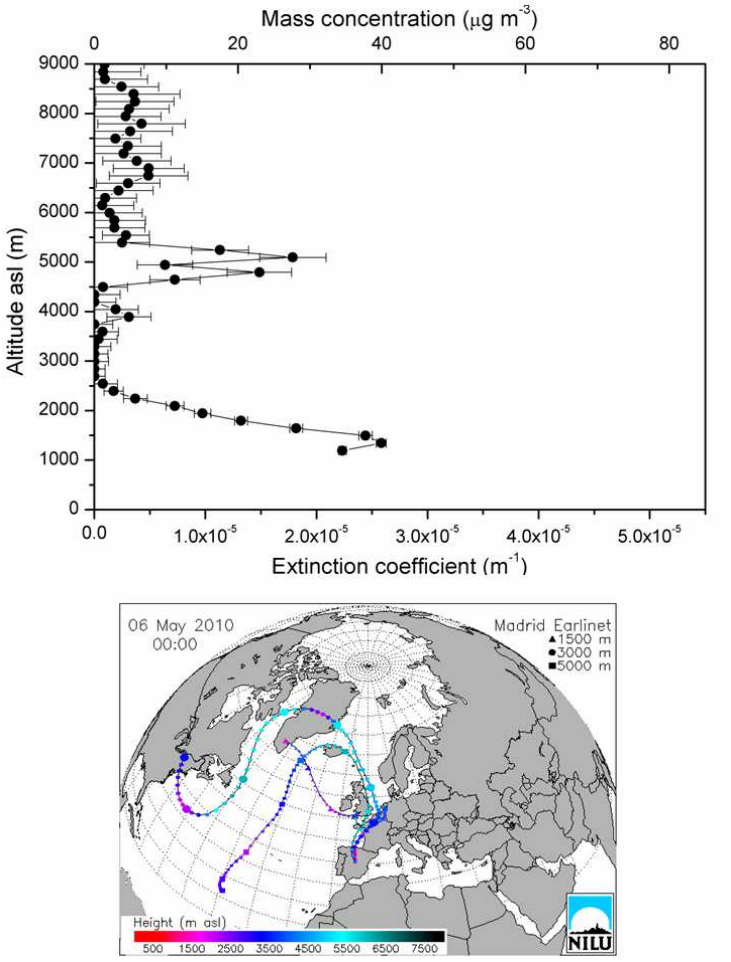

Figure 7.2. Extinction coefficient vertical profile provided by the lidar (top panel) over Madrid on 06/05/2010 00:00 UTC and 7-days backward trajectories provided by FLEXTRA model ending over Madrid at 1500 m (triangles), 3000 m (circles) and 5000 m (squares), (bottom panel).

As mentioned in the introduction of this chapter, one of the most critical parameters for aviation is aerosol mass concentration, so that there was a demand for timely mass loading estimates during the volcanic event in order to determine the damaging potential of the plume on jet engines. Lidar systems were the only remote sensing measurements from which vertically-resolved mass concentration could be estimated, although large uncertainties remain in the conversion from extinction coefficient to mass concentration profiles. In CIEMAT, the extinction coefficient profiles were converted into mass concentration profiles using a so-called specific extinction coefficient or cross-section value of 0.64 $m^2 \cdot g^{-1}$ at 550 nm, provided by the OPAC (Optical Properties of Aerosol and Clouds) software (Hess et al., 1998), assuming that the refractive index of volcanic ash is close to that of mineral dust and that the

refractive index of sulphate droplets is close to that of water soluble aerosols. The same assumption of desert dust similarity was employed in Ansmann et al. (2010), obtaining a slightly smaller value of 0.51 $m^2 \cdot g^{-1}$. This conversion implies large uncertainties because the specific extinction coefficient is a function of size, shape and refractive index of the particles, all of them unknown for the aerosols in aloft layers detected by lidar. The top panel of Figure 7.2 shows the extinction coefficient profile provided by the lidar system, with a mixing layer up to 2.5 km, and a double-lobed aerosol layer between 4.5 and 5.4 km, with a maximum value of 1.83×10^{-5} (±0.32) m^{-1} (bottom x-axes). This value converts into a mass concentration value of 28.6 (±5) μg m^{-3} (top x-axes). The error assigned to the mass concentration value corresponds to the experimental error estimated for the extinction coefficient, but due to the aforementioned uncertainties regarding the specific extinction coefficient, this error can be significantly larger. However, no further estimates could be made for it with the data available.

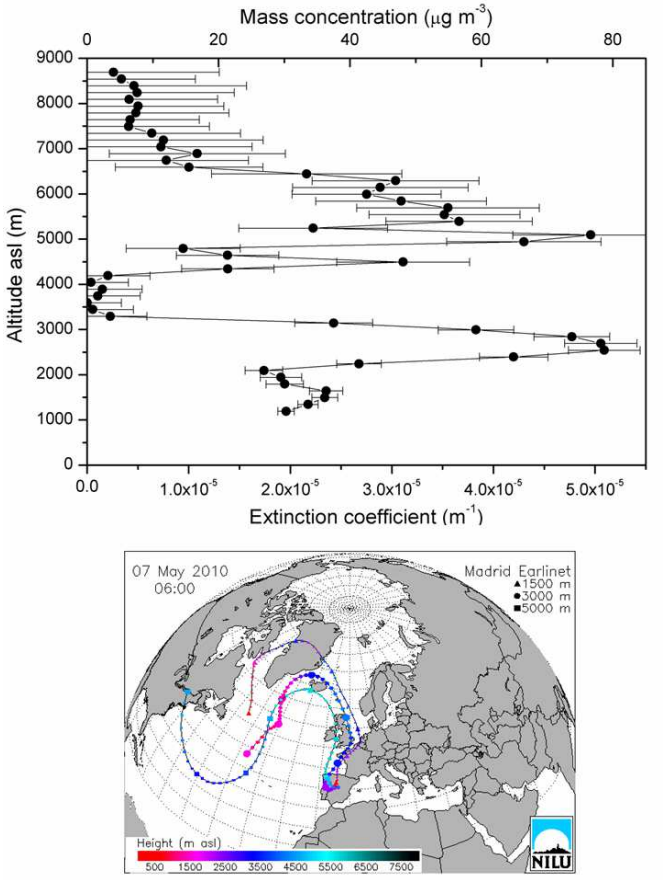

Figure 7.3. Same as figure 7.2, for 07/05/2010 01:00 UTC.

Figure 7.3 shows the moment at which the volcanic layers reached the highest optical depth observed during the whole event. This occurred on 7 May, at 01:00 UTC in several layers located between 4 and 6.5 km asl. The extinction coefficient peak reached $4.93 \cdot 10^{-5}$ (±0.63) m^{-1}, corresponding to a maximum detected value for volcanic layers of 77 (±9.6) $\mu g \cdot m^{-3}$. Therefore, the maximum mass concentration detected is well below the critical limit suggested by aircraft and engine manufacturers during the event (2 $mg \cdot m^{-3}$). The provenance of those layers is again confirmed by the back-trajectories provided by the FLEXTRA model ending on 7 May 06:00 UTC. Several layers were detected during the day, slowly subsiding toward the mixing layer. During 7 May afternoon and 8 May, volcanogenic particles were detected at ground level in Madrid, as will be explained further below.

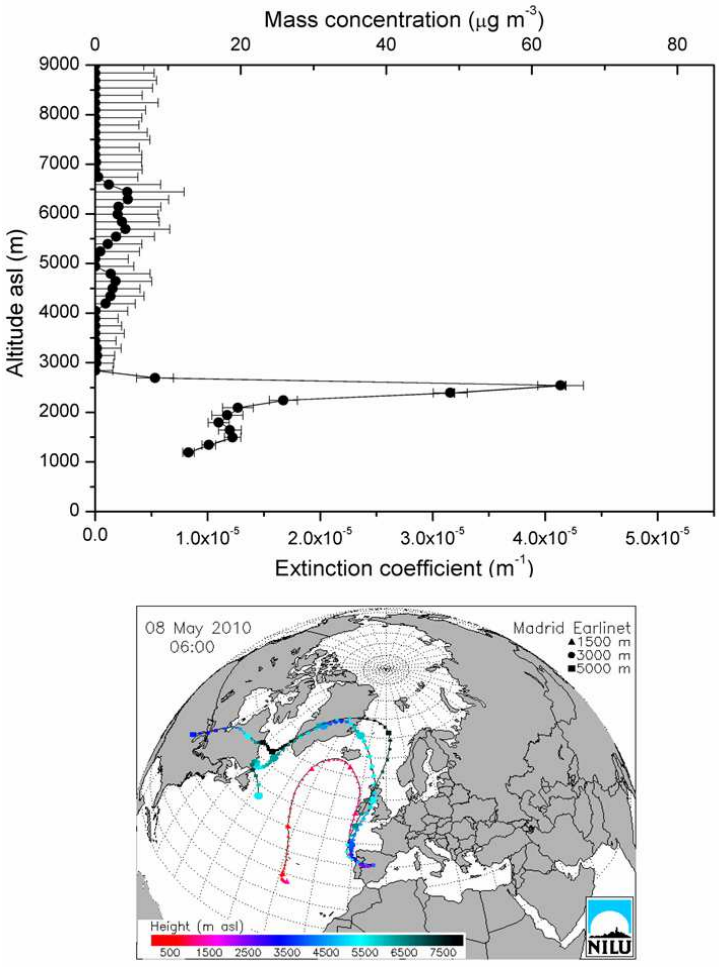

Figure 7.4. Same as figure 7.2, for 08/05/2010 03:00 UTC.

Figure 7.4 depicts the situation 26 h after the maximum volcanic layers were detected. In this case, a mixing layer is observed up to 2.8 km and residual aerosol layers are

detected between 4 and 6.9 km, with extinction coefficient values below $0.4 \cdot 10^{-5}$ m^{-1}. The air masses seem to come from North of the British Isles but not directly from Iceland, according to back-trajectories. No further lidar measurements were possible after this, due to low clouds and rain caused by a clean air mass from the Atlantic Ocean that washed the atmosphere from the West. The clean atmosphere observed over Madrid 7 h before volcanogenic aerosols were detected at the CIEMAT site, highlights the inherent difficulty of characterizing the plume from a single lidar station.

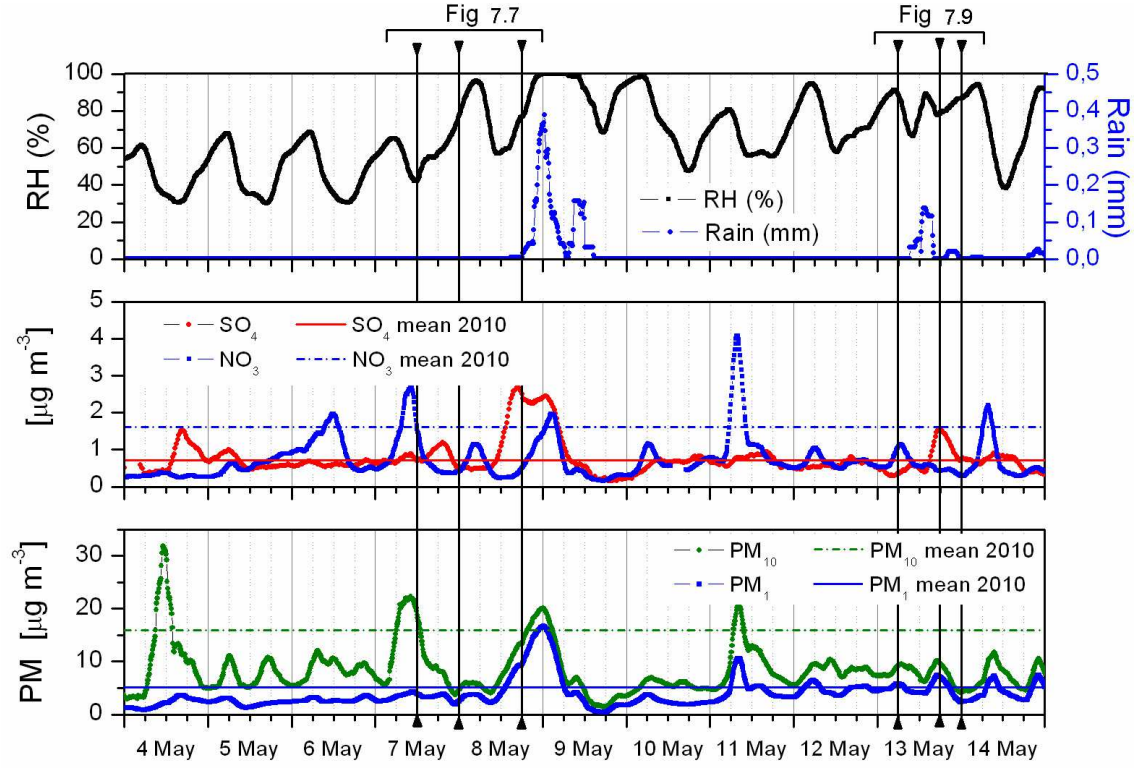

Figure 7.5. Temporal evolution of relative humidity and rain (top panel), PM_1 particulate sulphate and $PM_{2.5}$ nitrate concentration (central panel) and particle concentration (bottom panel) from 4 to 14 May at CIEMAT. Vertical lines indicate the times for which aerosol volume distributions are depicted in Figures 7.7 and 7.9.

In Figure 7.5, the temporal evolution of the particle mass concentration and particulate sulphate and nitrate concentration at the CIEMAT site between 4 and 14 May is depicted together with relative humidity (RH) and rain, meteorological parameters with a clear influence on particle concentration. Vertical lines indicate the times for

which aerosol volume distributions have been depicted in Figures 7.7 and 7.9, as will be explained below.

The first remarkable sulphate peak appears on 4 May at 13:00 UTC (middle panel), in coincidence with the sulphur dioxide peaks observed at the O Saviñao, Peñausende and San Pablo EMEP stations. Sulphate concentration increases sharply during 4 hours, while RH remains at low values. The previous level is not recovered until 5 May in the afternoon. The ratio SO_4^{2-}/PM_1 increases 0.20 during this event (from 0.20 on 4 May at 13:00 UTC to 0.40 on 4 May between 15:00 and 21:00 UTC).

During 7 May afternoon a small sulphate peak was detected, nevertheless, the most remarkable event happened on 8-9 May. A sharp increase in PM_1 sulphate levels took place on 8 May at 10:30 UTC, and five hours later sulphate reached a maximum of 3 $\mu g \cdot m^{-3}$. This value is more than three times higher than the average level of 2010 (0.72 µg m-3) and 3 times higher than the 80th percentile. SO_4^{2-}/PM_1 increased 0.15 during the rise of the peak (from 0.20 on 8 May at 10:30 UTC to 0.35 at 15:00 UTC). RH at this time remained below 65% at all times, so this increase cannot be attributed to hygroscopic sulphate formation. SO_2 peaks were observed at the San Pablo, Peñausende, Víznar and Zarra stations on this day. At the CIEMAT site, the aerosol was removed by rain scavenging during the early hours of 9 May. The increase was also seen in PM_1 concentration, reflecting both the sulphate event and also the later increase in nitrate levels. Results suggest that the hygroscopic nitrate formation was due to the high RH levels starting after the sulphate concentration reached its maximum. Hygroscopic nitrate formation has already been detected at this site in previous studies (Gomez-Moreno et al, 2007). The aerosol coarse fraction was not affected during this event.

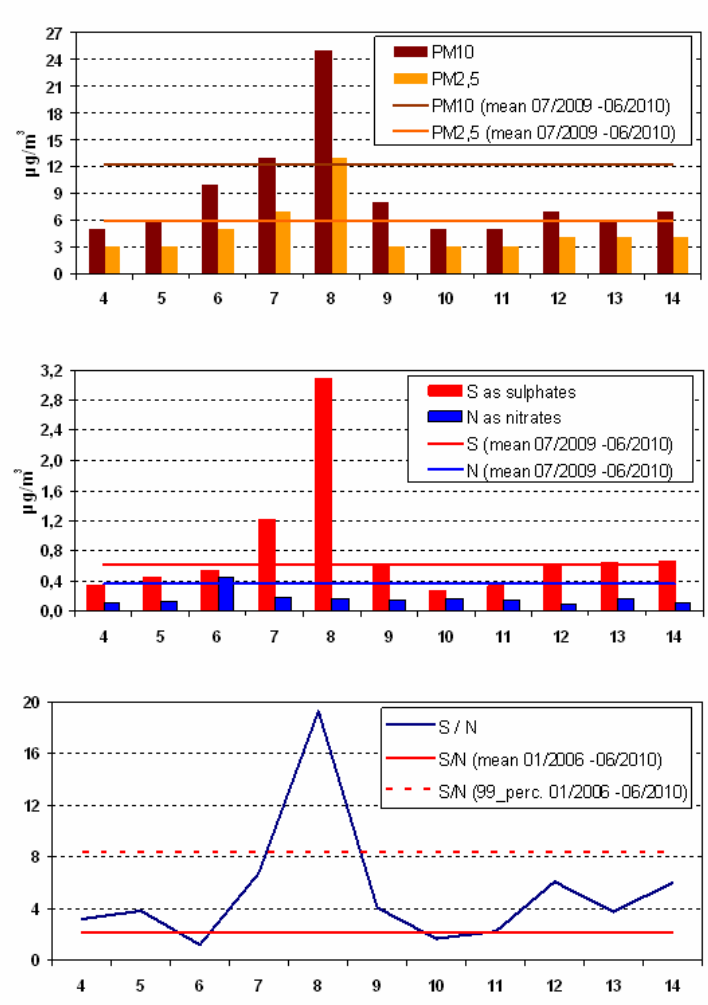

Figure 7.6. (Top) PM_{10} and $PM_{2.5}$ concentrations at Zarra. The mean values are calculated from July 2009 to June 2010. (Middle) Sulphur as sulphates (S) and nitrogen as nitrates (N) concentrations in PM_{10} at Zarra. The mean values are calculated from July 2009 to June 2010. (Bottom) S/N ratio obtained in PM_{10} at Zarra. The mean values are calculated from January 2006 to June 2010.

Although the PM_{10} and $PM_{2.5}$ mass concentrations recorded by the EMEP Network during this period were not at unusually high values, at most of the sites relative maxima are observed and sulphate content in PM_{10} presents very high values together with very low values of nitrates. Therefore, the S/N ratio (where S is sulphur as sulphate and N is nitrogen as nitrate) obtained in daily PM_{10} filters is high at almost all of the stations of the network. A high S/N ratio might indicate a possible volcanic origin of the aerosols. Figure 7.6 shows the 24-h averages of PM_{10} and $PM_{2.5}$ mass concentrations in the top panel, PM_{10}-sulphate, PM_{10}-nitrate concentrations (middle

panel) and the S/N ratio (bottom panel) from 4 to 14 May at the Zarra station. On 8 May, the S/N ratio stands out at Zarra, in coincidence with the highest value of $PM_{2.5}$ for the period, indicating a strong contribution of small sulphate-rich particles.

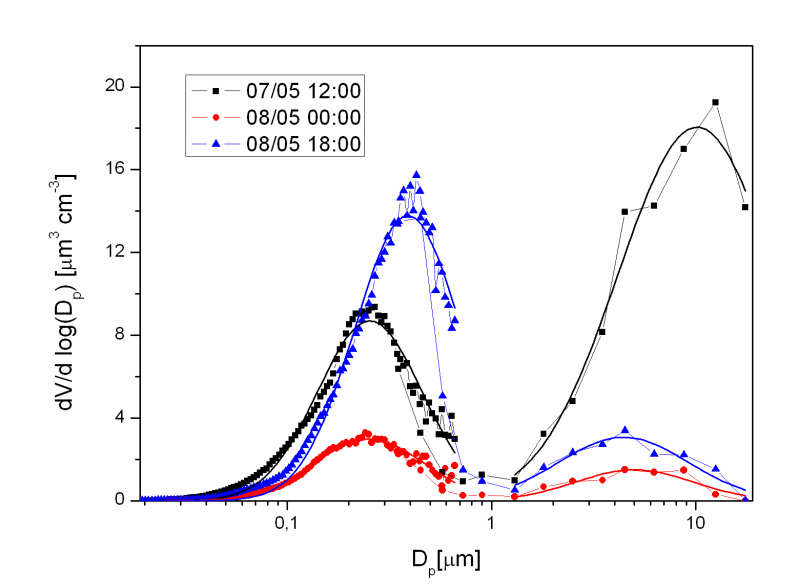

Figure 7.7. 3h-averaged volume distributions for the event of the 7-9 May. Markers refer to experimental data (SMPS 0.015-0.60 µm, GRIMM1108 0.3-20 µm). Solid lines are lognormal curve fits.

Figure 7.7 depicts 3-h averaged volume distributions, obtained from both SMPS and OPC instruments at the CIEMAT site, exhibiting a bimodal size distribution in the range 0.015 – 20 µm. Lognormal distributions were fitted to the fine mode and coarse mode separately. Values and errors for geometric diameter (dg) and geometric standard deviation (σg) of the distributions, given by the fitting algorithm, are shown in Table 7.1. The modal diameter (Dp) was obtained from these parameters using the Hatch-Choate equations (eq. 3.15), and is also shown in Table 7.1. ΔDp was calculated by error propagation (eq. 3.2).

Three different situations are shown, a local pollution event measured on 7 May at 12:00 (squares), the arrival of volcanic aerosol obtained on 8 May at 18:00 (triangles) and also a clean-atmosphere situation observed on 8 May at 00:00 (circles).

Mode	Date	Time	d_g (μm)	σ_g	D_P (μm)
Fine	07/05/2010	12:00	0.359±0.005	1.802±0.015	0.254±0.004
	08/05/2010	00:00	0.370±0.006	1.859±0.018	0.252±0.005
	08/05/2010	18:00	0.556±0.011	1.816±0.019	0.390±0.009
	13/05/2010	06:00	0.358±0.005	1.871±0.017	0.242±0.004
	13/05/2010	18:00	0.353±0.002	1.450±0.007	0.307±0.002
	14/05/2010	00:00	0.287±0.002	1.458±0.007	0.249±0.002
Coarse	07/05/2010	12:00	22.4±4.6	2.44±0.19	10.1±2.5
	08/05/2010	00:00	7.8±1.2	1.94±0.19	5.0±1.0
	08/05/2010	18:00	7.5±1.0	2.07±0.15	4.4±0.7
	13/05/2010	06:00	10.3±3.1	2.39±0.37	4.8±2.0
	13/05/2010	18:00	12.1±6.8	2.62±0.70	4.8±3.7
	14/05/2010	00:00	4.1±0.2	1.68±0.07	3.1±0.2

Table 7.1. Values obtained for the fitting of lognormal distribution to the fine mode, measured by the SMPS instrument, and coarse mode, measured by the GRIMM 1108 OPC.

During the morning of 7 May, a pollution event yields a significant PM_{10} peak simultaneously with an increase in particulate nitrate levels and no remarkable fine sulphate and PM_1 level increase. The nitrate concentration increase reveals the anthropogenic origin of pollutants. The clean atmosphere case shows low values of all parameters measured. In both cases the fine mode has a modal diameter of 0.25 μm, as can be seen in table 7.1. However, when the volcanic event was detected at ground level (curve 8 May at 18:00, triangles) the modal diameter is displaced to 0.39 μm. This value is small compared with those estimated by remote sensing for the plume that affected Central Europe in April, where ash-related low Ångström exponent indicated the presence of a considerable amount of large to very large particles with diameters larger than 20 μm in the ash layers (Ansmann et al, 2010). The coarse distribution was similar under the clean and volcanic cases, being significantly higher in magnitude and modal diameter for the local event. On 8 May an increase in the fine mode (PM_1) caused by the arrival of the volcanogenic aerosol was clearly seen on figure 7.5 (bottom panel). Nevertheless, aerosol size at 18:00 might already reflect some secondary production due to hygroscopicity since rising RH values reached 75% around that

time. Previous works have stated hygroscopic secondary aerosol production at RH levels over 70% (Chen et al, 2003).

7.3.2-Minor Eyjafjallajökull event

On the evening of 13 May another noticeable sulphate peak was observed at the CIEMAT site (see figure 7.5, middle panel). Shortly after a rain event the concentration tripled its value in less than three hours. The increase in SO_4^{2-}/PM_1 was similar to the events of 4-5 and 7-9 May (from 0.15 on 13 May at 15:00 UTC to 0.35 at 23:00 UTC), but in this case RH values remained over 70%. No nitrate production was detected and coarse particulate matter did not suffer any significant change. Small SO_2 peaks were also measured in O Saviñao, Peñausende, Víznar and Els Torms (figure 7.1).

Figure 7.8 shows the vertical extinction coefficient profile measured over Madrid at 08:00 UTC. In this case, a mixing layer with clouds on top is observed up to 3 km and a double-lobed aerosol layer is detected between 4.5 and 5.5 km, with extinction coefficient values around $1.25 \cdot 10^{-5}$ (±0.53) m^{-1}, corresponding to a mass concentration value of 19.5 (±8.3) $\mu g \cdot m^{-3}$. Although in this case back-trajectories indicate Icelandic provenance, contributions can come also from an Atlantic air mass polluted with volcanic aerosols from previous days.

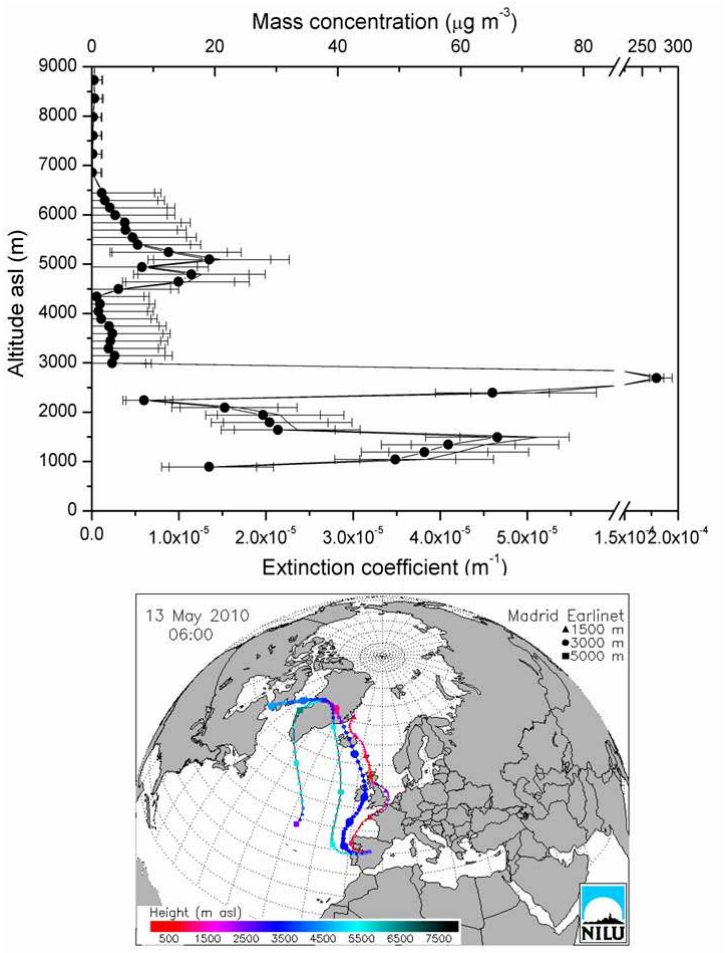

Figure 7.8. Same as figure 7.2, for 13/05/2010 08:00 UTC.

Figure 7.9 shows the distributions obtained during a local pollution event (13 May at 6:00, squares), the volcanic event (13 May at 18:00, circles) and a clean-atmosphere situation (14 May at 00:00, triangles). On 13 May at 6:00, figure 7.5 showed a PM_1 peak event correlated with an increase in nitrate, indicating an anthropogenic event. On 13 May at 18:00, another volcanogenic event was identified by the sulphate peak without nitrate concentration increase. Finally, on 14 May at 0:00, the event has nearly ceased and values reflect a clean atmosphere. In the first and last cases the fine mode of the distribution is under 0.25 μm, while during the sulphate event it grows to over 0.30 μm. The coarse fraction presents a small contribution to the aerosol in all three cases. On 13 and 14 May, an increase in the fine mode is seen again during the sulphate event. RH is over 80% in the three moments studied, before, during and after the event, so that by itself it cannot explain the increase in aerosol size.

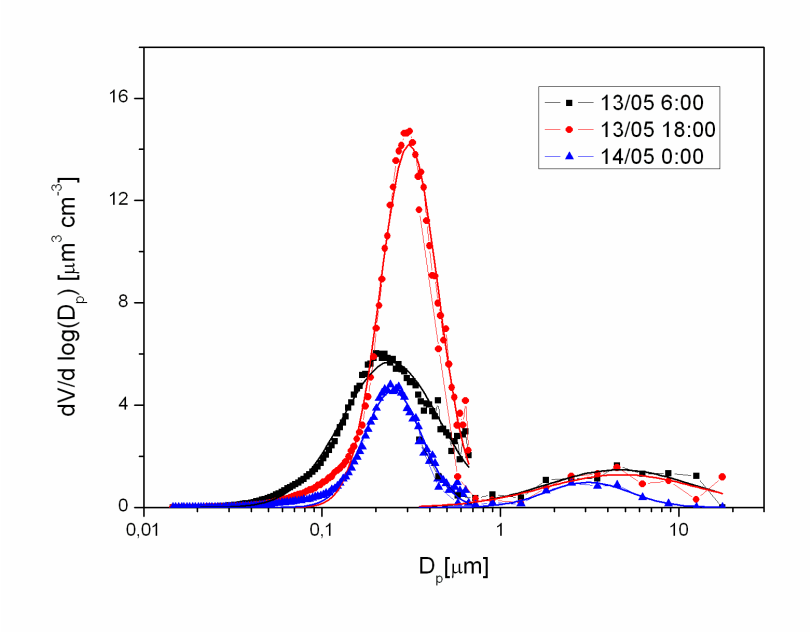

Figure 7.9. Same as figure 7.7, for the event of the 13-14 May

Size distributions of ions present in aerosols sampled at ground level near volcanoes have been obtained by other researchers, finding a major sulphate modal diameter of 0.5 μm (Mather et al, 2003) and 0.1-0.25 μm (Ilyinskaya et al, 2010). In both cases the importance of background meteorological conditions for particle evolution was stated, observing an increase in sulphate aerosol size in high humidity conditions for the former. A recent study (Ilyinskaya et al, 2011) has shown the near-source size distribution of aerosol emitted by Eyjafjallajökull on 2010 eruption. The authors found, in the eruptive phase between 18 April and May 5, a bimodal distribution with a fine mode below 0.4 μm and a coarse mode > 1 μm. Our results are consistent with these, showing a modal diameter Dp of 0.39 μm when volcanogenic sulphate aerosol impacts on the ground. This value is distinguishable from the local accumulation mode, typically with a Dp on the order of 0.25 μm. No impact is seen on the coarse aerosol mode. These results suggest a possible growth of the fine mode through condensation and/or coagulation processes from the source to the arrival of the plume at the sampling point, and also the removal of the larger ash particles.

7.3.3-Etna event

Throughout 2011, the Etna showed high activity (Coltelli et al, 2012). On the evening of 28 September 2011, the New Southeast Crater of Etna produced its 15th eruptive episode since the beginning of the year. This eruption coincided with high sulphate concentrations above the European continent, which reached Madrid on the 13th of September. On the 28th, there is an enhancement of the sulphate cloud, registering maximum extension and concentrations on the 1st of October (See figure 7.10). FLEXTRA back-trajectories show eastern provenance at 1500, 3000 and 5000 m. From 5 Oct on an Atlantic air mass cleaned away the sulphate cloud.

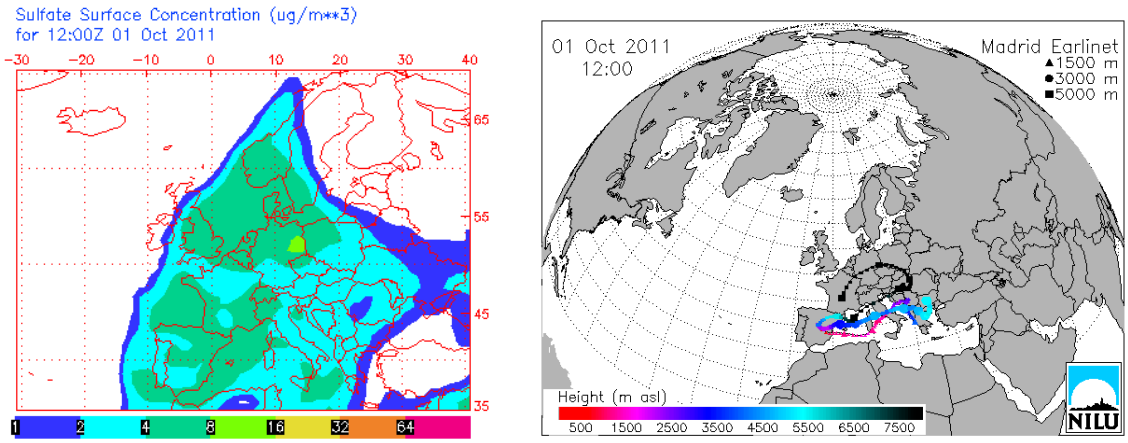

Figure 7.10. (Left) Sulphate surface concentration estimated by NAAPS. (Right) Trajectories arriving in Madrid on 1 Oct 2011 at 12:00 UTC

The increase in sulphate levels was registered in CIEMAT and also in the three EMEP rural stations in the central Iberian Peninsula: ES01, ES09 and ES13. The daily evolution of this pollutant was very similar in all of them (figure 7.11).

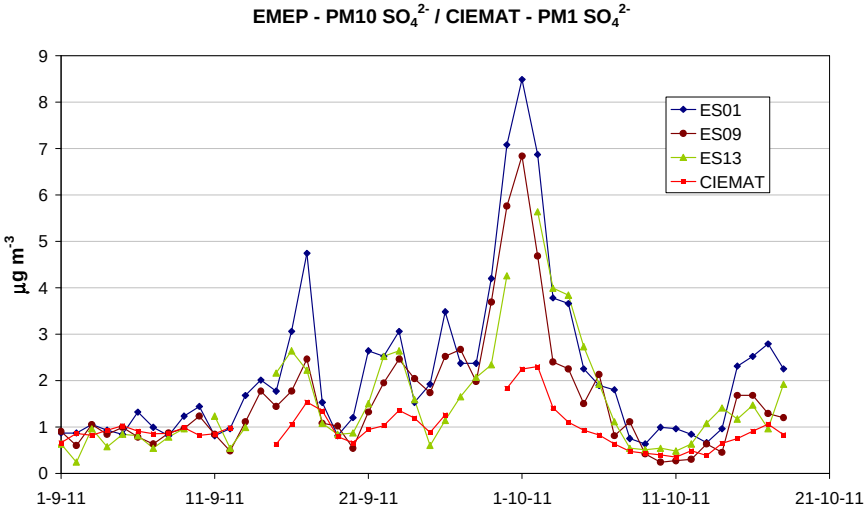

Figure 7.11. Evolution of daily averaged particulate sulphate in CIEMAT and three EMEP sites

In this case, we can estimate the size of the particles that reached Madrid by means of the ratio $PM_{2.5}/PM_{10}$ in the EMEP stations. Figure 7.12 shows the evolution of $PM_{2.5}/PM_{10}$ in September and October 2009, the period in which the transport episode from the European continent was previously characterised, and September-October 2011. Some data have been excluded at the end of Oct 2011 due to highly noisy ratios.

The days corresponding to the main events (22 Sept-10 Oct 2009 and 28 Sept-5 Oct 2011) show very similar maximum $PM_{2.5}/PM_{10}$ ratios, with values around 70%. The 0.5 percentiles calculated for Sept-Oct 2009 and 2011 are 56% and 42% respectively. The bottom panel of figure 7.12 shows that during the days of the main event the particle size of the aerosols measured at the three stations was significantly smaller than for the rest of the 2-month period.

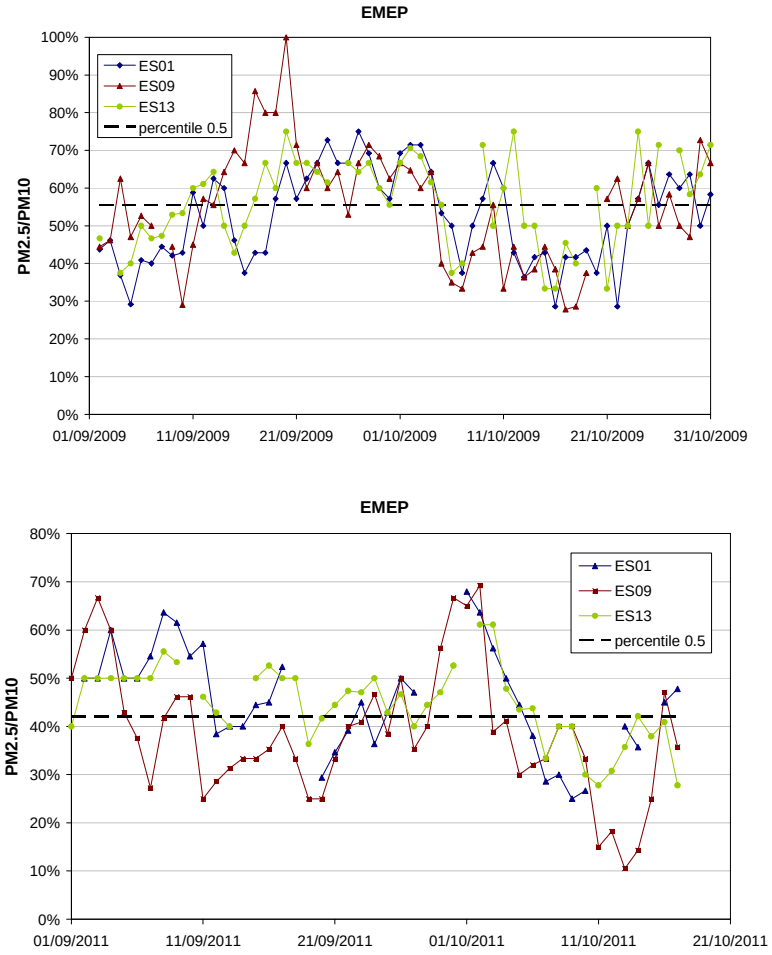

Figure 7.12. Evolution of the ratio $PM_{2.5}/PM_{10}$ in ES01, ES09 and ES13 during the European long-range transport episode 2009 (top) and the Etna episode 2011 (bottom)

7.4-Conclusions

Physico-chemical characteristics of the volcanic aerosol emitted by the Icelandic volcano Eyjafjallajökull during May 2010 and detected at several sites of the Iberian Peninsula have been presented. Ground-based on-site observations from the Spanish EMEP network were affected by the volcanic plume. The concentrations of sulphur dioxide and sulphate in PM_{10} and $PM_{2.5}$ reached relative maxima not correlated with other pollutants such as nitrogen oxides and ozone. The first effects appeared on 4 and 5 May from the northwest to the southeast of Spain, but they intensified between 7 and 9 May at the sites in the centre and south of the Iberian Peninsula. In this period no influence was detected in the Eastern Spain stations, Cabo de Creus and Mahón. At the CIEMAT site, an estimation of the vertical profiles of mass concentration was

calculated from the extinction coefficient profiles, obtaining a maximum value (77 (±9.6) $\mu g \cdot m^{-3}$) well below the threshold established for safe aircraft operation. In this site the aerosol size distribution and chemical composition were continuously monitored during the event, detecting a large increase in the fine mode in coincidence with an increase in sulphate concentration, while the coarse mode remained almost unaltered. Volume distributions at ground level indicate particles mainly in the 0.1-0.7 μm size range, in contrast with studies of the plume that affected Central Europe in April, where particles with diameters larger than 20 μm were present in the ash layers. These results are consistent with the bimodal size distribution obtained near-source by Ilyinskaya et al, 2010, and suggest a possible growth of the fine mode through condensation and/or coagulation processes from the source to the arrival of the plume at the sampling point, and also the removal of the larger ash particles. The information on volcanic aerosol characteristics after long-range transport provided by this study might contribute to better assess the type of aerosol that reach distant locations.

On 28 September 2011, the Sicilian volcano Etna started a violent eruption. Meteorological conditions present at the time made that the material ejected into the atmosphere might get to Madrid. This event coincided with a period in which the NAAPS model and FLEXTRA back-trajectories described a situation similar to the conditions present at the time of the European transport episode described in the previous chapter. $PM_{2.5}/PM_{10}$ ratio calculated in EMEP stations is similar for both episodes. Due to this fact, the contribution of the Etna emissions to the event detected in the central Iberian Peninsula is difficult to quantify.

8-SIZE-SEGREGATED INORGANIC AEROSOL COMPOUNDS

8-SIZE-SEGREGATED INORGANIC AEROSOL COMPOUNDS

8.1-Introduction

In previous chapters we have studied the time evolution of sulphate and nitrate in the fine aerosol (PM_1 and $PM_{2.5}$ size fractions respectively) at an urban background site in Madrid. The high resolution time series database acquired on both compounds and the complementary information allowed us also to study in detail characteristic episodes taking place in the Madrid airshed and specific events of special interest. Nevertheless, some behaviours and observed patterns of these species have not been fully understood. One reason can be that a complete characterization of the processes involved in the formation of secondary compounds must be addressed taking into account different size fractions simultaneously (Cabada et al, 2004; Wall et al, 1988). As discussed in the introduction of this thesis (Chapter 1), the processes leading to the generation of particulate nitrate and sulphate are related to the particle size, therefore their study must contemplate a size distribution characterization of these compounds, which will provide valuable information about the processes involved in the formation of SIA in the study area.

So that, this analysis was carried by re-analyzing , in the light of our main findings, the work of Plaza et al., 2011, which was designed to study the mass size distribution of inorganic species at the CIEMAT site. It was based on a field campaign carried out throughout one year (February 2007 to February 2008). Annual and seasonal averages were obtained, and some case studies under specific atmospheric conditions (winter stagnation, summer conditions and fog) were discussed. As a result, a very remarkable amount of sulphate not neutralised by ammonium was detected below 0.056 μm. The presence of nanometric particles was confirmed by the SMPS number size distributions.

On the other hand, as exposed in Chapter 5, the comparison with other regions with different emissions and meteorology has been deemed not only interesting but necessary, since it contributes to identify and explain characteristic behaviours of the study area, in this case the Madrid airshed. To this end we present here the ion size

distributions in the area of Barcelona which were obtained in the frame of the DAURE campaign and compare them with the results previously achieved in Madrid.

DAURE (Determination of the sources of atmospheric Aerosols in Urban and Rural Environments in the western Mediterranean) was an international campaign which took place during winter 2009 (February 25 to March 26) and summer 2009 (July). The objective of DAURE was to characterise the sources of fine aerosols in the Barcelona region, paying particular attention to the formation mechanisms of secondary aerosols. During DAURE, measurements were made in winter and summer, at two sampling sites, an urban background site close to the centre of Barcelona city (BCN) and a rural background site in the Montseny Natural Park (MSY), but not all the measurements were performed in every site and season. For this reason in this work we will analyse the properties of SIC in BCN site during winter conditions.

The aerosol formation and transformation processes in the Western Mediterranean Basin (WMB) are complex and not yet fully understood. Large pollutant emissions from densely populated and industrialised areas together with regional atmospheric dynamics lead to extremely high concentrations of $PM_{2.5}$ and PM_1 in the region (Pey et al, 2010a). In winter, the weather has an influence on air pollutants similar to that in Madrid. Atlantic air masses often reach the study area, replacing aged air masses and reducing pollution levels. However, under anticyclonic conditions thermal inversions are formed and highly polluted air masses are accumulated in the region. Moreover, under weak synoptic forcing conditions mesoscale phenomena are developed, consisting on strong sea-land breezes and mountain and valley breezes (Pérez et al, 2008).

The high concentrations of SIC registered in the Barcelona area and the important contribution of SIC to the total aerosol have led to numerous studies in recent years. In Querol et al (2004c), the maximum daily average values for SIC in $PM_{2.5}$ in Spain were obtained in a kerb-side site in the Barcelona metropolitan area, 4 $\mu g \cdot m^{-3}$ for nitrate and 5.8 $\mu g \cdot m^{-3}$ for sulphate –notably higher than the 1.3 and 3.8 $\mu g \cdot m^{-3}$ registered in a traffic site in Madrid in the same 1–year study. The secondary inorganic aerosol contribution to the total aerosol mass can reach values around 30% in the fine fraction,

being the study of nitrate especially important (Pey et al., 2010b). The differences in source profiles –traffic predominance in Madrid and significant industrial and shipping contributions in Barcelona- and meteorology –influence of the sea in Barcelona- raise the interest in the comparison of the ion distributions in the two largest Spanish cities, which will be determined by the sources and formation processes.

In this chapter we present results obtained at the BCN urban background site in the winter DAURE campaign. Ion size distribution and balances obtained from chemical analysis are shown (Artíñano et al, 2010).

In both the work of Plaza et al (2011) and the DAURE campaign ion size fractions were studied in 11 stages, spanning a range from 18 μm down to particles smaller than 0.056 μm. Those works have been expanded with a study which includes smaller size fractions, not covered in the previous experiments. We present a field experiment that implies an extension to particles smaller than 0.010 μm. These measurements were taken at the CIEMAT site in different meteorological scenarios during winter 2011, and among them three case studies were selected. A heavy fog episode was compared to a typical intense winter stagnation situation. A third scenario represented the transition between a clean period and the fog, where a slight haze was present. This allowed studying the efficiency of sulphate and nitrate formation by aqueous phase oxidation in comparison with the typical photochemical episodes which take place in winter under anticyclonic conditions.

8.2-Methods

8.2.1- Measurement sites

In Madrid, all the measurements analysed in this chapter were taken in the CIEMAT station already described in Chapter 3.

The area selected for the DAURE campaign is located in the NE of the Iberian Peninsula, in the WMB. Barcelona is located on the Mediterranean coast between the mouths of the rivers Llobregat and Besòs and is bounded to the west by the Serra de

Collserola ridge (512 m). It is the second most populated city in Spain and the tenth in the EU. Its official metropolitan area covers an area of 636 km² and more than 3.2 million inhabitants with a density of population of 5000 km⁻². However, the estimated region of influence of the city includes about 5 million inhabitants. It is not only densely populated but also densely industrialised and traffic congested. According to the 2010 data supplied by the Metropolitan Transport Authority, the weekly mobility distribution in the Metropolitan Region of Barcelona is: 31% private cars, 20.5% public transport, 48.5% pedestrian. Traffic (>45% diesel) constitutes the major source of air pollution in the area, although the contributions from industry and the harbour are also significant.

The Barcelona urban background site (BCN) is located 150 m away from Diagonal Avenue, one of the busiest traffic streets of the city (see Figure 8.1). At BCN, local emission sources in addition to meteorological factors determine the PM levels (Pey et al, 2010a). In spite of being classified as an urban background site, as CIEMAT, the distance to traffic streets is smaller than in the second case, being the CIEMAT site located in a greener area. This fact must be taken into account when comparing results from both sites.

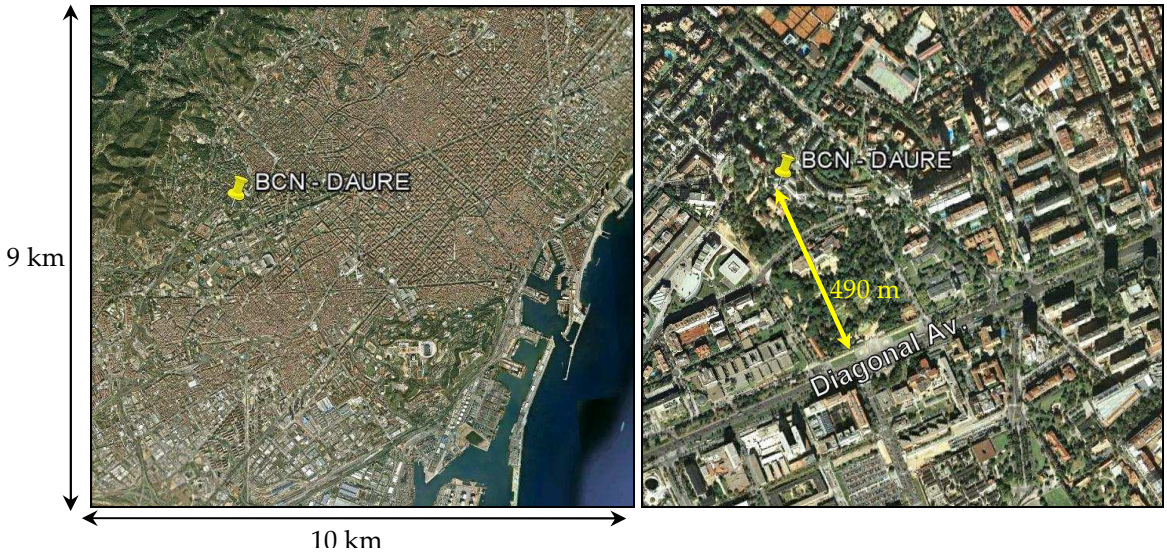

Figure 8.1. BCN site in the DAURE campaign (left). BCN site and Diagonal Av. (right)

An overview of the meteorological conditions during the DAURE campaigns can be found in Jorba et al (2011). During the winter case, which will be analysed here, three

main meteorological regimes were identified: (A) high pressure conditions over the WMB, high insolation and the development of thermally-driven wind flows; (B) a strong north-western advection producing a cleansing action over the atmosphere; and (C) strong stagnant conditions produced by nocturnal thermal inversions which decoupled the low troposphere of plain and coastal areas from mountainous terrains.

8.2.2. Instrumentation and sampling

Particle size distributions were obtained by a micro-orifice deposit impactor (MOUDI M110R, MSP Corporation). This impactor collected ten size fractions on uncoated aluminium substrates and a quartz fiber backup filter.

In Madrid, Plaza et al (2011) obtained a total of 20 sample pairs starting in February 2007 and throughout a complete year. The sampling periods were designed to discriminate nocturnal and diurnal periods. The diurnal sample collected aerosol in the period 8-15 h UTC and the nocturnal sample collected aerosol after sunset, in the period 18-7 h UTC. Atmospheric conditions were rather variable during the sampling days. Several cases with poor dispersive or stagnant atmospheric conditions were observed in different seasons.

Samples were taken during the DAURE winter campaign at the BCN site from February 24th to March 12th on a 12 hour basis (9 to 21 and 21 to 9 h UTC). Stable meteorological conditions favouring the accumulation of pollutants were present during most of the time period sampled. The first sampling period attempted to collect secondary aerosol as it started after the early morning emission period. The second sample collected the night aerosol and the morning emission period.

Further measurements were taken in Madrid during the winter of 2011. Three scenarios were selected with the objective of expanding the work of Plaza et al (2011). These scenarios where similar to others analysed by the authors of the previous work in which high concentrations of SIC had been identified. A heavy fog scenario (S1; 17/01/2011 8:15-18/01/2011 8:10 UTC) was compared to a typical intense winter stagnation situation (S2; 07/02/2011 8:15-08/02/2011 8:15) which corresponds to the same winter stagnation event described in chapter 7.3.3. S3 scenario (13/01/2011 13:30-

14/01/2011 13:30 UTC) represents the transition period between a clean period and S1, where a slight haze preceded the formation of S1. For these three case studies, the MOUDI M110R and MSP Nano-MOUDI Model 115 were used in combination to obtain 13 size fractions on uncoated aluminium substrates and a quartz fibre backup filter. These selected scenarios were also characterised by the semi-continuous PM_1 sulphate concentration and $PM_{2.5}$ nitrate concentration, gaseous SO_2, particle number concentration, and meteorological parameters all at the CIEMAT site.

After sampling, all substrates and filters were chemically analysed by ion chromatography (IC) for soluble ions, obtaining a size distribution for each of the following ions: sulphate, nitrate, nitrite, ammonium, calcium, sodium, magnesium, potassium and chloride. The analytical procedure is described in Plaza et al (2011).

8.3-Results

8.3.1-Previous results in Madrid

The results from Plaza et al (2011) showed that in the urban background site studied the sulphate and ammonium masses were mainly concentrated in the accumulation range (0.18-0.56 μm), which is consistent with the gas-phase photochemical formation of ammonium sulphate and nitrate from their gaseous precursors. However, annual lognormal bimodal fits showed accumulation modes around 0.35 μm for sulphate, nitrate and ammonium and coarse modes in 5.6 μm and 4.3 μm for nitrate and ammonium. For nitrate the coarse mode dominated over the accumulation mode in all seasons and time periods. This is probably due to the interaction of nitric acid with crustal material.

Ammonia neutralised the acidity in the range 0.056-1.8 μm, being an excess of NO_3^- in the range 1.8-18 μm. In the coarse range the nitrate acidity was neutralised mainly by the calcium ion.

A very remarkable amount of sulphate not neutralised by ammonium was detected below 0.056 μm (Figure 8.2). This might be explained by the presence of sulphuric acid nanoparticles. Sulphuric acid is one of the key components in aerosol nucleation and

growth from the initial stable clusters to detectable sizes (Wehner et al, 2005; Kulmala et al, 2004). The presence of nanometric particles was confirmed by the SMPS number size distributions. Due to the harmful effects of these particles on health it is important to go deeper into this issue. The adverse health effects of these particles would be given on one hand by its small size, which confers them a great ability to penetrate the human body, and on the other hand by its acidity, which makes them capable of reacting with biological tissues (Leikauf et al, 1981).

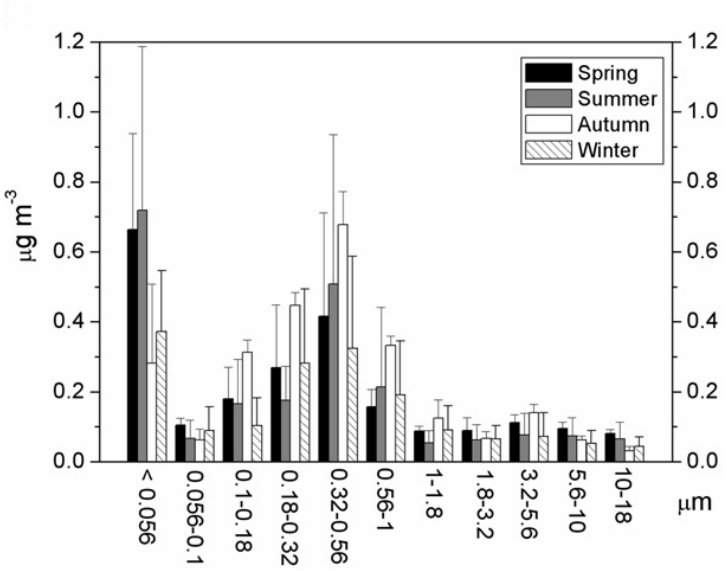

Figure 8.2. Seasonally averaged mass size distributions obtained for sulphate in Madrid by Plaza et al (2011). Standard deviations of averages (±2σ) are also shown.

Nitrate in the accumulation mode presented a marked seasonal evolution, with maximum values in the cold season because of the volatilization of ammonium nitrate in summer. In contrast, maximum concentrations of coarse nitrate were found in spring and summer. In the case of sulphate, in autumn and winter the accumulation mode dominates this ion mass size distribution, but during the warm season nanometric sulphate prevails.

The concentrations of sulphate, nitrate and ammonium were slightly higher during the day, since the traffic emission period was included in the diurnal sample. The highest averaged concentrations of sulphate and nitrate per stage in winter –season which will be compared with the results in Barcelona- were around 0.30-0.35 $\mu g \cdot m^{-3}$, and 0.25 $\mu g \cdot m^{-3}$ for ammonia.

Regarding the results for different case studies, the size distributions obtained in winter episodic conditions are very similar to the winter averages already described. In contrast with this scenario, an example of a windy summer day with very effective dispersion was studied. Under this second scenario, the nanometric sulphate fraction below 0.056 μm was enhanced. Particles concentrate on this primary or freshly nucleated particles, in contrast with the poor dispersion winter scenario, which would favour agglomeration and coagulation of particles. Finally, a fog event was studied. Very high concentrations of sulphate (over 2 $\mu g \cdot m^{-3}$) were detected in the stages 0.56-1 μm and 1-1.8 μm. Nitrate concentration also accumulated in the range 0.056-1.8 μm, showing values over 1 $\mu g \cdot m^{-3}$. The presence of fog indicates strong atmospheric stability conditions and hence the same processes taking place in the first case study would apply in this case. However, the dominance of the sulphate and nitrate aqueous formation, not seen under the typical winter episodic conditions, was confirmed by these results.

8.3.2- Ion size distributions at urban background sites in winter: results from BCN and comparison with Madrid

-Mass size distributions-

The mean mass concentrations of sulphate, nitrate, ammonium and calcium ions per size fraction during the whole campaign in Barcelona were fitted to bimodal log-Gaussian distributions (eq. 3.16) and are shown in figure 8.3. The size fractions sampled by the MOUDI and nano-MOUDI stages have been designed to obtain discrete aerosol mass distributions similar to the discrete aerosol number distribution shown in figure 3.18. The size fraction sampled by the backup filter does not fulfill the requirements to be part of that mass distribution, so data for the backup filter stage have not been taken into account in the calculation.

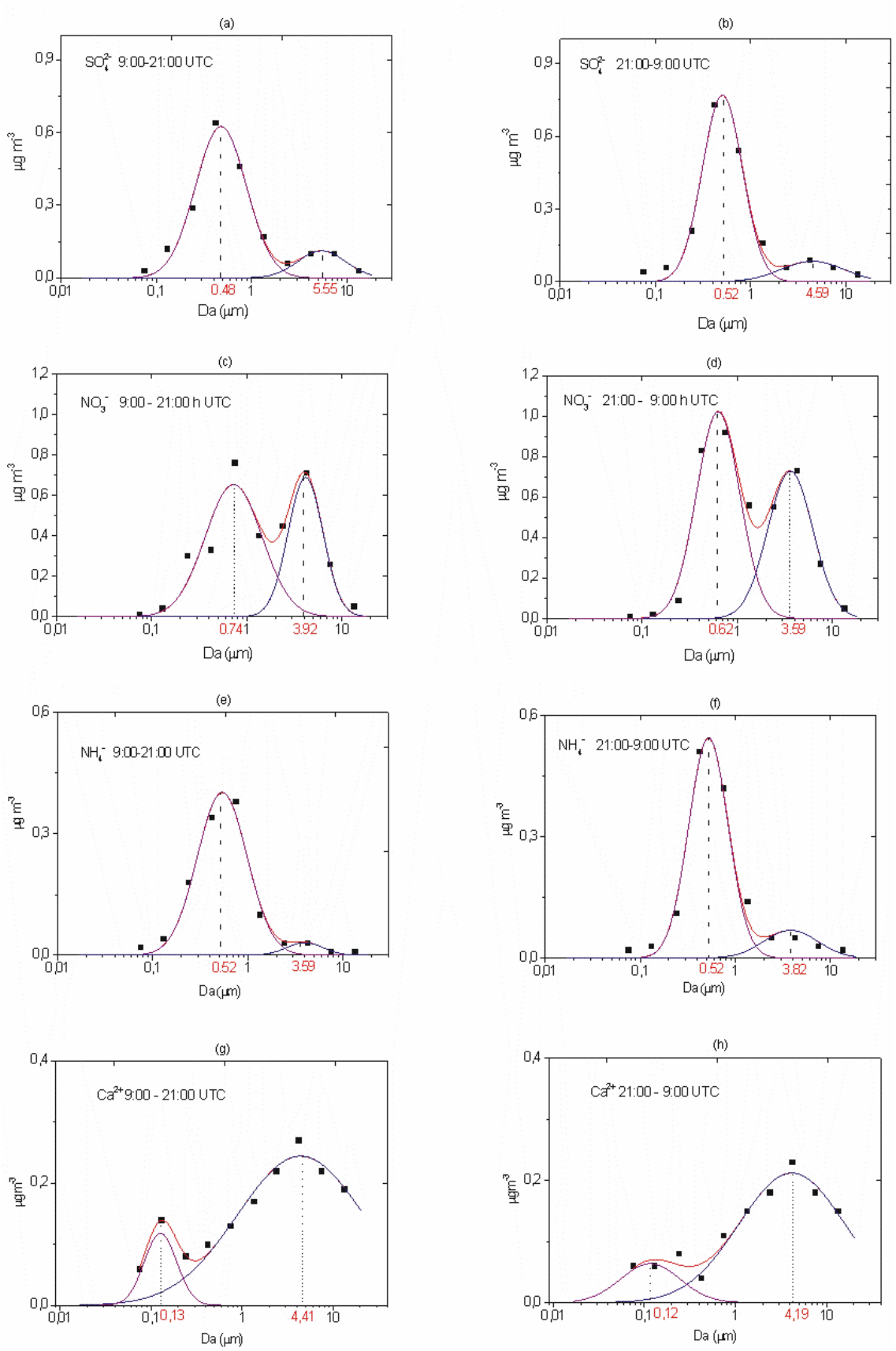

Figure 8.3. Averaged ion mass distributions by day/night period (left/ right panel) in BCN during the DAURE winter campaign.

The nitrate mass was found to be concentrated in two modes, an accumulation one around 0.75 μm and other coarse one around 3.90 μm. The sulphate and ammonium masses were concentrated in the accumulation mode, around 0.50 μm, although a small peak in the coarse range also appeared for both ions. The calcium mass also presented a bimodal distribution, although mainly concentrated in the coarse fraction, with a modal diameter ~ 4 μm. All ions showed slightly higher concentrations during the night-time due to the inclusion of the emissions period in the nocturnal sample. The differences in the modal distributions between day and night were small, only the particulate nitrate showed a dominant accumulation mode during the night while during the day the two modes accounted for a similar amount of nitrate. This could be caused by the fact that during daytime nitric acid concentration is higher, as temperature is higher and the equilibrium between solid nitrate and precursor gases favours the gas phase. Gaseous nitric acid can react with crustal or soil material. The formation of mineral sulphates in the coarse range cannot be discarded either, since the low water solubility of these compounds does not allow their detection by the techniques employed.

The highest averaged concentrations per stage were found in stages 6 and 7 (0.32-1 μm), reaching values around 0.7 $\mu g \cdot m^{-3}$ for sulphate and nitrate and around 0.5 $\mu g \cdot m^{-3}$ for ammonia.

Accumulation modal diameters were significantly smaller, especially for nitrate, in Madrid than in Barcelona. This can be explained by the dominance of a droplet mode in Barcelona. The accumulation mode may split into a (hygroscopic) droplet mode and a (non-hygroscopic) condensation mode. In addition, gas-phase pollutants may dissolve and react in the particle-bound water of hygroscopic particles, leading to an increase in the dry size (EPA, 2004). Other researchers observed that sulphate showed two sub-modes in the accumulation mode, peaking in the condensation mode at 0.2 μm, and in the droplet mode at 0.7 μm (John et al., 1990; Meng and Seinfeld, 1994). The size distributions observed in Barcelona are compatible with a non-resolved double accumulation mode with a dominant droplet mode, while in Madrid the condensation mode would dominate in the accumulation range. This can be explained taking into account the location of both cities. While Barcelona is a coastal city, therefore with high

relative humidity conditions, Madrid is located inland where dry atmospheric conditions prevail. Relative humidity during the 17 days sampled in BCN showed daily means >60% (except for two days) and >80% for four days in the Barcelona region (Jorba et al, 2011). In Madrid, rain events are frequent during the cold season, but when anticyclonic conditions prevail, relative humidity rarely exceeds 70%. A double accumulation mode was also found in a coastal site in Hong Kong by Zhuang et al (1999b), who used similar MOUDI samplers.

The dominance of the nitrate coarse mode in Madrid had been explained by the reaction of nitric acid with crustal or soil material, since limestone crustal aerosol is abundant in the Madrid air basin. This aerosol can be dominant when local and regional circulations prevail in the airshed (Coz et al, 2010). However, on an annual basis, the percentage of mineral aerosol in PM_{10} is similar (~30%) in Barcelona and Madrid (Querol et al, 2008; Querol et al, 2004a).

The highest averaged concentrations of sulphate and nitrate per stage in winter in Madrid were around half of the concentrations measured in Barcelona.

-Ion balances-

Ion balances were performed to study the aerosol neutralization. Figure 8.4 shows the results obtained for the full sample set collected at BCN in the range 0.056-18 μm. The soluble fraction of sulphate and nitrate was fully neutralised by ammonium. Moreover, taking into account all the soluble ions analysed, we can see than in average there exists an excess of cations.

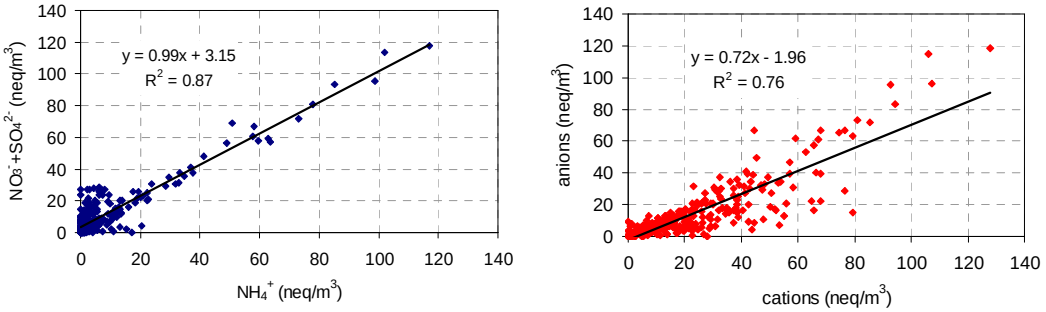

Figure 8.4. Neutralisation balances at the BCN site during the DAURE winter campaign

Figure 8.5 depicts the ion balances by size fraction and day/night time period taking into account the measured concentrations of nitrate, sulphate, ammonium and calcium. The results showed that acidic ions were neutralised, except those in the range below 0.056 μm, where the sulphate and nitrate ions produced acidity for both sampling periods. This acidic fraction was more remarkable during daytime.

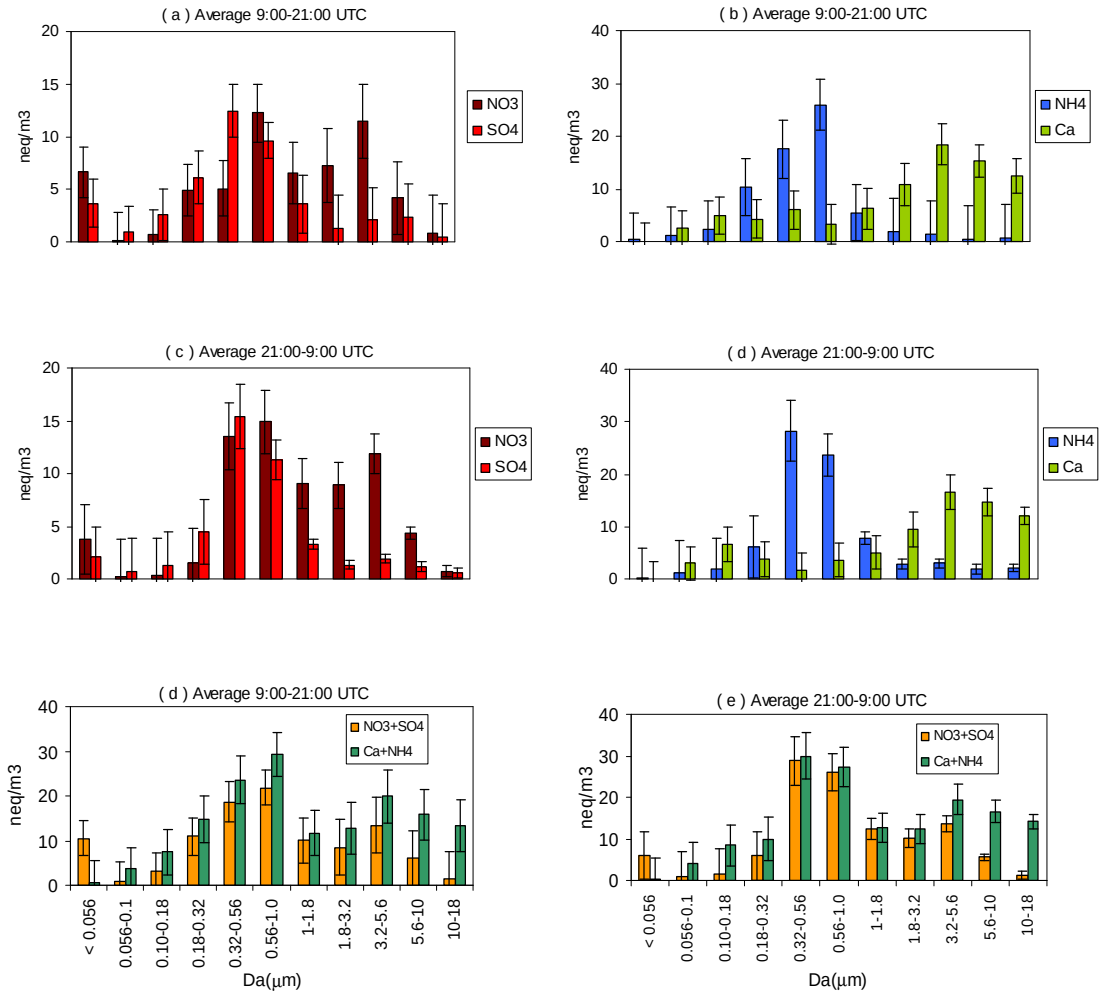

Figure 8.5. Ion balances at BCN site during the DAURE winter campaign by day/night period (left/ right panel) and size fraction.

The ammonium measured in the accumulation mode was able to neutralise the inorganic acidity caused by the nitrate and sulphate, but not the acidity in the coarse mode caused by the nitrate. During most of the campaign in BCN the particulate nitrate in this mode was generated by the reaction of gaseous nitric acid with crustal calcium carbonate (reaction 1.9) replacing the carbonate (Saul et al, 2006; McNaughton et al, 2009). In the few cases where the calcium ion concentration was not enough, i.e.

from March 6 to 10 (B meteorological regime), sodium became the neutralizing cation (reaction 1.8).

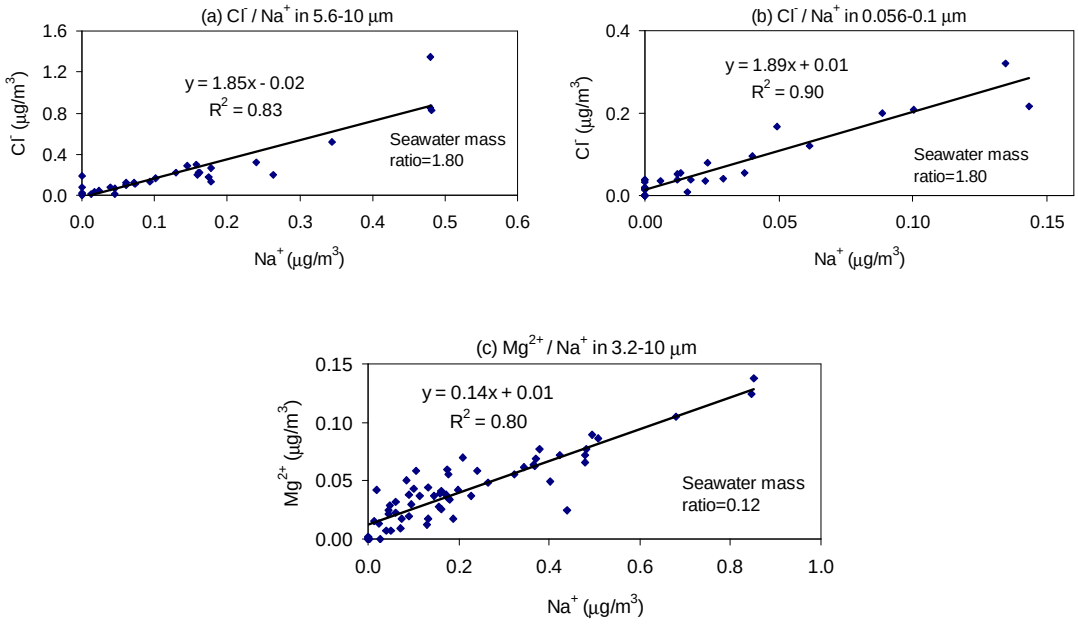

Figure 8.6. Ion mass ratios and comparison with seawater ratios

Figure 8.6 depicts ion mass ratios for the marine elements during the full period sampled at BCN. In the coarse range the slope between Cl^- and Na^+ was close to the Cl^-/Na^+ seawater ratio in mass (1.80) in the stage 5.6-10 µm. In the range 3.2-10 µm the slope between Mg^{2+} and Na^+ was close to the Mg^{2+}/Na^+ seawater ratio in mass (0.12) (seawater ratios from Seinfeld and Pandis, 2006). This suggests the marine origin of Cl^-, Na^+ and Mg^{2+} ions in the coarse fraction. However, the best correlation between chloride and sodium ions was found in the range 0.056-0.1 µm, with a ratio slightly higher than the seawater ratio. A significant amount of Cl^-, Na^+ and also Ca^{2+} was found in the submicronic fraction. It is known that the crustal species Ca^{2+} and Mg^{2+} may exist in small amounts in the nuclei mode. Sea salt, commonly found in coarse particles, may also exist as nanoparticles, generated by sea spray (Pey et al, 2009). A review of the characteristics of nanoparticles in the urban atmosphere was performed by Kumar et al (2010).

In short, in both cities sulphate and nitrate ions were neutralised by ammonium in the accumulation range, while nitrate in the coarse range was neutralised mainly by calcium. Acidic nitrate and sulphate were detected in Barcelona below 0.056 µm. Non-

neutralised sulphate in this range was also observed in Madrid, although the presence of nitrate cannot be confirmed from the results of Plaza et al (2011), since nitrate concentration was not analysed in the backup filter. In Madrid the nanometric sulphate fraction was enhanced with respect to Barcelona, exhibiting higher sulphate concentrations than any other substrate in winter, and also in spring and summer.

8.3.3-Selected case studies in Madrid

To obtain further insight about the origin and generation processes of sulphate and nitrate in the Madrid atmosphere, and especially to study in more detail the nanometric fraction observed in previous studies, a sampling campaign was carried out during winter 2011. MOUDI and nano-MOUDI were deployed together with the semicontinuous instrumentation available at CIEMAT. The results obtained for three selected episodes S1 (fog), S2 (winter stagnation), S3 (haze) are presented below.

-Mass size distributions-

Figure 8.7 shows the mass size distributions obtained for sulphate, nitrate and ammonium during the three cases.

During the fog episode S1, ion analysis showed a very pronounced accumulation mode of 1-1.8 μm of both sulphate and nitrate. Sulphate total concentration measured was over 2 $\mu g \cdot m^{-3}$ and nitrate over 3.2 $\mu g \cdot m^{-3}$. Nitrate maximum concentration per stage was 1.2 $\mu g \cdot m^{-3}$, similar as in the fog case studied by Plaza et al (2011). However, sulphate maximum concentration per stage is 0.8 $\mu g \cdot m^{-3}$, significantly lower than the 2.5 $\mu g \cdot m^{-3}$ registered in the previous study. This can be attributed to the fall in sulphur compounds emissions between the winters when the first and the second studies took place (2008 and 2011), as was seen in Chapter 4. Other researchers have recently found an inorganic salt supermicron mode associated to fog processing by the use of MOUDI (Yao and Zhang, 2012).

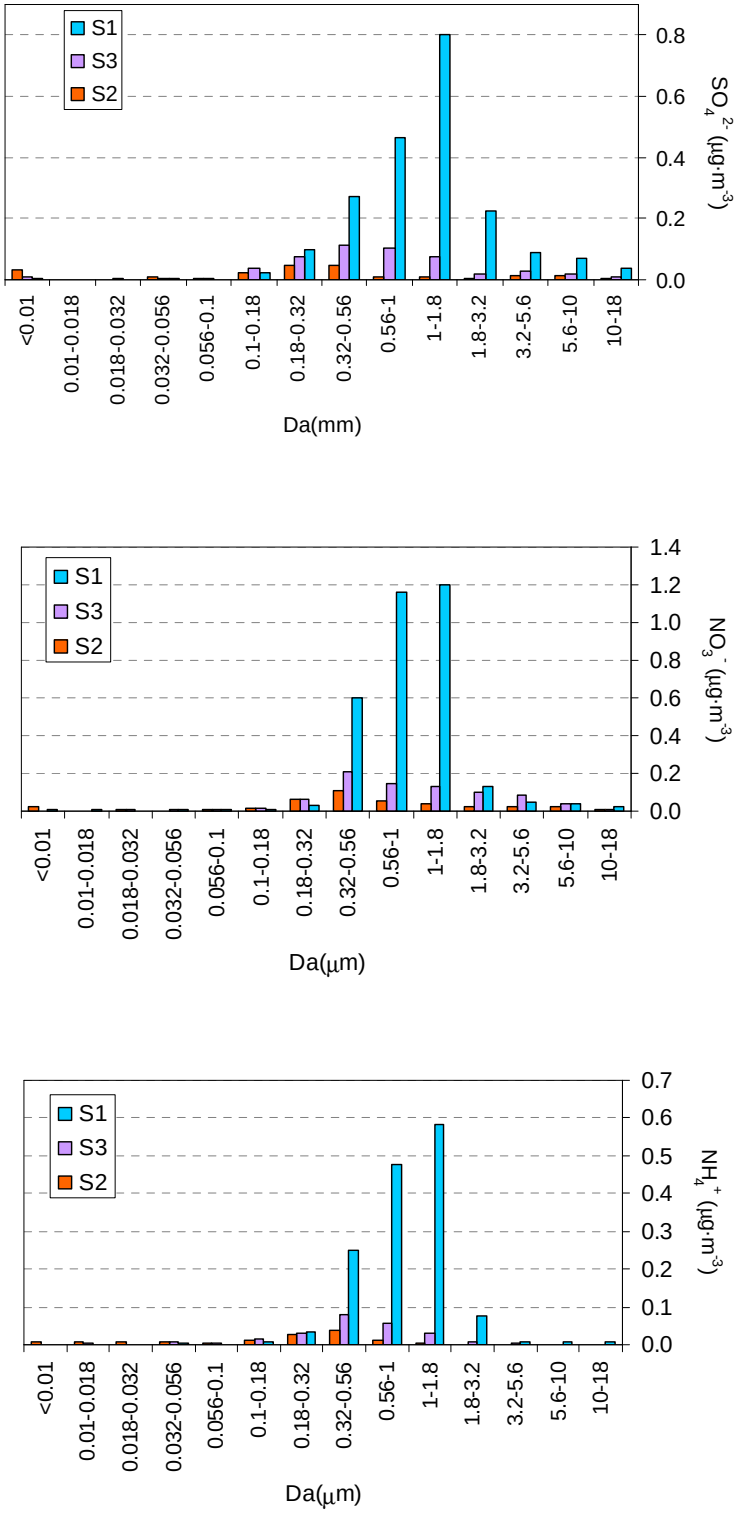

Figure 8.7: Size-segregated sulphate (top), nitrate (medium) and ammonia (bottom) in S1, S2 and S3 case studies in Madrid

During the stagnation episode S2, the prevailing aerosol mode was also in the accumulation range, but the highest concentrations were found in smaller sizes (sulphate 0.18-0.56 μm, nitrate 0.32-0.56 μm). A secondary coarse mode was found.

Total concentrations were one order of magnitude lower than in S1. Concentrations of the main ions were also lower than in the winter episodic case studied by Plaza et al (2011).

S3 showed intermediate characteristics between S1 and S2. The main ion distributions were unimodal, showing maximum mass values in the range 0.32-1 μm. Ion concentrations were higher than in S2, but very far from those found in S1.

The analysis of the nano-MOUDI stages showed a significant fraction of both sulphate and nitrate below 0.01 μm for the episode of winter stagnation (Figure 8.8). This remarkable fraction did not appear for the other cases, suggesting the shift of the nanometric particles to the accumulation mode. This mode shift can take place through aggregation and coagulation processes, or can be the result of direct SIC production in the droplet mode. Nanometric nitrate and sulphate have been found by other researchers using similar techniques. Lin et al (2007) found both compounds in a traffic site. Hsieh et al (2009) found $(NH_4)_2 SO_4$, but not nitrate, in a suburban site.

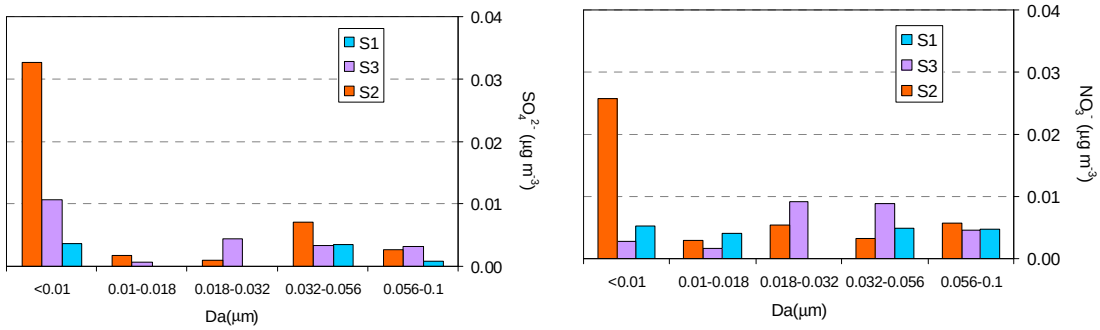

Figure 8.8: Ultrafine sulphate (left) and nitrate (right) in S1, S2 and S3 case studies in Madrid

The presence of Cl^-, Na^+, Mg^{2+} and Ca^{2+} in nano-MOUDI stages has been detected. As was exposed above, these ions have been identified in Barcelona in the lower stages of MOUDI. Hsieh et al (2009) obtained the same result using nano-MOUDI in a suburban site in Taiwan.

-Ion balances-

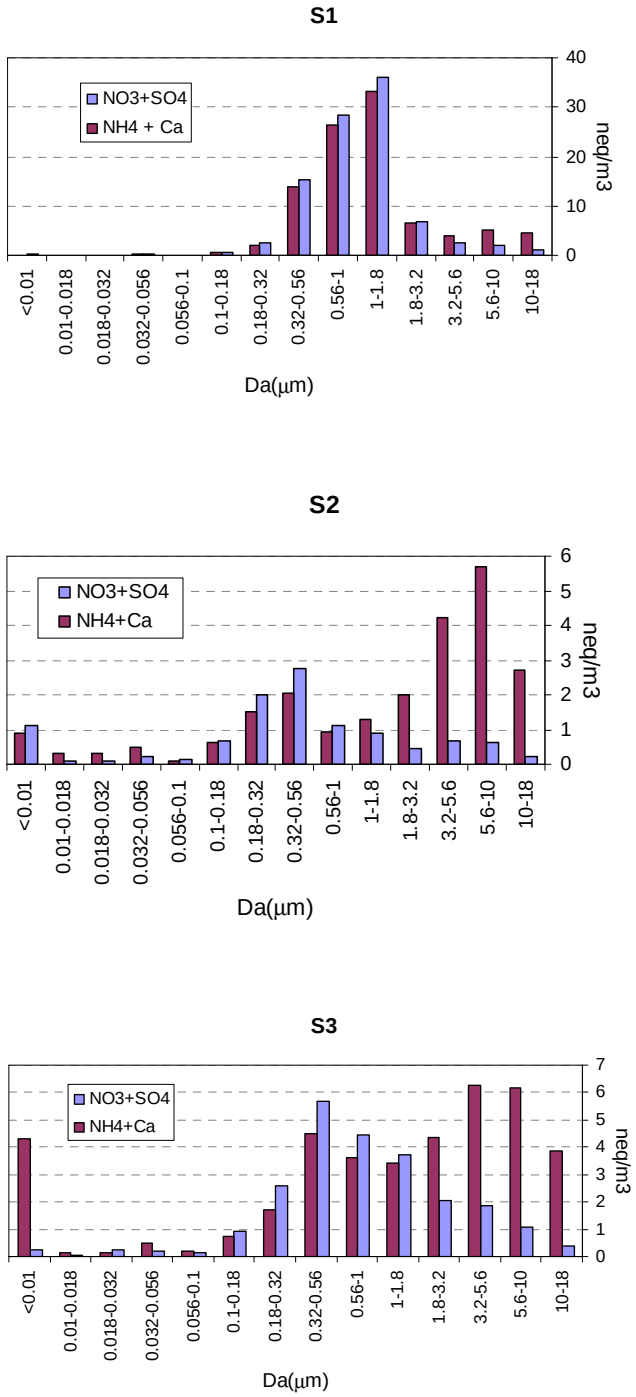

Figure 8.9. Ion balances at Madrid during S1, S2 and S3

Figure 8.9 shows the balances between NO_3^- + SO_4^{2-} and NH_4^+ + Ca^{2+} for the three selected case studies. Again, ammonia in the fine mode and calcium in the coarse mode are the main neutralizing agents. The distributions showed a slight acidity in the

accumulation mode. The percentage of non-neutralised aerosol below 1.8 μm is ~20% in all three cases. This acidity has not been seen in the averaged studies shown before.

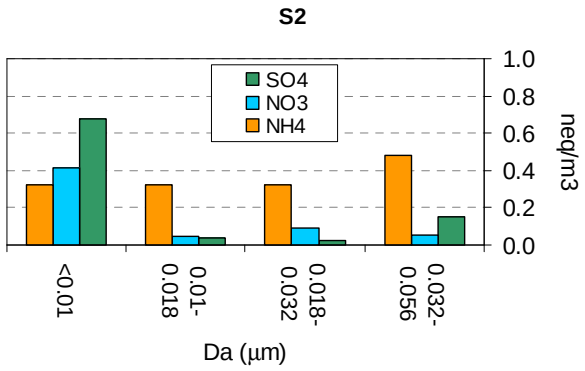

Figure 8.10. Nano-MOUDI ion balances at Madrid during S2

As seen in figure 8.8, nano-MOUDI showed very low sulphate and nitrate concentrations for the episodes of haze and fog. In contrast, for the winter stagnation episode a significant fraction of SIC is present. Ammonium neq exceeds SO_4^{2-} + NO_3^- neq in the range 0.018-0.056 μm, but below 0.010 μm remarkable sulphate and nitrate amounts not neutralised by ammonium appear (figure 8.10). The presence of other inorganic compounds different from ammonium salts -such as calcium nitrate- cannot be dismissed, but the data obtained so far do not allow confirmation. Care must be taken with this result, since studies have shown that the mass collected on Nano-MOUDI stages (<0.40 um) can be contaminated by particle bounce from upper stages (Park K. et al, 2003). In this case the presence of particles below 0.010 μm cannot be confirmed by the comparison with the SMPS, since the detection limit of this instrument is 0.015 μm.

-Temporal evolution-

The temporal evolution of particulate sulphate, nitrate, gaseous SO_2 and meteorological parameters during the three case studies selected is depicted in figure 8.11.

During S1 time series showed production of sulphate and nitrate during day and night, with a similar evolution of both pollutants under relative humidities always above

85%. The decrease in solar radiation on January 17 is a consequence of the present fog. SO_2 fell dramatically coinciding with SIC production, suggesting heterogeneous SO_2 to sulphate oxidation following the reactions (1.2). Gaseous N_2O_5 and HNO_3 measurements are not available, so HNO_3(g) generation on hydrated aerosols (1.5) and absorption of HNO_3(g) by water droplets could not be studied in more detail.

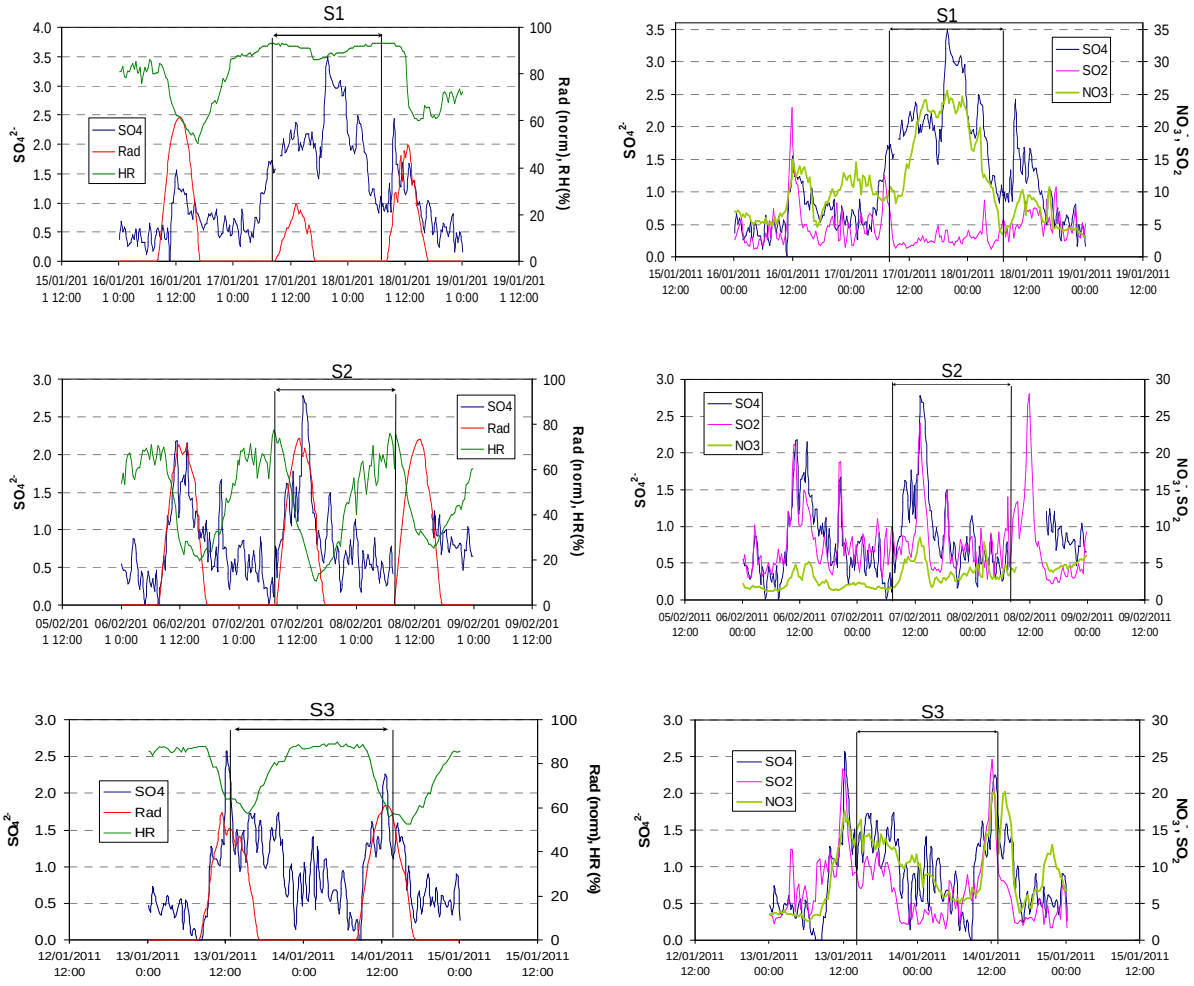

Figure 8.11. Temporal evolution of particulate sulphate, nitrate, gaseous SO_2 and meteorological parameters during S1 (top), S2 (middle) and S3 (bottom)

During S2 time series showed daily SIC and SO_2 increases correlated to solar radiation. As was discussed in previous chapters, nitrate is formed by photochemical production, while SO_2 and sulphate are more dependent on the air mass evolution and thus their short-term increases are more likely related to transport from the city centre. Relative humidity was under 70% most of the time (see Figure 8.11). Previous works have stated hygroscopic secondary aerosol production at RH levels over 70% (Chen et al,

2003), therefore, during S2 RH was likely to be below the threshold to trigger aqueous phase SIC generation.

S3 time evolution parameters suggest both aqueous nocturnal SIC production and diurnal photochemical production (nitrate) and accumulation. Relative humidity was in the range 50% - 90% during this episode.

Ion concentrations were the highest for the fog episode and lowest for the winter stagnation episode. However, the differences in mass measured during the three events were smaller than the differences found for the water-soluble ions sampled with the MOUDI cascade impactor. This is probably related to variations in the detection efficiency of the various types of aerosol with both techniques. Table 8.1 shows a comparison between the nitrate in $PM_{2.5}$ and sulphate in PM_1 measured by the semi-continuous instruments and the cascade impactors and the ratios between both measurements.

NO_3^- in $PM_{2.5}$	R&P NO_3^-	MOUDI	MOUDI/RP NO_3^-
S1	16.76	13.23	**0.79**
S2	4.02	1.32	**0.33**
S3	10.57	2.71	**0.26**

SO_4^{2-} in PM_1	SPA SO_4^{2-}	MOUDI	MOUDI/SPA SO_4^{2-}
S1	2.04	3.67	**1.80**
S2	0.95	0.63	**0.67**
S3	1.07	1.43	**1.34**

Table 8.1. Nitrate in $PM_{2.5}$ and sulphate in PM_1 measured by the semi-continuous instruments and the cascade impactors

Ratios are the highest for the fog event for both compounds. In the case of sulphate, the detection efficiency is even higher for the MOUDI for the haze and fog episodes. This might be related to a reduction in the losses due to bouncing in the MOUDI substrates when the particles are hydrated, which might be also related to the higher concentrations of ions sampled by nano-MOUDI under S2 with respect to S1 and S3. Test results by Chen et al (2011) showed that decreasing RH in general increased particle bounce from uncoated aluminium foils, causing oversampling of $PM_{0.1}$. Particle

bounce did not influence the overall mass distribution of ambient fine particles when RH was in the range 40-80%, whereas it led to undersampling of particles greater than 2.5 μm severely. Particle bounce was found to be negligible, and both $PM_{0.1}$ and $PM_{2.5}$ could be sampled accurately with less than 5% error at a RH range of 75%–80%.

Losses due to evaporation of semivolatile compounds can also account for the differences in ratios for nitrate and sulphate shown in Table 8.1. Intercomparisons performed by Nie et al (2010) between a MOUDI, a Thermo Anderson Chemical Speciation Monitor (RAAS) and a real-time ambient ion monitor (AIM, URG9000B) showed that a MOUDI using aluminium substrates suffered a significant loss of nitrate (50-70%) under summer conditions due to evaporation. In this study some nitrate loss is also expected in spite of the wooden box which protected the instrument against high temperatures.

Semi-continuous instruments are not artefact-free either. Grover et al (2006) evaluated the response of different instruments to both non-volatile and semivolatile material during one month, reporting lower nitrate concentrations measured with a R&P 8400N under conditions of high humidity. Nitrate measured by the 8400N was lower during fog events compared to the other two systems (Dionex ion chromatographic system and integrated PC-BOSS).

Therefore, variations in the detection efficiency of the different compounds with both techniques require careful analysis and further study.

8.4-Conclusions

Mass size segregated ions have been studied in a winter 3-week campaign at a suburban site in Barcelona in the range 18 μm down to <0.056 μm and compared with a previous study at the CIEMAT site in Madrid. This comparison has allowed establishing significant differences in the dominant SIC modes related to aerosol formation and evolution processes.

In Barcelona, lognormal bimodal fits showed accumulation modes around 0.5 μm for sulphate and ammonia and 0.6-0.75 μm for nitrate. This accumulation modal diameter is higher than the one found in Madrid –around 0.35 μm for all three ions. This can be

explained by the presence of a droplet mode in Barcelona due to the higher relative humidity conditions of this coastal city. In contrast, in Madrid the accumulation range only showed the vapour condensation mode. The coarse mode of these ions was in the range 3.5-5.5 μm in both cities. Sulphate and ammonia distributions were dominated by the accumulation mode, although the presence of a coarse mode formed by insoluble mineral sulphates cannot be discarded. However, the coarse mode dominated the nitrate size distribution in Madrid and also in Barcelona at night. This result shows the relevance of the reaction between nitric acid and mineral elements, especially $CaCO_3$, producing $Ca(NO_3)_2$, although neutralisation by marine Na^+ was found in especial cases in Barcelona.

The ion concentrations measured in winter in Madrid were around half of the concentrations measured in Barcelona. Higher SIC concentrations have been detected in Barcelona with respect to Madrid in other studies (Querol et al, 2004c) on an annual basis, but it must be taken into account also that the suburban site in Barcelona has a higher influence of traffic than the one in Madrid.

Balances show fully neutralised acidity in both cities taking into account ammonia in the fine range and ammonia and calcium in the coarse range, except for the particles <0.056 μm. In Madrid the sulphate concentration in this stage was the highest. In Barcelona significant non-neutralised sulphate and nitrate concentration were also found, although concentrations were much smaller than in Madrid.

Additionally, size segregated secondary inorganic aerosol compounds were studied in the Madrid CIEMAT site during three different meteorological scenarios in the range 18 μm down to <0.010 μm: heavy fog (S1), typical winter stagnation (S2) and transition from a clean period to fog (S3).

The highest sulphate and nitrate concentrations were found for S1 in the range 1-1.8 μm. This interval is significantly higher than the range found for S2 (sulphate 0.18-0.56 μm, nitrate 0.32-0.56 μm). Moreover, a significant fraction of nitrate and sulphate below 0.01 μm was found only for S2. Plaza et al (2011) study stated the efficiency of sulphate and nitrate formation by aqueous phase oxidation under a fog event. In the present work this efficiency has been corroborated. The results suggest the aqueous

phase generation in the accumulation mode. A shift of nanometric compounds to the accumulation mode through aggregation and coagulation processes in fog and haze scenarios is also possible. These processes can explain the lower amount of sulphate and nitrate found below 0.056 μm in the Barcelona campaign in comparison with the Madrid winter average, since in Barcelona the higher relative humidity results in a droplet mode not typically seen in Madrid.

Near real-time measurements confirmed the efficiency of aqueous-phase SIC generation over photochemical and transport processes which take place during the typical winter stagnation scenarios. Deviations were found in the mass ratios of nitrate and sulphate for S1, S2 and S3 measured with both techniques. This is probably related to variations in the detection efficiency of the various types of aerosol and requires further study.

9- CONCLUSIONS AND FUTURE WORK

9. CONCLUSIONS AND FUTURE WORK

9.1-Summary of results and conclusions of this work

The aim of this thesis has been to deepen in the knowledge of the inorganic fraction of secondary urban aerosol in the city of Madrid, with special emphasis on particulate nitrate and sulphate measured by semi-continuous techniques. Specific campaigns with sampling equipment were carried out to obtain further information on the size fractions and chemical state in which SIC are found in the aerosol. The data acquired at an urban background site in Madrid (CIEMAT) were compared and contrasted with analogous experimental data in the London region and Barcelona. A compendium of the results obtained is presented below.

First we have summarised the available information on concentrations of precursor gases (NO_2, NOx, SO_2 and NH_3), particulate matter and SIC at representative locations -urban, urban background and rural- of the Madrid air basin in the last decade. In general, concentrations were highest at the urban site and lowest at the rural, showing intermediate values at the urban background site. Different seasonal patterns have been found depending on the pollutant and sampling site.

PM and gases showed descending trends in the last decade except for gaseous NH_3, which kept constant annual values at the rural site. The falls in NOx and PM can be due to various measures to reduce emisions, such as the incorporation of catalytic converters in vehicles. These converters have been proved to lead to outstanding reductions in NOx emissions, but also to generate gaseous ammonia.Drops in SO_2 and particulate sulphate are due to the limitations of S in fuels. The urban site studied in Madrid (Escuelas Aguirre) showed a 40% reduction in SO_2 levels from winter 2008-2009 to winter 2009-2010. On 1 January 2009 the European Directive 2003/17/EC limited sulphur in all vehicle fuels to a maximum of 10 $mg \cdot kg^{-1}$.

- The results are compatible with prevailing nitrate local generation at the urban area of Madrid with seasonal cycles dominated by thermal decomposition.

- Local sources contributed significantly to sulphate levels in winter at the urban site studied; however, the rural background in the air basin is dominated by enhanced photochemical oxidation of SO_2 at summer.

The scarcity of measurements of gaseous NH_3 in comparison with other inorganic pollutants led to a characterisation of ammonia ambient levels and sources in the Madrid atmosphere in 2011. 10-day integrated measurements were obtained in winter and summer using passive samplers.

- Sites close to sewage treatment plants and an incinerator registered the highest ammonia concentrations, followed by traffic sites. The latter showed significantly higher values than the urban background sites in both seasons.
- In Madrid, average ammonia levels were similar to measurements in other European cities and remarkably lower than the levels found in Barcelona on the same year.

An analysis of temporal mean patterns of sulphate, nitrate and precursor gases on annual, weekly and daily timescales has been performed for urban background and rural sites in the Madrid airshed and the London region in the period 2005-2010. This study identifyied similarities and discrepancies that contribute to determine the main processes and relevant parameters in each case.

- The seasonal fine nitrate pattern in Madrid was found to be dominated by temperature-driven evolution. In contrast, the annual nitrate pattern in London showed thermal decomposition in summer, but also a notable maximum from February to April which can be related to pollutant transport from mainland Europe.
- In both cities fine nitrate weekend reductions around 20% were found in summer with statistical significance. In contrast, weekend sulphate reductions in the range 13-18 % were found at both urban background sites in winter.

The daily pattern followed by NOx is similar in both cities; however, nitrate behaviour was very different in winter. In Madrid, low temperatures and the small vertical extent of the mixing layer allowed the dominance of photochemistry in nitrate formation, resulting in a single maximum at noon. High concentrations were registered in an urban background site in London at night-time, explained as a consequence of nitrate

formation under high humidity conditions. In summer, higher temperatures and a greater mixing height resulted in a dominant morning peak associated to the traffic rush hour plus a secondary evening peak. The evening peak has been explained in terms of the contraction of the mixing layer by other researchers, which is consistent with our results.

- The results from both cities indicate that nitrate hourly evolution is predominantly determined by meteorological factors rather than by the evolution of precursor gases.
- In Madrid in winter SO_2 and SO_4^{2-} peaked at noon. The same phenomenon had been observed in London for SO_2.

The data analyses for London complement the process-based work carried out in the REPARTEE experiments. This work shows that behaviour seen in London is not representative of that in Madrid.

- The processes controlling nitrate and sulphate concentrations may vary substantially across Europe. Observations in one city should not be assumed to be applicable elsewhere.

Three types of events which led to high concentrations of particulate sulphate and nitrate at the urban area of Madrid have been characterised. These events are: a regional recirculation episode (E1), transport from Central Europe-Western Mediterranean (E2a –sulphate- and E2b –nitrate and sulphate-) and local accumulation in a winter stagnant anticyclonic situation (E3). These episodes were differentiated using HYSPLIT back-trajectory analysis, data from rural stations and FLEXTRA and NAAPS model results, and daily evolution of pollutants at the CIEMAT site. Since the importance of local emissions has been stated, regional and long range transport has also been found to be relevant for particulate sulphate ambient concentrations at a suburban site at Madrid.

- The highest $PM_{2.5}$ nitrate values (over 20 $\mu g \cdot m^{-3}$) were associated to the local accumulation situation E3, while the maximum concentrations reached under transport episodes E1 and E2b were less than half of that value.

- The highest short-term PM_1 sulphate values registered at the site (7 $\mu g \cdot m^{-3}$) were associated to the pollutant long-range transport E2a. Sulphate concentrations reached 5 and only 3.5 $\mu g \cdot m^{-3}$ during E1 and E3 respectively.

An unusual volcanic event which took place during the course of the measurements carried out at CIEMAT has been also characterised in detail. The eruption of the Icelandic volcano Eyjafjallajökull disrupted the air traffic in Europe during spring 2010. The passage of the volcanic plume was identified in the EMEP network stations. The concentrations of sulphur dioxide and sulphate in PM_{10} and $PM_{2.5}$ reached relative maxima not correlated with other pollutants. The first effects appeared on 4 and 5 May, but they intensified between 7 and 9 May at the centre and south of the Peninsula. Physico-chemical characteristics of the aerosol that reached the CIEMAT site have been presented.

- An estimation of the vertical profiles of mass concentration was calculated from the extinction coefficient profiles, obtaining a maximum value (77±9.6 $\mu g \cdot m^{-3}$) well below the threshold established for safe aircraft operation.
- A large increase in the fine aerosol mode was detected in coincidence with an increase in sulphate concentration, while the coarse mode remained almost unaltered. Volume distributions at ground level indicate particles mainly in the 0.1-0.7 μm size range, in contrast with studies of the plume that affected Central Europe in April, where coarse particles were present.
- Results are consistent with the bimodal size distribution obtained near-source and suggest the growth of the fine mode through condensation and/or coagulation processes and also the removal of the larger ash particles.

Mass size segregated ions in the range 18 μm down to <0.056 μm have been studied in winter at a suburban site in Barcelona and compared with a previous study in Madrid. The ion concentrations measured in winter in Madrid were around half of the concentrations measured in Barcelona.

- In Barcelona, accumulation modes around 0.5 μm for sulphate and ammonia and 0.6-0.75 μm were found for nitrate. In Madrid the accumulation modal diameter was around 0.35 μm for all three ions. This is consistent with the presence of a droplet mode in Barcelona due to higher ambient relative

humidity. In Madrid the accumulation range only showed the vapour condensation mode.

- Ion size distributions were dominated by the accumulation mode in the case of sulphate and ammonia, and by the coarse one (3.5-5.5 μm) in the case of nitrate in Madrid and also in Barcelona at night. This result shows the relevance of the reaction between nitric acid and mineral elements, especially $CaCO_3$, producing $Ca(NO_3)_2$.

- Balances show fully neutralised acidity except for the particles <0.056 μm.

In Madrid the sulphate concentration in the stage below 0.056 μm was the highest. In Barcelona non-neutralised sulphate and nitrate concentration were also found in the same stage, although concentrations were much smaller. To get a deeper insight into this problem size segregated secondary inorganic aerosol compounds were studied in Madrid during three different meteorological winter scenarios in the range 18 μm down to <0.010 μm: heavy fog (S1), typical winter stagnation (S2, which coincides with E3) and transition from a clean period to fog (S3).

- The highest sulphate and nitrate concentrations were found for S1 in the range 1-1.8 μm (droplet mode). This interval is significantly higher than the range found for S2 (sulphate 0.18-0.56 μm, nitrate 0.32-0.56 μm).

- A significant fraction of nitrate and sulphate below 0.01 μm was found only for S2.

The results suggest the aqueous phase generation in the droplet mode, but a shift of nanometric compounds to the accumulation mode through aggregation and coagulation processes in high ambient humidity scenarios is also possible. These processes can also explain the lower amount of sulphate and nitrate found below 0.056 μm in Barcelona.

Semi-continuous measurements confirmed the efficiency of aqueous-phase SIC generation over photochemical and transport processes which take place during the typical winter stagnation scenarios. Deviations were found in the mass ratios of nitrate and sulphate for S1, S2 and S3 measured with both techniques. This is probably related to variations in the detection efficiency of the various types of aerosol.

9.2- Future research and open questions

This thesis has involved a deep study of the behaviour of secondary inorganic aerosol compounds in the region of Madrid. The semi-continuous techniques have allowed the study of features which were concealed in previous works. However, there are still unresolved problems.

In the Madrid air basin the measurements of some gaseous precursors (NOx and SO_2) are abundant, but existing information on ammonia is insufficient, especially in the urban area of Madrid. The campaign carried out made a first step in this direction, but further studies covering larger time periods are needed. Semi-continuous measurements of this compound would allow a better characterization of the traffic source, since it would enable the analysis of correlations with primary pollutants emitted by vehicles.

The interpretation of the diurnal evolution of secondary compounds has proven to be complex. In literature, morning and evening peaks in urban areas are related to the traffic rush hours and changes in the height of the boundary layer. In contrast, the occurrence of maxima at noon-afternoon has been explained in different ways in several sites in the US. In the case of nitrate, Park et al (2005) and Rattigan et al (2006) interpreted that they were driven by local photochemical production and Wittig et al (2004) explained the same for sulphate. In contrast, Chow et al (2008) attributed them to a combination of local photochemical production in urban areas and nighttime transport followed by daytime vertical mixing. Recently, Doraiswamy et al (2010) found discrepancies between model forecasts and near real-time fine nitrate and sulphate. Underpredictions of sulphate concentrations at urban sites at noon were attributed to the underprediction of secondary formation due to sensitiveness to cloud properties, which influence water-phase production. In the case of Madrid, the evolution patterns found can be explained in terms of photochemical formation but taking into account the diurnal transport pattern prevailing in the air basin. The comparison of hourly evolution of precursors together with secondary compounds in two different cities highlighted the difficulties of this study.

Semi-continuous measurements allowed differentiating local events from transport events, since only in the former case a clear daily pattern is seen. Quantification of the amount of nitrate and sulphate which is attributable to each

type of episode remains open, and especially to long-range transport of fine nitrate. The results shown indicate that the airborne nitrate contribution is less relevant than for sulphate, but noticeable.

This work has provided advances in the study of the nanometric fraction of inorganic aerosols present in the urban atmosphere of Madrid. Different mass contributions of every ion to each size fraction in the nanometric range has been found when dry and hydrated aerosols are present. To obtain conclusive results further research is needed, determining the response of the technique employed (cascade impactors) to different types of aerosol.

9.3-Scientific publications

THIS THESIS LED TO THE FOLLOWING PUBLICATIONS:

-Scientific Papers-

• **Revuelta, M. A.**, R. M. Harrison, L. Núñez, F. J. Gómez-Moreno, M. Pujadas, B. Artíñano. Comparison of temporal features of sulphate and nitrate at urban and rural sites in Spain and the UK. Atmospheric Environment 60, December 2012, p 383-91.

• **Revuelta, M. A.**, M. Sastre, A. J. Fernández, L. Martín, R. García, F. J. Gómez-Moreno, B. Artíñano, M. Pujadas, F. Molero. Characterization of the Eyjafjallajökull volcanic plume over the Iberian Peninsula by lidar remote sensing and ground-level data collection. Atmospheric Environment 48, March 2012, p 46-55.

-In preparation-

• Secondary inorganic aerosol behavior in urban and rural background sites during the DAURE campaign.

-Other scientific papers-

• Jorba, O., M. Pandolfi, M. Spada, J. M. Baldasano, J. Pey, A. Alastuey, D. Arnold, M. Sicard, B. Artíñano, **M. A. Revuelta**, X. Querol. The DAURE field campaign: meteorological overview. Atmos. Chem. Phys. Discuss., 11, 4953-5001, 2011

-Conference proceedings-

• **Revuelta, M. A.**, R. M. Harrison, L. Núñez, F. J. Gómez-Moreno, M. Pujadas, B. Artíñano. Patrones de evolución de contaminantes atmosféricos en diferentes emplazamientos de España y el Reino Unido. XXXII Jornadas Científicas de la

Asociación Meteorológica Española, Museo de la Ciencia COSMOCAIXA, Alcobendas, Madrid (2012). ISBN: 978-84-695-6430-1

• **Revuelta, M. A.**, F. J. Gómez-Moreno, L. Núñez, P. Salvador, F. Molero, B. Artíñano. Temporal analysis and characterization of events of fine particulate sulphate in Madrid. V Reunión Española de Ciencia y Tecnología de Aerosoles (2011). ISBN: 978-84-7834-662-2

• Artíñano, B., **M. A. Revuelta**, J. Plaza, E. Coz, F. J. Gómez-Moreno, M. Pujadas. Experimental Characterization of Aerosol Properties during the DAURE 2009 Campaigns. IV Reunión Española de Ciencia y Tecnología de Aerosoles (2010). ISBN: 978-84-693-4839-0

OTHER PUBLICATIONS OF THE AUTHOR NOT INCLUDED IN THIS THESIS**:**

-Scientific papers-

• Fernández-Gálvez, J., J. L. Guerrero-Rascado, F. Molero, H. Lyamani, **M. A. Revuelta**, F. Navas-Guzmán, M. Sastre, J. A. Bravo-Aranda, A. J. Fernández, M. J. Granados-Muñoz, F. J. Gómez-Moreno, F. J. Olmo, M. Pujadas, L. Alados-Arboledas. Aerosol size distribution from inversion of solar radiances and measured at ground-level during SPALI10 campaign. Atmospheric Research. In press. doi: 10.1016/j.atmosres.2012.03.015

-Conference proceedings-

• Mirante, F., C. Alves, C. Pio, **M. A. Revuelta**, B. Artiñano. Chemical characterisation and source mass balance of roadside aerosol from Madrid in summer. V Reunión Española de Ciencia y Tecnología de Aerosoles (2011). ISBN: 978-84-7834-662-2

• **Revuelta, M. A**., G. McIntosh, J. Pey, M. L. Osete. Environmental Magnetic Proxies In The Field Of Atmospheric Aerosol. III Reunión Española de Ciencia y Tecnología de Aerosoles (2009).

REFERENCES

REFERENCES

Abdalmogith, S. S., Harrison, R. M. (2005). "The use of trajectory cluster analysis to examine the long-range transport of secondary inorganic aerosol in the UK." Atmospheric Environment 39(35): 6686-6695.

Adachi, K., Buseck, P. R. (2008). Internally mixed soot, sulfate, and organic matter in aerosol particles from Mexico City. Atmospheric Chemistry and Physics 8, 6469-6481.

Al-Horr, R., Samanta, G., and Dasgupta, P. K. (2003). A Continuous Analyzer for Soluble Anionic Constituents and Ammonium in Atmospheric Particulate Matter, Environ. Sci. Technol. 37:5711–20.

Allen, A. G., Oppenheimer, C., Ferm, M., Baxter, P. J., Horrocks, L. A., Galle, B., McGonigle, A. J. S., Duffell, H. J. (2002). Primary sulfate aerosol and associated emissions from Masaya Volcano, Nicaragua. Journal of Geophysical Research-Atmospheres 107(D23).

Anatolaki, Ch, Tsitouridou, R. (2007). Atmospheric deposition of nitrogen, sulfur and chloride in Thessaloniki, Greece. Atmospheric Research 85, 413-428.

Ansmann, A., J. Bosenberg, A. Chaikovsky, A. Comeron, S. Eckhardt, R. Eixmann, V. Freudenthaler, P. Ginoux, L. Komguem, H. Linne, M. A. L. Marquez, V. Matthias, I. Mattis, V. Mitev, D. Muller, S. Music, S. Nickovic, J. Pelon, L. Sauvage, P. Sobolewsky, M. K. Srivastava, A. Stohl, O. Torres, G. Vaughan, U. Wandinger, and M. Wiegner. (2003). "Long-Range Transport of Saharan Dust to Northern Europe: The 11-16 October 2001 Outbreak Observed with Earlinet." Journal of Geophysical Research-Atmospheres 108, no. D24.

Ansmann, A., Tesche, M., Groß, S., Freudenthaler, V., Seifert, P., Hiebsch, A., Schmidt, J., Wandinger, U., Mattis, I., Müller, D., and Wiegner, M. (2010). The 16 April 2010 major volcanic ash plume over central Europe: EARLINET lidar and AERONET photometer observations at Leipzig and Munich, Germany, Geophys. Res. Lett., 3.

Artíñano, B., M. A. Revuelta, J. Plaza, E. Coz, F. J. Gómez-Moreno, M. Pujadas. Experimental Characterization of Aerosol Properties during the DAURE 2009 Campaigns. IV Reunión Española de Ciencia y Tecnología de Aerosoles (2010). ISBN: 978-84-693-4839-0.

Artíñano, B., Salvador, P., Alonso, D. G., Querol, X., Alastuey, A. (2003). "Anthropogenic and Natural Influence on the PM10 and PM2.5 Aerosol in Madrid (Spain). Analysis of High Concentration Episodes." Environmental Pollution 125, no. 3: 453-65.

Artíñano, B., P. Salvador, D. G. Alonso, X. Querol, and A. Alastuey (2004). "Influence of Traffic on the PM10 and PM2.5 Urban Aerosol Fractions in Madrid (Spain)." Science of the Total Environment 334: 111-23.

ATLAS CLIMÁTICO IBÉRICO. Agencia Estatal de Meteorología (AEMET) (2011). ISBN: 978-84-7837-079-5.

Ayuntamiento de Madrid. Ordenanza General de Protección del Medio Ambiente Urbano ANM 1985\3 (2009). Boletín Oficial del Ayuntamiento de Madrid n. 6033.

Baker, J (2010). "A Cluster Analysis of Long Range Air Transport Pathways and Associated Pollutant Concentrations within the UK." Atmospheric Environment 44, no. 4: 563-71.

Baldasano, J. M., L. P. Guereca, E. Lopez, S. Gasso, and P. Jimenez-Guerrero (2008). "Development of a High-Resolution (1 Km X 1 Km, 1 H) Emission Model for Spain: The High-Elective Resolution Modelling Emission System (Hermes)." Atmospheric Environment 42, no. 31: 7215-33.

Bampardimos, I., Nufer, M., Oderbolz, D. C., Keller, J., Aksoyoglu, S., Hueglin, C., Baltensperger, U., Prévôt, A. S. H. (2011). "The weekly cycle of ambient concentrations and traffic emissions of coarse (PM10–PM2.5) atmospheric particles." Atmospheric Environment 45(27): 4580-4590.

Bari, A., Ferraro, V., Wilson, L. R., Luttinger, D., Husain, L. (2003). "Measurements of gaseous HONO, HNO3, SO2, HCl, NH3, particulate sulfate and PM2.5 in New York, NY." Atmospheric Environment 37(20): 2825-2835.

Barlow, J. F., Dunbar, T. M., Nemitz, E. G., Wood, C. R., Gallagher, M. W., Davies, F., O'Connor, E., Harrison, R. M. (2011). "Boundary layer dynamics over London, UK, as observed using Doppler lidar during REPARTEE-II." Atmospheric Chemistry and Physics 11(5): 2111-2125.

Benton, A. K., Langridge, J. M., Ball, S. M., Bloss, W. J., Dall'Osto, M., Nemitz, E., Harrison, R. M., Jones R. L. (2010). "Night-time Chemistry above London: Measurements of NO3 and N2O5 from the BT Tower during REPARTEE-II." Atmospheric Chemistry & Physics 10: 9781-9795.

Berndt, T., F. Stratmann, S. Brasel, J. Heintzenberg, A. Laaksonen, and M. Kulmala. (2008) "SO2 Oxidation Products Other Than H2SO4 as a Trigger of New Particle Formation. Part 1: Laboratory Investigations". Atmospheric Chemistry and Physics 8, no. 21: 6365-74.

Bertram, T. H., and J. A. Thornton (2009). "Toward a General Parameterization of N2o5 Reactivity on Aqueous Particles: The Competing Effects of Particle Liquid Water, Nitrate and Chloride." Atmospheric Chemistry and Physics 9, no. 21: 8351-63.

Bigi, A., Harrison, R. M. (2010). "Analysis of the air pollution climate at a central urban background site." Atmospheric Environment 44(16): 2004-2012.

Bobbink, R., M. Hornung, and J. G. M. Roelofs (1998). "The Effects of Air-Borne Nitrogen Pollutants on Species Diversity in Natural and Semi-Natural European Vegetation." Journal of Ecology 86, no. 5: 717-38.

Bodhaine, B. A., Wood, N. B., Dutton, E. G., Slusser, J. R. (1999). On Rayleigh optical depth calculations. Journal of Atmospheric and Oceanic Technology 16(11): 1854-1861.

Borge, R., Lumbreras, J., Vardoulakis, S., Kassomenos, P., Rodríguez, E. (2007). "Analysis of long-range transport influences on urban PM10 using two-stage atmospheric trajectory clusters." Atmospheric Environment 41(21): 4434-4450.

Bösenberg, J., A. Ansmann, J.M. Baldasano, D. Balis, Ch. Böckmann, B. Calpini, A. Chaikovsky, P. Flamant, A. Hagard, V. Mitev, A. Papayannis, J. Pelon, D. Resendes, J. Schneider, N. Spinelli, Th. Trickl, G. Vaughan, G. Visconti, M. Wiegner (2001). EARLINET: A European Aerosol Research Lidar Network, in A. Dabas, C. Loth, and J. Pelon (eds.), Advances in Laser Remote Sensing, pp. 155–158. ISBN 2-7302-0798-8

Bouwman, A. F., D. S. Lee, W. A. H. Asman, F. J. Dentener, K. W. Van Der Hoek, and J. G. J. Olivier (1997). "A Global High-Resolution Emission Inventory for Ammonia." Global Biogeochem. Cycles 11, no. 4 : 561-87.

Brown, S.S., Stark, H., Ryerson, T.B., Williams, E.J., Nicks, D.K., Trainer, M., Fehsenfeld, F.C., Ravishankara, A.R. (2003). Nitrogen oxides in the nocturnal boundary layer: simultaneous in situ measurements of NO3, N2O5, NO2, NO and O3. Journal of Geophysical Research 108, D9.

Builtjes, P. J. H. (1992). The LOTOS – Long Term Ozone Simulation – project, Summary report, TNO-report, TNO-MW-R92/240.

Cabada J.C., Rees, S., Takahama, S., Khlystov, A., Pandis, S.N., Davidson, C.I., Robinson, A.L. (2004). Mass size distributions and size resolved chemical composition of fine particulate matter at the Pittsburgh supersite. Atmospheric Environment 38, 3127-3141.

Cachier, Helene, Marie-Pierre Bremond, and Patrick Buat-Menard (1989). "Determination of Atmospheric Soot Carbon with a Simple Thermal Method." Tellus Series B-Chemical and Physical Meteorology 41, no. 3: 379-90.

Carbone, C., Decesari, S., Mircea, M., Giulianelli, L., Finessi, E., Rinaldi, M., Fuzzi, S., Marinoni, A., Duchi, R., Perrino, C., Sargolini, T., Vardè, M., Sprovieri, F., Gobbi, G.P., Angelini, F., Facchini, M.C. (2010). Size-resolved aerosol chemical composition over the Italian Peninsula during typical summer and winter conditions. Atmospheric Environment 44, 5269-5278.

Carslaw D.C., Beevers S.D., Tate J.E., Westmoreland E.J., Williams M.L. (2011). Recent evidence concerning higher NOx emissions from passenger cars and light duty vehicles. Atmospheric Environment, 45, 7053-7063.

Carslaw, D. C., Carslaw, N. (2007). Detecting and characterising small changes in urban nitrogen dioxide concentrations. Atmospheric Environment 41 (22), 4723–4733. 181.

Carslaw, David C., and Karl Ropkins. (2012). "Openair - an R Package for Air Quality Data Analysis." Environmental Modelling & Software 27-28, no. 0: 52-61.

Chang, M.C., Kim, S., Sioutas, C. (1999). Experimental studies on particle impaction and bounce: effects of substrate design and material. Atmospheric Environment 33, 2313-2322.

Charlson, R. J., Vanderpo.Ah, D. S. Covert, A. P. Waggoner, and N. C. Ahlquist (1974). "Sulfuric Acid Ammonium Sulfate Aerosol - Optical Detection in St-Louis Region." Science 184, no. 4133: 156-58.

Chen, Lu-Yen, Jeng, Fu-Tien, Chen, Chih-Chieh, Hsiao, Ta-Chih (2003). Hygroscopic behavior of atmospheric aerosol in Taipei. Atmospheric Environment 37(15): 2069-2075.

Chow, Judith C., Prakash Doraiswamy, John. G. Watson, L.-W. Antony Chen, Steven Sai Hang Ho, David A. Sodeman (2008). Advances in Integrated and Continuous Measurements for Particle Mass and Chemical Composition, Journal of the Air & Waste Management Association, 58:2, 141-163.

Christensen, J. H. (1997). The Danish eulerian hemispheric model - A three-dimensional air pollution model used for the Arctic. Atm. Env., 31, 4169-4191.

Clarisse, L., C. Clerbaux, F. Dentener, D. Hurtmans, and P. F. Coheur (2009). "Global Ammonia Distribution Derived from Infrared Satellite Observations." Nature Geoscience. Nature Geoscience 2, 479 – 483.

Colette, A., O. Favez, F. Meleux, L. Chiappini, M. Haeffelin, Y. Morille, L. Malherbe, A. Papin, B. Bessagnet, L. Menut, E. Leoz, and L. Rouil (2010). "Assessing in near Real Time the Impact of the April 2010 Eyjafjallajökull Ash Plume on Air Quality." Atmospheric Environment 45, no. 5: 1217-21.

Collins, W. J., S. Sitch, and O. Boucher (2010). How vegetation impacts affect climate metrics for ozone precursors. Journal of Geophysical Research-Atmospheres, 115.

Coltelli, M.; Patanè, D.; Aiuppa, A.; Aliotta, M.; Aloisi, M.; Behncke, B.; Cannata, A.; Cannavò, F.; Di Grazia, G.; Gambino, S.; Gurrieri, S.; Mattia, M.; Montalto, P.; Prestifilippo, M.; Puglisi, G.; Salerno, G.; Scandura, D. (2012). Insight into eruptive cyclic behavior of Mount Etna during 2011: geophysical and

geochemical constraints. EGU General Assembly 2012, held 22-27 April, 2012 in Vienna, Austria, p.1992.

Coz , E., F. J. Gómez-Moreno, G. S. Casuccio, and B. Artíñano (2010), Variations on morphology and elemental composition of mineral dust particles from local, regional, and long-range transport meteorological scenarios, J. Geophys. Res., 115, D12204.

Coz, E., F. J. Gomez-Moreno, M. Pujadas, G. S. Casuccio, T. L. Lersch, and B. Artíñano (2009). "Individual Particle Characteristics of North African Dust under Different Long-Range Transport Scenarios." Atmospheric Environment 43, no. 11: 1850-63.

Crespi, S. N., Artíñano, B., Cabal, H. (1995). "Synoptic classification of the mixed-layer height evolution." Journal of Applied Meteorology 34(7): 1666-1677.

Cziczo, D. J., J. B. Nowak, J. H. Hu, and J. P. D. Abbatt (1997), Infrared spectroscopy of model tropospheric aerosols as a function of relative humidity: Observation of deliquescence and crystallization, J. Geophys. Res., 102(D15), 18,843–18,850.

Dall'Osto, M., Harrison, R. M., Coe, H., Williams, P. I., Allan, J. D. (2009). "Real time Chemical characterization of local and regional nitrate aerosols." Atmospheric Chemistry & Phyics 9: 3709-3720.

Donaldson, D. J. (1999). "Adsorption of Atmospheric Gases at the Air-Water Interface. I. Nh3." Journal of Physical Chemistry A 103, no. 1: 62-70.

Draxler, R.R. and Hess, G.D. (1998). Description of the hysplit_4 modeling system. NOAA Tech. Memo, ERLARL-224, 24 pp.

Duce, R. A., C. K. Unni, B. J. Ray, J. M. Prospero, and J. T. Merrill (1980). "Long-Range Atmospheric Transport of Soil Dust from Asia to the Tropical North Pacific - Temporal Variability." Science 209, no. 4464: 1522-24.

Dusek, U., G. P. Frank, L. Hildebrandt, J. Curtius, J. Schneider, S. Walter, D. Chand, F. Drewnick, S. Hings, D. Jung, S. Borrmann, and M. O. Andreae (2006). "Size Matters More Than Chemistry for Cloud-Nucleating Ability of Aerosol Particles." Science 312, no. 5778: 1375-78.

Dzubay, T. G., R. K. Stevens, and L. W. Richards (1967). "Composition of Aerosols over Los Angeles Freeways." Atmospheric Environment 13, no. 5 (1979): 653-59.

EU Directive 2003/17/EC of the European Parliament and of the Council (2003) amending Directive 98/70/EC relating to the quality of petrol and diesel fuels. Official Journal of the European Union, L 76.

EU Directive 2008/50/EC of the European Parliament and of The Council (2008) on ambient air quality and cleaner air for Europe. Official Journal of the European Union, L 152/1.

EU Directive 96/62/CE of the European Parliament and of The Council (1996) on ambient air quality assessment and management. Official Journal of the European Union, L 296/55.

European Environment Agency (1999). "Criteria for EUROAIRNET. The EEA Air Quality Monitoring and Information Network". Technical Report No. 12.

European Environment Agency (2012). Air quality in Europe. EEA Technical report nº 4/2012.

European Environment Agency: European Union emission inventory report 1990–2009 under the UNECE Convention on Long-range Transboundary Air Pollution (LRTAP, 2011). EEA Technical report 9.

European Standard EN 12341 (1999). Air Quality – Determination of the PM10 fraction of suspended particulate matter – Reference method and field test procedure to demonstrate reference equivalence of measurement methods.

European Standard EN14907 (2005). Ambient air quality - Standard gravimetric measurement method for the determination of the PM2,5 mass fraction of suspended particulate matter.

Feng, Y., and J. Penner. (2007). Global modeling of nitrate and ammonium: Interaction of aerosols and tropospheric chemistry. J. Geophys. Res., 112(D01304).

Fernández-Gálvez, J., J. L. Guerrero-Rascado, F. Molero, H. Lyamani, M. A. Revuelta, F. Navas-Guzmán, M. Sastre, J. A. Bravo-Aranda, A. J. Fernández, M. J. Granados-Muñoz, F. J. Gómez-Moreno, F. J. Olmo, M. Pujadas, and L. Alados-Arboledas. "Aerosol Size Distribution from Inversion of Solar Radiances and Measured at Ground-Level During Spali10 Campaign." Atmospheric Research, in press.

Flentje, H., Claude, H., Elste, T., Gilge, S., Kohler, U., Plass-Dulmer, C., Steinbrecht, W., Thomas, W., Werner, A., Fricke, W. (2010). The Eyjafjallajokull eruption in April 2010-detection of volcanic plume using in-situ measurements, ozone sondes and lidar-ceilometer profiles. Atmospheric Chemistry and Physics 10(20): 10085-10092.

Galloway, J. N., F. J. Dentener, D. G. Capone, E. W. Boyer and R. W. Howarth (2004). Nitrogen Cycles: Past, Present, and Future. Biogeochemistry, Volume 70, Number 2, Pages 153-226.

Gangoiti, G., M. M. Millan, R. Salvador, E. Mantilla (2001). Long-range transport and re-circulation of pollutants in the western Mediterranean during the project Regional Cycles of Air Pollution in the West-Central Mediterranean Area. Atmospheric Environment 35, 6267.

Gebauer, G., A. Giesemann, E. D. Schulze, and H. J. Jager (1994). "Isotope Ratios and Concentrations of Sulfur and Nitrogen in Needles and Soils of Picea-Abies

Stands as Influenced by Atmospheric Deposition of Sulfur and Nitrogen-Compounds." Plant and Soil 164, no. 2: 267-81.

Gómez-Moreno, F. J., M. Pujadas, J. Plaza, J. J. Rodríguez-Maroto, P. Martínez-Lozano, and B. Artíñano (2011). "Influence of Seasonal Factors on the Atmospheric Particle Number Concentration and Size Distribution in Madrid." Atmospheric Environment 45, no. 18: 3169-80.

Gomez-Moreno, F. J., Nunez, L., Plaza, J., Alonso, D., Pujadas, M., Artíñano, B. (2007). Annual evolution and generation mechanisms of particulate nitrate in Madrid. Atmospheric Environment 41(2): 394-406.

Grabke, H. J., E. Reese, and M. Spiegel (1995). "The Effects of Chlorides, Hydrogen-Chloride, and Sulfur-Dioxide in the Oxidation of Steels Below Deposits." Corrosion Science 37, no. 7: 1023-43.

Grimm, H. and D. J. Eatough (2009). Aerosol Measurement: The Use of Optical Light Scattering for the Determination of Particulate Size Distribution, and Particulate Mass, Including the Semi-Volatile Fraction. Journal of the Air & Waste Management Association 59(1): 101-107.

Grover, Brett D., Norman L. Eatough, Delbert J. Eatough, Judith C. Chow, John G. Watson, Jeffrey L. Ambs, Michael B. Meyer, Philip K. Hopke, Rida Al-Horr, Douglas W. Later, William E. Wilson (2006). Measurement of both Non-volatile and Semi-Volatile Fractions of Fine Particulate Matter in Fresno, CA, Aerosol Science and Technology, 40:10, 811-826.

Hameri, K., M. Vakeva, H. C. Hansson, A. Laaksonen (2000). "Hygroscopic Growth of Ultrafine Ammonium Sulphate Aerosol Measured Using an Ultrafine Tandem Differential Mobility Analyzer." Journal of Geophysical Research-Atmospheres 105, no. D17: 22231-42.

Harrison, D., S.S. Park, J. Ondov, T. Buckley, S.R. Kim, R.K.M. Jayanty (2004). Highly time resolved fine particulate nitrate measurements at the Baltimore supersite. Atmospheric Environment 38, pp. 5321–5332.

Harrison, R. M., and C. A. Pio (1983). "Major Ion Composition and Chemical Associations of Inorganic Atmospheric Aerosols." Environmental Science & Technology 17, no. 3: 169-74.

Harrison, R. M., J. Stedman, and D. Derwent (2008). "New Directions: Why Are PM10 Concentrations in Europe Not Falling?" Atmospheric Environment 42, no. 3: 603-606.

Harrison, R. M., and M. Jones (1995). "The Chemical-Composition of Airborne Particles in the Uk Atmosphere." Science of the Total Environment 168, no. 3: 195-214.

Harrison, R. M., Laxen, D., Moorcroft, S., Kieran, L. (2012a). "Processes affecting concentrations of fine particulate matter (PM2.5) in the UK atmosphere." Atmospheric Environment 46: 115-124.

Harrison, R. M., Dall'Osto, M., Beddows, D. C. S., Thorpe, A. J., Bloss, W. J., Allan, J. D., Coe, H., Dorsey, J. R., Gallagher, M., Martin, C., Whitehead, J., Williams, P. I., Jones, R. L., Langridge, J. M., Benton, A. K., Ball, S. M., Langford, B., Hewitt, C. N., Davison, B., Martin, D., Petersson, K. F., Henshaw, S. J., White, I. R., Shallcross, D. E., Barlow, J. F., Dunbar, T., Davies, F., Nemitz, E., Phillips, G. J., Helfter, C., Di Marco, C. F., Smith, S. (2012b). Atmospheric chemistry and physics in the atmosphere of a developed megacity (London): an overview of the REPARTEE experiment and its conclusions, Atmos. Chem. Phys., 12, 3065-3114.

Harrison, R.M., R.E. van Grieken (eds). Atmospheric Particles Wiley, Chichester (1998) 610 pp.

Harrison, Roy M., and Casimiro A. Pio (1967). "Size-Differentiated Composition of Inorganic Atmospheric Aerosols of Both Marine and Polluted Continental Origin." Atmospheric Environment 17, no. 9 (1983): 1733-38.

Heffter, J.L. and Taylor, A.D. (1975) Trajectory model – Part I. A regional-continental scale transport, diffusion, and deposition model. NOAA Tech. Memo, ERL-ARL-50, 28 pp.

Hering, S. V., Stolzenburg, M. R., Hand, J. L., Kreidenweis, S. M., Lee, T., Collett, J. L., Jr., Dietrich, D., and Tigges, M. (2003). Hourly Concentrations and Light Scattering Cross Sections for Fine Particle Sulphate at Big Bend National Park, Atmos. Environ. 37:1175–1183.

Hess, M., Koepke, P., Schult, I. (1998). Optical properties of aerosols and clouds: The software package OPAC. Bulletin of the American Meteorological Society 79(5): 831-844.

Hinds, W. C., (1982). Aerosol Technology. Properties, Behaviour and Measurement of Airborne Particles, in: John Wiley and Sons (Eds.), Wiley Interscience, pp. 91-100.

Hogan, T. F., L. R. Brody (1993). Sensitivity studies of the Navy's global forecast model parameterizations and evaluation of improvements to NOGAPS. Mon. Wea. Rev., 121, 2373-2395.

Hogan, T. F., T. E. Rosmond (1991). The description of the Navy operational global atmospheric prediction system's spectral forecast model. Mon. Wea. Rev., 119, 1786-1815.

Hogrefe, O., F. Drewnick, G.G. Lala, J.J. Schwab, K.L. Demerjian (2004). Development, operation and applications of an aerosol generation, calibration and research facility. Aerosol Science and Technology, 38, pp. 196–214.

Hsieh, L. Y., Kuo, S. C., Chen, C. L., Tsai, Y. I. (2009). Size distributions of nano/micron dicarboxylic acids and inorganic ions in suburban PM episode and non-episodic aerosol, Atmos. Environ., 43(29), 4396–4406.

Hudson, J. G., X. Y. Da (1996) "Volatility and Size of Cloud Condensation Nuclei." Journal of Geophysical Research-Atmospheres 101, no. D2: 4435-42.

Ilyinskaya, E., Oppenheimer, C., Mather, T. A., Martin, R. S., Kyle, P. R. (2010). Size-resolved chemical composition of aerosol emitted by Erebus volcano, Antarctica. Geochemistry Geophysics Geosystems 11: 14.

Ilyinskaya, E., V. I. Tsanev, R. S. Martin, C. Oppenheimer, J. Le Blond, G. M. Sawyer, and M. T. Gudmundsson (2011). "Near-Source Observations of Aerosol Size Distributions in the Eruptive Plumes from Eyjafjallajökull Volcano, March-April 2010". Atmospheric Environment 45, no. 18: 3210-16.

IDAEA-CSIC, CIEMAT, Instituto de Salud Carlos III (2012). Niveles, Composición y fuentes de PM10, PM2.5 y PM1 en España: Aragón, Asturias, Castilla la Mancha y Madrid. Ministerio de Medio Ambiente y Medio Rural y Marino. S.D.G. de Calidad del Aire y Medio Ambiente Industrial. In preparation.

IPCC, 2001: Climate Change 2001: The Scientific Basis Contribution of Working Group I to the Third Assessment Report of the Intergovernmental Panel on Climate Change (IPCC), J. T. Houghton, Y. Ding, D.J. Griggs, M. Noguer, P. J. van der Linden and D. Xiaosu (Eds.), Cambridge University Press, UK, pp. 944.

IPCC, 2007: Climate Change 2007: Synthesis Report. Contribution of Working Groups I, II and III to the Fourth Assessment Report of the Intergovernmental Panel on Climate Change [Core Writing Team, Pachauri, R.K and Reisinger, A.(eds.)]. IPCC, Geneva, Switzerland, 104 pp.

Izquierdo, R, A. Avila, M. Alarcón (2012). Trajectory statistical analysis of atmospheric transport patterns and trends in precipitation chemistry of a rural site in NE Spain in 1984-2009. Atmospheric Environment 61, pp. 400-408.

Jacobson, M. C., H. C. Hansson, K. J. Noone, R. J. Charlson (2000), Organic atmospheric aerosols: Review and state of the science, Rev. Geophys., 38(2), 267–294, doi:10.1029/1998RG000045.

Jaecnike, R. (2005). Abundance of cellular material and proteins in the Atmosphere, Science, 308, 73.

Jayne, J. T., Leard, D. C., Zhang, X., Davidovits, P., Smith, K. A.,Kolb, C. E., and Worsnop, D. R. (2000). Development of an Aerosol Mass Spectrometer for Size and Composition Analysis of Submicron Particles, Aerosol Sci. Technol. 33:49–70.

John,W., Wall, S.M., Ondo, J.L., Winklmavr,W. (1990). Models in the size distributions of atmospheric inorganic aerosol. Atmospheric Environment 24A, 2349-2359.

Jones, A. M., Harrison, R. M. (2011). "Temporal trends in sulphate concentrations at European sites and relationships to sulphur dioxide." Atmospheric Environment 45(4): 873-882.

Jones, A. M., R. M. Harrison, B. Barratt, and G. Fuller (2012). "A Large Reduction in Airborne Particle Number Concentrations at the Time of the Introduction Of " Sulphur Free" Diesel and the London Low Emission Zone." Atmospheric Environment 50: 129-38.

Jones, A. M., Yin, J., Harrison, R. M. (2008). "The weekday–weekend difference and the estimation of the non-vehicle contributions to the urban increment of airborne particulate matter." Atmospheric Environment 42(19): 4467-4479.

Jorba, O., Pandolfi, M., Spada, M., Baldasano, J. M., Pey, J., Alastuey, A., Arnold, D., Sicard, M., Artiñano, B., Revuelta, M. A., Querol, X. (2011). The DAURE field campaign: meteorological overview. Atmos. Chem. Phys. Discuss., 11, 4953-5001.

Kadowaki, Satoshi (1967). "Size Distribution of Atmospheric Total Aerosols, Sulfate, Ammonium and Nitrate Particulates in the Nagoya Area." Atmospheric Environment 10, no. 1 (1976): 39-43.

Kalnay E, Kanamitsu M, Kistler R, Collins W, Deaven D, Gandin L, M. Iredell, S. Saha, G. White, J. Woollen, Y. Zhu, A. Leetmaa, R. Reynolds, M. Chelliah, W. Ebisuzaki, W. Higgins, J. Janowiak, K. C. Mo, C. Ropelewski, J. Wang, Roy Jenne, Dennis Joseph (1996). The NCEP/NCAR 40-year reanalysis project. B Am Meteorol Soc 77:437–70.

Karydis, Vlassis A., Alexandra P. Tsimpidi, Christos Fountoukis, Athanasios Nenes, Miguel Zavala, Wenfang Lei, Luisa T. Molina, Spyros N. Pandis (2010). "Simulating the Fine and Coarse Inorganic Particulate Matter Concentrations in a Polluted Megacity." Atmospheric Environment 44, no. 5: 608-20.

Kean,A.J., Harley,R.A., Littlejohn,D., Kendall,G.R. (2000). On-road measurement of ammonia and other motor vehicle exhaust emissions. Environmental Science and Technology. 34,3535–35 39.

Kerminen, V. M., T. A. Pakkanen, and R. E. Hillamo (1997). "Interactions between Inorganic Trace Gases and Supermicrometer Particles at a Coastal Site." Atmospheric Environment 31, no. 17: 2753-65.

Keuken, M. P., M. G. M. Roemer, P. Zandveld, R. P. Verbeek, and G. J. M. Velders (2012). "Trends in Primary NO2 and Exhaust PM Emissions from Road Traffic for the Period 2000-2020 and Implications for Air Quality and Health in the Netherlands." Atmospheric Environment 54, no. 0: 313-19.

Khlystov, A., Wyers, G. P., and Slanina, J. (1995). The Steam-Jet Aerosol Collector, Atmos. Environ. 29:2229–2234.

Klett, J. D. (1981). Stable Analytical Inversion Solution for Processing Lidar Returns. Applied Optics 20(2): 211-220.

Koebel, M., M. Elsener, and M. Kleemann (2000). "Urea-Scr: A Promising Technique to Reduce Nox Emissions from Automotive Diesel Engines." Catalysis Today 59, no. 3-4: 335-45.

Kolb, C. E., R. A. Cox, J. P. D. Abbatt, M. Ammann, E. J. Davis, D. J. Donaldson, B. C. Garrett, C. George, P. T. Griffiths, D. R. Hanson, M. Kulmala, G. McFiggans, U. Poeschl, I. Riipinen, M. J. Rossi, Y. Rudich, P. E. Wagner, P. M. Winkler, D. R. Worsnop, C. D. O' Dowd (2010). "An Overview of Current Issues in the Uptake of Atmospheric Trace Gases by Aerosols and Clouds." Atmospheric Chemistry and Physics 10, no. 21: 10561-605.

Koutrakis, P., C. Sioutas, S. T. Ferguson, J. M. Wolfson, James D. Mulik, and Robert M. Burton (1993). "Development and Evaluation of a Glass Honeycomb Denuder/Filter Pack System to Collect Atmospheric Gases and Particles." Environmental Science & Technology 27, no. 12: 2497-501.

Krupa, S. V. (2003). Effects of atmospheric ammonia (NH3) on terrestrial vegetation: A review. Environ. Pollut. 124, 179–221.

Kulmala, M., V.-M. Kerminen, T. Anttila, A. Laaksonen, and C. D. O'Dowd (2004), Organic aerosol formation via sulphate cluster activation, J. Geophys. Res., 109.

Kumar, P. , A. Robins, S. Vardoulakis, R. Britter (2010). A review of the characteristics of nanoparticles in the urban atmosphere and the prospects for developing regulatory control. Atmospheric Environment, 44, pp. 5035–5052.

Laakso, L., T. Gronholm, U. Rannik, M. Kosmale, V. Fiedler, H. Vehkamaki, M. Kulmala (2003). "Ultrafine Particle Scavenging Coefficients Calculated from 6 Years Field Measurements." Atmospheric Environment 37, no. 25: 3605-13.

Laaksonen, A., M. Kulmala, T. Berndt, F. Stratmann, S. Mikkonen, A. Ruuskanen, K. E. J. Lehtinen, M. Dal Maso, P. Aalto, T. Petaja, I. Riipinen, S. L. Sihto, R. Janson, F. Arnold, M. Hanke, J. Ucker, B. Umann, K. Sellegri, C. D. O'Dowd, Y. Viisanen. (2008) "SO2 Oxidation Products Other Than H2SO4 as a Trigger of New Particle Formation. Part 2: Comparison of Ambient and Laboratory Measurements, and Atmospheric Implications". Atmospheric Chemistry and Physics 8, no. 23: 7255-64.

Langmann, Baerbel, Arnau Folch, Martin Hensch, Volker Matthias. (2012) "Volcanic Ash over Europe During the Eruption of Eyjafjallajökull on Iceland, April-May 2010." Atmospheric Environment 48, no. 0: 1-8.

Larssen, S., Sluyter, R. and Helmis, C. (1999). Criteria for EUROAIRNET. The European Environmental Agency Air Quality Monitoring and Information Network. Technical Report No. 12.

Leikauf G, Yeates DB, Wales KA, Spektor D, Albert RE, Lippmann M (1981). Effects of sulfuric acid aerosol on respiratory mechanics and mucociliary particle clearance in healthy nonsmoking adults. Am Ind Hyg Assoc J. 42:273–282.

LEY 34/2007, de 15 de noviembre, de calidad del aire y protección de la atmósfera (2007). Boletín Oficial de Estado 16 de noviembre de 2007.

Li, W. J., and L. Y. Shao (2009). "Observation of Nitrate Coatings on Atmospheric Mineral Dust Particles." Atmospheric Chemistry and Physics 9, no. 6: 1863-71.

Li, Yongquan, James J. Schwab, and Kenneth L. Demerjian (2006). "Measurements of Ambient Ammonia Using a Tunable Diode Laser Absorption Spectrometer: Characteristics of Ambient Ammonia Emissions in an Urban Area of New York City." J. Geophys. Res. 111, no. D10: D10S02.

Liao, Hong, Daven K. Henze, John H. Seinfeld, Shiliang Wu, Loretta J. Mickley (2007). "Biogenic Secondary Organic Aerosol over the United States: Comparison of Climatological Simulations with Observations." Journal of Geophysical Research-Atmospheres 112, no. D6.

Likens, G. L. and Bormann, F. H. (1974). Acid Rain: A Serious Regional Environmental Problem. Science, Vol. 184 no. 4142 pp. 1176-1179.

Lin, C.C., Chen, S.J., Huang, K.L., Lee, W.J., Lin, W.Y., Liao, C.J., Chaung, H.C., Chiu, C.H., (2007). Water soluble ions in nano/ultrafine/fine/coarse particles collected near a busy road and at a rural site. Environmental Pollution 145, 562-570.

Long, R. W. and W. A. McClenny (2006). Laboratory and field evaluation of instrumentation for the semicontinuous determination of particulate nitrate (and other water-soluble particulate components). Journal of the Air & Waste Management Association 56(3): 294-305.

Long, R.W.; Eatough, N.L.; Eatough, D.J.; Meyer, M.B. (2005). Continuous Determination of PM2.5 Mass in the Salt Lake City EPA EMPACT Project: A Comparison of RAMS, SES-TEOM and Conventional TEOM Monitor Results; J. Air & Waste Manage. Assoc. 55, 1839-1846.

Long, R.W.; Eatough, N.L.; Mangelson, N.F.; Thompson, W.; Fiet, K.; Smith, S.; Smith, R.; Eatough, D.J.; Pope, C.A.; Wilson, W.E (2003). The Measurement of PM2.5, Including Semi-Volatile Components, in the EMPACT Program: Results From the Salt Lake City Study. Atmos. Environ. 37, 4407-4417.

Marple, V. A., and Olson, B. A. (1999). A Micro-Orifice Impactor with Cut Sizes Down to 10 Nanometers for Diesel Exhaust Sampling, Final Report. Generic Center for Respirable Dust, Pennsylvania State University, University Park, PA.

Marple, V.A., Rubow, K.L., Behm, S.M. (1991). A micro-orifice uniform deposit impactor (MOUDI): description, calibration and use. Aerosol Science and Technology 14, 434-446.

Mather, T. A., Allen, A. G., Oppenheimer, C., Pyle, D. M., McGonigle, A. J. S. (2003). Size-resolved characterisation of soluble ions in the particles in the tropospheric plume of Masaya volcano, Nicaragua: Origins and plume processing. Journal of Atmospheric Chemistry 46(3): 207-237.

Mather, T. A., C. Oppenheimer, A.G. Allen A.J.S. McGonigle, (2004). Aerosol chemistry of emissions from three contrasting volcanoes in Italy, Atmospheric Environment, 38(33), 5637-5649.

McInnes, L. M., D. S. Covert, P. K. Quinn, M. S. Germani (1994). "Measurements of Chloride Depletion and Sulfur Enrichment in Individual Sea-Salt Particles Collected from the Remote Marine Boundary-Layer." Journal of Geophysical Research-Atmospheres 99, no. D4: 8257-68.

McMurry, P. H. (2000). A Review of Atmospheric Aerosol Measurements, Atmos. Environ. 34:1959–1999.

McNaughton, C. S., Clarke, A. D., Kapustin, V., Shinozuka, Y., Howell, S. G., Anderson, B. E., Winstead, E., Dibb, J., Scheuer, E., Cohen, R. C., Wooldridge, P., Perring, A., Huey, L. G., Kim, S., Jimenez, J. L., Dunlea, E. J., DeCarlo, P. F., Wennberg, P. O., Crounse, J. D., Weinheimer, A. J., and Flocke, F. (2009). Observations of heterogeneous reactions between Asian pollution and mineral dust over the Eastern North Pacific during INTEX-B. Atmos. Chem. Phys., 9, 8283-8308.

Meng, Z. Y., Lin, W. L., Jiang, X. M., Yan, P., Wang, Y., Zhang, Y. M., Jia, X. F., Yu, X. L. (2011). Characteristics of atmospheric ammonia over Beijing, China, Atmos. Chem. Phys., 11, 6139-6151, doi:10.5194/acp-11-6139-2011.

Meng, Z. and J. H. Seinfeld (1994). On the Source of the Submicrometer Droplet Mode of Urban and Regional Aerosols, Aerosol Science and Technology, 20:3, 253-265.

Middleton, Paulette, C. S. Kiang, Volker A. Mohnen (1967). "Theoretical Estimates of the Relative Importance of Various Urban Sulfate Aerosol Production Mechanisms". Atmospheric Environment 14, no. 4 (1980): 463-72.

Millán MM, Salvador R, Mantilla E, Kallos G (1997). Photo-oxidant dynamics in the Mediterranean basin in summer: results from European research projects. J Geophys Res ;102:8811–23.

Miller, K.A., M.S., David S. Siscovick, Lianne Sheppard, Kristen Shepherd, Jeffrey H. Sullivan, Garnet L. Anderson, Joel D. Kaufman (2007). Long-term exposure to air pollution and incidence of cardiovascular events in women. N Engl J Med. 356:447–458.

Millstein, D. E., Harley, R. A., Hering, S. V. (2008) "Weekly cycles in fine particulate nitrate." Atmospheric Environment 42(4): 632-641.

Molero, F. and F. Jaque (1999). The laser as a tool in environmental problems. Optical Materials 13(1): 167-173.

Moreno, T., X. Querol, A. Alastuey, M. Viana, W. Gibbons (2009). "Profiling Transient Daytime Peaks in Urban Air Pollutants: City Centre Traffic Hotspot Versus Urban Background Concentrations." J. Environ. Monit. 11, no. 8: 1535-42.

Mozurkewich, M. (1993). "The Dissociation-Constant of Ammonium-Nitrate and Its Dependence on Temperature, Relative-Humidity and Particle-Size." Atmospheric Environment Part a-General Topics 27, no. 2: 261-70.

N. Pérez, J. Pey, S. Castillo, A. Alastuey, X. Querol, M. Viana (2008). Interpretation of the variability of regional background aerosols in the Western Mediterranean. Sci Total Environ, pp. 527–540.

Ng, N. L., Herndon, S. C., Trimborn, A., Canagaratna, M. R., Croteau, P. L., Onasch, T. B., D. Sueper, D. R. Worsnop, Q. Zhang, Y. L. Sun, J. T. Jayne (2011). An Aerosol Chemical Speciation Monitor (ACSM) for Routine Monitoring of the Composition and Mass Concentrations of Ambient Aerosol. Aerosol Sci. Technol. 45:780–794.

Nicolas, J. F., N. Galindo, E. Yubero, C. Pastor, R. Esclapez, J. Crespo (2009). "Aerosol Inorganic Ions in a Semiarid Region on the Southeastern Spanish Mediterranean Coast." Water Air and Soil Pollution 201, no. 1-4 : 149-59.

Nie, W., T. Wang, X. M. Gao, R. K. Pathak, X. F. Wang, R. Gao, Q. Z. Zhang, L. X. Yang, W. X. Wang (2010). "Comparison among Filter-Based, Impactor-Based and Continuous Techniques for Measuring Atmospheric Fine Sulfate and Nitrate." Atmospheric Environment 44, no. 35: 4396-403.

O'Dowd, Colin D., Gerrit De Leeuw (2007). "Marine Aerosol Production: A Review of the Current Knowledge." Philosophical Transactions of the Royal Society a-Mathematical Physical and Engineering Sciences 365, no. 1856: 1753-74.

Olivier, J.G.J., A.F. Bouwman, K.W. van der Hoek, J.J.M. Berdowski (1998). Global Air Emission Inventories for Anthropogenic Sources of NOx, NH3 and N2O in 1990. Environmental Poll., 102, 135-148.

Oppenheimer, C., Kyle, P., Eisele, F., Crawford, J., Huey, G., Tanner, D., Kim, S., Mauldin, L., Blake, D., Beyersdorf, A., Buhr, M., Davis, D. (2010). Atmospheric chemistry of an Antarctic volcanic plume. Journal of Geophysical Research-Atmospheres 115: 15.

Ovadnevaite, J., Ceburnis, D., Plauskaite-Sukiene, K., Modini, R., Dupuy, R., Rimselyte, I., Ramonet, M., Kvietkus, K., Ristovski, Z., Berresheim, H., O'Dowd, C. D.

(2009). Volcanic sulfate and arctic dust plumes over the North Atlantic Ocean. Atmospheric Environment 43(32): 4968-4974.

Pandolfi, M., Amato, F., Reche, C., Alastuey, A., Otjes, R. P., Blom, M. J., Querol, X (2012). Summer ammonia measurements in a densely populated Mediterranean city. Atmos. Chem. Phys., 12, 7557-7575.

Pakkanen, Tuomo A (1996). "Study of Formation of Coarse Particle Nitrate Aerosol." Atmospheric Environment 30, no. 14: 2475-82.

Park, K., Cao, F., Kittelson, D.B., McMurry, P.H., (2003). Relationship between particle mass and mobility for diesel exhaust particles. Environmental Science and Technology, 37 (3), pp 577–583.

Park, R. J., D. J. Jacob, M. Chin, R. V. Martin (2003). "Sources of Carbonaceous Aerosols over the United States and Implications for Natural Visibility." Journal of Geophysical Research-Atmospheres 108, no. D12.

Park, S.S., J.M. Ondov, D. Harrison, N.P. Nair (2005). Seasonal and shorter-term variations in particulate atmospheric nitrate in Baltimore. Atmospheric Environment, 39, pp. 2011–2020

Park, Seung S., John M.Ondov, David Harrison, Narayanan P. Nair (2005). Seasonal and shorter-term variations in particulate atmospheric nitrate in Baltimore. Atmospheric Environment 39: 2011–2020

Pay, María T., Pedro Jiménez-Guerrero, José M. Baldasano (2012). Assessing Sensitivity Regimes of Secondary Inorganic Aerosol Formation in Europe with the Caliope-Eu Modeling System. Atmospheric Environment 51, no. 0: 146-64.

Penner, J.E., 1995: Carbonaceous aerosols influencing atmospheric radiation: black and organic carbon, in Aerosol Forcing of Climate, ed. R.J. Charlson and J. Heintzenberg, John Wiley and Sons, Chichester, 91-108.

Penttinen, P., K. L. Timonen, P. Tiittanen, A. Mirme, J. Ruuskanen, J. Pekkanen (2001). "Ultrafine Particles in Urban Air and Respiratory Health among Adult Asthmatics." European Respiratory Journal 17, no. 3: 428-35.

Perrino, C., M. Catrambone, A. Di Menno Di Bucchianico, I. Allegrini (2002). "Gaseous Ammonia in the Urban Area of Rome, Italy and Its Relationship with Traffic Emissions." Atmospheric Environment 36, no. 34: 5385-94.

Peters, T. M., Ott, D., O'Shaughnessy, P. T. (2006). Comparison of the Grimm 1.108 and 1.109 portable aerosol spectrometer to the TSI 3321 aerodynamic particle sizer for dry particles. Annals of Occupational Hygiene 50(8): 843-850.

Peterson, T. W. and Seinfeld, J. H. (1997). Mathematical model for transport, interconversion, and removal of gaseous and particulate air pollutants -

Application to the urban plume. Atmospheric Environment. Vol. 11, no. 12, pp. 1171-1184.

Petters, M. D., and S. M. Kreidenweis (2007). "A Single Parameter Representation of Hygroscopic Growth and Cloud Condensation Nucleus Activity." Atmospheric Chemistry and Physics 7, no. 8: 1961-71.

Petterssen, S. (1940). Weather Analysis and Forecasting. Mc-Graw-Hill Book Company, New York, pp. 221–223.

Pey, Jorge, Noemí- Pérez, Xavier Querol, Andrés Alastuey, Michael Cusack, Cristina Reche (2010a). "Intense Winter Atmospheric Pollution Episodes Affecting the Western Mediterranean." Science of The Total Environment 408, no. 8: 1951-59.

Pey J., Querol X ., Alastuey A. (2010b) Discriminating the regional and urban contributions in the North-Western Mediterranean: PM levels and composition. Atmospheric Environment 44,13,1587-1596.

Pey J., Querol X., Alastuey A., Rodríguez S., Putaud J.P., Van Dingenen R. (2009). "Source apportionment of urban fine and ultra fine particle number concentration in a Western Mediterranean city". Atmospheric Environment, 43, 4407-4415.

Pey, J., X. Querol, J. de la Rosa, Y. Gonzalez-Castanedo, A. Alastuey, G. Gangoiti, A. S. de la Campa, L. Alados-Arboledas, M. Sorribas, C. Pio, V. Cachorro, M. Pineiro, P. Lopez-Mahia, D. Garcia-Gacio (2008). "Characterization of a Long Range Transport Pollution Episode Affecting Pm in Sw Spain." Journal of Environmental Monitoring 10, no. 10: 1158-71.

Pio, CA., Ramos, MM., Duarte, AC (1998). "Atmospheric aerosol and soiling of external surfaces in an urban environment ". ATMOSPHERIC ENVIRONMENT 32, 11: 1979-1989.

Pio, C.A., Santos, I.M., Anacleto, T.D., Nunes, T.V. (1991). Particulate and gaseous air pollutants levels at the Portuguese West Coast. Atmospheric Environment 25A, 669-680.

Plaza, J., M. Pujadas, L. Núñez, P. Salvador, B. Artíñano (2007). Estimation of NO2/NOx traffic emission ratio from ambient measurements in Madrid. Particles and photooxidants in Europe. Conference and Exhibition. Prague, 26-27 September.

Plaza, Javier, Begoña Artíñano, Pedro Salvador, Francisco J. Gómez-Moreno, Manuel Pujadas, and Casimiro A. Pio. Short-Term Secondary Organic Carbon Estimations with a Modified OC/EC Primary Ratio Method at a Suburban Site in Madrid (Spain) (2011). Atmospheric Environment 45, no. 15: 2496-506.

Pope, C. A. and Schwartz, J. (1992). Daily moratality and PM10 pollution in Utah Valley. Archives of Environmental Health, 47:211-217.

Potukuchi, S., and A. S. Wexler (1995a). Identifying Solid-Aqueous Phase-Transitions in Atmospheric Aerosols. 1. Neutral-Acidity Solutions. Atmospheric Environment 29, no. 14: 1663-76.

Potukuchi, S., and A. S. Wexler (1995b). Identifying Solid-Aqueous-Phase Transitions in Atmospheric Aerosols. 2. Acidic Solutions. Atmospheric Environment 29, no. 22: 3357-64.

Prakash Doraiswamy, Christian Hogrefe, Winston Hao, Kevin Civerolo, Jia-Yeong Ku & Gopal Sistla (2010): A Retrospective Comparison of Model-Based Forecasted PM2.5 Concentrations with Measurements, Journal of the Air & Waste Management Association, 60:11, 1293-1308.

Putaud, J. P., Raes, F., Van Dingenen, R., Brüggemann, E., Facchini, M. C., Decesari, S., Fuzzi, S., Gehrig, R., Hüglin, C., Laj, P., Lorbeer, G., Maenhaut, W., Mihalopoulos, N., Müller, K., Querol, X., Rodriguez, S., Schneider, J., Spindler, G., ten Brink, H., Tørseth, K., Wiedensohler, A. (2004). "A European Aerosol Phenomenology—2: Chemical Characteristics of Particulate Matter at Kerbside, Urban, Rural and Background Sites in Europe." Atmospheric Environment 38, no. 16: 2579-95.

Putaud, J. P., Van Dingenen, R., Alastuey, A., Bauer, H., Birmili, W., Cyrys, J., Flentje, H., Fuzzi, S., Gehrig, R., Hansson, H. C., Harrison, R. M., Herrmann, H., Hitzenberger, R., Hüglin, C., Jones, A. M., Kasper-Giebl, A., Kiss, G., Kousa, A., Kuhlbusch, T. A. J., Löschau, G., Maenhaut, W., Molnar, A., Moreno, T., Pekkanen, J., Perrino, C., Pitz, M., Puxbaum, H., Querol, X., Rodriguez, S., Salma, I., Schwarz, J., Smolik, J., Schneider, J., Spindler, G., ten Brink, H., Tursic, J., Viana, M., Wiedensohler, A., Raes, F. (2010). A European Aerosol Phenomenology – 3: Physical and Chemical Characteristics of Particulate Matter from 60 Rural, Urban, and Kerbside Sites across Europe. Atmospheric Environment 44, no. 10: 1308-20.

QUARG (1996). Airborne Particulate Matter in the United Kingdom. Third Report. Quality of Urban Air Review Group. Dept. Envir. London. 176 pp.

Querol, X., A. Alastuey, J.A. Puicercus, E. Mantilla, C.R. Ruiz, A. López-Soler, F. Plana, R. Juan (1998a). Seasonal evolution of suspended particles around a large coal-fired power station: chemical characterisation. Atmospheric Environment, 32 (11): 719–731.

Querol, X., A Alastuey, J.A Puicercus, E Mantilla, J.V Miros, A Lopez-Soler, F Plana, B Artíñano (1998b). Seasonal evolution of suspended particles around a large coal-fired power station: particles levels and sources. Atmospheric Environment, 32 (11): 1963–1978.

Querol, X. et al. (2009). Niveles, Composición y Fuentes De PM10, PM2.5 Y PM1 en España: Cantabria, Castilla-León, Madrid y Melilla. Final Report. Ministry of Environment.

Querol, X., A. Alastuey, M. M. Viana, S. Rodriguez, B. Artíñano, P. Salvador, S. G. do Santos, R. F. Patier, C. R. Ruiz, J. de la Rosa, A. S. de la Campa, M. Menendez, J. I. Gil (2004a). Speciation and Origin of PM10 and PM2.5 in Spain. Journal of Aerosol Science 35, no. 9: 1151-72.

Querol, X., A. Alastuey, C. R. Ruiz, B. Artiñano, H. C. Hansson, R. M. Harrison, E. Buringh, H. M. ten Brink, M. Lutz, P. Bruckmann, P. Straehl, J. Schneider (2004b). Speciation and Origin of PM10 and PM2.5 in Selected European Cities. Atmospheric Environment 38, no. 38 (2004a): 6547-55.

Querol X., Alastuey A., Rodríguez S., Viana M.M., Artíñano B., Salvador P., Mantilla E., Santos S.G.D., Patier R.F., Rosa J.D.L., Sánchez de la Campa A., Menendez M. (2004c). Levels of PM in rural, urban and industrial sites in Spain. The Science of Total Environment , 334-335, pp. 359-376.

Querol, X., A. Alastuey, T. Moreno, M. M. Viana, S. Castillo, J. Pey, S. Rodriguez, B. Artíñano, P. Salvador, M. Sanchez, S. G. Dos Santos, M. D. H. Garraleta, R. Fernandez-Patier, S. Moreno-Grau, L. Negral, M. C. Minguillon, E. Monfort, M. J. Sanz, R. Palomo-Marin, E. Pinilla-Gil, E. Cuevas, J. de la Rosa, A. S. de la Campa (2008). Spatial and Temporal Variations in Airborne Particulate Matter (PM10 and PM2.5) across Spain 1999-2005. Atmospheric Environment 42, no. 17: 3964-79.

Querol, X., Andrés Alastuey, Sergio Rodriguez, Felicià Plana, Enrique Mantilla, Carmen R Ruiz (2001), Monitoring of PM10 and PM2.5 around primary particulate anthropogenic emission sources. Atmospheric Environment 35(5): 845-858.

Rattigan, O. V., Hogrefe, O., Felton, H. D., Schwab, J. J., Roychowdhury, U. K., Husain, L., Dutkiewicz, V. A., Demerjian, K. L. (2006) "Multi-year urban and rural semi-continuous PM2.5 sulfate and nitrate measurements in New York state: Evaluation and comparison with filter based measurements." Atmospheric Environment 40: 192-205.

Real Decreto 102/2011, de 28 de enero, relativo a la mejora de la calidad del aire (2011). Boletín Oficial del Estado 29 de enero de 2011.

Real Decreto 61/2006, de 31 de enero, por el que se determinan las especificaciones de gasolinas, gasóleos, fuelóleos y gases licuados del petróleo y se regula el uso de determinados biocarburantes (2006). Boletín Oficial del Estado 17 de febrero 2006

Reche, Cristina, Mar Viana, Marco Pandolfi, Andrés Alastuey, Teresa Moreno, Fulvio Amato, Anna Ripoll, Xavier Querol (2012). "Urban NH3 Levels and Sources in a Mediterranean Environment." Atmospheric Environment 57, no. 0: 153-64.

Regulation (EC) no 715/2007 of the European Parliament and of the Council (2007). On type approval of motor vehicles with respect to emissions from light passenger

and commercial vehicles (Euro 5 and Euro 6) and on access to vehicle repair and maintenance information. Official Journal of the European Union, L171.

Revuelta, M. A., R. M. Harrison, L. Núñez, F. J. Gómez-Moreno, M. Pujadas, B. Artíñano (2012a). Comparison of temporal features of sulphate and nitrate at urban and rural sites in Spain and the UK. Atmospheric Environment 60, p 383-91.

Revuelta, M. A., R. M. Harrison, L. Núñez, F. J. Gómez-Moreno, M. Pujadas, B. Artíñano (2012b). Patrones de evolución de contaminantes atmosféricos en diferentes emplazamientos de España y el Reino Unido. XXXII Jornadas Científicas de la Asociación Meteorológica Española, Museo de la Ciencia COSMOCAIXA, Alcobendas.

Revuelta, M. A., M. Sastre, A. J. Fernández, L. Martín, R. García, F. J. Gómez-Moreno, B. Artíñano, M. Pujadas, F. Molero (2012c). Characterization of the Eyjafjallajökull volcanic plume over the Iberian Peninsula by lidar remote sensing and ground-level data collection. Atmospheric Environment 48, p 46-55.

Revuelta, M. A., Gómez-Moreno, F. J., Núñez, L., Salvador, P., Molero, F., Artíñano, B. (2011) Temporal analysis and characterization of events of fine particulate sulfate in Madrid. Proceedings of the V RECTA. ISBN: 978-84-7834-662-2.

Rigby, M., Timmis, R., Toumi, R. (2006) "Similarities of Boundary Layer Ventilation and Particulate Matter Roses." Atmospheric Environment 40, no. 27: 5112-24.

Rodhe, H. (1978) Budgets and turn-over times of atmospheric sulfur compounds, Atmos. Environ. 12, 671-680.

Rodríguez, S., González, Y., Cuevas, E., Ramos, R., Romero, P.M., Abreu-Afonso, J., Redondas, A. (2009). "Atmospheric nanoparticle observations in the low free troposphere during upward orographic flows at Izaña Mountain Observatory". Atmospheric Chemistry and Physics, 9, 6319-6335, 2009.

Rodríguez, S., R. Van Dingenen, J.P. Putaud, A. Dell'Acqua, X. Querol, A. Alastuey, J. Pey, R.M. Harrison, K.F. Ho, S. Chenery, R. Tardivo, V. Gemelli, B. Scarnato (2007). A study on the relationship between mass concentrations, chemistry and number size distribution of urban fine PM2.5 aerosols in Milan, Barcelona, London. Atmospheric Chemistry and Physics, 7, 2217-2232.

Rodriguez, S., X. Querol, A. Alastuey, G. Kallos, and O. Kakaliagou (2001). Saharan Dust Contributions to Pm10 and Tsp Levels in Southern and Eastern Spain. Atmospheric Environment 35, no. 14: 2433-47.

Rua, A., Ehjd Parras, I. Martin, L. Gimeno (1998) "Sources of So2, So42-, Nox, and No3- in the Air of Four Spanish Remote Stations". Journal of the Air & Waste Management Association 48, no. 9: 838-45.

Salvador P., Artíñano B., Querol X. Alastuey A. (2008). A combined analysis of backward trajectories and aerosol chemistry to characterize long-range transport episodes of particulate matter: the Madrid air basin, a case study. Science of the Total Environment 390/2-3 pp. 496-507.

Salvador, P. (2004a). Caracterización de la contaminación atmosférica producida por las partículas en suspensión en Madrid, Tesis Doctoral, Universidad Complutense de Madrid. ISBN: 84-669-2560-0.

Salvador, P., Artíñano, B., Alonso, D. G., Querol, X., Alastuey, A. (2004b). Identification and characterisation of sources of PM10 in Madrid (Spain) by statistical methods. Atmospheric Environment 38(3): 435-447.

Salvador, P., B. Artíñano, M. M. Viana, X. Querol, A. Alastuey, I. González-Fernández, R. Alonso (2010). "Spatial and Temporal Variations in PM10 and PM2.5 across Madrid Metropolitan Area in 1999-2008." Procedia Environmental Sciences 4, no. 0: 198-208.

Salvador, P., B. Artíñano, M. Viana, A. Alastuey, X. Querol (2012). "Evaluation of the Changes in the Madrid Metropolitan Area Influencing Air Quality: Analysis of 1999-2008 Temporal Trend of Particulate Matter." Atmospheric Environment 57, 175-185.

Saul, T. D., Tolocka, M. P., and Johnston, M. V., (2006). Reactive Uptake of Nitric Acid onto Sodium Chloride Aerosols Across a Wide Range of Relative Humidities. J. Phys. Chem. A, 110, 7614-7620.

Savoie, D. L., and J. M. Prospero (1982). "Particle-Size Distribution of Nitrate and Sulfate in the Marine Atmosphere." Geophysical Research Letters 9, no. 10: 1207-10.

Schaap, M., M. Van Loon, H. M. Ten Brink, F. J. Dentener, and P. J. H. Builtjes (2004). Secondary inorganic aerosol simulations for Europe with special attention to nitrate. Atmospheric Chemistry and Physics 4, 3; 857-874.

Schumann, U., Weinzierl, B., Reitebuch, O., Schlager, H., Minikin, A., Forster, C., Baumann, R., Sailer, T., Graf, K., Mannstein, H., Voigt, C., Rahm, S., Simmet, R., Scheibe, M., Lichtenstern, M., Stock, P., Rüba, H., Schäuble, D., Tafferner, A., Rautenhaus, M., Gerz, T., Ziereis, H., Krautstrunk, M., Mallaun, C., Gayet, J. F., Lieke, K., Kandler, K., Ebert, M., Weinbruch, S., Stohl, A., Gasteiger, J., Groß, S., Freudenthaler, V., Wiegner, M., Ansmann, A., Tesche, M., Olafsson, H., Sturm, K. (2011) Airborne observations of the Eyjafjalla volcano ash cloud over Europe during air space closure in April and May 2010, Atmos. Chem. Phys., 11, 2245-2279.

Schwab, J. J., Hogrefe, O., Demerjian, K. L., Dutkiewicz, V. A., Husain, L., Rattigan, O. V., Felton, H. D. (2006). Field and laboratory evaluation of the Thermo Electron

5020 Sulfate Particulate Analyzer. Aerosol Science and Technology 40(10): 744-752.

Seinfeld, J.H., Pandis, S.N. (1998). Atmospheric Chemistry and Physics: From Air Pollution to Global Change. Wiley, New York.

Seinfeld, J.H., Pandis, S.N. (2006). Atmospheric Chemistry and Physics: From Air Pollution to Global Change (2nd edition). Wiley, New York.

Serrano, E., E. Zurita, M. Castro (1989). Analysis of the Annual Trend in SO2 and Particulate Matter Emissions in Madrid (Spain). Atmospheric Environment 23, no. 3: 631-42.

Serrano, E., M. Castro, R. González (1997). "An Update on SO2 and Particulate Matter Emissions Trends in Madrid (Spain)." Anales de Física 93, no. 2, 93-97.

Shindell, D. T., G. Faluvegi, D. M. Koch, G. A. Schmidt, N. Unger, S. E. Bauer (2009). Improved Attribution of Climate Forcing to Emissions. Science, 326, 716-718.

Sioutas, C., R. J. Delfino, M. Singh (2005). "Exposure Assessment for Atmospheric Ultrafine Particles (Ufps) and Implications in Epidemiologic Research." Environmental Health Perspectives 113, no. 8: 947-55.

Sorribas, M., B. A. de la Morena, B. Wehner, J. F. Lopez, N. Prats, S. Mogo, A. Wiedensohler, V. E. Cachorro (2011). "On the Sub-Micron Aerosol Size Distribution in a Coastal-Rural Site at El Arenosillo Station (Sw - Spain)." Atmospheric Chemistry and Physics 11, no. 21: 11185-206.

Stein, S.W., Turpin, B.J., Cai, X.P., Huang, C.P.F., McMurry, P.H., (1994). Measurements of relative humidity-dependent bounce and density for atmospheric particles using the DMA-impactor technique. Atmospheric Environment 28, 1739-1746.

Stein, A. F. and Saylor, R. D. (2012): Sensitivities of sulfate aerosol formation and oxidation pathways on the chemical mechanism employed in simulations, Atmos. Chem. Phys., 12, 8567–8574.

Stohl, A., and P. Seibert (1998): Accuracy of trajectories as determined from the conservation of meteorological tracers. Q. J. Roy. Met. Soc. 124, 1465-1484.

Stohl, A., G. Wotawa, P. Seibert, H. Kromp-Kolb (1995): Interpolation errors in wind fields as a function of spatial and temporal resolution and their impact on different types of kinematic trajectories. J. Appl. Meteor. 34, 2149-2165.

Stolzenburg, M. R., Hering, S. V. (2000). Method for the automated measurement of fine particle nitrate in the atmosphere. Environmental Science & Technology, 34, 907–914.

Stuut, J.B., I. Smalley, K. O'Hara-Dhand (2009). Aeolian dust in Europe: African sources and European deposits. Quaternary International 198, Issues 1–2: 234–245.

Surratt, J. D., Kroll, J. H., Kleindienst, T. E., Edney, E. O., Claeys, M., Sorooshian, A., Ng, N. L., Offenberg, J. H., Lewandowski, M., Jaoui, M., Flagan, R. C. Seinfeld, J. H. (2007). Evidence for organosulfates in secondary organic aerosol. Environmental Science & Technology, 41, 517-27.

Tandon, P., and D. E. Rosner (1999). Monte Carlo Simulation of Particle Aggregation and Simultaneous Restructuring. Journal of Colloid and Interface Science 213, no. 2: 273-86.

Tang, Y.S., Cape, J.N., Sutton, M.A. (2001). Development and types of passive samplers for monitoring atmospheric NO2 and NH3 concentrations. In Proceedings of the International Symposium on Passive Sampling of Gaseous Air Pollutants in Ecological Effects Research. TheScientificWorld 1, 513–529.

Tanner, R. L., D'Ottavio, T., Garber, R., Newman, L. (1980). Determination of Ambient Aerosol Sulfur Using a Continuous Flame Photometric Detection System. 1. Sampling System for Aerosol Sulphate and Sulfuric Acid, Atmos. Environ. 14:121–127.

Tegen, I., M. Werner, S.P. Harrison, and K.E. Kohfeld (2004). Relative importance of climate and land use in determining present and future global soil dust emission. Geophys. Res. Lett., 31, L05105.

Toledano, C., V. E. Cachorro, A. M. de Frutos, M. Sorribas, N. Prats, B. A. de la Morena (2007). Inventory of African Desert Dust Events over the Southwestern Iberian Peninsula in 2000-2005 with an Aeronet Cimel Sun Photometer. Journal of Geophysical Research-Atmospheres 112, no. D21: 14.

Ulbrich, I. M., M. R. Canagaratna, Q. Zhang, D. R. Worsnop, J. L. Jimenez (2009). "Interpretation of Organic Components from Positive Matrix Factorization of Aerosol Mass Spectrometric Data." Atmospheric Chemistry and Physics 9, no. 9: 2891-918.

US EPA (2004). Air quality criteria for particulate matter. Research Triangle Park, NC: Office of Research and Development, EPA/600/P-99/002aF.

Van Dingenen, R., F. Raes, J. P. Putaud, U. Baltensperger, A. Charron, M. C. Facchini, S. Decesari, S. Fuzzi, R. Gehrig, H. C. Hansson, R. M. Harrison, C. Hüglin, A. M. Jones, P. Laj, G. Lorbeer, W. Maenhaut, F. Palmgren, X. Querol, S. Rodriguez, J. Schneider, H. ten Brink, P. Tunved, K. Tørseth, B. Wehner, E. Weingartner, A. Wiedensohler, P. Wåhlin (2004). "A European Aerosol Phenomenology—1: Physical Characteristics of Particulate Matter at Kerbside, Urban, Rural and Background Sites in Europe." Atmospheric Environment 38, no. 16: 2561-77.

Venkataraman, C., and J. Raymond (1998). "Estimating the Lung Deposition of Particulate Polycyclic Aromatic Hydrocarbons Associated with Multimodal Urban Aerosols." Inhalation Toxicology 10, no. 3: 183-204.

Viana, M., X. Querol, A. Alastuey, G. Gangoiti, M. Menéndez (2003). "PM Levels in the Basque Country (Northern Spain): Analysis of a 5-Year Data Record and Interpretation of Seasonal Variations." Atmospheric Environment 37, no. 21: 2879-2891.

Virkkula, A. (1997). Performance of a differential optical absorption spectrometer for surface O3 measurements in the Finnish Arctic. Atmospheric Environment, 31 (4): 545–555.

Vogt, E., Held, A., Klemm, O. (2005). Sources and concentrations of gaseous and particulate reduced nitrogen in the city of Münster (Germany). Atmospheric Environment 38, 7393-7402.

Wagstrom, K. M., and S. N. Pandis (2011). "Contribution of Long Range Transport to Local Fine Particulate Matter Concerns." Atmospheric Environment 45, no. 16: 2730-35.

Wahlin, P. (2009). Measured Reduction of Kerbside Ultrafine Particle Number Concentrations in Copenhagen. Atmospheric Environment 43, no. 22-23 (2009): 3645-47.

Wall, S. M., John, W., Ondo, J. L. (1988). "Measurement Of Aerosol Size Distributions For Nitrate And Major Ionic Species". Atmospheric Environment 22, 1649-1656.

Wang, S. C. and R. C. Flagan (1990). Scanning Electrical Mobility Spectrometer. Aerosol Science and Technology 13(2): 230-240.

Wang, W, D. Gong, Z. Zhou, Y. Guo (2012). Robustness of the aerosol weekly cycle over Southeastern China. Atmospheric Environment 61, 409-418.

Wayne, R.P., Barnes, I., Biggs, P., Burrows, J.P., Canosa-Mas, C.E., Hjorth, J., Le Bras, G., Moortgat, G.K., Perner, D., Poulet, G., Restelli, G., Sidebottom, H. (1991). The nitrate radical: physics, chemistry, and the atmosphere. Atmospheric Environment, Part A 25, 1–203.

Weber, R. J., Orsini, D., Daun, Y., Lee, Y.-N., Klotz, P. J., and Brechtel, F. (2001). A Particle-into-Liquid Collector for Rapid Measurment of Aerosol Bulk Chemical Composition, Aerosol Sci. Technol. 35:718– 727.

Wehner, B., T. Petäjä, M. Boy, C. Engler, W. Birmili, T. Tuch, A. Wiedensohler, M. Kulmala (2005), The contribution of sulfuric acid and non-volatile compounds on the growth of freshly formed atmospheric aerosols, Geophys. Res. Lett., 32, L17810.

Whitby, K. T. (1978). The physical characteristics of sulfur aerosols. Atmos. Environ. 12: 135-159.

Whitehead, J., I. Longley, M. Gallagher (2007). Seasonal and Diurnal Variation in Atmospheric Ammonia in an Urban Environment Measured Using a Quantum Cascade Laser Absorption Spectrometer. Water, Air, & Soil Pollution 183, no. 1: 317-29.

WHO, Regional office for Europe (2006). Regional risks of particulate matter from long-range transbourdary air pollution. World Health Organization.

Wiegner, M., Gasteiger, J., Groß, S., Schnell, F., Freudenthaler, V., Forkel, R., (2012). Characterization of the Eyjafjallajökull ash-plume: Potential of lidar remote sensing. J. Phys. Chem. Earth. 45–46: 79–86.

Wittig, A. E., Takahama, S., Khlystov, A. Y., Pandis, S. N., Hering, S., Kirby, B., Davidson, C. (2004). Semi-continuous PM2.5 inorganic composition measurements during the Pittsburgh Air Quality Study. Atmospheric Environment 38(20): 3201-3213.

World Urbanization Prospects, the 2011 Revision (2012). United Nations, Department of Economic and Social Affairs, Population Division. New York.

Wurzler, S., T. G. Reisin, Z. Levin (2000). "Modification of Mineral Dust Particles by Cloud Processing and Subsequent Effects on Drop Size Distributions." Journal of Geophysical Research-Atmospheres 105, no. D4: 4501-12.

Xie, R., Jackson, K.A., Seip, H.M., McLeod, C.W., Wibetoe, G., Schofield, M.J., Anderson D. Hanssen J.E. (2009). Characteristics of water-soluble inorganic chemical components in size-resolved airborne particulate matters. J. Environ. Monit. 11, 336-343.

Yao and Zhang (2012). Modes in the size distributions and neutralization extent of fog-processed ammonium salt aerosols observed at Canadian rural locations. Atmos. Chem. Phys. Discuss., 12, 5519–5550.

Zhang, Q., Jiménez, J.L., Woorsnop, D.R., Canagaratna, M. (2007). A case study of urban particle acidity and its influence on secondary organic aerosol. Environmental Science & Technology 41, 3213-3219.

Zhang, R. Y., Wang, L., Khalizov, A. F., Zhao, J., Zheng, J., Mcgraw, R. L. & Molina, L. T. (2009). Formation of nanoparticles of blue haze enhanced by anthropogenic pollution. Proceedings of the National Academy of Sciences of the United States of America, 106, 17650-17654.

Zhuang, H., C. K. Chan, M. Fang, A. S. Wexler (1999a). Formation of Nitrate and Non-Sea-Salt Sulfate on Coarse Particles. Atmospheric Environment 33, no. 26: 4223-33.

Zhuang, H., Chan, C.K., Fang, M., Wexler, A.S., (1999b). Size distributions of particulate sulfate, nitrate, and ammonium at a coastal site in Hong Kong. Atmospheric Environment 33, 843-853.

APPENDIX I

Code	*Station name*	*Coordinates*	*NO_2-NO-NOx*	*SO_2*	*NH_3*	*PM_{10} (+ions)*	*$PM_{2.5}$*	*Precipitation*
ES01	San Pablo de los Montes (Toledo)	***39.55° N, 4.35° W, 917 m asl.***	Y	Y	***	Y	Y	Y
ES02	La Cartuja (Granada)	***37.12°N, 3.35°W, 800 m asl.***	Y	Y	***	Y	Y	***
ES03	Roquetas (Tarragona)	***40.49°N, 0.29°E, 44 m asl.***	Y	Y	***	Y	Y	***
ES04	Logroño (La Rioja)	***42.27°N, 2.30°W, 445 m asl.***	Y	Y	***	Y	Y	***
ES05	Noia (A Coruña)	***42.72° N, 8.92° W, 685 m asl.***	Y	Y	***	Y	***	Y
ES06	Mahón (Menorca)	***39.88° N, 4.32° E, 78 m asl.***	Y	Y	***	Y	***	Y
ES07	Víznar (Granada)	***37.24° N, 3.53° W, 1230 m asl.***	Y	Y	***	Y	Y	Y
ES08	Niembro-Llanes (Asturias)	***43.44° N, 4.85° W, 134 m asl.***	Y	Y	***	Y	Y	Y
ES09	Campisábalos (Guadalajara)	***41.27° N, 3.14° W, 1360 m asl.***	Y	Y	Y	Y	Y	Y
ES10	Cabo de Creus (Girona)	***42.32° N, 3.31° E, 23 m asl.***	Y	Y	***	Y	Y	***
ES11	Barcarrota (Badajoz)	***38.47° N, 6.92° W, 393 m asl.***	Y	Y	***	Y	Y	Y
ES12	Zarra (Valencia)	***39.08° N, 1.10° W, 885 m asl.***	Y	Y	***	Y	Y	Y
ES13	Peñausende (Zamora)	***41.23° N, 5.89° W, 985 m asl.***	Y	Y	***	Y	Y	Y
ES14	Els Torms (Lleida)	***41.39° N, 0.73° E, 470 m asl.***	Y	Y	***	Y	Y	Y
ES15	Risco Llano (Toledo)	***39.31°N, 4.21°W, 1208 m asl.***	Y	Y	***	Y	Y	Y
ES16	O Saviñao (Lugo)	***42.63° N, 7.70° W, 506 m asl.***	Y	Y	***	Y	Y	Y
ES17	Doñana (Huelva)	***37.05° N, 6.56° W, 5 m asl.***	Y	Y	***	Y	***	Y

Table AI.1 shows the coordinates of the EMEP stations in Spain and the parameters used in this work (Y=YES)

NO_2-NO-NOx	*SO_2*	*NH_3*	*PM_{10} (+ions)*	*$PM_{2.5}$*	*Precipitation*
Chemiluminescence	UV-fluorescence	Visible spectrophotometry	Gravimetry (+IC, atomic absorption spectrometry and visible spectrometry)	Gravimetry	Water collector

Table AI.2 shows the measurement techniques of the EMEP parameters used

APPENDIX II

Table AII.1 shows the sampling sites selected in the winter NH_3 campaign in Madrid. In red, sewage treatment plants. In green, stations belonging to the city hall air quality network (*Red de Calidad de Aire del Ayuntamiento de Madrid*). Sites marked with I and II (samplers D14-D15; D25-D26; D30-D31; D59-D60) were separated a few meters. One of them was adjacent to a sewer. The sampler at Rejas was replicated (D17, D28) to check the reproducibility of the procedure. However, the results obtained for D28 were discarded since the sampler was shielded and might have not been exposed to representative ambient ammonia concentrations.

The following samplers were not deployed in the summer campaign: D7, D11, D13, D15, D26, D29, D31, D39, D42, D47, D56, D58 and D59.

Sampler	Site name	Latitude	Longitude	Type
D1	Puerta de Hierro	40°27'3"N	3°44'36"W	STP
D2	E05-B° del Pilar	40°28'40"N	3°42'43"W	Traffic
D3	E10-Cuatro Caminos	40°26'43"N	3°42'26"W	Traffic
D4	E11-Ramón y Cajal	40°27'4"N	3°40'39"W	Traffic
D5	E48-Castellana	40°26'22"N	3°41'25"W	Traffic
D6	E50-Plaza de Castilla	40°27'56"N	3°41'20"W	Traffic
D7	E57-San Chinarro	40°29'43"N	3°39'33"W	Urban bg
D8	E58-El Pardo	40°31'6"N	3°46'31"W	Urban bg
D9	E86-Tres Olivos	40°30'1"N	3°41'22"W	Urban bg
D10	P2-Plaza 2 de Mayo	40°25'40"N	3°42'13"W	Traffic
D11	P4-Tetuán	40°27'40"N	3°41'51"W	Traffic
D12	P10-Molins de Rey	40°29'39"N	3°41'34"W	Urban bg
D13	P16-Pinar de Chamartín	40°28'35"N	3°40'22"W	Urban bg
D14	P21a-Antonio Machado I	40°27'55"N	3°43'17"W	Urban bg
D15	P21b-Antonio Machado II	40°27'55"N	3°43'17"W	Urban bg
D16	P22-CIEMAT	40°27'23.25"N	3°43'31.87"W	Urban bg
D17	Rejas	40°27'4.46"N	3°32'7.16"W	STP
D18	Valdebebas	40°29'39.31"N	3°32'54.86"W	STP
D19	E16-Arturo Soria	40°26'24.17"N	3°38'21.24"W	Traffic
D20	E27-Barajas Pueblo	40°28'36.93"N	3°34'48.11"W	Urban bg
D21	E55-Urb. Embajada	40°27'41.02"N	3°34'55.21"W	Urban bg
D22	E59-Juan Carlos I	40°27'54.80"N	3°36'32.70"W	Urban bg
D23	P1-Gran Vía de Hortaleza	40°28'2.21"N	3°39'8.61"W	Urban bg
D24	P3-Silvano	40°27'28.60"N	3°38'38.28"W	Urban bg
D25	P7a-Arcentales I	40°26'4.24"N	3°36'28.70"W	Traffic
D26	P7b-Arcentales II	40°25'59.61"N	3°36'27.94"W	Traffic
D27	P15-Alcalá	40°25'46.26"N	3°39'55.16"W	Traffic

D28	Rejas	40°27'4.46"N	3°32'7.16"W	STP
D29	P18-Sorzano	40°27'7.68"N	3°39'24.61"W	Urban bg
D30	P20a-G. Noblejas I	40°25'55.80"N	3°38'2.40"W	Traffic
D31	P20b-G. Noblejas II	40°25'55.80"N	3°38'2.40"W	Traffic
D32	P26-El Capricho	40°27'16.04"N	3°35'56.22"W	Urban bg
D33	Butarque	40°19'59.5"N	3°39'40.2"W	STP
D34	La Gavia	40°21'8.9"N	3°39'31.7"W	STP
D35	E08-Escuelas Aguirre	40°25'22.1"N	3°40'51.9"W	Traffic
D36	E13-Pte. De Vallecas	40°23'22"N	3°39'1"W	Urban bg
D37	E20-Moratalaz	40°24'32.7"N	3°38'38.4"W	Traffic
D38	E47-Plaza del Amanecer	40°24'0.8"N	3°41'1.7"W	Traffic
D39	E49-Retiro	4025'15.5"N	3°40'44.9"W	Urban bg
D40	Retiro viveros	40°24'40"N	3°41'4.2"W	Urban bg
D41	E54-Pau de Vallecas	40°22'27.0"N	3°36'39.4"W	Urban bg
D42	SODAR-RASS	40°25'22.1"N	3°38'7.1"W	Urban bg
D43	P6-Vicálvaro	40°24'26.2"N	3°36'15.5"W	Traffic
D44	P14-Valdebernardo	40°24'13.8"N	3°37'8.8"W	Traffic
D45	P24-P. Cotos	40°24'6.8"N	3°39'26.6"W	Traffic
D46	P25-G. Dávila	40°22'41.0"N	3°38'17.3"W	Urban bg
D47	P27-S. Alcaraz	40°23'29"N	3°40'0.9"W	Urban bg
D48	P28-Valdemingómez	40°20'10.4"N	3°35'38.3"W	Incinerator
D49	E03-Plaza del Carmen	40°25'07.67"N	3°42'12.91"W	Traffic
D50	E04-Plaza de España	40°25'25.89"N	3°42'45.10"W	Traffic
D51	E17-Villaverde	40°20'51.15"N	3°42'47.95"W	Urban bg
D52	E18-Farolillo	40°23'41.38"N	3°43'55.25"W	Urban bg
D53	E24-Casa de Campo	40°25'06.07"N	3°44'14.19"W	Urban bg
D54	E56-Pza. Fdez. Ladreda	40°23'07.10"N	3°42'59.83"W	Traffic
D55	P5-Aluche A5	40°23'40.58"N	3°46'06.22"W	Traffic
D56	P8-Valle del Oro	40°23'18.58"N	3°43'52.14"W	Traffic
D57	P9-Cava Baja	40°24'43.80"N	3°42'35.00"W	Traffic
D58	P11-Zoo	40°24'28.54"N	3°45'44.54"W	Urban bg
D59	P12a-Lavapies I	40°24'32.64"N	3°42'04.92"W	Traffic
D60	P12b-Lavapies II	40°24'33.26"N	3°42'05.09"W	Traffic
D61	P13-Templo de Debod	40°25'26.59"N	3°43'07.40"W	Urban bg
D62	P19-Carabanchel Alto	40°22'25.92"N	3°45'02.82"W	Traffic
D63	P23-R. Ybarra	40°22'07.86"N	3°42'44.15"W	Traffic
D64	P29-Cuatro Vientos	40°22'39.88"N	3°46'49.59"W	Traffic

Table AII.1. Sampling sites in the winter NH_3 campaign in Madrid. STP=sewage treatment plant. Urban bg=urban background.

APPENDIX III

III.1-Back trajectories in every cluster for the periods Aug-Nov 2009 and Dec 2010-Mar 2011

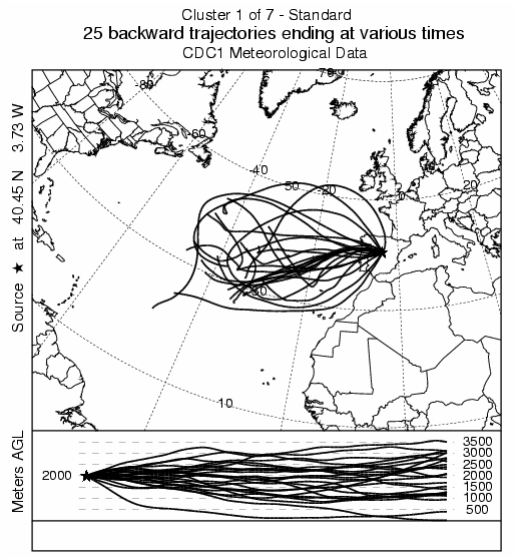

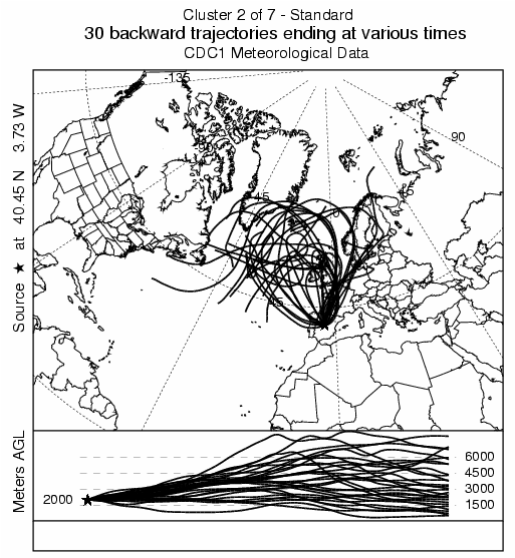

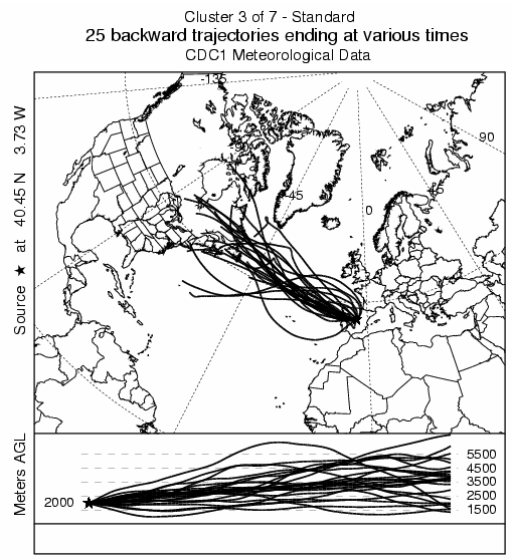

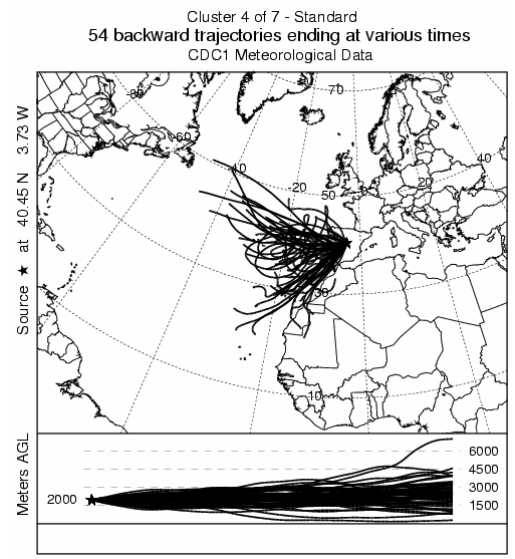

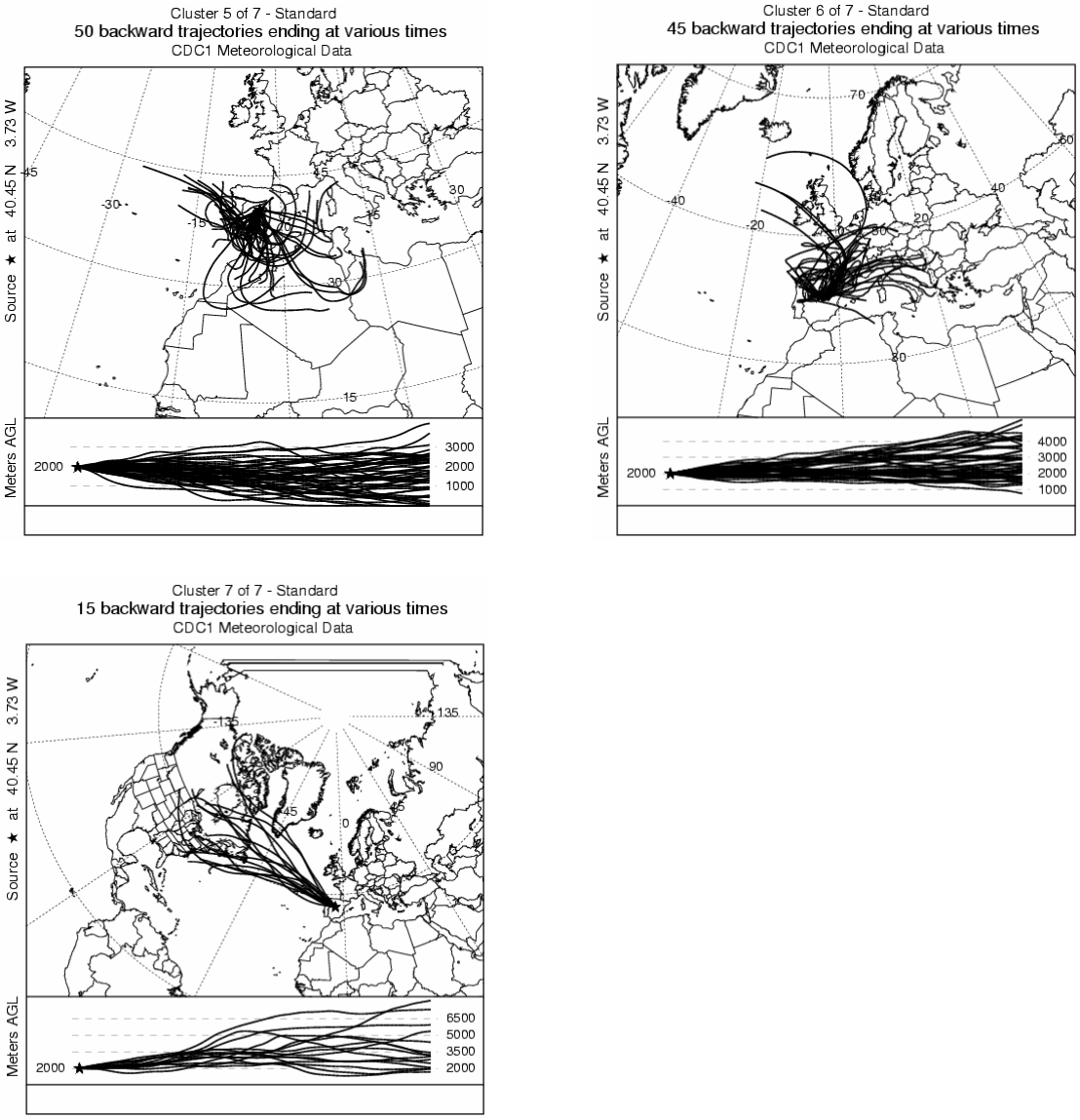

Figure AIII.1. Back trajectories in every cluster for the period Aug-Nov 2009

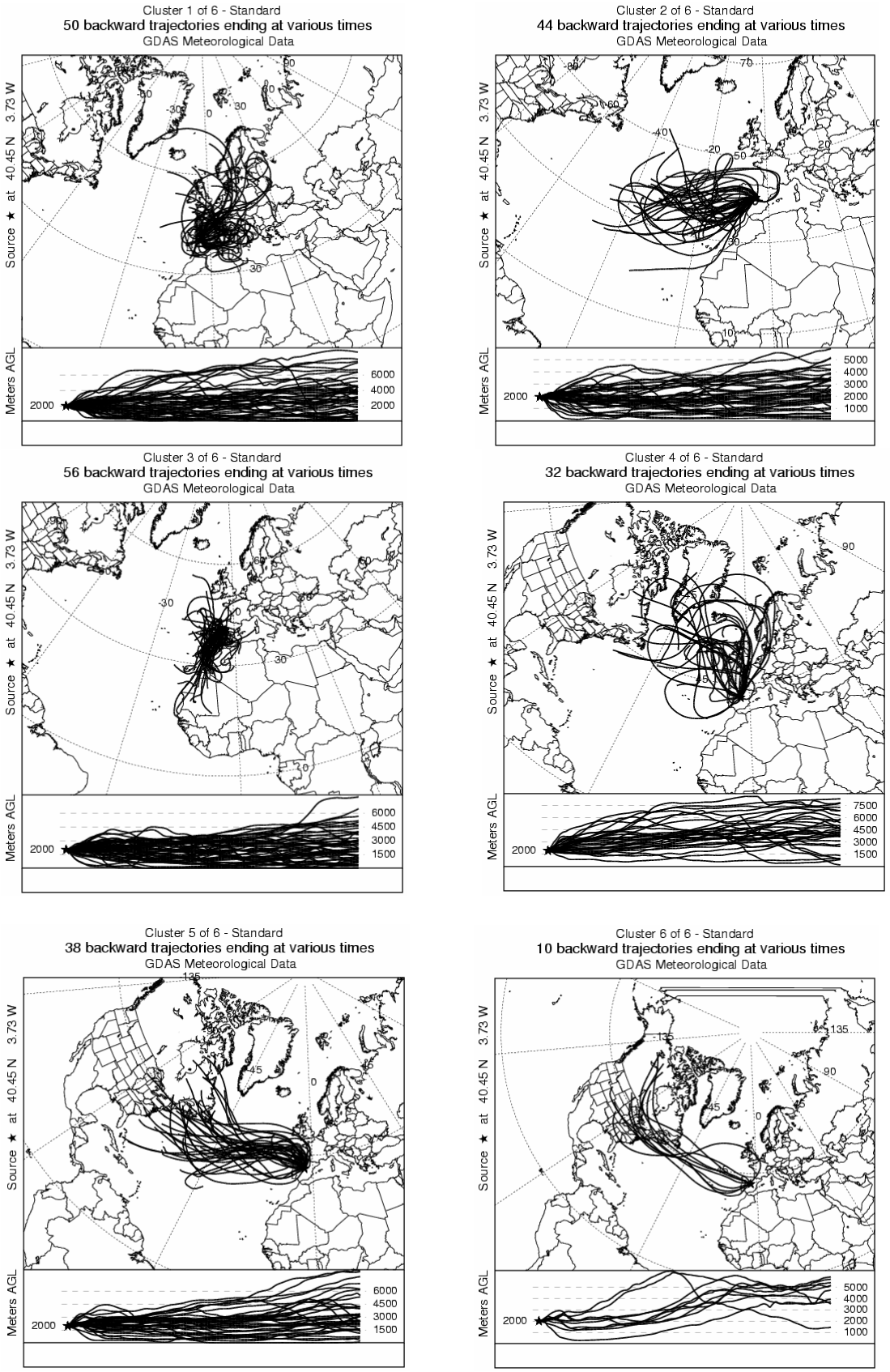

Figure AIII.2. Back trajectories in every cluster for the period Dec 2010-Mar 2011

III.2- Comparison of the daily evolution of sulphate modelled by NAAPS and at CIEMAT during E2a event

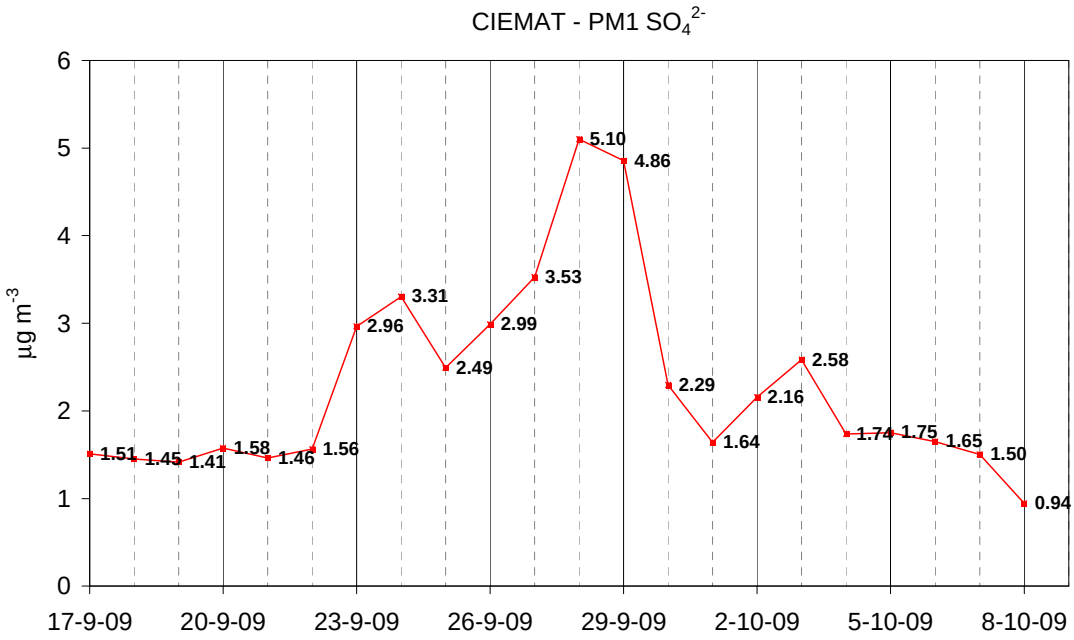

Figure AIII.3. Daily evolution of PM₁ sulphate at CIEMAT

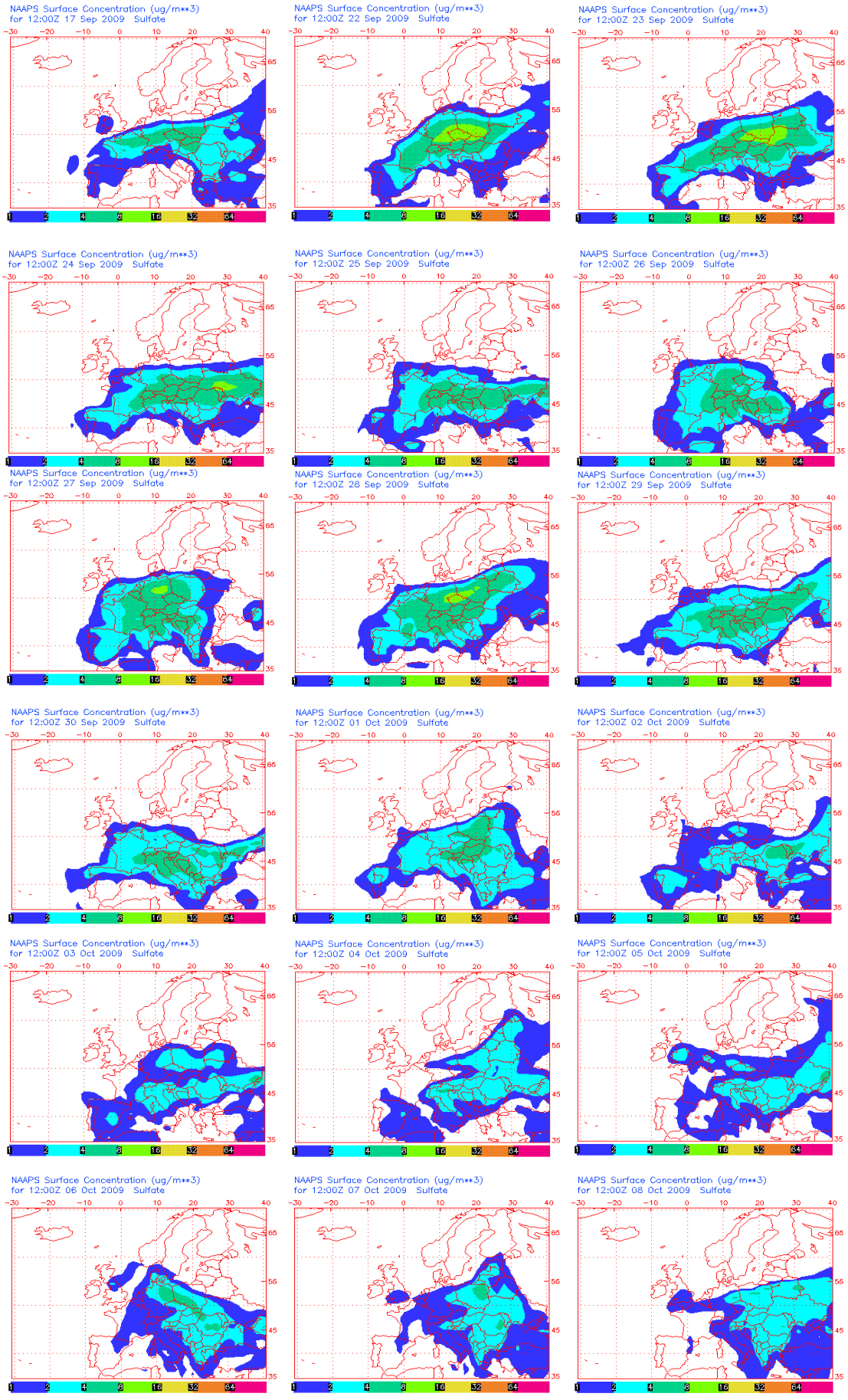

Figure AIII.4. Evolution of particulate sulphate modelled by NAAPS